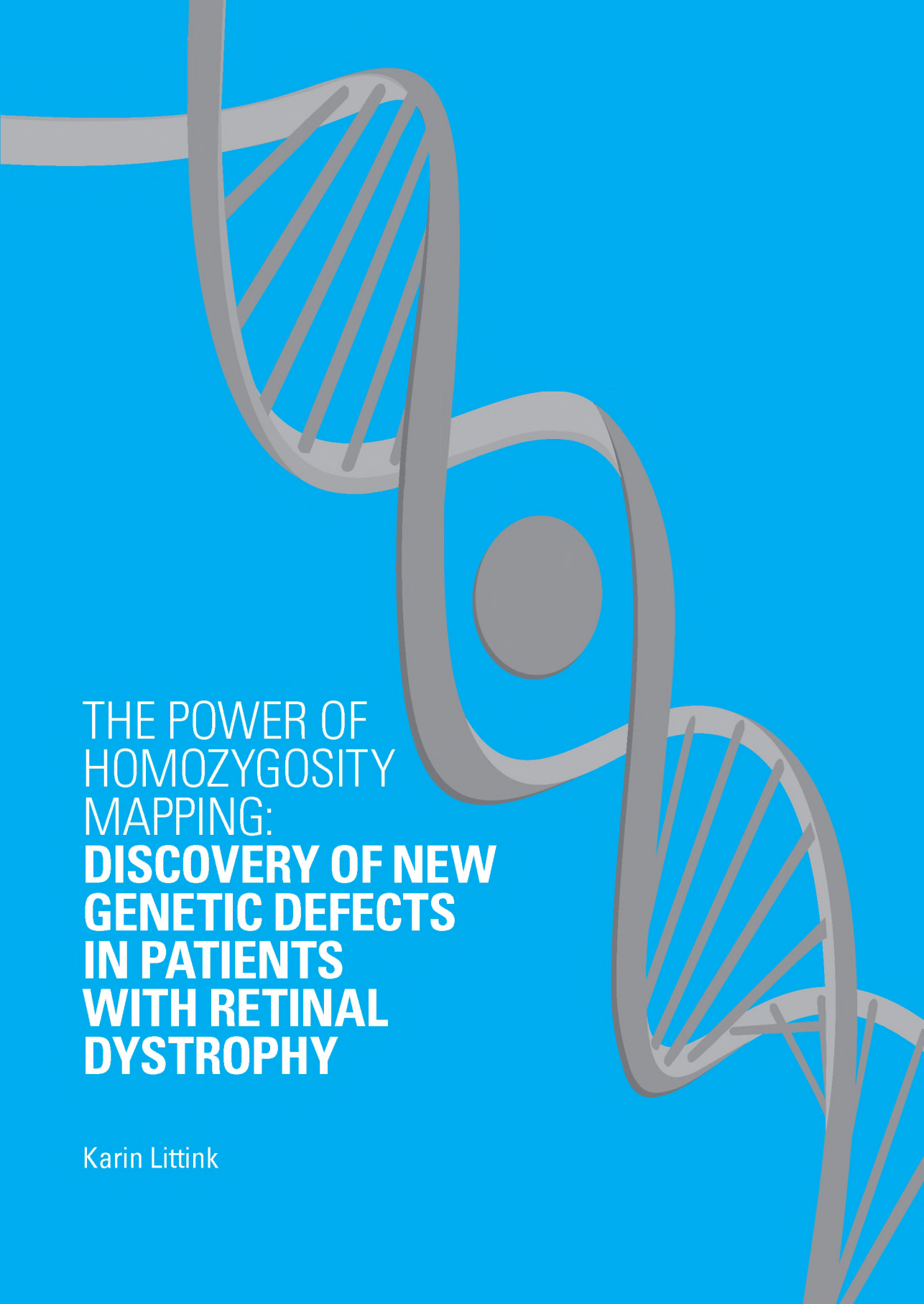

THE POWER OF HOMOZYGOSITY MAPPING: **DISCOVERY OF NEW GENETIC DEFECTS IN PATIENTS WITH RETINAL DYSTROPHY**

Karin Littink

Stellingen behorende bij het proefschrift:

THE POWER OF HOMOZYGOSITY MAPPING: DISCOVERY OF NEW GENETIC DEFECTS IN PATIENTS WITH RETINAL DYSTROPHY

1 Uit het feit dat homozygotie mapping ook leidt tot het vinden van het genetisch defect in niet-consanguine patienten uit Nederland – *dit proefschrift* – zou men kunnen concluderen dat sommige Nederlanders minder reislustig zijn ingesteld dan onze VOC geschiedenis doet vermoeden.

2 Fenotypische variatie is waarschijnlijk vaker dan we weten het resultaat van een modifier allel. – *dit proefschrift* – De huidige opvatting dat retina dystrofie een monogenetische aandoening is, wordt daarmee discutabel.

3 De bevinding dat next generation sequencing ~80 pathogene mutaties in één humaan genoom detecteert, leidt tot de vraag of monogenetische ziektebeelden überhaupt bestaan.

4 Hoewel interculturele relaties de effectiviteit van homozygotie mapping niet bevorderen, zijn ze vanuit persoonlijk oogpunt toch een aanrader.

5 Als "ik heb het gen voor ...*(aandoening)*..." een correcte uitspraak zou zijn, dan zou ieder mens een zeer groot aantal erfelijke aandoeningen hebben.

6 Zonder artsen geen patiënten, zonder lab geen mutaties.

7 Iedere onderzoeker lijdt een beetje aan tunnelvisie.

8 Het schrijven van een proefschrift is als een trekking in de bergen; de eerste dag is vreselijk, maar als je eenmaal het ritme te pakken hebt wil je niet meer stoppen. Dit in tegenstelling tot de 4daagse, waarbij de finish meer dan welkom is.

9 You can reach anything if the desire to reach the goal is bigger than the fear to fail. *(Medical genetics course, Bertinoro, may 2008)*

10 Logic will get you from A to B. Imagination will take you everywhere. *(Albert Einstein)*

11 Geluk is niet afhankelijk van dingen buiten ons, maar van de manier waarop wij die zien. *(Lev Tolstoj)*

12 Too much thinking – bad for health *(Health museum, Hyderabad, India)*

Karin Littink, 03-11-2010

THE POWER OF HOMOZYGOSITY MAPPING: DISCOVERY OF NEW GENETIC DEFECTS IN PATIENTS WITH RETINAL DYSTROPHY

Karin Littink

'What is essential is invisible to the eye'

(Antoine de Saint-Exupéry. in "Le petit prince")

THE POWER OF HOMOZYGOSITY MAPPING: DISCOVERY OF NEW GENETIC DEFECTS IN PATIENTS WITH RETINAL DYSTROPHY

Karin Littink, 2010

Publication of this thesis was financially supported by the Department of Human Genetics, Radboud University Nijmegen Medical Centre; Stichting Wetenschappelijk Onderzoek Het Oogziekenhuis - prof.dr. H.J. Flieringa; Landelijke Stichting voor Blinden en Slechtzienden; Alcon Nederland B.V.; Novartis Pharma B.V.; Bayer HealthCare; Stichting Blindenhulp; Allergan B.V.; Rotterdamse Vereniging Blindenbelangen.

Design: Nicole Ellenbroek (www.studio-zout.nl)
Cover design: Iris Benites Estrada
Printed by: Zalsman, Kampen
ISBN: 978-90-9025562-0

THE POWER OF HOMOZYGOSITY MAPPING: DISCOVERY OF NEW GENETIC DEFECTS IN PATIENTS WITH RETINAL DYSTROPHY

EEN WETENSCHAPPELIJKE PROEVE OP HET
GEBIED VAN DE MEDISCHE WETENSCHAPPEN

Proefschrift

ter verkrijging van de graad van doctor aan de Radboud Universiteit Nijmegen op gezag van de rector magnificus prof. mr. S.C.J.J. Kortmann, volgens besluit van het college van decanen in het openbaar te verdedigen op woensdag 3 november 2010 om 13:30 uur precies

door

Karin Willemijn Littink
geboren op 25 juni 1981 te Sleeuwijk

Promotor:
Prof. Dr. F.P.M. Cremers

Copromotores:
Dr. L.I. van den Born
Dr. A.I. den Hollander

Manuscriptcommissie:
Prof. Dr. B.G.M. van Engelen (voorzitter)
Prof. Dr. W. Berger (University of Zürich, Switzerland)
Dr. H. Kremer

TABLE OF CONTENTS

CHAPTER 1

GENERAL INTRODUCTION

Vision is a fascinating phenomenon, and over the last millennia scientists have reflected on a large number of theories to explain the actual mechanism of sight. Although the earliest scientists probably understood that the eye was the organ that mediated vision, the actual formation of an image remained a mystery.

One of the first reports about the eye go back to Hippocrates (~460-377 B.C.), who described several components of the eye and distinguished the retina as a separate membrane. About one century later Greek anatomists were able to describe a more detailed anatomy by dissecting animal eyes. During dissections, the retina easily detached from the eyeball and appeared as a collapsed membrane in the shape of a fishing net, and was therefore called 'retina', meaning 'netlike-membrane' in Latin. The next characterization that improved the knowledge about the different eye components was made by the Roman physician and philosopher Galen of Pergamum (129-199 A.D.), who described the retina as a displaced part of the brain, based on its similarity in color and consistency with the brain.[1]

In contrast to the relatively correct ideas about anatomy, the speculations about the function of the different components of the eye were far from our current knowledge. Several theories were posed to explain how the eye was able to perceive an image: 'the water inside the eyeball is the photosensitive organ' (Hippocrates), 'objects continuously send images of themselves' (Democritos, 460-370 B.C.), 'rays of light emanated from an object meet with the rays of light sent from the pupil' (Plato, 427-347 B.C.), 'objects discharge countless shell-like moulds that leave a print in the visual organ' (Epicuros, 341-270 B.C.). Eventually, two main thoughts continued to exist. First, the eye was thought to send light – like a sun – in a cone shaped projection, with the tip of the cone in the pupil and the base of the cone projected on the subject of interest ('the emanation theory', by Pythagoras in 532 B.C). Second, the lens was thought to be the photosensitive organ in the eye. The retina appeared to contain many blood vessels, and was thought to be the provider of nutrition as well as the conveyor of the 'visual spirit' – a mysterious force by which vision was effectuated.

After the decline of the Classical Civilization due to invasion of the barbarians, the ophthalmic knowledge passed on to the Arab Civilization. It was at the end of the first millennium that the Arab optics student Ibn al-Haitham (965-1039) criticized the emanation theory and proposed that 'vision is accomplished by rays coming from external objects and entering into the visual organ'. Around the 12th century, the Greek and Arab knowledge slowly reached Western Europe when Arab manuscripts were translated into Latin, and it was only in the 16th century that the anatomist Platter (1536-

1614) overthrew the long-lasting idea of a photosensitive role of the lens. In his opinion, the lens was 'the spectacle of the optic nerve', and the true photoreceptor was the retina. The model of vision was finalized by Kepler (1571-1630), who explained that an image is projected to the retina inverted and diminished in size based on refraction.

The knowledge of retinal anatomy accelerated after the invention of the microscope by Anthonie van Leeuwenhoek (1632-1723), which made it possible to visualize the photoreceptor cells and the retinal layers. The first observations were confusing, because the order of the retinal layers seemed to be inside-out, with the photoreceptor layer in the posterior position. Nevertheless, it was in the 19th century that Helmholtz (who also developed the first ophthalmoscope), Corti and Koelliker (~1850) laid the foundation for the present understanding of the three-layered retina and its connection to the optic nerve. The distribution of photoreceptors and the difference in diurnal and nocturnal function between cone and rod photoreceptors was clarified by Schultz in 1872. In 1877 Boll discovered the visual pigment 'rhodopsin'. The bipolar, horizontal and amacrine cells were elucidated by Cajal around 1900.[1]

From then on there was an expansion of understanding the visual processes due to the elucidation of the phototransduction cascade, which gave the first insights into the inner part of the retinal cells. Since two decades this knowledge is expanded to the genetic level, due to the identification of genes involved in retinal dystrophies. In 1990, only 113 years after the discovery of the visual pigment, the gene encoding this rhodopsin molecule, termed rhodopsin (*RHO*), was identified as the first genetic cause of retinal dystrophy.[2] In the same year, Cremers et al. published the identification of the choroideremia – an X-linked chorioretinal dystrophy – gene.[3] These two studies marked the beginning of an era of positional candidate gene cloning. Since then, the number of genes associated with retinal dystrophies has grown tremendously, which has led to a detailed knowledge about the visual processes, insight into disease mechanisms that cause the different types of retinal dystrophies, and – most importantly – to the development of possible interventions of degeneration of retinal cells in humans. This all has led to the first clinical trials of gene-specific therapy in patients with retinal dystrophy,[4-7] which emphasizes the need to continue exploration of the unknown.

The next paragraphs will focus on the present knowledge about the retina, visual processes and the molecular genetics of mainly three retinal dystrophies; cone-rod dystrophy (CRD), Leber congenital amaurosis (LCA) and retinitis pigmentosa (RP).

THE RETINA

Retinal anatomy

The retina consists of two layers: the neural retina and the retinal pigment epithelium (RPE). The RPE is a single layer of cells that separates the photoreceptors from the choroid (Figure 1), and exchanges nutrients and waste products between the retina and the choroidal blood vessels. The neural retina is a section of the central nervous system that covers the inner back side of the eye, and consists of three layers (Figure 1).[8 and refs therein] The first layer – which is the posterior layer from the perspective of the incoming light – consists of photoreceptor cells (cones and rods), which convert the energy of an absorbed photon into an electrical signal that is then transferred via their synaptic terminal to the second layer of bipolar, horizontal and amacrine cells (the second order neurons). These cells are responsible for interconnecting the input from single photoreceptors, which is the first stage of image processing. The signals are then communicated to the third layer of cells; the ganglion cells, which transport the neuronal signal via the optic nerve to the visual cortex of the brain.

The blood supply to the retina is provided by the retinal artery (15-35%) and the choroidal vessels (65-85%).[9] The blood supply of the choroidal vessels is vital for the maintenance of the photoreceptors in the outer retina, which makes the 'inside-out design' of the retina – with the photoreceptors (the cells that absorb the light) separated from the light with two layers of cells – more logical.[9, 10]

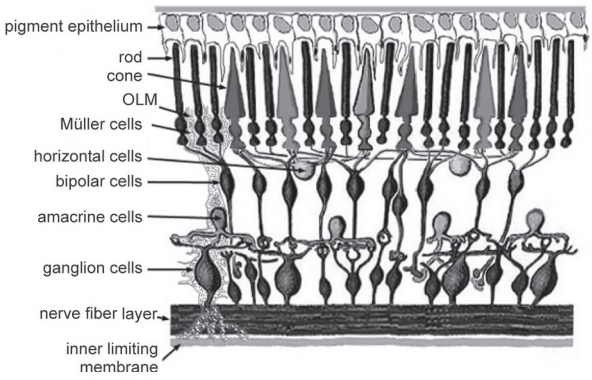

FIGURE 1. Schematic overview of the various cells within the three retinal layers. *(Figure derived from http://webvision.med.utah.edu).*

There are two types of photoreceptors, both with a specialized function. Only 5% of the photoreceptors (~3 million) are cones, which are concentrated in the central retina (the fovea), and are responsible for the visual acuity, bright light (photopic)

vision and for color vision. The other 95% (~60 million) are rods, which mediate dim light (scotopic) vision. Rods are absent in the inner part of the fovea, but are highly concentrated in a rim surrounding the fovea and they are the major photoreceptor cells in the mid-peripheral and peripheral retina (Figure 2A). Rods are able to detect even a single photon, which explains why stars can be seen when focusing slightly beside a star, so that the photons project to the rods, and may not be visible when focusing straight at a star with the cones, that are not sensitive enough to process this low-intensity light.[8]

Photoreceptors have an inner segment in which proteins are synthesized, which are then transported towards the outer segment via the connecting cilium of the cell (Figure 2B). The outer segment contains membranous discs that carry the photopigment – color opsins in case of cones and rhodopsin in case of rods – and other proteins necessary for phototransduction. The anatomy of the outer segment differs among cone and rod photoreceptors; the rod outer segments are rod shaped and contain internalized discs, which do not attach to the cell membrane, the cone outer segments are cone shaped and the discs and surface membrane are continuous.

Every day, new discs are generated from the base of the outer segment, and – at the apical end – daily 10% of the discs are phagocytosed by the RPE cells. The high turnover of photoreceptor discs makes the RPE cells the most active phagocytic cells in the human body.[8]

FIGURE 2. Distribution of rod and cone photoreceptors over the retina, and anatomy of the rod photoreceptor.

A. Distribution of the cones and rods, showing a high concentration of cones and absence of rods in the fovea, and a high concentration of rods in the peripheral retina *(Figure derived from http://www.cogsci.bme.hu/).*

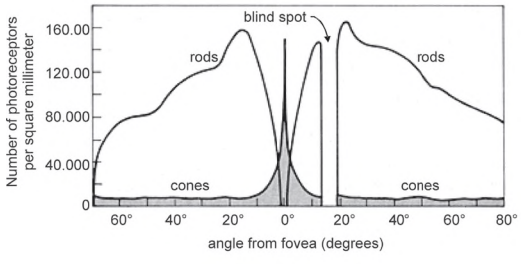

B. Detailed anatomy of the rod photoreceptor *(Figure designed by and published with permission of E.A. Pierce).*

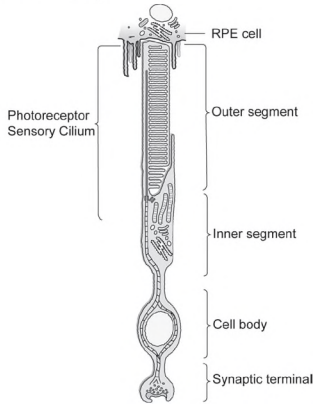

Retinal processes

Two major processes are important for the conversion of light into an electrical signal. First, the phototransduction cascade; the process by which the photoreceptors convert the energy of an absorbed photon into a neuronal signal. Second, the visual cycle; a continuous recycling process in which the chromophores (all-*trans*-retinal) used in the phototransduction cascade are recycled into newly usable chromophores (11-*cis*-retinal).
Both processes are described in more detail below.

Phototransduction cascade

The phototransduction cascade (Figure 3) takes place in the photoreceptor outer segment. The membranous discs of the outer segment contain a photosensitive pigment; a membrane protein that consists of an opsin protein (rhodopsin in rods, green, red or blue opsin in cones) joined with an 11-*cis*-retinal chromophore. When a light photon reaches the retina, it activates rhodopsin by changing the 11-*cis*-retinal into all-*trans*-retinal. The activated rhodopsin (metarhodopsin II) triggers the activation of transducin, which – when bound to GTP – then activates cGMP specific phosphodiesterase (PDE). The activated PDE α and β subunit hydrolyze cGMP to 5-GMP. The subsequent decrease of cytoplasmic cGMP leads to the closure of cGMP channels in the plasma membrane and, as a result, sodium cannot freely enter the cell, which leads to the hyperpolarization of the cell. Due to hyperpolarization of the plasma membrane voltage-gated calcium channels (for example the $Ca_v1.4$ channel) at the synaptic terminal will close. As a result, the intracellular calcium concentration suddenly decreases, which leads to the inhibition of neurotransmitter (glutamate) release. Thus, counter-intuitively, in the dark state there is a constant neurotransmitter release, while activation of the photoreceptor leads to a decrease of neurotransmitter release.[11, 12 and refs therein]

Following activation of the phototransduction cascade, used molecules are converted into their initial conformation during the recovery phase (Figure 3).[13] Metarhodopsin II is inactivated via phosphorylation by rhodopsin kinase and by binding to arrestin which results in free opsin and all-*trans*-retinal. Subsequently, activated transducin and PDE are deactivated by a complex of GTPase accelerator protein (Regulators of G-protein Signaling; *RGS9-1*) and Gβ5L, which together stimulate GTP hydrolysis. From this GTP, cGMP is synthesized by guanylate cyclase enzymes (GC-1 and GC-2) as a result of which cGMP concentration are restored to 'dark levels'. The end result is an outer segment in dark state, in which the cation channels are open, the photoreceptor is depolarized, neurotransmitter is steadily released from the synaptic

terminal, all proteins involved in the phototransduction cascade are ready for the next activation, and all-*trans*-retinal is ready to be recycled in the visual cycle.

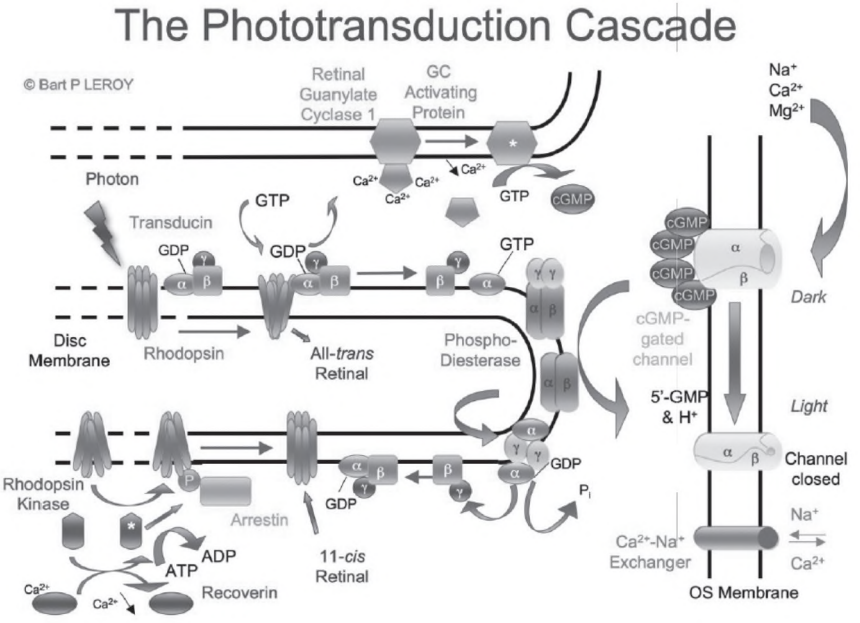

FIGURE 3. **Schematic overview of the activation and recovery of the phototransduction cascade.** A photoreceptor outer segment disk membrane and plasma membrane are shown with the most important molecules that participate in the phototransduction cascade. Activation of rhodopsin by a photon induces a cascade of chemical reactions, leading to closure of the plasma membrane cGMP-gated channel, leading in turn to hyperpolarization of the photoreceptor cell. *(Figure designed by and published with permission of B.P. Leroy.)*

Visual cycle

The rod visual cycle is a recycle machinery that takes place in the RPE and photoreceptor outer segment, where it recycles 'used' all-*trans*-retinal into 11-*cis*-retinal that can be re-utilized in the phototransduction cascade (Figure 4A).[14 and refs therein] Following inactivation of the phototransduction cascade, all-*trans*-retinal dissociates from the opsin into the disc membranes of the photoreceptor outer segment, is then transferred to the cytoplasmic space facilitated by the ABCR protein in the disc membrane, and converted into all-*trans*-retinol by retinol dehydrogenase (*RDH12*).

All-trans-retinol (vitamin A) is then released into the interphotoreceptor matrix, which is accelerated by interphotoreceptor retinoid-binding protein (*IRBP*); a protein localized in the interphotoreceptor matrix that strongly binds all-*trans*-retinol. All-*trans*-retinol is then taken up by the RPE cells, facilitated by cellular retinol-binding protein-1 (*CRBP1*). RPE cells also take up vitamin A from blood in the choroidal circulation. In the RPE cell, all-*trans*-retinol is esterified by lecithin retinol acyl transferase (*LRAT*) into all-trans-retinyl ester, which is the stable and non-cytotoxic storage form of vitamin A. Subsequently, RPE-specific 65-kDa protein (*RPE65*) isomerizes all-*trans*-retinyl ester into 11-*cis*-retinol, and – since free 11-*cis*-retinol inhibits the isomerization of more all-*trans*-retinyl ester – it then binds to cellular retinal-binding protein (*CRALBP*), and may be temporarily removed from the chemical equilibrium by conversion into 11-*cis*-retinyl by *LRAT*. 11-*cis*-retinol is subsequently oxidized into 11-*cis*-retinal, catalyzed by 11-*cis*-retinol dehydrogenase (*RDH5*), and then released from the RPE cell into the interphotoreceptor matrix, again facilitated by IRBP. Finally, 11-*cis*-retinal is taken up by the photoreceptor, where it binds to rhodopsin to be part of the phototransduction cascade again.

The rod photoreceptors are fully dependent on the visual cycle in the RPE for the regeneration of 11-*cis*-retinal. Remarkable, the visual pigment regeneration in cones is 2000-fold higher than in rods, and the maximum throughput of the visual cycle is too slow to explain the sustained photosensitivity of cones in bright light. Based on these observations, a new pathway for regeneration of visual pigment was discovered that revealed that part of the visual cycle in cones takes place in the Müller cells, instead of the RPE cells (Figure 4B).[15] Analysis of cone-dominated retinas (from chickens and ground squirrels) revealed that all-*trans*-retinol was directly isomerized to 11-*cis*-retinol without the formation of all-*trans*-retinyl ester as intermediate. Subsequently, 11-*cis*-retinol is removed from the equilibrium reaction by binding to CRALBP and by a palmitoyl-coenzyme A (palm-CoA)-dependent esterification of 11-*cis*-retinol, to stimulate 11-*cis*-retinol synthesis. The existence of this alternative visual cycle may function in conjunction with the visual cycle in the RPE-cells, to provide visual chromophores to the cone in the high rate that is required for daylight-vision.

ON and OFF pathways

The conversion of a neuronal signal from a photon is step one in vision. Step two comprises the processing of the neuronal signals into signals that eventually can build an image. This is conducted by two separate pathways: one that is activated by light input and by images that are lighter than their background, and one that is activated by a dark input, or when a stimulus is darker than its background. These pathways are called the ON and OFF pathway, respectively, and were discovered

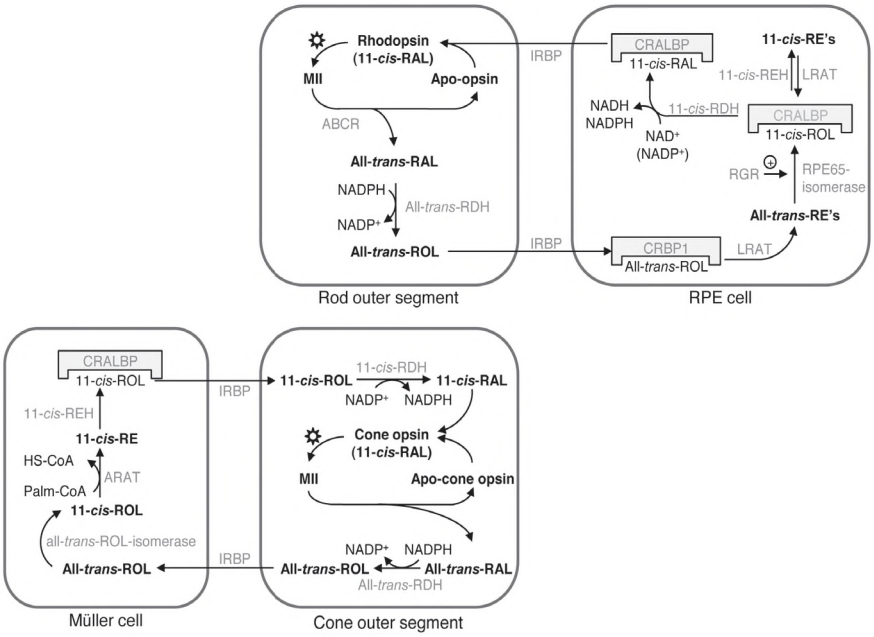

FIGURE 4. Schematic presentation of the rod and cone visual cycles. All-*trans*-retinal is recycled via several steps into 11-*cis*-retinal that can be reused in the phototransduction cascade. **A.** The rod visual cycle takes place in the rod outer segment and the retinal pigment epithelium. **B.** The cone visual cycle takes place in the cone outer segment and the Müller cells. *, photon; MII, metarhodopsin II; RAL, retinal; RDH, retinol dehydrogenase; RE, retinyl ester; REH, retinyl ester hydrolase; ROL, retinol; palm CoA, palmitoyl coenzyme A. Proteins are presented in grey, and are encoded by the following genes (in italic): 11-cis-RDH, *RDH5*; ABCR, *ABCA4*; All-trans-RDH, *RDH12*; CRALP, *RLBP1*, CRBP1, *CRBP1*, IRBP, *IRBP*; LRAT, *LRAT*; RGR, *RGR*; RPE65 isomerase; *RPE65*.

when measurement of the optic nerve revealed that some nerve fibers fire when the light is switched on, while other nerve fibers fire when light is turned off. These separate pathways implicate that sensing black and white is not a continuum of grey intensity, but two separate pathways, one from gray to black, and one from gray to white.[16]

The separation into the ON and OFF pathways starts at the synapse between the photoreceptor and the bipolar cells. As mentioned before, neurotransmitter release is favored in a dark state, and drops during light input. There are no separate ON and OFF photoreceptors, the bidirectional signaling appears at the stage of the bipolar

cells. There are mainly two types of bipolar cells; the ON (rod and cone) and OFF (cone) bipolar cells. These cells differ in the type of receptor molecules expressed at the synapse. ON bipolar cells have a metabotropic mGLuR6 receptor and OFF bipolar cells have an ionotropic glutamate receptor. Due to different properties of the receptors, OFF bipolar cells are excited when glutamate levels are high, i.e. a dark stimulus, and ON cone bipolar cells are excited when glutamate levels drop, i.e. a light stimulus (Figure 5). The cone ON or OFF signal is passed on to the ON and OFF ganglion cells, respectively, and subsequently passed on via the optic nerve towards the visual cortex. The rod ON bipolar cells cannot transfer their signal directly to the ganglion cells. Instead, there are three possible routes. First, the classical pathway (ON1/OFF1, Figure 5), in which a signal from a rod bipolar cell is transferred to the amacrine cells in the inner plexiform layer. The amacrine cells then sum the input from several rod bipolar cells and transfer the signal to the axon terminal of the ON cone bipolar cell. These cone bipolar cells, in turn, synapse onto the ganglion cells. This rod bipolar pathway is the most sensitive pathway, and is able to detect one single photon. The alternative pathways transfer the signal via a gap junction between the rod synaptic terminal and the cone synaptic terminal, and on to the cone bipolar cells (ON2/OFF2, Figure 5), and some rods have a direct synaptic connection to the OFF cone bipolar cells (OFF3, Figure 5).

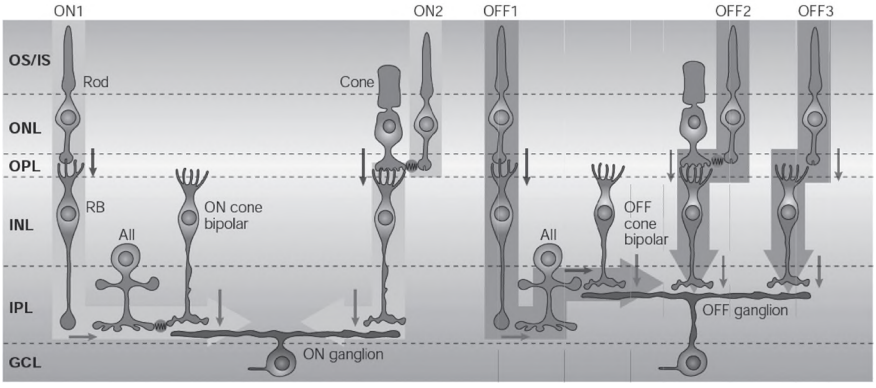

FIGURE 5. The various ON and OFF signal transmission paths from rod and cone photoreceptors to bipolar cells.

OS, outer segment; IS, inner segment; ONL, outer nuclear layer; OPL, outer plexiform layer; INL, inner nuclear layer; IPL, inner plexiform layer; GCL, ganglion cell layer. AII, amacrine cell; RB, rod bipolar cell. Dark arrows depict "OFF-signaling" via glutamate receptors, whereas light grey arrows depict "ON-signaling" through mGLuR6 receptors. *(Figure derived from Wässle, 2004,[16] and published with permission.)*

RETINAL DYSTROPHIES; THE CLINICAL FEATURES

Monogenic retinal dystrophies affect approximately 1/2000 people, which corresponds to more than 2 million people worldwide.[17] There are several types of retinal dystrophies, representing a spectrum of cone-dominated (achromatopsia, cone dystrophy, cone-rod dystrophy) to rod-dominated (retinitis pigmentosa [i.e. rod-cone dystrophy]) diseases, or diseases that can present as either cone- or rod-dominated (Leber congenital amaurosis). Beside the type of photoreceptor that is primarily involved, the sub-classification is based on the age of onset, the clinical features, and the course of the disease. However, clinical features can be very heterogeneous. Retinal dystrophies account for ~5% of blindness worldwide, in which blindness is defined by the World Health Organization as a visual acuity lower than 20/400 in the best eye and/or a visual field smaller than 10 degrees.

The three types of retinal dystrophy included in this thesis will be discussed in more detail below.

Cone-rod dystrophy

Cone-rod dystrophy (CRD) is characterized by the primary loss of cone photoreceptors followed by or simultaneous with the loss of rod photoreceptors.[18, 19] The disease commonly becomes apparent during primary school years. The symptoms include photo-aversion, a decrease in visual acuity with or without nystagmus, color vision defects, and decreased sensitivity of the central visual field. Rod photoreceptors can become affected as well, leading to night blindness and loss of peripheral vision. In comparison to the rod-cone type of disease, CRD patients have fewer difficulties to move independently in the initial stage, due to the remaining peripheral visual field, but are practically blind at a relatively young age, due to early and more rapid loss of macular function. The fundus of CRD patients is characterized by maculopathy and, in later stages, attenuated vasculature, pallor of the optic disc and pigmentary changes in the periphery can be seen.

The diagnosis of CRD is mainly based on electroretinogram (ERG) recordings, in which cone (photopic) responses are more severely reduced than or equally reduced as rod (scotopic) responses.[20] Goldmann kinetic perimetry can reveal a relative or absolute central scotoma. Fundus autofluorescence shows a predominant involvement of the macular region, and to a lesser extend, the peripheral region.

The prevalence of CRD is ~1:40,000 and it can be inherited in an autosomal recessive, autosomal dominant and X-linked manner.[18] Usually CRD is a non-syndromic disease,

but it can also appear as part of a syndrome, like in Bardet-Biedl syndrome (BBS) and spinocerebellar ataxia type 2 (Jalili syndrome), or in combination with ectodermal diseases like amelogenesis imperfecta.

Leber congenital amaurosis

Leber congenital amaurosis (LCA), sometimes referred to as congenital blindness, is the earliest and most severe form of all retinal dystrophies. The diagnosis is established on the following clinical features: severe and early visual loss, wandering nystagmus, amaurotic pupils (i.e. no pupillary reflex on light sensation), and absent or severely reduced signals on ERG testing before the age of one year.[21-23] In the initial stage, LCA can be difficult to distinguish from other severe congenital retinal dystrophies like (complete or incomplete) achromatopsia, congenital stationary night blindness (CSNB; type 1 or 2), and albinism. However, early ERG responses are usually low or non-detectable for both cones and rods in LCA, whereas rod signals remain detectable in achromatopsia, ERG responses are electro-negative in CNSB, and supernormal in albinism. Hanein et al.[22] divided the LCA phenotype in two groups; LCA type I is the cone-rod type of LCA, in which photophobia is most remarkable. In this group, patients often have a hypermetropic refractory error, macular as well as peripheral abnormalities on ophthalmoscopy, and the course of disease is usually stationary. In LCA type II, night blindness is more prominent, which suggests a rod-cone type of disease, and it has a more progressive nature.

The prevalence of LCA is ~1:30,000-81,000,[21, 23] and in most cases LCA is inherited in an autosomal recessive mode, but cases of autosomal dominant inheritance have also been described. Like many other retinal dystrophies, LCA can be a symptom of a syndrome as well, for examples in Joubert syndrome, Senior-Løken syndrome and Alström syndrome.

Retinitis pigmentosa

Retinitis pigmentosa (RP) is a retinal dystrophy in which the rods are primarily affected. The age of onset of symptoms is highly variable in RP, ranging from early childhood to later than 50 years of age. The initial symptoms are night blindness and loss of peripheral vision.[24, 25] Both symptoms may be difficult to notice by a patient, because the current electrical night-time illumination is sufficient for cone-dependent vision, and loss of the peripheral field can be unnoticed until ~50 degrees of remaining visual field.[26] Eventually, the cone photoreceptors become affected as well, often leading to blindness due to a combination of restricted visual fields and maculopathy. Although there is no established

treatment for RP yet, treatment of common complications, like posterior subcapsular cataract or cystoid maculopathy, can be of help for preserving a visual function.

The fundus of RP patients in the initial stage shows minimal changes, but in advanced stages pathognomic bone-spicule shaped pigmentation usually appear in the mid-peripheral retina. These pigmentations are the result of RPE cells that migrate into the neural retina in response to photoreceptor cell death. Furthermore, the fundus shows a waxy pale optic disc and a narrow retinal vasculature. Chorioretinal atrophy can appear, which makes the choroidal vessels more abundantly visible due to pronounced atrophy of the RPE.

The diagnosis is based on the ERG responses, in which rods are more severely affected than cones. Goldmann perimetry can document the loss of peripheral visual field, and usually shows a ring scotoma, or loss of the peripheral visual field.

The prevalence of non-syndromic RP is ~1:4,000.[24, 25] RP can appear as a symptom of a syndrome as well, for example in Usher syndrome, Jeune syndrome, metabolic syndromes like Refsum disease and Zellweger syndrome, and neurological syndromes like neuronal ceroid lipofuscinosis (Batten disease). Non-syndromic RP can be inherited in an autosomal recessive (50-60%), autosomal dominant (30-40%), X-linked (5-15%) and digenic manner. RP is the leading cause of visual disability in adults below the age of 60.[27]

MOLECULAR GENETICS OF AUTOSOMAL RECESSIVE CRD, LCA AND RP

In order to achieve a neuronal signal from an absorbed photon, a properly working visual cycle, phototransduction cascade, and a well-developed and well-maintained retinal architecture are essential. Consequently, many mutations leading to CRD, LCA and/or RP are detected in genes that play an important role in the visual processes or the development of photoreceptors. Table 1 shows an overview of genes associated with autosomal recessive (ar) CRD, LCA and RP, and their accompanying function.[17, 21, 28] Some genes are responsible for a substantial percentage of CRD, RP and LCA patients, whereas most genes are involved in only one or two percent of cases (percentages indicated in Table 1). Still, in ~55%, ~35% and ~50% of arCRD, arLCA and arRP patients, respectively,[18, 21, 25] the genetic defect remains unsolved, and the discovery of new mutations and new genes associated to these phenotypes is

ongoing. New genes and gene mutations can be discovered trough several methods, of which three have led to the identification of most of the genetic causes. In candidate gene analysis genes that turned out to play an important role in one of the visual processes were screened in large cohorts of patients.[2, 29-31] In positional gene cloning the disease locus in the DNA of a patient was first established, for example by linkage analysis, followed by a screening of genes in that particular genomic region.[3, 32-34] The third method includes screening of genes that are mutated in animal models that exhibit a phenotype comparable to the human disease.[35-37] Recently, one gene was identified by using mRNA expression profiling.[38]

In this thesis, homozygosity mapping has been used in order to identify the genetic defect in patients affected by CRD or allied disorders.

TABLE 1. **Overview of genes involved in autosomal recessive cone-rod dystrophy, autosomal recessive Leber congenital amaurosis and autosomal recessive retinitis pigmentosa.**

Gene	arCRD*	arLCA ‡	arRP*	Other associated diseases	Function
ABCA4	40%		1-2%	MD, STGD1	Visual cycle[32, 39, 40]
ADAM9	1-2%				Involved in outer segment-RPE junction[41]
AIPL1		5,3%		adCRD	Involved in posttranslational modification[42-44]
CABP4		<1%		CCSD	Synaptic transmission[45]
CEP290		15%		EOSRD, JBTS, SLSN, BBS	Transport across the photo-receptor connecting cilium[46]
CERKL	1-2%		1-2%		Cellular apoptosis and survival[47]
CNGA1			2%		Phototransduction[48]
CNGB1			1-2%		Phototransduction[49]
CRB1		9,9%	2%		Photoreceptor development and structure[50]
CRX		1,0%		adRP, adLCA, adCRD	Transcriptional regulation (photoreceptor development)[51]
EYS	<1%		5-12%		Photoreceptor morphogenesis[52, 53]
GUCY2D		11,7%		adCRD	Phototransduction[54]
IDH3B			1-2%		Krebs cycle[38]
LCA5		1,8%			Transport across the photo-receptor connecting cilium[55]
LRAT		0,5%	1-2%		Visual cycle[56]

MERTK		0,6%	1-2%		Photoreceptor outer segment phagocytosis[57]
NR2E3			1-2%	adRP, ESC	Transcriptional regulation (photoreceptor development)[58, 59]
NRL			1-2%	adRP	Transcriptional regulation (photoreceptor development)[60-62]
PDE6A			4%		Phototransduction[30]
PDE6B			4%		Phototransduction[36]
PRCD			<1%		Present in photoreceptor cytoplasm[63]
PROM1	1-2%		1-2%		Photoreceptor disk membrane morphogenesis[64]
RBP3 (IRBP)			<1%		Visual cycle[65]
RD3		0,1%			Early postnatal retinal development[66]
RDH12		2,7%		adRP	Visual cycle[67]
RGR			1-2%		Visual cycle[68]
RHO			1-2%	adCSNB, adRP	Phototransduction[69]
RLBP1			1-2%	FA, RPA	Visual cycle[70]
RP1			1-2%	adRP	Photoreceptor structure[71, 72]
RPE65		6,0%	2%		Visual cycle[56, 73]
RPGRIP1	1-2%	4,2%			Transport across the photo-receptor connecting cilium[74]
SAG			2%	CSNB	Phototransduction[75]
SPATA7		1-2%	1-2%		Expressed in cytoplasm of photoreceptor inner segment[76]
TULP1		0,8%	1-2%		Transport across the photo-receptor connecting cilium[37]
USH2A			5%	Usher syndrome	Signaling, photoreceptor development[77, 78]
Total % estimated	~45%	~65%	~50%		

Grey boxes indicate involvement in the above-mentioned disease. In *italic*, brief description of putative function or localization of the gene; in **bold**, associations that were identified in this thesis. *, percentages of genes involved in arCRD and arRP are a rough estimate. ǂ, percentages of genes involved in arLCA are calculated on the basis of publications up to 2008, except for SPATA7.[21] ad, autosomal dominant; ar, autosomal recessive; BBS, Bardet-Biedl syndrome; CCSD, congenital cone-rod synaptic disorder (this thesis); CRD, cone-rod dystrophy; CSNB, congenital stationary night blindness; ESC, enhanced S-cone syndrome; EOSRD, early onset severe retinal dystrophy; FA, fundus albipunctatus; JBTS, Joubert syndrome; LCA, Leber congenital amaurosis; MD, macular degeneration; RP, retinitis pigmentosa; RPA, retinitis punctata albescens; SLSN, Senior-Løken syndrome; STGD1, Stargardt disease. *(Information derived from RetNet™ (Retinal Information Network; http://www.sph.uth.tmc.edu/Retnet), den Hollander et al. 2008,[21] Berger et al. 2010,[17] and den Hollander et al. 2010[79])*

HOMOZYGOSITY MAPPING

The human genome consists of 23 chromosome pairs: one set from the mother and one set from the father. The total of 46 chromosomes consists of ~3.200.000.000 basepairs, in which ~25.000 genes are encoded. The human genome is 99.5% identical between people, and the 0.5% variation is created by numerous insertions or deletions, by thousands of copy number variations, and by about 3 million single nucleotide polymorphisms (SNPs).[80, 81] A SNP is a nucleotide that can differ between people (for example, a guanine (G) in one person and an adenine (A) in another person) in most cases without causing an obvious defect. As SNPs can be found throughout the entire genome, they can be used for linkage analysis or for the detection of homozygous regions. In contrast, a change in nucleotide is called a mutation only when it has a deleterious effect on the protein function. Analysis of all coding regions ('the exome') of a human genome revealed that a person may carry ~1.500 possible pathogenic variants.[81]

In autosomal recessive diseases, a person needs to carry mutations in both copies of one gene in order to become affected. These can be either two identical mutations, called homozygous mutations, as well as two different mutations, called compound heterozygous mutations. Compound heterozygous mutations are most frequently found in patients in so-called mixed populations; i.e. populations in which people are moving easily, and in which people can choose a partner without clear restrictions (Figure 6A). In an isolated population, people tend to stay in the same place, and/or the choice for a partner is based for example on religious or cultural restrictions. In such a society people have a higher chance to marry someone that is (distantly) related, and therefore their children, when affected by an autosomal recessive disease, mostly carry a homozygous defect (Figure 6B).[82-84] Examples of (relatively) isolated populations are island populations, places with a low percentage of migration, or a secluded population due to religious, cultural or language reasons.

Approximately 35% of mostly Dutch and German patients affected by a retinal dystrophy carry a homozygous mutation (F.P.M. Cremers, personal communication 2010), and a similar percentage was detected in several genetic studies on autosomal recessive diseases in western European populations.[85-89] The relatively high percentage of homozygous mutations in these populations may implicate that several western European populations are a combination of mixed and isolated populations.

Homozygous mutations may be detected by a method, named homozygosity mapping, as follows. When a mutation is passed on to the next generation, only part of the

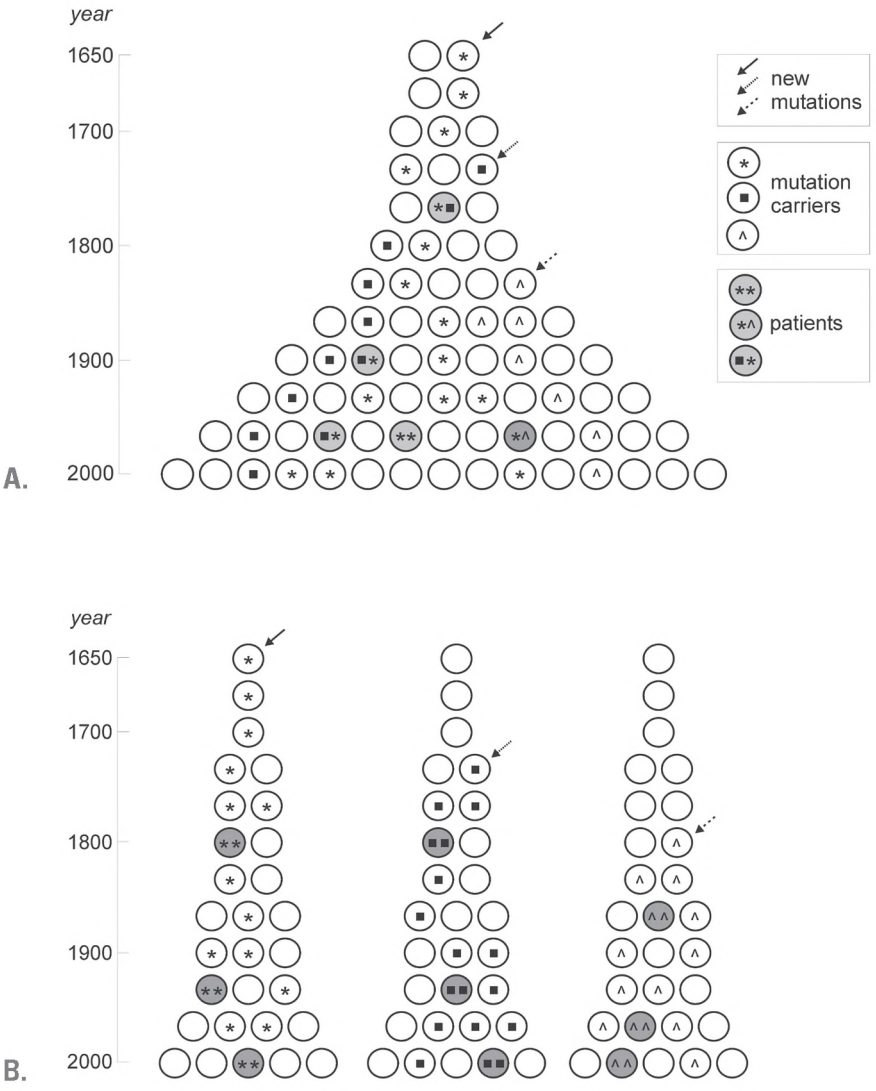

FIGURE 6. Schematic overview of mutation distribution in two types of populations over several generations.

A. Mixed population: mutations enter the population by *de novo* occurrence or by the immigration of an individual from another population. As there is complete mixture of variants, they can appear identical (homozygous; two identical mutation symbols), but will often appear non-identical (compound heterozygous; two different mutation symbols) in an affected individual.
B. The chance for one ancestral mutation to be present on both alleles (homozygous) in one person is higher in a relatively isolated population in which parents of a patient are likely to be distantly related.

surrounding chromosomal region will be passed on as well. A combination of alleles that a person inherits is called the 'haplotype'. The length and position of the original parental haplotype that will be present in a child depends on the positions of recombination during meiosis. Recombination occurs in reproductive cells during meiosis and implies the physical exchange between the two homologous chromosomes at random positions. As a result a person's genome is a mosaic of the preceding ancestors. Figure 7A illustrates the transfer of a mutation through different generations in a first-cousin marriage. The mutation, present in the great-grandmother, was passed on to the next generations, including part of the surrounding genomic region. When the ancestral mutation is passed on via father and mother to their child, part of the original haplotype is still present, and in the child will be present as an identical-by-descent (i.e. homozygous) region. In a first-cousin family the size of a homozygous segment that harbors the mutation is on average 26 Mb.[90] When an ancestor who carried the mutation lived several generations ago, more recombinations took place, and as a result the homozygous region containing the mutation in a patient will be smaller (Figure 7B).

A homozygous region can be detected by using genome-wide genotyping arrays on which thousands of SNPs in the DNA of a person can be determined. When a SNP on one allele is identical to the SNP at the other allele, the SNP is called homozygous. A stretch of homozygous SNPs can indicate that this region may originate from a common ancestor. Stretches of DNA can be homozygous by chance as well, for example in genomic regions that have a limited haplotype diversity, in a centromeric region, or in regions with little historical recombination (i.e. haplotype blocks).[91] Nevertheless, homozygosity mapping has been proven to be an effective method to identify the disease locus and, subsequently, the genetic defect in patients affected by autosomal recessive retinal diseases.[52, 55, 92-94]

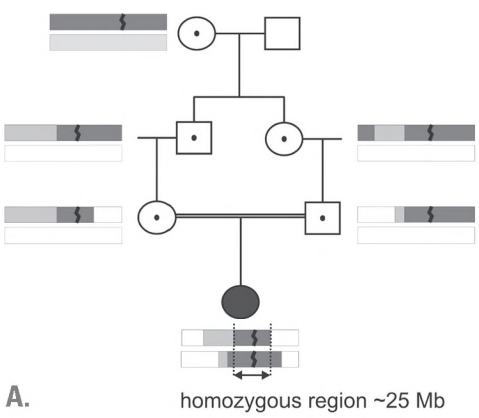

FIGURE 7. Schematic presentation of the inheritance of an ancestral chromosome that harbors a mutation. Every generation the original ancestral chromosome becomes 'smaller' due to recombination between homologous chromosomes.

A. In consanguineous families, the mutation is likely inherited from a recent common ancestor. Because the limited number of generations between the ancestor and the patient, a large fraction of the ancestral haplotype is present in both chromosome copies of the patient, resulting in a relatively large homozygous region.[90]

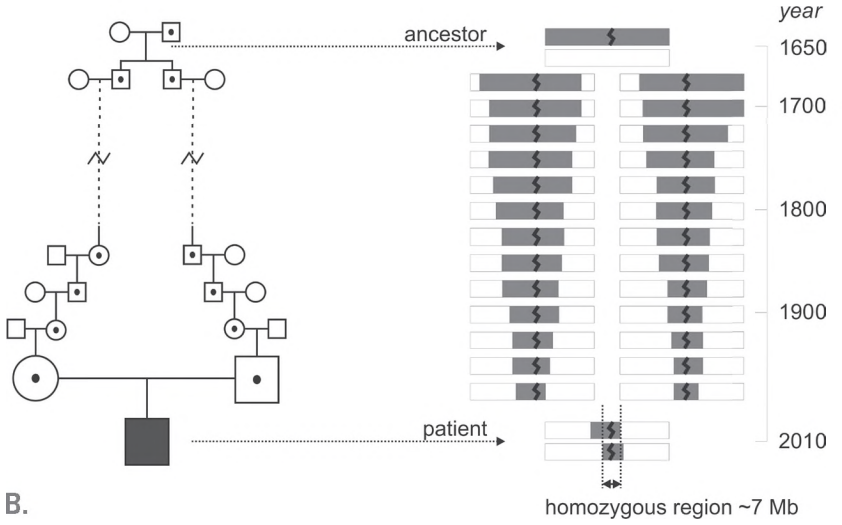

B. When the ancestor who carried the mutation lived many generations ago, only a small fraction of the ancestral haplotype will be present on both chromosome copies of a patient, and therefore the homozygous region in such a patient will be relatively small.

AIM OF THIS THESIS

The aim of this thesis was to identify the genetic defect underlying retinal dystrophy in patients affected by retinal dystrophy; mainly by cone-rod dystrophy or retinitis pigmentosa. The localization of the genetic defect was detected by using high density genome-wide SNP arrays, followed by homozygosity mapping or linkage analysis.

Chapter 2 summarizes all mutations that were identified using high-throughput SNP array analysis followed by homozygosity mapping in 108 CRD patients, and shows the detailed clinical features of the CRD patients in whom a mutation was identified.

Chapters 3 presents a detailed description of the phenotype that results from a *CABP4* p.Arg216X mutation, as the detailed clinical examinations, including 15Hz electroretinogram measurements, in both siblings led to the characterization of a distinctive phenotype that is associated with a defect in processes in the photoreceptor synapse. In **chapter 4**, a family is presented in which we identified mutations in *CEP290* and *MERTK* by linkage analysis. A novel nonsense mutation in *CEP290* appeared to have a hypomorphic character, and led to a relatively mild phenotype, coined early onset severe retinal dystrophy. A third patient from the same family, affected by Leber congenital amaurosis, carried the same *CEP290* mutations, and a heterozygous mutation in *MERTK*, which may act as modifier allele.

Chapter 5A present the discovery of a new gene involved in retinitis pigmentosa; the *EYS* gene. In **chapters 5B and 5C** the prevalence of *EYS* mutations is determined in a Dutch and Israelian/Palestinian cohort, respectively, and the characteristics of the *EYS*-associated phenotype are described.

A general discussion on the genetics of retinal dystrophies is given in **chapter 6**.

REFERENCES

1. Polyak S. The vertebrate visual system. Chicago, IL: University of Chicago Press; 1957

2. Dryja TP, McGee TL, Reichel E, et al. A point mutation of the rhodopsin gene in one form of retinitis pigmentosa. Nature. 1990;343:364-366.

3. Cremers FPM, van de Pol DJ, van Kerkhoff LP, Wieringa B, Ropers HH. Cloning of a gene that is rearranged in patients with choroideraemia. Nature. 1990;347:674-677.

4. Bainbridge JW, Smith AJ, Barker SS, et al. Effect of gene therapy on visual function in Leber's congenital amaurosis. N Engl J Med. 2008;358:2231-2239.

5. Maguire AM, Simonelli F, Pierce EA, et al. Safety and efficacy of gene transfer for Leber's congenital amaurosis. N Engl J Med. 2008;358:2240-2248.

6. Cideciyan AV, Hauswirth WW, Aleman TS, et al. Human RPE65 gene therapy for Leber congenital amaurosis: persistence of early visual improvements and safety at 1 year. Hum Gene Ther. 2009;20:999-1004.

7. Maguire AM, High KA, Auricchio A, et al. Age-dependent effects of RPE65 gene therapy for Leber's congenital amaurosis: a phase 1 dose-escalation trial. Lancet. 2009;374:1597-1605.

8. Rattner A, Sun H, Nathans J. Molecular genetics of human retinal disease. Annu Rev Genet. 1999;33:89-131.

9. Henkind P, Hansen RI, Szalay J. Ocular circulation. Physiology of the human eye and visual system. New York: Harper & Row; 1979:98-155.

10. Lamb TD. Evolution of vertebrate retinal photoreception. Philos Trans R Soc Lond B Biol Sci. 2009;364:2911-2924.

11. Yau KW. Phototransduction mechanism in retinal rods and cones. The Friedenwald Lecture. Invest Ophthalmol Vis Sci. 1994;35:9-32.

12. Jindrova H. Vertebrate phototransduction: activation, recovery, and adaptation. Physiol Res. 1998;47:155-168.

13. Burns ME, Baylor DA. Activation, deactivation, and adaptation in vertebrate photoreceptor cells. Annu Rev Neurosci. 2001;24:779-805.

14. Travis GH, Golczak M, Moise AR, Palczewski K. Diseases caused by defects in the visual cycle: retinoids as potential therapeutic agents. Annu Rev Pharmacol Toxicol. 2007;47:469-512.

15. Mata NL, Radu RA, Clemmons RC, Travis GH. Isomerization and oxidation of vitamin a in cone-dominant retinas: a novel pathway for visual-pigment regeneration in daylight. Neuron. 2002;36:69-80.

16. Wässle H. Parallel processing in the mammalian retina. Nat Rev Neurosci. 2004;5:747-757.

17. Berger W, Kloeckener-Gruissem B, Neidhardt J. The molecular basis of human retinal and vitreoretinal diseases. Prog Retin Eye Res. 2010:in press.

18. Hamel CP. Cone rod dystrophies. Orphanet J Rare Dis. 2007;2:7-14.

19. Michaelides M, Hardcastle AJ, Hunt DM, Moore AT. Progressive cone and cone-rod dystrophies: phenotypes and underlying molecular genetic basis. Surv Ophthalmol. 2006;51:232-258.

20. Szlyk JP, Fishman GA, Alexander KR, Peachey NS, Derlacki DJ. Clinical subtypes of cone-rod dystrophy. Arch Ophthalmol. 1993;111:781-788.

21. den Hollander AI, Roepman R, Koenekoop RK, Cremers FPM. Leber congenital amaurosis: genes, proteins and disease mechanisms. Prog Retin Eye Res. 2008;27:391-419.

22. Hanein S, Perrault I, Gerber S, et al. Leber congenital amaurosis: comprehensive survey of the genetic heterogeneity, refinement of the clinical definition, and genotype-phenotype correlations as a strategy for molecular diagnosis. Hum Mutat. 2004;23:306-317.

23. Koenekoop RK. An overview of Leber congenital amaurosis: a model to understand human retinal development. Surv Ophthalmol. 2004;49:379-398.

24. Hamel C. Retinitis pigmentosa. Orphanet J Rare Dis. 2006;1:40-52.

25. Hartong DT, Berson EL, Dryja TP. Retinitis pigmentosa. Lancet. 2006;368:1795-1809.

26. Szlyk JP, Seiple W, Fishman GA, Alexander KR, Grover S, Mahler CL. Perceived and actual performance of daily tasks: relationship to visual function tests in individuals with retinitis pigmentosa. Ophthalmology. 2001;108:65-75.

27. Buch H, Vinding T, La Cour M, Appleyard M, Jensen GB, Nielsen NV. Prevalence and causes of visual impairment and blindness among 9980 Scandinavian adults: the Copenhagen City Eye Study. Ophthalmology. 2004;111:53-61.

28. den Hollander AI, Black A, Bennett J, Cremers FPM. Lighting a candle in the dark: advances in genetics and gene therapy of recessive retinal dystrophies. J Clin Invest. Submitted.

29. Dryja TP, Finn JT, Peng YW, McGee TL, Berson EL, Yau KW. Mutations in the gene encoding the alpha subunit of the rod cGMP-gated channel in autosomal recessive retinitis pigmentosa. Proc Natl Acad Sci U S A. 1995;92:10177-10181.

30. Huang SH, Pittler SJ, Huang X, Oliveira L, Berson EL, Dryja TP. Autosomal recessive retinitis pigmentosa caused by mutations in the alpha subunit of rod cGMP phosphodiesterase. Nat Genet. 1995;11:468-471.

31. Marlhens F, Bareil C, Griffoin JM, et al. Mutations in RPE65 cause Leber's congenital amaurosis. Nat Genet. 1997;17:139-141.

32. Allikmets R, Singh N, Sun H, et al. A photoreceptor cell-specific ATP-binding transporter gene (ABCR) is mutated in recessive Stargardt macular dystrophy. Nat Genet. 1997;15:236-246.

33. den Hollander AI, van Driel MA, de Kok YJM, et al. Isolation and mapping of novel candidate genes for retinal disorders using suppression subtractive hybridization. Genomics. 1999;58:240-249.

34. Maw MA, Corbeil D, Koch J, et al. A frameshift mutation in prominin (mouse)-like 1 causes human retinal degeneration. Hum Mol Genet. 2000;9:27-34.

35. Farrar GJ, Kenna P, Jordan SA, et al. A three-base-pair deletion in the peripherin-RDS gene in one form of retinitis pigmentosa. Nature. 1991;354:478-480.

36. McLaughlin ME, Ehrhart TL, Berson EL, Dryja TP. Mutation spectrum of the gene encoding the beta subunit of rod phosphodiesterase among patients with autosomal recessive retinitis pigmentosa. Proc Natl Acad Sci U S A. 1995;92:3249-3253.

37. Hagstrom SA, North MA, Nishina PL, Berson EL, Dryja TP. Recessive mutations in the gene encoding the tubby-like protein TULP1 in patients with retinitis pigmentosa. Nat Genet. 1998;18:174-176.

38. Hartong DT, Dange M, McGee TL, Berson EL, Dryja TP, Colman RF. Insights from retinitis pigmentosa into the roles of isocitrate dehydrogenases in the Krebs cycle. Nat Genet. 2008;40:1230-1234.

39. Sun H, Molday RS, Nathans J. Retinal stimulates ATP hydrolysis by purified and reconstituted ABCR, the photoreceptor-specific ATP-binding cassette transporter responsible for Stargardt disease. J Biol Chem. 1999;274:8269-8281.

40. Sun H, Nathans J. Stargardt's ABCR is localized to the disc membrane of retinal rod outer segments. Nat Genet. 1997;17:15-16.

41. Parry DA, Toomes C, Bida L, et al. Loss of the metalloprotease ADAM9 leads to cone-rod dystrophy in humans and retinal degeneration in mice. Am J Hum Genet. 2009;84:683-691.

42. van der Spuy J, Chapple JP, Clark BJ, Luthert PJ, Sethi CS, Cheetham ME. The Leber congenital amaurosis gene product AIPL1 is localized exclusively in rod photoreceptors of the adult human retina. Hum Mol Genet. 2002;11:823-831.

43. Ramamurthy V, Roberts M, van den Akker F, Niemi G, Reh TA, Hurley JB. AIPL1, a protein implicated in Leber's congenital amaurosis, interacts with and aids in processing of farnesylated proteins. Proc Natl Acad Sci U S A. 2003;100:12630-12635.

44. Akey DT, Zhu X, Dyer M, et al. The inherited blindness associated protein AIPL1 interacts with the cell cycle regulator protein NUB1. Hum Mol Genet. 2002;11:2723-2733.

45. Haeseleer F, Imanishi Y, Maeda T, et al. Essential role of Ca2+-binding protein 4, a Cav1.4 channel regulator, in photoreceptor synaptic function. Nat Neurosci. 2004;7:1079-1087.

46. Sayer JA, Otto EA, O'Toole JF, et al. The centrosomal protein nephrocystin-6 is mutated in Joubert syndrome and activates transcription factor ATF4. Nat Genet. 2006;38:674-681.

47. Tuson M, Marfany G, Gonzalez-Duarte R. Mutation of CERKL, a novel human ceramide kinase gene, causes autosomal recessive retinitis pigmentosa (RP26). Am J Hum Genet. 2004;74:128-138.

48. Dhallan RS, Macke JP, Eddy RL, et al. Human rod photoreceptor cGMP-gated channel: amino acid sequence, gene structure, and functional expression. J Neurosci. 1992;12:3248-3256.

49. Korschen HG, Beyermann M, Muller F, et al. Interaction of glutamic-acid-rich proteins with the cGMP signalling pathway in rod photoreceptors. Nature. 1999;400:761-766.

50. Pellikka M, Tanentzapf G, Pinto M, et al. Crumbs, the Drosophila homologue of human CRB1/RP12, is essential for photoreceptor morphogenesis. Nature. 2002;416:143-149.

51. Akagi T, Mandai M, Ooto S, et al. Otx2 homeobox gene induces photoreceptor-specific phenotypes in cells derived from adult iris and ciliary tissue. Invest Ophthalmol Vis Sci. 2004;45:4570-4575.

52. Collin RWJ, Littink KW, Klevering BJ, et al. Identification of a 2 Mb human ortholog of Drosophila eyes shut/spacemaker that is mutated in patients with retinitis pigmentosa. Am J Hum Genet. 2008;83:594-603.

53. Abd El-Aziz MM, Barragan I, O'Driscoll CA, et al. EYS, encoding an ortholog of Drosophila spacemaker, is mutated in autosomal recessive retinitis pigmentosa. Nat Genet. 2008;40:1285-1287.

54. Duda T, Venkataraman V, Goraczniak R, Lange C, Koch KW, Sharma RK. Functional consequences of a rod outer segment membrane guanylate cyclase (ROS-GC1) gene mutation linked with Leber's congenital amaurosis. Biochemistry. 1999;38:509-515.

55. den Hollander AI, Koenekoop RK, Mohamed MD, et al. Mutations in LCA5, encoding the ciliary protein lebercilin, cause Leber congenital amaurosis. Nat Genet. 2007;39:889-895.

56. Xue L, Gollapalli DR, Maiti P, Jahng WJ, Rando RR. A palmitoylation switch mechanism in the regulation of the visual cycle. Cell. 2004;117:761-771.

57. Gal A, Li Y, Thompson DA, et al. Mutations in MERTK, the human orthologue of the RCS rat retinal dystrophy gene, cause retinitis pigmentosa. Nat Genet. 2000;26:270-271.

58. Cheng H, Khanna H, Oh EC, Hicks D, Mitton KP, Swaroop A. Photoreceptor-specific nuclear receptor NR2E3 functions as a transcriptional activator in rod photoreceptors. Hum Mol Genet. 2004;13:1563-1575.

59. Peng GH, Ahmad O, Ahmad F, Liu J, Chen S. The photoreceptor-specific nuclear receptor Nr2e3 interacts with Crx and exerts opposing effects on the transcription of rod versus cone genes. Hum Mol Genet. 2005;14:747-764.

60. Mitton KP, Swain PK, Khanna H, Dowd M, Apel IJ, Swaroop A. Interaction of retinal bZIP transcription factor NRL with Flt3-interacting zinc-finger protein Fiz1: possible role of Fiz1 as a transcriptional repressor. Hum Mol Genet. 2003;12:365-373.

61. Yoshida S, Mears AJ, Friedman JS, et al. Expression profiling of the developing and mature Nrl-/- mouse retina: identification of retinal disease candidates and transcriptional regulatory targets of Nrl. Hum Mol Genet. 2004;13:1487-1503.

62. MacLaren RE, Pearson RA, MacNeil A, et al. Retinal repair by transplantation of photoreceptor precursors. Nature. 2006;444:203-207.

63. Zangerl B, Goldstein O, Philp AR, et al. Identical mutation in a novel retinal gene causes progressive rod-cone degeneration in dogs and retinitis pigmentosa in humans. Genomics. 2006;88:551-563.

64. Yang Z, Chen Y, Lillo C, et al. Mutant prominin 1 found in patients with macular degeneration disrupts photoreceptor disk morphogenesis in mice. J Clin Invest. 2008;118:2908-2916.

65. Fong SL, Liou GI, Landers RA, et al. Characterization, localization, and biosynthesis of an interstitial retinol-binding glycoprotein in the human eye. J Neurochem. 1984;42:1667-1676.

66. Friedman JS, Chang B, Kannabiran C, et al. Premature truncation of a novel protein, RD3, exhibiting subnuclear localization is associated with retinal degeneration. Am J Hum Genet. 2006;79:1059-1070.

67. Haeseleer F, Jang GF, Imanishi Y, et al. Dual-substrate specificity short chain retinol dehydrogenases from the vertebrate retina. J Biol Chem. 2002;277:45537-45546.

68. Chen P, Hao W, Rife L, et al. A photic visual cycle of rhodopsin regeneration is dependent on RGR. Nat Genet. 2001;28:256-260.

69. Nathans J, Hogness DS. Isolation and nucleotide sequence of the gene encoding human rhodopsin. Proc Natl Acad Sci U S A. 1984;81:4851-4855.

70. Sparkes RS, Heinzmann C, Goldflam S, et al. Assignment of the gene (RLBP1) for cellular retinaldehyde-binding protein (CRALBP) to human chromosome 15q26 and mouse chromosome 7. Genomics. 1992;12:58-62.

71. Liu Q, Zhou J, Daiger SP, et al. Identification and subcellular localization of the RP1 protein in human and mouse photoreceptors. Invest Ophthalmol Vis Sci. 2002;43:22-32.

72. Liu Q, Lyubarsky A, Skalet JH, Pugh Jr. EN, Pierce EA. RP1 is required for the correct stacking of outer segment discs. Invest Ophthalmol Vis Sci. 2003;44:4171-4183.

73. Moiseyev G, Chen Y, Takahashi Y, Wu BX, Ma JX. RPE65 is the isomerohydrolase in the retinoid visual cycle. Proc Natl Acad Sci U S A. 2005;102:12413-12418.

74. Castagnet P, Mavlyutov T, Cai Y, Zhong F, Ferreira P. RPGRIP1s with distinct neuronal localization and biochemical properties associate selectively with RanBP2 in amacrine neurons. Hum Mol Genet. 2003;12:1847-1863.

75. Yamaki K, Tsuda M, Kikuchi T, Chen KH, Huang KP, Shinohara T. Structural organization of the human S-antigen gene. cDNA, amino acid, intron, exon, promoter, in vitro transcription, retina, and pineal gland. J Biol Chem. 1990;265:20757-20762.

76. Wang H, den Hollander AI, Moayedi Y, et al. Mutations in SPATA7 cause Leber congenital amaurosis and juvenile retinitis pigmentosa. Am J Hum Genet. 2009;84:380-387.

77. Reiners J, van Wijk E, Marker T, et al. Scaffold protein harmonin (USH1C) provides molecular links between Usher syndrome type 1 and type 2. Hum Mol Genet. 2005;14:3933-3943.

78. van Wijk E, Kersten FF, Kartono A, et al. Usher syndrome and Leber congenital amaurosis are molecularly linked via a novel isoform of the centrosomal ninein-like protein. Hum Mol Genet. 2009;18:51-64.

79. den Hollander AI, Black A, Bennett J, Cremers FPM. Lighting a candle in the dark: advances in genetics and gene therapy of recessive retinal dystrophies. J Clin Invest. 2010:in press.

80. Levy S, Sutton G, Ng PC, et al. The diploid genome sequence of an individual human. PLoS Biol. 2007;5:e254.

81. Ng PC, Levy S, Huang J, et al. Genetic variation in an individual human exome. PLoS Genet. 2008;4:e1000160.

82. McQuillan R, Leutenegger AL, Abdel-Rahman R, et al. Runs of homozygosity in European populations. Am J Hum Genet. 2008;83:359-372.

83. Yzer S, van den Born LI, Schuil J, et al. A Tyr368His RPE65 founder mutation is associated with variable expression and progression of early onset retinal dystrophy in 10 families of a genetically isolated population. J Med Genet. 2003;40:709-713.

84. den Hollander AI, ten Brink JB, de Kok YJM, et al. Mutations in a human homologue of Drosophila crumbs cause retinitis pigmentosa (RP12). Nat Genet. 1999;23:217-221.

85. Sandoval N, Platzer M, Rosenthal A, et al. Characterization of ATM gene mutations in 66 ataxia telangiectasia families. Hum Mol Genet. 1999;8:69-79.

86. Krone N, Braun A, Roscher AA, Knorr D, Schwarz HP. Predicting phenotype in steroid 21-hydroxylase deficiency? Comprehensive genotyping in 155 unrelated, well defined patients from southern Germany. J Clin Endocrinol Metab. 2000;85:1059-1065.

87. Wissinger B, Gamer D, Jagle H, et al. CNGA3 mutations in hereditary cone photoreceptor disorders. Am J Hum Genet. 2001;69:722-737.

88. Roux AF, Faugere V, Le Guedard S, et al. Survey of the frequency of USH1 gene mutations in a cohort of Usher patients shows the importance of cadherin 23 and protocadherin 15 genes and establishes a detection rate of above 90%. J Med Genet. 2006;43:763-768.

89. Yzer S, Leroy BP, De Baere E, et al. Microarray-based mutation detection and phenotypic characterization of patients with Leber congenital amaurosis. Invest Ophthalmol Vis Sci. 2006;47:1167-1176.

90. Woods CG, Cox J, Springell K, et al. Quantification of homozygosity in consanguineous individuals with autosomal recessive disease. Am J Hum Genet. 2006;78:889-896.

91. Wall JD, Pritchard JK. Haplotype blocks and linkage disequilibrium in the human genome. Nat Rev Genet. 2003;4:587-597.

92. den Hollander AI, Lopez I, Yzer S, et al. Identification of novel mutations in patients with Leber congenital amaurosis and juvenile RP by genome-wide homozygosity mapping with SNP microarrays. Invest Ophthalmol Vis Sci. 2007;48:5690-5698.

93. den Hollander AI, Koenekoop RK, Yzer S, et al. Mutations in the CEP290 (NPHP6) gene are a frequent cause of Leber congenital amaurosis. Am J Hum Genet. 2006;79:556-561.

94. Thiadens AA, den Hollander AI, Roosing S, et al. Homozygosity mapping reveals PDE6C mutations in patients with early-onset cone photoreceptor disorders. Am J Hum Genet. 2009;85:240-247.

Adapted from: *Investigative Ophthalmology & Visual Science.* June 2010

Karin W. Littink,[1,2,13] Robert K. Koenekoop,[3,13] L. Ingeborgh van den Born,[1] Rob W.J. Collin,[2,4,5] Luminita Moruz,[2,6] Joris A. Veltman,[2,7] Susanne Roosing,[2] Marijke N. Zonneveld,[1,2] Amer Omar,[3] Mahshad Darvish,[3] Irma Lopez,[3] Hester Y. Kroes,[8] Maria M. van Genderen,[9] Carel B. Hoyng,[5] Klaus Rohrschneider,[10] Mary J. van Schooneveld,[11,12] Frans P.M. Cremers,[2,4] Anneke I. den Hollander[2,5]

[1] The Rotterdam Eye Hospital, Rotterdam, The Netherlands; [2] Department of Human Genetics, Radboud University Nijmegen Medical Centre, Nijmegen, The Netherlands; [3] McGill Ocular Genetics Laboratory, Montreal Children's Hospital Research Institute, McGill University Health Centre, Montreal, Canada; [4] Nijmegen Centre for Molecular Life Sciences, Radboud University Nijmegen Medical Centre, Nijmegen, The Netherlands; [5] Department of Ophthalmology, Radboud University Nijmegen Medical Centre, Nijmegen, The Netherlands; [6] Center for Biomembrane Research, Department of Biochemistry and Biophysics, Stockholm University, Stockholm, Sweden; [7] Institute for Genetic and Metabolic Disease, Radboud University Nijmegen Medical Centre, Nijmegen, The Netherlands; [8] Department of Medical Genetics, University Medical Centre Utrecht, Utrecht, The Netherlands; [9] Bartiméus Institute for the Visually Impaired, Zeist, The Netherlands; [10] Department of Ophthalmology, University of Heidelberg, Heidelberg, Germany; [11] Netherlands Institute of Neuroscience, Amsterdam, The Netherlands; [12] Department of Ophthalmology, Academic Medical Centre, Amsterdam, The Netherlands.
[13] These authors contributed equally.

CHAPTER 2

HOMOZYGOSITY MAPPING IN PATIENTS WITH CONE-ROD DYSTROPHY: NOVEL MUTATIONS AND CLINICAL CHARACTERIZATIONS

ABSTRACT

PURPOSE. To determine the genetic defect, and to describe the clinical characteristics in a cohort of mainly non-consanguineous cone-rod dystrophy (CRD) patients.

METHODS. We collected 139 patients diagnosed with CRD. Ninety patients were screened for known mutations in *ABCA4*, and those carrying one or two mutations were excluded from further research. Genome-wide homozygosity mapping was performed in the remaining 108 patients. Known genes associated with autosomal recessive retinal dystrophies located within a homozygous region were screened for mutations. Patients in whom a mutation was detected underwent further ophthalmological examinations.

RESULTS. We identified homozygous sequence variants in eight CRD families, six of which were non-consanguineous. The variants were detected in the following six genes: *ABCA4*, *CABP4*, *CERKL*, *EYS*, *KCNV2*, or *PROM1*. Patients carrying mutations in *ABCA4*, *CERKL* and *PROM1* had typical CRD symptoms, but a variety of retinal appearances on fundoscopy, optical coherence tomography and autofluorescence imaging.

CONCLUSIONS. Homozygosity mapping led to the identification of new mutations in consanguineous as well as in non-consanguineous retinal dystrophy patients. Detailed clinical characterization revealed a variety of retinal appearances, ranging from nearly normal to extensive retinal remodeling, retinal thinning and debris accumulation. Although all patients were initially clinically diagnosed as CRD, the molecular findings led to a reappraisal of the clinical diagnosis in patients carrying mutations in *EYS*, *CABP4* and *KCNV2*.

INTRODUCTION

Cone-rod dystrophies (CRDs) belong to a heterogeneous group of inherited retinal dystrophies, characterized by the primary dysfunction or loss of cone photoreceptors followed by the dysfunction or loss of rod photoreceptors. The diagnosis is established by documenting decreased visual acuity – usually noticed during childhood – dyschromatopsia, central scotomas on visual field testing and an electroretinogram (ERG) that shows more severely reduced cone- than rod responses.[1] The clinical course involves progressive loss of central vision, followed by peripheral visual field loss and progressive nyctalopia as more rod photoreceptors become involved in the disease process, and eventually may lead to complete blindness. CRD often presents as an isolated disease, but can be part of a syndrome as well, as in Bardet-Biedl syndrome or Jalili syndrome.[2,3] Isolated CRD can be inherited as an autosomal recessive, autosomal dominant or X-linked trait, and is genetically heterogeneous. Currently, autosomal recessive CRD (arCRD) is associated with mutations in five genes, of which *ABCA4* is the major contributing gene (40%).[4-7] The other four genes (*ADAM9*, *CERKL*, *PROM1*, and *RPGRIP1*) all account for only few cases (1-2% each).[8-11]

Autosomal recessive disorders such as CRD can be caused by homozygous or by compound heterozygous mutations. Homozygous mutations are most frequently detected in patients of consanguineous parents, or in patients from relatively isolated populations, where the chance for the parents to have a common ancestor is relatively high. However, homozygous mutations are also detected in patients of non-consanguineous unions, and based on several genetic studies in large cohorts of patients with autosomal recessive diseases from western European countries, it is estimated that ~35% of those patients carry their mutation homozygously.[12-16] A homozygous mutation is likely to reside within a homozygous region that is detectable with a high resolution single nucleotide polymorphism (SNP) array.[17,18] Mapping of these homozygous regions (homozygosity mapping) may lead to the identification of the genetic defect both in consanguineous and in non-consanguineous patients, as shown as proof-of-principle in patients with autosomal recessive kidney diseases,[19] and as a successful method for the detection of new disease genes,[20-23] and new mutations in known genes implicated in retinal dystrophies.[24]

The goal of this study was to identify and map homozygous regions in a large cohort of CRD patients, mainly born of non-consanguineous marriages, and to subsequently identify the causal mutations. Using this approach, we identified eight genetic variants, of which seven were novel, in four families and four sporadic patients, respectively. All patients carrying disease-causing mutations were clinically re-evaluated.

PATIENTS AND METHODS

Patients

A total of 126 probands and 13 affected siblings diagnosed as or suspected to have autosomal recessive or isolated CRD were included in this study by ophthalmologists from the Netherlands (LIvdB, MMvG, CBH, MJvS), Germany (KR) and Canada (RKK). The study was approved by the ethical review board of the participating centers, and all patients signed an informed consent adhering to the tenets of the Declaration of Helsinki. After discovering the genetic defect clinical data were retrospectively reviewed, and patients were invited for ophthalmological examination by their own ophthalmologist. Clinical evaluation included best-corrected projected Snellen visual acuity, objective refractive error after cycloplegia, biomicroscopy, and fundoscopy. Visual fields were assessed using Goldmann kinetic perimetry (targets V-4e and I-4e). Color vision was tested using the American Optical Hardy-Rand-Rittler Test (AO-HRR), the Farnsworth D-15 Panel (saturated and desaturated) or the Ishihara color plates. Spectral domain optical coherence tomography (OCT) and fundus autofluorescence (FAF) imaging (Spectralis, Heidelberg Engineering, Heidelberg, Germany) were performed in four patients. Fundus photographs were made in all patients.

Homozygosity mapping

Blood samples for molecular genetic testing were obtained from all probands and affected family members. Total genomic DNA was extracted from leukocytes by a standard salting out procedure.[25] DNA samples of 90 probands, mainly from the Netherlands and Germany were screened for known mutations in *ABCA4* by the *ABCA4* arrayed-primer extension (APEX) microarray (Asper Ophthalmics, Tartu, Estonia).[26] The 46 probands and 13 siblings who did not carry known mutations in *ABCA4*, were genotyped on the GeneChip Mapping 250K *Nsp*I array (Affymetrix, Santa Clara, CA), containing 262,000 SNPs. Forty-nine probands, mainly from eastern Canada, were included in the study in a later stage, and were not prescreened for known mutations in *ABCA4*. These samples were genotyped on the GeneChip Genome-Wide Human SNP Array 6.0 (Affymetrix), containing 906,600 polymorphic SNPs. Array experiments were performed according to protocols provided by the manufacturer. For both array platforms, genotypes were called by Genotype Console software (Affymetrix). For 250K-analyzed samples, the default confidence threshold was adjusted to 0.3 for samples with a quality control value of <93%. All samples analyzed on the 6.0 array had a quality control value of >93%, and for those samples default settings were used. Regions of homozygosity were determined by PLINK software,[27] using a sliding window of 50 SNPs, and allowing 2 heterozygous SNPs

(miscalls) and 10 missing SNPs (no-calls) per window. Because the 250K and 6.0 arrays contain different SNP densities, we defined regions to be homozygous when they contained 200 or more consecutive homozygous SNPs on the 250K array and 600 or more consecutive homozygous SNPs on the 6.0 array. The minimal length of the regions appeared to be on average ~3 Mb.

Analysis of homozygous regions

Homozygous regions were ranked based on the number of SNPs. SNP positions were derived from the UCSC human genome browser build hg18, March 2006 (http://genome.ucsc.edu/). All arCRD and autosomal dominant CRD (adCRD) genes residing in a homozygous region were selected for mutation analysis. We also analyzed all autosomal recessive retinal dystrophy genes (derived from RetNet: www.sph.uth.tmc.edu/Retnet/) residing in the six largest homozygous regions of each patient or, in case of multiple affected siblings, in the six largest homozygous regions shared by the siblings. Finally, we determined overlap of the detected homozygous regions with known, published retinal dystrophy loci (RetNet).

Sequence analysis

We selected a total of 15 retinal dystrophy genes for mutation analysis. Six genes known to be associated with arCRD and adCRD were analyzed (arCRD genes: *ABCA4*, 2 patients; *ADAM9*, 3 patients; *CERKL*, 3 patients; *PROM1*, 3 patients. adCRD genes: *SEMA4A*, 2 patients; *UNC119*, 2 patients). In addition, 9 genes associated with other retinal dystrophies were screened (*CABP4*, *KCNV2*, and *RLBP1* each in 2 patients; *C2orf71*, *CNGA1*, *IDH3B*, *RDH5*, *RDS*, and *RP1* each in 1 patient). All coding exons of the selected genes were PCR amplified and analyzed in sense or anti-sense direction on an automated sequencer (BigDye Terminator, ver. 3 on a 3730 DNA analyzer; Applied Biosystems, Inc., Foster City, CA). Primers were designed using Primer3 software.[28] Ethnically matched control individuals were screened for newly identified mutations using the amplification-refractory mutation system (ARMS), or restriction fragment length polymorphism.[29] Primer sequences and PCR conditions are available on request.

RESULTS

Patient cohort and *ABCA4* prescreening

A total of 126 probands and 13 affected siblings, who received a clinical diagnosis of autosomal recessive or isolated CRD were included in this study. This cohort included ten families with two or three affected siblings. Six sporadic CRD patients and one

TABLE 1. **Overview of the genes in which mutations were detected, and the size ranking of the homozygous regions in which these genes resided.**

Retinal dystrophy gene	Patient or family ID (# of siblings)	Consanguinity	Country (origin)	Ranking of region (total # of regions)
ABCA4	W00-409 (3)	Yes	Germany (*Iraq*)	1st (1)
ABCA4	50417	No	Canada (*Pakistan*)	5th (10)
CABP4	W03-008 (2)	No	Netherlands	1st (2)
CERKL	50397	No	Canada	1st (4)
CERKL	51456	No	Canada (*French Canadian*)	1st (2)
EYS	W05-112 (2)	No	Netherlands	2nd (2)
KCNV2	50222	Yes	Netherlands (*Morocco*)	3rd (16)
PROM1	W02-077 (2)	No	Netherlands (Greece)	2nd (6)

#, number; *, in case of multiple affected siblings the mean percentage of the genome that is homozygous was calculated.

CRD family were reported to be consanguineous; the remaining patients and families were reported to be non-consanguineous. Prescreening of 90 probands, using the *ABCA4* APEX microarray (Asper Ophthalmics),[26] revealed mutations in *ABCA4* in 31 patients (1 homozygous, 15 compound heterozygous, and 15 heterozygous), of which 19 patients have been published previously.[4,7] All patients carrying one or two *ABCA4* mutations were excluded from further research.

Homozygosity mapping

A total of 59 CRD samples were analyzed for 262,000 SNPs (250K array) and 49 samples were analyzed for 906,600 SNPs (6.0 array), and homozygous regions were determined. Supplemental Table 1 gives an overview of the number and sizes of the homozygous regions for each individual patient, and the percentage of the total genome that was homozygous.

Significant homozygous regions were identified in 76 (77%) of the non-consanguineous CRD patients. The average number of homozygous regions in these patients was 3 (range: 1-10), and the average total length of homozygous regions was 17.5 Mb (range: 1.7-83.3 Mb), which corresponds to 0.5% (range: 0.1-2.9%) of the genome. Twenty-three (23%) non-consanguineous patients carried no significant homozygous regions. All consanguineous patients carried multiple large homozygous regions;

Size (Mb)	% of genome that is homozygous (regions >~3 Mb)	Homozygous mutations	Reference for mutation
27.8	5.7%*	c.160T>G; p.C54G	Ozgül et al.[31]
4.2	1.5%	c.6729+5_19del15; splice defect	This study
8.9	0.9%*	c.646C>T; p.Arg216X	Littink et al.[36]
28.4	1.6%	c.375C>G; p.C125W	This study
10.6	0.5%	c.847C>T; p.R283X	This study
5.0	0.9%*	c.9468T>A; p.Y3156X	Collin et al.[22]
10.9	7.0%	c.162C>A; p.Y54X	This study
10.4	1.2%*	c.1142-1G>A; splice defect	This study

on average each patient carried 18 (range: 8-27) homozygous regions, with a total length of 204.3 Mb (range: 107.3-332.9 Mb), which corresponds to 7.2% of the genome (range: 3.8-11.7%).

In affected siblings, we compared the individual homozygous regions and included only those regions that were shared between siblings and displayed the same haplotype. In two non-consanguineous families, no shared homozygous regions were present. Five families (of which one consanguineous) had one shared homozygous region and three families had two shared homozygous regions.

Figure 1 presents an overview of all detected homozygous regions sorted by chromosome. In these plots, known retinal dystrophy loci, centromeric regions (which are less likely to recombine), and common homozygous regions are indicated. A common homozygous region was defined as a region of ≥100 homozygous SNPs present in ≥25% of individuals in a cohort of 144 healthy controls.[30] A small number of homozygous regions seem to be shared among four, five or six individuals. However, when excluding patients who carry mutations in another homozygous region, common homozygous regions, and regions close to the centromere, only regions shared among a maximum of three patients remain. This indicates that no major novel locus for arCRD is detected in this cohort by our homozygosity mapping approach.

FIGURE 1. Chromosome plots showing homozygous regions identified in 108 patients with cone-rod dystrophy.

The chromosomal positions are plotted on the x-axis, and the patientnumbers are displayed on the y-axis. Centromeric positions and retinal dystrophy loci are indicated in the lower part of each plot, and the chromosomal position of retinal dystrophy genes are indicated at the top of each plot.
Wxx-xxx numbers in the y-axis designate homozygous regions that are shared by all affected siblings of a family. Black lines indicate homozygous regions in non-consanguineous patients. Dotted lines display homozygous regions in consanguineous patients, and grey lines indicate that a mutation was identified in another homozygous region of that patient. Black star indicates the identification of a mutation at that position.

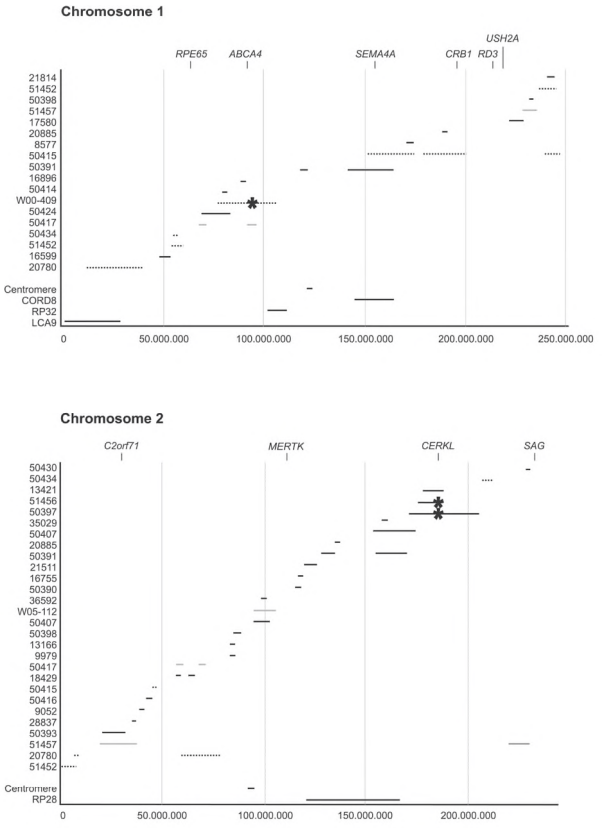

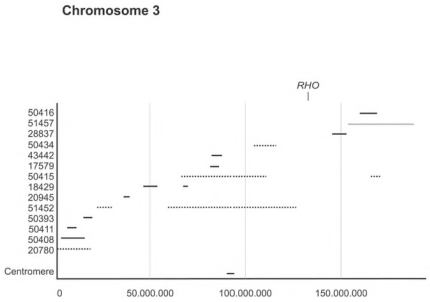
Chromosome 3
RHO
50416
51457
28837
50434
43442
17579
50415
18429
20945
51452
50393
50411
50408
20780
Centromere
0
50.000.000
100.000.000
150.000.000

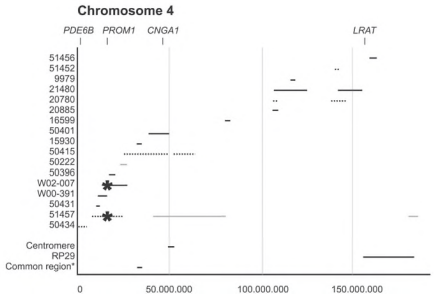
Chromosome 4
PDE6B
PROM1
CNGA1
LRAT
51456
51452
9979
21480
20780
20885
16599
50401
15930
50415
50222
50396
W02-007
W00-391
50431
51457
50434
Centromere
RP29
Common region*
0
50.000.000
100.000.000
150.000.000

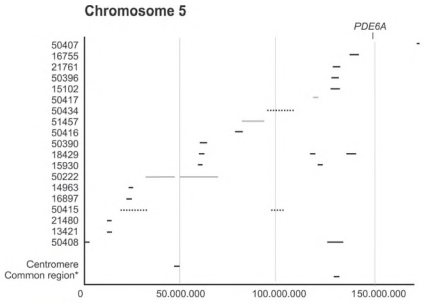
Chromosome 5
PDE6A
50407
16755
21761
50396
15102
50417
50434
51457
50416
50390
18429
15930
50222
14963
16897
50415
21480
13421
50408
Centromere
Common region*
0
50.000.000
100.000.000
150.000.000

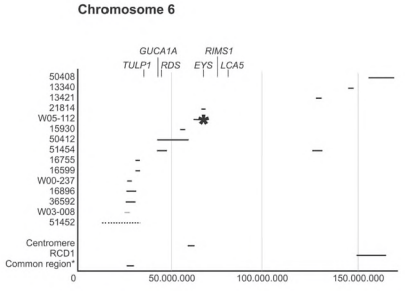
Chromosome 6
GUCA1A
RIMS1
TULP1
RDS
EYS
LCA5
50408
13340
13421
21814
W05-112
15930
50412
51454
16755
16599
W00-237
16896
36592
W03-008
51452
Centromere
RCD1
Common region*
0
50.000.000
100.000.000
150.000.000

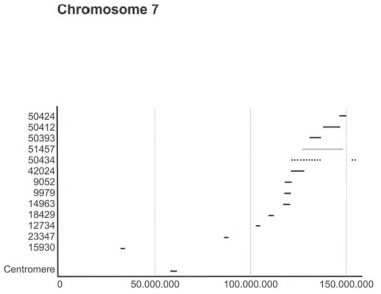
Chromosome 7
50424
50412
50393
51457
50434
42024
9052
9979
14963
18429
12734
23347
15930
Centromere
0
50.000.000
100.000.000
150.000.000

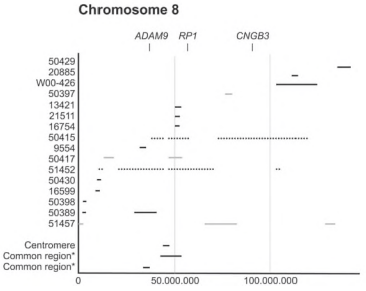
Chromosome 8
ADAM9
RP1
CNGB3
50429
20885
W00-426
50397
13421
21511
16754
50415
9554
50417
51452
50430
16599
50398
50389
51457
Centromere
Common region*
Common region*
0
50.000.000
100.000.000

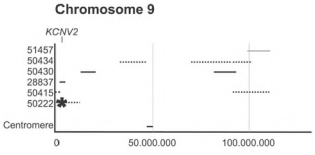
Chromosome 9
KCNV2
51457
50434
50430
28837
50415
50222
Centromere
0
50.000.000
100.000.000

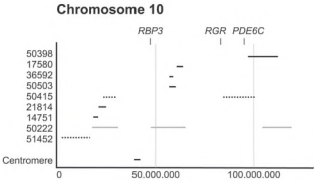
Chromosome 10
RBP3
RGR
PDE6C
50398
17580
36592
50503
50415
21814
14751
50222
51452
Centromere
0
50.000.000
100.000.000

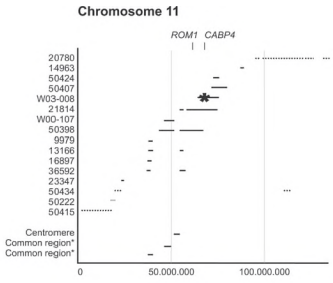
Chromosome 11
ROM1
CABP4
20780
14963
50424
50407
W03-008
21814
W00-107
50398
9979
13166
16897
36592
23347
50434
50222
50415
Centromere
Common region*
Common region*
0
50.000.000
100.000.000

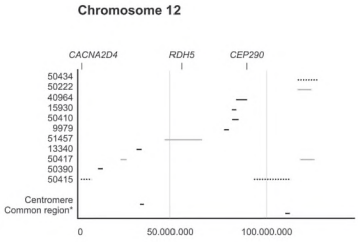
Chromosome 12
CACNA2D4
RDH5
CEP290
50434
50222
40964
15930
50410
9979
51457
13340
50417
50390
50415
Centromere
Common region*
0
50.000.000
100.000.000

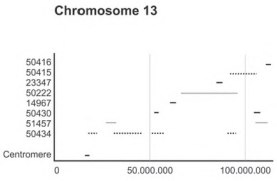
Chromosome 13
50416
50415
23347
50222
14967
50430
51457
50434
Centromere
0
50.000.000
100.000.000

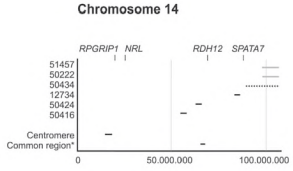
Chromosome 14
RPGRIP1
NRL
RDH12
SPATA7
51457
50222
50434
12734
50424
50416
Centromere
Common region*
0
50.000.000
100.000.000

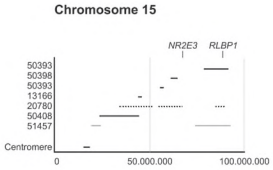
Chromosome 15
NR2E3
RLBP1
50393
50398
50393
13166
20780
50408
51457
Centromere
0
50.000.000
100.000.000

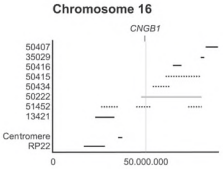
Chromosome 16
CNGB1
50407
35029
50416
50415
50434
50222
51452
13421
Centromere
RP22
0
50.000.000

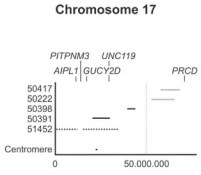
Chromosome 17
PITPNM3
UNC119
AIPL1
GUCY2D
PRCD
50417
50222
50398
50391
51452
Centromere
0
50.000.000

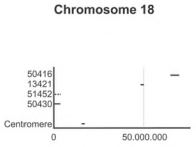
Chromosome 18
50416
13421
51452
50430
Centromere
0
50.000.000

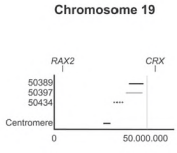
Chromosome 19
RAX2
CRX
50389
50397
50434
Centromere
0
50.000.000

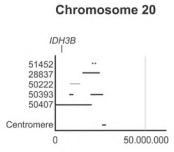
Chromosome 20
IDH3B
51452
28837
50222
50393
50407
Centromere
0
50.000.000

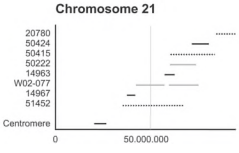
Chromosome 21
20780
50424
50415
50222
14963
W02-077
14967
51452
Centromere
0
50.000.000

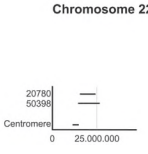
Chromosome 22
20780
50398
Centromere
0
25.000.000

Mutation analysis

Mutation analysis of four arCRD genes (*ABCA4, ADAM9, CERKL* and *PROM1*) in a total of 11 probands (eight sporadic CRD patients and three families) revealed sequence variants in seven of them (five sporadic patients and two families; Table 1). Screening of 9 other retinal dystrophy genes in a total of 12 probands, led to the identification of novel homozygous mutations in one sporadic patient (*KCNV2*), and in one family (*CABP4*) (Table 1).

FIGURE 2. Evolutionary conservation of the three missense variants detected in *ADAM9, CERKL* and *PROM1*. The p.C125 residue in CERKL shows full conservation up to Danio rerio (zebrafish). The p.Q800 in ADAM9 is fully conserved in at least five out of six residues, and the p.S649 residue in PROM1 shows a similar amino acid in six out of seven residues, but both appeared to be non-pathogenic.

White lettered residues on a black background are fully conserved. White letters on a gray background are relatively well-conserved or form a block of similar amino acids. The amino acid sequences are aligned using default settings in Vector NTI software (Invitrogen, Breda, The Netherlands). Protein sequences of CERKL, PROM1 and ADAM9 orthologs were derived from the NCBI database (http://www.ncbi.nlm.nih.gov/homologene). Accession numbers of the protein sequences used for sequence comparison are as follows.

ADAM9:
Homo sapiens, NP_003807.1;
Pan troglodytes, XP_519719;
Canis lupus familiaris, XP_532798.2;
Mus musculus, NP_031430.1;
Rattus norvergicus, NP_001014772.1;
Gallus gallus, NP_001026567.1;
Danio rerio, NP_001107911.1.

CERKL:
Homo sapiens, NP_963842.1;
Pan troglodytes, XP_515955.2;
Canis lupus familiaris, XP_545552.2;
Mus musculus, NP_001041641.1;
Rattus norvergicus, XP_578135.2;
Gallus gallus, XP_421973.2;
Danio rerio, NP_001082943.1.

PROM1:
Homo sapiens, NP_006008.1;
Pan troglodytes, XP_517115.2;
Canis lupus familiaris, XP_545934.2;
Bos taurus, XP_875477.2;
Mus musculus, NP_032961.1;
Gallus gallus, XP_001232165.1;
Danio rerio, NP_001108615.1

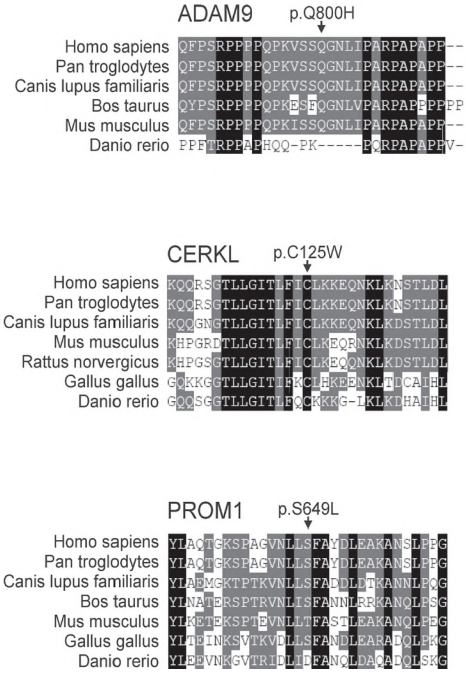

The p.C54G change in *ABCA4* (family W04-009) is a known mutation, which was not present yet on the 2001 version of the *ABCA4* APEX array at the time the patient's DNA was screened.[31] The other mutation in *ABCA4* (c.6729+5_19del15) is new, and was not detected in 180 control alleles. This mutation may result in defective splicing, since the splice site consensus score decreases from 81.8 to 61.7, as calculated by the method of Shapiro & Senapathy.[32]

TABLE 2. **Overview of characteristics of the missense variants detected in CRD patients.**

Sequence change	Blosum-62 score*	Polyphen	SIFT prediction (score)†	Grantham score ‡	Segregation analysis	Presence in control individuals	Conclusion
ADAM9, c.2400G>T, p.Q800H	3	Possibly damaging	Not tolerated (0.03)	24	Homozygously present in unaffected brother	Excluded in 210 Dutch alleles§	Not pathogenic
CERKL, c.375C>G, p.C125W	-2	Probably damaging	Tolerated (0.08)	215	Homozygously present in affected brother	Excluded in 200 alleles	Pathogenic
PROM1, c.1946C>T, p.S649L	-3	Possibly damaging	Tolerated (0.14)	145	Both parents heterozygous, wildtype in non-affected brother	Present homozygously in 1/90 control individuals	Not pathogenic

*, the more negative the BLOSUM62 score, the more likely that a variant is pathogenic; †, SIFT score of <0.05 is predicted to be pathogenic; ‡, Grantham score: > 60 possibly damaging; §, no ethnically matched controls available.

A homozygous nonsense mutation (c.847C>T; p.R283X) and a homozygous missense mutation (c.375C>G; p.C125W) were identified in *CERKL*, which are both novel. The missense mutation replaces a cysteine by a tryptophan, which does not occur commonly during evolution (BLOSUM62 score -2; Table 2).[33] The mutation affects a fully conserved residue (Figure 2), was also identified homozygously in the patient's affected sibling (patient 54684), and was not present in 200 ethnically matched control alleles, and is therefore likely to be pathogenic. The novel splice site mutation in *PROM1* (c.1142-1G>A) affects the invariable AG-dinucleotide of the splice acceptor site of intron 10, and is predicted to impair splicing. The missense changes in *PROM1* (c.1946C>T; p.S649L) and *ADAM9* (c.2400G>T; p.Q800H) both affect highly conserved residues (Figure 2). However, the variant in *PROM1* was identified homozygously

in one out of 90 ethnically matched control individuals, and is therefore likely to be nonpathogenic. The *ADAM9* variant was detected homozygously in an unaffected brother, and is therefore likely to be nonpathogenic as well (Table 2).

Overlap with retinal disease loci

One homozygous region in a non-consanguineous Dutch CRD family from this cohort overlapped with the RP25 locus, which led to the discovery of *EYS* and the identification of a p.Y3156X mutation in the affected siblings. We published this finding elsewhere.[22] In addition, several other homozygous regions were detected which overlapped with previously published retinal dystrophy loci: LCA9, RP22, RP28, RP29, RCD1, and most interestingly, the 5.8 Mb CORD8 locus.[34,35] Two CRD patients of this study show an overlap with the entire CORD8 locus, a region that harbors more than 100 genes, of which *SEMA4A* was excluded as being causative. No other obvious candidate genes were identified it this region. Since most of the published retinal dystrophy loci are very large, overlap with one of our homozygous regions might be coincidental.

Clinical features

All 13 patients from eight families, in whom mutations were identified, underwent detailed ophthalmologic examinations. An overview of the clinical data is presented in Table 3. Nine patients showed clear signs of CRD. Remarkably, four patients from three families (two patients with mutations in *CABP4*, one of the patients with *EYS* mutations, and one patient with *KCNV2* mutations) originally diagnosed as cone-rod dysfunction and therefore entered into this study, appeared not to be affected with CRD. We have described the phenotype of the patients carrying mutations in *CABP4* and in *EYS* elsewhere.[22,36] The fourth patient, carrying a homozygous *KCNV2* mutation, initially received the diagnosis CRD. However, additional ERG testing at the age of 11 showed supernormal and delayed rod responses and decreased cone responses, characteristic for cone dystrophy with supernormal rod responses (RCD3; OMIM entry 610024). The detection of the novel p.Y54X mutation in *KCNV2* confirmed the corrected diagnosis, since this phenotype is specifically associated with mutations in *KCNV2*.[37]

The remaining patients showed the typical signs of CRD, with a wide range of phenotypic features and severity. Visual acuity ranged from 20/50 at age 48 in patient 50397 (*CERKL*, p.C125W) to light perception (LP) at age 53 in patient 51456 (*CERKL*, p.R283X). All patients experienced color vision abnormalities, central defects of the visual field on Goldmann perimetry, and – when measurable – more decreased cone

TABLE 3. Clinical features of patients in which a genetic defect was identified.

Patient ID (family number)	Gene defect	Age (yrs)	Age of diagnosis	Visual acuity (best eye)	Color vision	Goldmann perimetry	ERG, rod†	ERG, cone‡
CRD patients								
16875 (W00-409)	*ABCA4*, p.C54G	17	15	20/200	Diffuse errors	Small central scotoma	Sub-normal	NR
16876 (W00-409)		15	14	20/400	Diffuse errors, mostly protan axis	Large central scotoma	↓	↓↓
16877 (W00-409)		13	8	20/300	Diffuse errors	NP	↓↓	NR
50417	*ABCA4*, c.6729+5_19del15	48	30	20/400	Abnormal	Central scotoma and decreased sensitivity	NR	NR
50397 (W09-0340)	*CERKL*, p.C125W	48	30	20/50	Abnormal	Central scotoma	↓↓	↓↓
54684 (W09-0340)		51	28	3/400	Abnormal	Central scotoma	NR	NR
51456	*CERKL*, p.R283X	53	29	LP	NP	Not measurable	NR	NR
20695 (W02-077)	*PROM1*, c.1142-1G>A	18	13	20/200	Severely disturbed	Substantial central scotoma	↓↓	NR
20696 (W02-077)		16	9	20/125	Severely disturbed	Central scotoma with relative ring scotoma	NR	NR
Patient affected by cone dystrophy with supernormal rod ERG responses								
50222	*KCNV2*, p.Y54X	11	10	20/32	Moderately disturbed	Normal	↑, delayed	↓

†, isolated rod response; ‡, single flash cone response; ↓, reduced; ↓↓, severely reduced; ↑, supernormal; LP, light perception; NR, no responses; NP, not performed; RPE, retinal pigment epithelium.

TABLE 4. **Overview of fundoscopy, autofluorescence imaging and spectral domain OCT of CRD patients.**

Patient ID (family number)	Gene defect	Fundoscopy	Autofluorescence	Spectralis OCT
16875 (W00-409)	*ABCA4*, c.160T>G, p.C54G	Central glittering maculopathy and some peripheral fishtail pigment clusters	NP	NP
16876 (W00-409)		Central glittering maculopathy and some peripheral fishtail pigment clusters	NP	NP
16877 (W00-409)		Granular macular changes with irregular RPE	NP	NP
50417	*ABCA4*, c.6729+5_ 19del15, splice defect	Advanced pigmentary maculopathy	Striking macular absence of FAF	Loss of the IS-OS junction, massive debris accumulation between the retina and RPE, retinal thickening and foveal thinning
50397 (W09-0340)	*CERKL*, c.375C>G, p.C125W	Peri-foveal atrophy with a central RPE island	Striking macular absence of FAF with remaining central island	Single retinal single cyst formation
54684 (W09-0340)		Advanced foveal and macular atrophy, choroidal show and sclerosis in the macula	Striking macular absence of FAF	Extensive retinal remodeling, severe diffuse retinal thinning to 1-2 layers
51456	*CERKL*, c.874C>T, p.R283X	Choroidal show and sclerosis in the macula	Striking macular absence of FAF	RPE thinning
20695 (W02-007)	*PROM1*, c.1142-1G>A, splice defect	Central atrophic lesions in the macula, severely attenuated retinal vessels	NP	NP
20696 (W02-007)		Discrete central atrophy in the macula, severely attenuated retinal vessels, granular pigmentation in periphery	NP	NP

FAF, fundus autofluorescence; IS-OS, inner segment-outer segment; NP, not performed; RPE, retinal pigment epithelium.

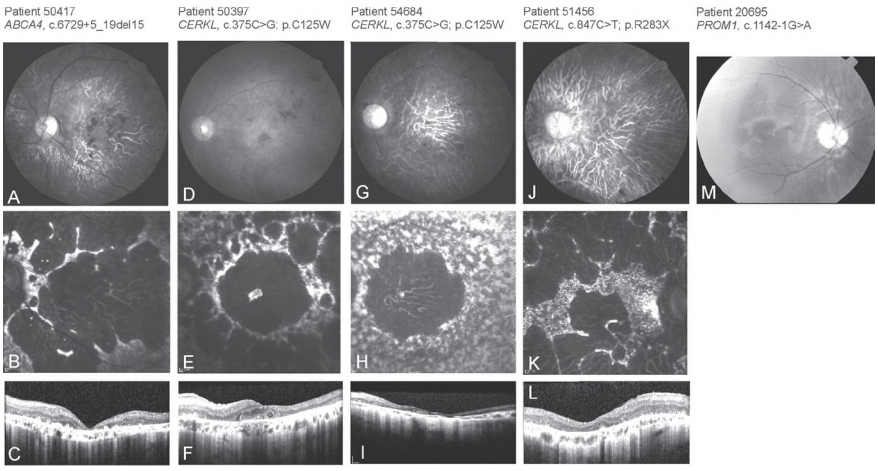

FIGURE 3. Fundus photographs, autofluorescence and spectral domain (Spectralis) OCT images of CRD patients with conclusive genetic defects. ***(See appendix for color figure)***

The retina of patient 50417 (*ABCA4*, c.6729+5_19del15; age 44) shows (**A**) extensive retinal pigment epithelium (RPE) cell loss, choroidal sclerosis and pigmentary macular changes on fundoscopy, (**B**) marked loss of central lipofuscin accumulation on fundus autofluoresence (FAF), and (**C**) a disorganized retina in which the six layers are not detectable, the fovea is extremely thin, with loss of the inner/outer segment junction. Extensive debris accumulation is noted. Patient 50397 (*CERKL*, p.C125W; age 48) has (**D**) a pigmentary maculopathy with choroidal sclerosis, (**E**) absence of central FAF, except in a tiny island, indicating nearly complete loss of lipofuscin deposition, and (**F**) very extensive retinal remodeling and an unusual subretinal cystic structure in the fovea. His older brother (54684, age 51), although carrying the same mutation in *CERKL*, has (**G**) extensive retinal, RPE and optic disc atrophy and sclerosis, (**H**) loss of central FAF, with a peculiar salt and pepper pattern of FAF outside the central retina, and (**I**) thinning and disorganization of the retina. A *CERKL* nonsense mutation (p.R238X) in patient 51456 (age 53) resulted in (**J**) extensive choroidal sclerosis, (**K**) loss of FAF, and (**L**) retinal remodeling with loss of inner/outer segment junction. The retina of patient 20695 (*PROM1*, c.1142-1G>A; age 18) showed (**M**) central atrophic lesions in the fovea and severely attenuated retinal vessels. No autofluorescence and spectral domain OCT images were available for this patient.

than rod responses. Fundus photographs, spectral domain OCT and FAF images of selected patients are presented in Figure 3, and described in Table 4.
In summary, macular appearances ranged from subtle RPE changes (*PROM1*) to pronounced atrophy of the RPE and choriocapillaris (*CERKL*). FAF showed an absence of autofluorescence in the macula in most of the patients. In vivo retinal architecture performed by spectral domain OCT, showed a variety of patterns, ranging from severe retinal thinning (*CERKL*) to thickening (*CERKL*), loss of architecture (*ABCA4*), cysts (*CERKL*) and accumulation of subfoveal hyper-reflective debris (*ABCA4*).

DISCUSSION

Homozygosity mapping in 95 probands and 13 affected siblings revealed significant homozygous regions in 77% of non-consanguineous patients and in all consanguineous patients, and led to the identification of the causative genetic defect in six non-consanguineous probands, and in two consanguineous probands. The percentage of homozygous regions in non-consanguineous patients seems to be high compared to other studies, in which homozygous regions were detected in 5-52% of patients from outbred populations.[24, 38, 39] This could be explained by the less stringent software settings were used to avoid false-negative regions. In addition, the cutoff for minimum length of homozygous regions varies among different studies. Genotyping studies in large cohorts show that individuals from outbred populations commonly carry homozygous regions, although they are usually shorter than those in individuals from isolated populations.[17, 40]

In all patients in whom a mutation was detected, the retinal phenotypes were reassessed. The mutations residing in *ABCA4*, *PROM1*, and *CERKL*, all previously associated with CRD,[4, 9, 10] indeed caused a CRD phenotype, although with variable characteristics. Three siblings carrying mutations in *ABCA4* and two siblings with PROM1 mutations showed a decrease in visual acuity during childhood (8-15 years of age), which is consistent with the previously described *ABCA4* and *PROM1*-related phenotypes.[9, 41] One patient (50417) carrying a defective splice site in *ABCA4* had a later age of onset at 30 years of age, which suggests that this mutation could have a moderately damaging effect on the protein. The three patients carrying mutations in *CERKL* had an age of onset around the age of 30 as well, but their visual acuity around the age of 50 differed considerable, even in the two brothers carrying the same mutation (20/50 at age 48, and 3/400 at the age of 51, respectively, and light perception at age 53 in the third patient). A wide variety of visual acuities in CRD patients with *CERKL* mutations, were described by Aleman et al. as well.[10]

A variability in retinal and macular appearances, retinal OCT findings and FAF patterns was noted, even for the same gene in different families (Figures 3D-3I versus 3J-3L) and the same mutation in the same family (Figure 3D-3F versus 3G-3I). A variety of maculopathies were documented, with geographic atrophy, choroidal show and sclerosis, and hyperpigmentations. Detailed OCT studies revealed retinal remodeling, loss of retinal layers, debris accumulation between the retina and RPE, single cysts, a subretinal cystic structure, and foveal thinning. Finally, FAF showed a complete absence of autofluorescence in the macular region in most patients, suggesting integral RPE- and photoreceptor loss. Documenting structural (OCT) and functional (FAF) disease patterns in genotyped patients are crucial for future therapeutic trials

and deciding the appropriate therapeutic modalities for the genotyped patients (gene replacement and drug trials in relatively intact retinas versus cell replacements in relatively destroyed maculas) but also for refining the clinical diagnosis and the visual prognosis.

Interestingly, one patient with *EYS* mutations was diagnosed as CRD, but her brother received the diagnosis RP. Mutations in *EYS* have been shown to be causative for ~5-12% of arRP cases, while no mutations were found in additional CRD patients.[42-45] *EYS* is therefore not a frequent cause of CRD. The clinical diagnoses of the patients carrying mutations in *CABP4* and *KCNV2* were revised to congenital cone-rod synaptic disorder and cone dystrophy with supernormal rod responses, respectively.[36, 37, 46] These revisions illustrate the complexity of diagnosing retinal dystrophies, the significant clinical overlap of genetically distinct disorders and the power and utility of molecular genetic testing.
Overall, the percentage of CRD cases that can be attributed to each gene in this cohort is ~1 % for *PROM1* (1/123), ~2 % for *CERKL* (2/123), and ~27 % for *ABCA4* (33/123), which is consistent with previous publications.[4-7, 9, 10] We identified *EYS* mutations in 1% (1/123) of the CRD patients, but no other mutations in CRD patients were identified in other studies.[42, 43] The percentages include patients in which homozygous and heterozygous *ABCA4* mutations were detected by APEX screening. For these calculations, we excluded the four patients in which other clinical diagnoses were established.

Which patients are most suitable for mutation detection by homozygosity mapping? Gibson et al. showed that long homozygous segments are common in unrelated individuals from the HapMap database.[40] However, long and numerous homozygous segments usually indicate parental relatedness.[17, 18] Also, the average genome-wide homozygosity in non-consanguineous patients of the entire cohort was 0.5% (0-2.9%), while the average was 1.06% (0.5-1.6%) in patients in whom homozygous mutations were identified. Although Carothers et al.[47] showed that the percentage of homozygosity is unreliable in predicting the relatedness, our data suggest that the chance to find a homozygous mutation is higher in patients with a high percentage of homozygosity. A better estimate to determine the chance to find a homozygous defect is to know the family origin. In at least four of our patients, the paternal and maternal grandparents originated from the same geographical region; one family from a province in Greece, one from the south-west of the Netherlands, one from the east of the Netherlands, and one family originated from the French-Canadian founder population. Therefore, detailed information about the origin of grandparents of

a patient is desired when considering whether homozygosity mapping will be efficient in identifying a genetic defect in a particular patient. Furthermore, for four out of eight probands in which the genetic defect was identified one or more affected siblings were available for homozygosity mapping.
In agreement with a previous study by Woods et al.,[48] families with two or more affected siblings are the most powerful to pinpoint the homozygous region containing the mutation.

The homozygosity data generated in this study are likely to be a valuable resource for the detection of novel disease genes. The discovery of the *EYS* gene in a family of this cohort, for example, shows how relatively small homozygous regions in non-consanguineous families can fine map the causative locus and thereby facilitate the identification of a new causative gene. Moreover, this type of data may be valuable now that "next generation sequencing" is emerging, which enables the screening of all genes within a homozygous region in one experiment.[49]

In conclusion, this study shows that homozygosity mapping can lead to the identification of novel genetic defects in consanguineous as well as non-consanguineous families. Our results show that many more CRD genes may exist. Finding them and identifying the associated detailed phenotypes will provide more insight into patients suitable for gene-specific therapies.

ACKNOWLEDGEMENT

The authors thank Christel Beumer, Saskia van der Velde-Visser, and Jinny Conte for technical assistance, Suzanne Keijzers-Vloet and Irene Janssen for performing the microarray experiments, and Kentar ArimadyoSulakso and Almudena Avila-Fernández for assistance in mutation analysis. This study was supported by the Stichting Wetenschappelijk Onderzoek Oogziekenhuis Prof. Dr. H.J. Flieringa Foundation, The Rotterdam Eye Hospital (grant 2005-13 [LIvdB, AIdH, FPMC]), Netherlands Organisation for Scientific Research (grant 916.56.160 [AIdH]), Foundation Fighting Blindness USA (grant BR-GE-0507-0381-RAD [AIdH]), the Landelijke Stichting voor Blinden en Slechtzienden [FPMC], Algemene Nederlandse Vereniging ter Voorkoming van Blindheid [FPMC], Canadian Institutes of Health Research [RKK], Foundation Fighting Blindness Canada [RKK], Fonds de la Recherche en Santé Quebec [RKK], National Institutes of Health [RKK], and Réseau de Vision [RKK].

SUPPLEMENTAL DATA

SUPPLEMENTAL TABLE 1. Overview of genomic homozygosity information for each patient.

NON-CONSANGUINEOUS PATIENTS							
Patient ID	**Country (origin)**	**Maximum number of consecutive homozygous SNPs**	**Size of region with largest amount of SNPs (Mb)**	**Number of regions**	**Total homo-zygous tract length (Mb)**	**% of genome (>~3 Mb) covered by homozygous segments**	**Genetic defect**
250K SNP array							
8577	Netherlands	210	2,9	1	2,9	0,1	
9052	Netherlands	247	3,3	2	5,5	0,2	
9554	Germany	376	3,0	1	3,0	0,1	
9661	Germany	0	0	0	0	0	
9979	Germany	230	3,1	5	11,6	0,4	
12734	Germany	264	2,2	2	4,2	0,1	
13165	Germany	0	0	0	0	0	
13166	Germany	254	2,4	4	8,2	0,3	
13340	Germany	205	2,1	2	4,4	0,2	
13421	Germany	987	9,9	6	29,3	1,0	
14751	Germany	271	1,7	1	1,7	0,1	
14963	Germany	337	2,5	4	9,2	0,3	
14967	Germany	295	3,0	2	5,0	0,2	
15102	Germany	360	4,5	1	4,5	0,2	
15930	Germany	242	2,5	6	12,7	0,4	
16599	Germany	263	5,1	4	11,3	0,4	
16754	Germany	249	2,1	1	2,1	0,1	
16755	Germany	228	2,2	3	7,6	0,3	
16896	Germany	472	7,4	2	7,4	0,3	
16897	Germany	207	2,5	2	4,5	0,2	
17579	Germany	328	3,9	1	3,9	0,1	
17580	Germany	542	6,6	2	9,4	0,3	
18429	USA	292	4,7	8	25,3	0,9	
20760	Germany	0	0	0	0	0	
20761	Germany	0	0	0	0	0	
20885	Netherlands	259	2,8	4	9,9	0,3	
20888	Germany	0	0	0	0	0	
20945	Netherlands	239	2,8	1	2,8	0,1	
21480	Netherlands	1781	17,7	3	32,8	1,2	
21511	Netherlands	554	5,9	2	7,9	0,3	
21761	Netherlands	249	3,7	1	3,7	0,1	
21814	Germany	850	16,4	5	26,4	0,9	
23347	Netherlands	320	3,0	3	6,8	0,2	
28837	Netherlands	1192	9,0	4	19,4	0,7	
35029	Netherlands (Suriname)	258	1,6	2	4,1	0,1	

Patient ID	Country (origin)	Maximum number of consecutive homozygous SNPs	Size of region with largest amount of SNPs (Mb)	Number of regions	Total homo-zygous tract length (Mb)	% of genome (>~3 Mb) covered by homozygous segments	Genetic defect
6.0 SNP array							
40964	Netherlands	1098	4,9	1	4,9	0,2	
42024	Netherlands	1744	6,2	1	6,2	0,2	
42297	Canada	0	0	0	0	0	
43442	Netherlands	1066	5,0	1	5,0	0,2	
50387	Canada	0	0	0	0	0	
50388	Canada	0	0	0	0		
50389	Canada	3132	11,2	3	19,9	0,7	
50390	Canada	972	3,4	3	7,7	0,3	
50391	Canada	5675	22,2	5	55,2	1,9	
50392	Canada	0	0	0	0	0	
50393	Canada	4210	12,5	7	43,6	1,5	
50394	Canada	0	0	0	0	0	
50396	Canada	888	3,1	2	6,5	0,2	
50397	Canada	7745	28,4	4	44,7	1,6	*CERKL*; c.375C>G; p.C125W
50398	Canada	4746	14,8	9	59,8	2,1	
50399	Canada	0	0	0	0	0	
50400	Canada	0	0	0	0	0	
50401	Canada	2673	10,6	1	10,6	0,4	
50402	Canada	0	0	0	0	0	
50403	Canada	0	0	0	0	0	
50404	Canada	0	0	0	0	0	
50405	Canada	0	0	0	0	0	
50406	Canada	0	0	0	0	0	
50407	Canada	9002	19,9	6	65,2	2,3	
50408	Canada	5941	20,2	5	55,4	1,9	
50409	Canada	0	0	0	0	0	
50410	Canada	744	2,8	1	2,8	0,1	
50411	Canada	2088	4,3	1	4,3	0,2	
50412	Canada	4734	16,3	2	25,2	0,9	
50413	Canada	0	0	0	0	0	
50414	Canada	684	2,0	1	2,0	0,1	
50416	Canada	1936	8,4	7	28,3	1,0	
50417	Canada	2810	9,5	10	43,9	1,5	*ABCA4*; c.6729+5_ 19del15; splice defect
50424	Canada	4084	13,8	5	26,3	0,9	
50425	Canada	0	0	0	0	0	
50427	Canada	0	0	0	0	0	
50429	Canada	3028	6,7	1	6,7	0,2	
50430	Canada	3881	10,4	7	28,9	1,0	
50431	Canada	860	1,8	1	1,8	0,1	
50503	Netherlands	906	2,7	1	2,7	0,1	

Patient ID	Country (origin)	Maximum number of consecutive homozygous SNPs	Size of region with largest amount of SNPs (Mb)	Number of regions	Total homo-zygous tract length (Mb)	% of genome (>~3 Mb) covered by homozygous segments	Genetic defect
51453	Canada (Middle East)	0	0	0	0	0	
51454	Canada (French Canadian)	1564	5,0	2	9,6	0,3	
51455	Canada (French Canadian)	0	0	0	0	0	
51456	Canada (French Canadian)	3097	10,6	2	14,3	0,5	*CERKL*; c.847C>T; p.R283X

CONSANGUINEOUS PATIENTS

Patient ID	Country (origin)	Maximum number of consecutive homozygous SNPs	Size of region with largest amount of SNPs (Mb)	Number of regions	Total homo-zygous tract length (Mb)	% of genome (>~3 Mb) covered by homozygous segments	Genetic defect
250K SNP array							
20780	Germany	2068	16,5	19	158,0	5,5	
6.0 SNP array							
50222	Netherlands	11970	32,1	16	198,7	7,0	*KCNV2*; c.162C>A; p.Y54X
50415	Canada	8438	29,6	27	332,9	11,7	
50434	Canada	7209	19,3	20	164,5	5,8	
51452	Canada (Italy)	10373	30,8	21	247,8	8,7	
51457	Canada (Middle East)	9178	33,7	21	246,8	8,7	

NON-CONSANGUINEOUS FAMILIES

Patient ID	Country (origin)	Maximum number of consecutive homozygous SNPs	Size of region with largest amount of SNPs (Mb)	Number of regions	Total homo-zygous tract length (Mb)	% of genome (>~3 Mb) covered by homozygous segments	Genetic defect
250K SNP array							
W97-037, overlap	Netherlands	0	0	0	0	0,0	
9007		223	2,5	1	2,5	0,1	
9033		252	3,9	2	6,3	0,2	
11253		218	2	1	2	0,1	
W98-057, overlap	Netherlands	0	0	0	0	0,0	
9519		1374	13,4	3	25,2	0,9	
13753		560	6	6	21,4	0,8	
W00-107, overlap	Germany	236	5,3	1	5,3	0,2	
14746		241	3,3	2	8,6	0,3	
14747		238	5,3	1	5,3	0,2	
W00-237, overlap	Germany	209	3,0	1	3,0	0,1	
15732		274	3,6	6	15,2	0,5	
15733		246	2,1	3	9,1	0,3	
W00-391, overlap	Germany	592	4,7	1	4,7	0,2	
21096		592	4,7	2	6,7	0,2	
21097		1767	15,2	6	36,6	1,3	
21098		1566	13,7	3	20,6	0,7	
W00-426, overlap	Germany	2156	20,8	1	20,8	0,7	
15104		3574	24,0	7	83,3	2,9	
20963		3280	31,4	6	50,0	1,8	
W02-077, overlap	Greece	2037	16,1	2	26,5	0,9	
20965		2646	20,7	3	34,4	1,2	*PROM1*; c.1142-1G>A; splice defect
20966		2037	16,0	2	32,0	1,1	
W03-008, overlap	Netherlands	538	11,3	2	15,7	0,5	
20867		790	5,6	8	33,0	1,2	*CABP4*; c.646C>T; p.Arg216X
20868		539	11,3	3	17,3	0,6	
W05-112, overlap	Netherlands	689	6,6	2	16,8	0,6	
26323		695	10,3	4	25,7	0,9	*EYS*; c.9468T>A; p.Y3156X
26836		694	6,7	4	26,0	0,9	

CONSANGUINEOUS FAMILY							
Patient ID	**Country (origin)**	**Maximum number of consecutive homozygous SNPs**	**Size of region with largest amount of SNPs (Mb)**	**Number of regions**	**Total homo-zygous tract length (Mb)**	**% of genome (>~3 Mb) covered by homozygous segments**	**Genetic defect**
250K SNP array							
W00-409	Iraq	2850	28,3	1	28,3	1,0	
16875		4003	38,1	12	166,5	5,8	*ABCA4*; c.160T>G; p.C54G
16876		3573	35,9	17	216,0	7,6	
16877		3278	32,9	8	107,3	3,8	

REFERENCES

1. Szlyk JP, Fishman GA, Alexander KR, Peachey NS, Derlacki DJ. Clinical subtypes of cone-rod dystrophy. Arch Ophthalmol. 1993;111:781-788.

2. Hamel CP. Cone rod dystrophies. Orphanet J Rare Dis. 2007;2:7-14.

3. Jalili IK, Smith NJ. A progressive cone-rod dystrophy and amelogenesis imperfecta: a new syndrome. J Med Genet. 1988;25:738-740.

4. Maugeri A, Klevering BJ, Rohrschneider K, et al. Mutations in the ABCA4 (ABCR) gene are the major cause of autosomal recessive cone-rod dystrophy. Am J Hum Genet. 2000;67:960-966.

5. Ducroq D, Rozet JM, Gerber S, et al. The ABCA4 gene in autosomal recessive cone-rod dystrophies. Am J Hum Genet. 2002;71:1480-1482.

6. Fishman GA, Stone EM, Eliason DA, Taylor CM, Lindeman M, Derlacki DJ. ABCA4 gene sequence variations in patients with autosomal recessive cone-rod dystrophy. Arch Ophthalmol. 2003;121:851-855.

7. Klevering BJ, Yzer S, Rohrschneider K, et al. Microarray-based mutation analysis of the ABCA4 (ABCR) gene in autosomal recessive cone-rod dystrophy and retinitis pigmentosa. Eur J Hum Genet. 2004;12:1024-1032.

8. Hameed A, Abid A, Aziz A, Ismail M, Mehdi SQ, Khaliq S. Evidence of RPGRIP1 gene mutations associated with recessive cone-rod dystrophy. J Med Genet. 2003;40:616-619.

9. Pras E, Abu A, Rotenstreich Y, et al. Cone-rod dystrophy and a frameshift mutation in the PROM1 gene. Mol Vis. 2009;15:1709-1716.

10. Aleman TS, Soumittra N, Cideciyan AV, et al. CERKL mutations cause an autosomal recessive cone-rod dystrophy with inner retinopathy. Invest Ophthalmol Vis Sci. 2009;50:5944-5954.

11. Parry DA, Toomes C, Bida L, et al. Loss of the metalloprotease ADAM9 leads to cone-rod dystrophy in humans and retinal degeneration in mice. Am J Hum Genet. 2009;84:683-691.

12. Yzer S, Leroy BP, De Baere E, et al. Microarray-based mutation detection and phenotypic characterization of patients with Leber congenital amaurosis. Invest Ophthalmol Vis Sci. 2006;47:1167-1176.

13. Wissinger B, Gamer D, Jagle H, et al. CNGA3 mutations in hereditary cone photoreceptor disorders. Am J Hum Genet. 2001;69:722-737.

14. Krone N, Braun A, Roscher AA, Knorr D, Schwarz HP. Predicting phenotype in steroid 21-hydroxylase deficiency? Comprehensive genotyping in 155 unrelated, well defined patients from southern Germany. J Clin Endocrinol Metab. 2000;85:1059-1065.

15. Sandoval N, Platzer M, Rosenthal A, et al. Characterization of ATM gene mutations in 66 ataxia telangiectasia families. Hum Mol Genet. 1999;8:69-79.

16. Roux AF, Faugere V, Le Guedard S, et al. Survey of the frequency of USH1 gene mutations in a cohort of Usher patients shows the importance of cadherin 23 and protocadherin 15 genes and establishes a detection rate of above 90%. J Med Genet. 2006;43:763-768.

17. McQuillan R, Leutenegger AL, Abdel-Rahman R, et al. Runs of homozygosity in European populations. Am J Hum Genet. 2008;83:359-372.

18. Broman KW, Weber JL. Long homozygous chromosomal segments in reference families from the centre d'Etude du polymorphisme humain. Am J Hum Genet. 1999;65:1493-1500.

19. Hildebrandt F, Heeringa SF, Ruschendorf F, et al. A systematic approach to mapping recessive disease genes in individuals from outbred populations. PLoS Genet. 2009;5:e1000353.

20. den Hollander AI, Koenekoop RK, Yzer S, et al. Mutations in the CEP290 (NPHP6) gene are a frequent cause of Leber congenital amaurosis. Am J Hum Genet. 2006;79:556-561.

21. den Hollander AI, Koenekoop RK, Mohamed MD, et al. Mutations in LCA5, encoding the ciliary protein lebercilin, cause Leber congenital amaurosis. Nat Genet. 2007;39:889-895.

22. Collin RWJ, Littink KW, Klevering BJ, et al. Identification of a 2 Mb human ortholog of Drosophila eyes shut/spacemaker that is mutated in patients with retinitis pigmentosa. Am J Hum Genet. 2008;83:594-603.

23. Thiadens AA, den Hollander AI, Roosing S, et al. Homozygosity mapping reveals PDE6C mutations in patients with early-onset cone photoreceptor disorders. Am J Hum Genet. 2009;85:240-247.

24. den Hollander AI, Lopez I, Yzer S, et al. Identification of novel mutations in patients with Leber congenital amaurosis and juvenile RP by genome-wide homozygosity mapping with SNP microarrays. Invest Ophthalmol Vis Sci. 2007;48:5690-5698.

25. Miller SA, Dykes DD, Polesky HF. A simple salting out procedure for extracting DNA from human nucleated cells. Nucleic Acids Res. 1988;16:1215.

26. Jaakson K, Zernant J, Kulm M, et al. Genotyping microarray (gene chip) for the ABCR (ABCA4) gene. Hum Mutat. 2003;22:395-403.

27. Purcell S, Neale B, Todd-Brown K, et al. PLINK: a tool set for whole-genome association and population-based linkage analyses. Am J Hum Genet. 2007;81:559-575.

28. Rozen S, Skaletsky H. Primer3 on the WWW for general users and for biologist programmers. Methods Mol Biol. 2000;132:365-386.

29. Little S. Amplification-refractory mutation system (ARMS) analysis of point mutations. Curr Protoc Hum Genet. 2001;Chapter 9:Unit 9.8.

30. Lencz T, Lambert C, DeRosse P, et al. Runs of homozygosity reveal highly penetrant recessive loci in schizophrenia. Proc Natl Acad Sci U S A. 2007;104:19942-19947.

31. Ozgul RK, Durukan H, Turan A, Oner C, Ogus A, Farber DB. Molecular analysis of the ABCA4 gene in Turkish patients with Stargardt disease and retinitis pigmentosa. Hum Mutat. 2004;23:523.

32. Shapiro MB, Senapathy P. RNA splice junctions of different classes of eukaryotes: sequence statistics and functional implications in gene expression. Nucleic Acids Res. 1987;15:7155-7174.

33. Henikoff S, Henikoff JG. Amino acid substitution matrices from protein blocks. Proc Natl Acad Sci U S A. 1992;89:10915-10919.

34. Khaliq S, Hameed A, Ismail M, et al. Novel locus for autosomal recessive cone-rod dystrophy CORD8 mapping to chromosome 1q12-q24. Invest Ophthalmol Vis Sci. 2000;41:3709-3712.

35. Ismail M, Abid A, Anwar K, Mehdi SQ, Khaliq S. Refinement of the locus for autosomal recessive cone-rod dystrophy (CORD8) linked to chromosome 1q23-q24 in a Pakistani family and exclusion of candidate genes. J Hum Genet. 2006;51:827-831.

36. Littink KW, van Genderen MM, Collin RWJ, et al. A novel homozygous nonsense mutation in CABP4 causes congenital cone-rod synaptic disorder. Invest Ophthalmol Vis Sci. 2009;50:2344-2350.

37. Wu H, Cowing JA, Michaelides M, et al. Mutations in the gene KCNV2 encoding a voltage-gated potassium channel subunit cause "cone dystrophy with supernormal rod electroretinogram" in humans. Am J Hum Genet. 2006;79:574-579.

38. Harville HM, Held S, Diaz-Font A, et al. Identification of 11 Novel Mutations in 8 BBS Genes by High-Resolution Homozygosity Mapping. J Med Genet. 2009.

39. Li LH, Ho SF, Chen CH, et al. Long contiguous stretches of homozygosity in the human genome. Hum Mutat. 2006;27:1115-1121.

40. Gibson J, Morton NE, Collins A. Extended tracts of homozygosity in outbred human populations. Hum Mol Genet. 2006;15:789-795.

41. Klevering BJ, Blankenagel A, Maugeri A, Cremers FPM, Hoyng CB, Rohrschneider K. Phenotypic spectrum of autosomal recessive cone-rod dystrophies caused by mutations in the ABCA4 (ABCR) gene. Invest Ophthalmol Vis Sci. 2002;43:1980-1985.

42. Littink KW, van den Born LI, Koenekoop RK, et al. Mutations in the EYS gene account for ~5% of autosomal recessive retinitis pigmentosa and cause a fairly homogeneous phenotype. Ophthalmology. 2010.

43. Bandah-Rozenfeld D, Littink KW, Ben-Yosef T, et al. Novel null mutations in the EYS gene are a frequent cause of autosomal recessive retinitis pigmentosa in the Israeli population. Invest Ophthalmol Vis Sci. 2010.

44. Abd El-Aziz MM, O'Driscoll CA, Kaye RS, et al. Identification of Novel Mutations in the ortholog of Drosophila eyes shut Gene (EYS) Causing Autosomal Recessive Retinitis Pigmentosa. Invest Ophthalmol Vis Sci. 2010.

45. Audo I, Sahel JA, Mohand-Said S, et al. EYS is a major gene for rod-cone dystrophies in France. Hum Mutat. 2010.

46. Zeitz C, Kloeckener-Gruissem B, Forster U, et al. Mutations in CABP4, the gene encoding the Ca2+-binding protein 4, cause autosomal recessive night blindness. Am J Hum Genet. 2006;79:657-667.

47. Carothers AD, Rudan I, Kolcic I, et al. Estimating human inbreeding coefficients: comparison of genealogical and marker heterozygosity approaches. Ann Hum Genet. 2006;70:666-676.

48. Woods CG, Cox J, Springell K, et al. Quantification of homozygosity in consanguineous individuals with autosomal recessive disease. Am J Hum Genet. 2006;78:889-896.

49. Metzker ML. Sequencing technologies - the next generation. Nat Rev Genet. 2010;11:31-46.

Adapted from: *Investigative Ophthalmology & Visual Science.* 2009;50:2344–2350.

Karin W. Littink,[1,2] Maria M. van Genderen,[3] Rob W. J. Collin,[2,4] Susanne Roosing,[2,4] Arjan P. M. de Brouwer,[2,4] Frans C. C. Riemslag,[3] Hanka Venselaar,[4,5] Alberta A. H. J. Thiadens,[6] Carel B. Hoyng,[7] Klaus Rohrschneider,[8] Anneke I. den Hollander,[2,4,7] Frans P. M. Cremers,[2,4] and L. Ingeborgh van den Born[1]

[1] The Rotterdam Eye Hospital, Rotterdam, The Netherlands; [2] Departments of Human Genetics, Radboud University Nijmegen Medical Centre, Nijmegen, The Netherlands; [3] Bartiméus Institute for the Visually Impaired, Zeist, The Netherlands; [4] Nijmegen Centre for Molecular Life Sciences, and [5] Centre for Molecular and Biomolecular Informatics, Radboud University Nijmegen Medical Centre, Nijmegen, The Netherlands; [6] Department of Ophthalmology, Erasmus Medical Center, Rotterdam, The Netherlands; [7] Departments of Ophthalmology, Radboud University Nijmegen Medical Centre, Nijmegen, The Netherlands and [8] Department of Ophthalmology, University of Heidelberg, Heidelberg, Germany.

CHAPTER 3

A NOVEL HOMOZYGOUS NONSENSE MUTATION IN *CABP4* CAUSES CONGENITAL CONE–ROD SYNAPTIC DISORDER

ABSTRACT

PURPOSE. The purpose of this study was to identify the causative gene defect in two siblings with an uncharacterized cone–rod dysfunction and to describe the clinical characteristics.

METHODS. Genome-wide homozygosity mapping, with a 250K SNP-array followed by a search for candidate genes, was performed. The patients underwent ophthalmic examination, including elaborate electroretinography.

RESULTS. In a Dutch sib pair, a shared 9-Mb homozygous region was found on 11q13.1-q13.5 that encompasses the *CABP4* gene, previously implicated in autosomal recessive incomplete congenital stationary night blindness (CSNB2) in two small families. A novel homozygous p.Arg216X mutation in *CABP4* was detected in the sib pair. Quantitative RT-PCR on RNA isolated from patient lymphoblast cells showed no nonsense mediated degradation of mutant *CABP4* mRNA. Clinically, patients presented with reduced visual acuity, photophobia, and abnormal color vision, but they did not experience night blindness. Electroretinograms showed electronegative mixed rod-cone responses and severely reduced cone responses, as in CSNB2. Isolated rod responses, however, were (sub)normal.

CONCLUSIONS. A novel homozygous nonsense mutation in *CABP4* in two siblings resulted in a phenotype with severely reduced cone function and only negligibly reduced rod function on electroretinography and psychophysical testing. Since these patients and two of three previously described patients do not experience night blindness, the name CSNB2 is confusing for patients as well as clinicians. Therefore, the authors propose to name the phenotype congenital cone–rod synaptic disorder.

INTRODUCTION

CABP4 (*C*alcium-*b*inding *p*rotein 4) has recently been described in association with autosomal recessive incomplete congenital stationary night blindness (CSNB2).[1] CSNB is a nonprogressive retinal disorder characterized by impaired night vision, myopia or hyperopia, nystagmus, and reduced visual acuity, with a wide intra- and interfamilial variability. All modes of Mendelian inheritance have been described for this disorder. The genes associated with CSNB encode different components of the phototransduction cascade or proteins involved in signaling from photoreceptor to the adjacent bipolar cells.[1-11] Most patients with CSNB (X-linked and autosomal recessive) have a characteristic electronegative electroretinogram (ERG) (Schubert-Bornschein type) – that is, a near-normal a-wave and a substantially reduced b-wave – on testing under scotopic conditions.[12] The X-linked type of CSNB was further subdivided by Miyake et al.[12] into complete CSNB (CSNB1) and incomplete CSNB (CSNB2), based on differences in electrophysiology. In CSNB1 (OMIM 310500), no residual rod function is detected. In CSNB2 (OMIM 300071) the rod contribution to the scotopic b-wave is reduced but recordable. At a 30-Hz flicker stimulation, amplitudes are overall decreased, but they increase in time with a characteristic double-peak appearance (wave separation phenomenon).[13] Miyake et al.[12] suggested distinct pathogenic mechanisms for the different forms of CSNB, which was confirmed by the identification of the molecular causes of CSNB. For CSNB1 mutations in *NYX* (MIM 300278)[7] were identified in patients with the X-linked form and mutations in *GRM6* (MIM 604096)[9, 14] in patients with the autosomal recessive form. Patients with mutations in *GRM6* and *NYX* can be distinguished clinically by a characteristic pattern at a 15-Hz flicker stimulation.[14] X-linked CSNB2 is caused by mutations in *CACNA1F* (MIM 300110),[6] which encodes the L-type voltage-dependent calcium channel 1.4 ($Ca_v1.4$).[15] In two small families with a CSNB2-like phenotype and an autosomal recessive mode of inheritance, Zeitz et al.[1] recently identified mutations in the *CABP4* gene (MIM 608965), which encodes the calcium binding protein CaBP4. CaBP4 colocalizes and interacts with $Ca_v1.4$ in both cone and rod photoreceptor synaptic terminals, thereby regulating the calcium influx in the photoreceptor. Patients carrying mutations in *CACNA1F* and *CABP4* show a comparable phenotype. A true genotype-phenotype correlation for *CABP4* has not been established yet, since only three patients have been described.[1]
In this article, we present two siblings, carrying a novel homozygous nonsense mutation in *CABP4*, with an ERG suggestive of CSNB2 but with nearly normal rod function and no night blindness. We show similarities between this phenotype and other disorders influencing photoreceptor synaptic calcium channels and propose to add this disorder to a novel spectrum of calcium channelopathies.

SUBJECTS AND METHODS

Patients

Two affected siblings were clinically and genetically examined. Blood samples were obtained from patients and their parents. Informed consents signed by the parents were obtained according to the tenets of the Declaration of Helsinki and the protocol was approved by the ethics committees of The Rotterdam Eye Hospital and the Radboud University Nijmegen Medical Centre. Clinical assessment included best corrected visual acuity, refractive error, slit lamp examination, funduscopy, kinetic Goldmann perimetry (targets V-4e and I-4e), color vision tests (Ishihara Test for Color Blindness, American Optical Hardy-Rand-Rittler Test (AO-HRR), Farnsworth Panel D15 Test) and dark adaptometry (Goldmann-Weekers dark adaptometer). Electroretinograms (ERGs) were recorded according to a previously described protocol.[12] For the standard ISCEV ERG measurements,[16] Xenon tube flashes (duration <10 μs) were delivered in a Ganzfeld (Color Dome; Diagnosys, Littleton, MA). The 15-Hz protocol was recorded intermixed with the standard ISCEV ERG at the appropriate intensities, using LED flashes of 4 ms duration.

Homozygosity mapping

Total genomic DNA was extracted from EDTA-treated blood samples by using standard procedures.[17] DNA samples for SNP analysis were genotyped for 262,000 SNPs (GeneChip Mapping 250K *Nsp*I array; Affymetrix, Santa Clara, CA). Array experiments were performed according to protocols provided by the manufacturer. The 250K SNP genotypes were analyzed with the software package CNAG,[18] and chromosomal segments were accepted as homozygous if the loss-of-heterozygosity (LOH) score was ≥15, which corresponds with an area of >200 SNPs.

Sequence analysis

All six coding exons, a noncoding exon and the intron/exon boundaries of the *CABP4* gene (NM_145200), were amplified by polymerase chain reaction (PCR). Genomic PCR was performed in 50 μL volumes containing 100 ng genomic DNA, 0.2 mM of each primer (Table 1), 2 mM $MgCl_2$, 1 mM dNTPs, PCR buffer provided by the manufacturer, and 5 U Taq polymerase (Invitrogen, Breda, The Netherlands). PCR reactions were performed as follows: 92°C (3 minutes); cycles with a denaturation at 95°C (30 seconds), an annealing temperature of 68°C (3 cycles), 66°C (3 cycles), 64°C (3 cycles), 62°C (31 cycles; 30 seconds) and an elongation at 72°C (45 seconds); and a final extension at 72°C (5 minutes). PCR products were purified (Qia Quick Gel Extraction Kit; Qiagen, Venlo, The Netherlands) according to the manufacturer's protocol and analyzed in sense and anti-sense directions

with dye termination chemistry (BigDye Terminator, version 3 on a 3730 DNA analyzer; Applied Biosystems, Inc., Foster City, CA). The control panel included 300 alleles from ethnically matched unrelated unaffected individuals and were screened for the c.646C>T mutation, detected in this study, using the Amplification-Refractory Mutation System (ARMS)[19] (Table 1). Furthermore, 71 patients with cone-rod dystrophy and 14 with cone dystrophy were screened for mutations in *CABP4*. DNA of 79 of these patients had been screened before for known *ABCA4* mutations with the *ABCA4* arrayed-primer extension microarray (Asper Ophthalmics, Tartu, Estonia).[20] In 62 patients, known *ABCA4* mutations were excluded, whereas in 17 patients, one mutation in *ABCA4* was detected.

Cell culture

Human B-lymphocytes were immortalized by transformation with the Epstein-Barr virus according to established procedures.[22] Epstein-Barr virus transformed lymphoblastoid cell lines (EBV-LCLs) of the patients and controls were grown to a density of 0.7 million cells per milliliter RPMI 1640 medium (Invitrogen-Gibco, Breda, The Netherlands) containing 10% (vol/vol) fetal calf serum (Sigma-Aldrich, Zwijndrecht, The Netherlands), 1% penicillin-streptomycin (Invitrogen-Gibco), and 1% cell culturing medium (GlutaMAX; Invitrogen-Gibco). Thirty-five million cells

TABLE 1. **Primers used for molecular studies of *CABP4***

Procedure Gene and exon	Sequence (5′→ 3′) Forward	Reverse	Product size (base pair)
Direct DNA sequencing			
CABP4 promotor	GGCCAGCAGGAAGAGGC	GACCCCAAATGGACACTACC	377
CABP4 exon 1	GGGTCCTGAAAGCCAAGG	GGTGAGCTGAGCCCAAGG	502
CABP4 exon 2-3	AGGGGATGAAGGAGGAAGG	CCACTAGCACCCCGATGG	426
CABP4 exon 4	TTTCTTCCTAGGTGCAGAGC	GCTGAGACCTGAGTGAGAGG	299
CABP4 exon 5-6	AGCTGGCTGAGGCTGAGG	CTGCTGGGTCTCCATCTCC	554
QPCR			
CABP4 exon 3-4	AGGTCTCGCAGCACATCAAG	CTCAGCTTTGGGCCTATCAG	81
GUSB	AGAGTGGTGCTGAGGATTGG	CCCTCATGCTCTAGCGTGTC	80
FTSJ1	CAACTCTTCCAAGGCGTGAC	ATCTTCTGGCTCAGCACCTG	80
	Sequence (5′→ 3′)		
ARMS primers			
Wildtype forward	5′-TGGGGGTGCGAGAGCTGCGCATCGCCTTAC-3′		
Mutant forward	5′-TGGGGGTGCGAGAGCTGCGCATCGCCTTAT-3′		
Reverse	5′-TAGCTGGTAGTGATCTGAACCATCTCTGA-3′		

Primers were designed using Primer3 software (http://frodo.wi.mit.edu/cgi-bin/primer3/primer3_www.cgi, provided in the public domain by the Whitehead Institute, Massachusetts Institute of Technology, Cambridge, MA).[21]

were harvested by centrifugation at 200 g for 5 minutes at room temperature and resuspended in 500 µL 8 mM Na_2HPO_4, 2 mM KH_2PO_4, 137 mM NaCl, and 2.7 mM KCl (pH 7.2; PBS). Cell pellets were subsequently stored at -80°C until RNA isolation.

Quantitative PCR analysis

Total RNA was isolated from EBV-LCLs according to the manufacturer's protocol (RNeasy minikit; Qiagen). cDNA was synthesized from 2.0 µg of total RNA using random primed hexamers (GE Healthcare, Hoevelaken, The Netherlands) and M-MLV reverse transcriptase (Invitrogen) in a total volume of 85 µL, according to the manufacturer s protocol. Primer pairs (Table 1) were validated by serial cDNA dilutions, synthesized from Universal Human Reference RNA (Stratagene, La Jolla, CA) in 5x to 80x dilutions, in triplicate. The primer pairs were 100% efficient, in that the amount of DNA was doubled in each cycle. The PCR conditions were 95°C (3 minutes) and cycles of 95°C (15 seconds) and 60°C (30 seconds) in a 25-µL reaction mix containing 5 µL of cDNA, supermix (IQ SYBR Green; Bio-Rad, Hercules, CA), and 0.3 µM of each primer. For the actual qPCR experiment, cDNA was diluted twice to make sure that the threshold cycles (C_t) were within the range of the dilution curve. qPCR reactions were performed on a thermocycler (7500 fast real-time PCR system; Applied Biosystems) and quantification was performed using the $^{\Delta\Delta}C_t$ method.[23,24] *GUSB* was used as a reference gene to normalize expression levels of *CABP4*, as this gene is stably expressed in EBV-LCLs.[25] RNA of a patient with a p.Q66X mutation in *FTSJ1*, known to result in nonsense-mediated decay (NMD), was used as a positive control for the occurrence of NMD.[26] The qPCR experiment was repeated for both patients on RNA isolated from two independently grown EBV-LCLs to confirm the results of the first qPCR experiment.

Molecular modeling

Since no crystal structure for CaBP4 was known, we performed homology modeling to predict the effect of the genomic mutation. The C-terminal residues of CaBP4 were modeled on a structure of calmodulin (PDB identifier 1a29, 44% identity).[27] Modeling of the N-terminal residues of CaBP4 was not possible as the calmodulin template contains no structural information for these residues. Homology modeling was performed with the WHAT IF Web Interface.[28] The effect of the genomic mutation on the three-dimensional structure of the protein was analyzed with YASARA NOVA.[29]

TABLE 2. Characteristics of two patients with p.Arg216X mutations in the *CABP4* gene

Patient	Sex	Age (y)	Visual acuity		N*	Refractive error†		Color vision‡	Goldmann perimetry (V4e)	DA (log units) §
			OD	OS		OD	OS			
II-1	M	12	20/200	20/200	pos	+5.0	+5.5	severely abnormal (deutan)	normal	0.5
II-2	F	10	20/200	20/400	pos	+4.5	+4.5	severely abnormal (deutan)	normal	0.75

*N, nystagmus (pos, positive); †, spherical equivalent in diopters; ‡, Ishihara, AO-HRR, D-15 Test; §DA, dark adapted final threshold elevation; OD, right eye; OS, left eye.

RESULTS

Clinical features

A brother and sister, 12 (patient II-1) and 10 (patient II-2) years of age, respectively, presented with a history of decreased visual acuity and nystagmus since early childhood. The clinical characteristics of the patients are shown in Table 2. Both reported photophobia, but did not experience night blindness. Visual acuities had not changed over the past 6 years. Slit lamp examinations were unremarkable and funduscopy showed no abnormalities, except for a mild granular aspect of the peripheral retinal pigment epithelium in patient II-1. Dark-adaptation curves were biphasic with a slightly elevated final threshold. The standard ISCEV ERG measurements[16] of both patients are shown in Figure 1. The amplitude of the rod isolated (scotopic) responses were normal in patient II-1 (124 µV) and were 2 SD below the mean in patient II-2 (46 µV; normal >45 µV).[30] In both children, the mixed rod-cone responses had absent cone a-waves, and an electronegative configuration with absent b-waves. Cone responses were severely reduced and 30-Hz photopic flicker responses showed the double-peak waveform characteristic of CSNB2. Rod ERG responses to a 15-Hz flicker stimulation are shown in Figure 2. The measurements showed intact, slow, sensitive rod pathway responses, but no minimum ERG response or 180° phase shift, indicating absent or severely abnormal fast insensitive rod pathway responses.

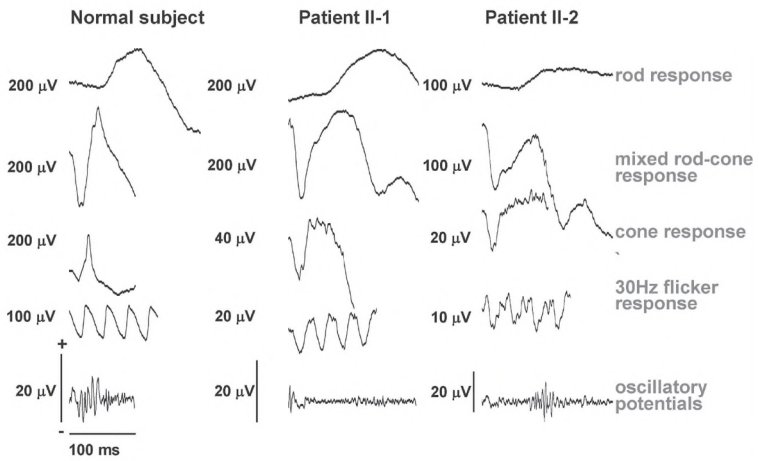

FIGURE 1. ISCEV standard ERG of a normal subject and patients II-1 and II-2. The amplitude of the rod response of patient II-1 was 124 µV and of patient II-2, 46 µV; normal is >45 µV.[30] In the mixed rod–cone responses, the a-wave in the normal subject contains two distinct peaks, one at 19 ms, supposedly the cone peak, and a later one at 24 ms, supposedly the rod peak. In both patients only one peak at 24 ms was distinguished. Therefore these mixed responses featured an absent cone a-wave, with a normal rod a-wave. The b-wave remained too small, resulting in a negative wave shape. Under photopic conditions, the b-wave amplitude was severely reduced but with normal implicit time in both patients. Photopic 30-Hz flicker stimulus revealed decreased amplitude with double peak waveform and normal implicit time. There were no recordable oscillatory potentials under scotopic conditions.

Genetic analysis

Genome-wide homozygosity mapping revealed two homozygous regions; a 9-Mb area on 11q13.1-q13.5 and a 4-Mb area on 6p22.1. The largest area comprised *CABP4*, a gene previously associated with CSNB.[1, 15] Sequence analysis of *CABP4* revealed a homozygous c.646C>T substitution in exon 4 in both patients, replacing an arginine residue at position 216 by a stop codon (p.Arg216X). In both parents this change was identified heterozygously (Figure 3). The mutation was not found in 300 alleles of ethnically matched control individuals. Jalkanen et al.[32] showed that a splice-site mutation in the *CACNA1F* gene, the causative gene for X-linked CSNB2, resulted in cone-rod dystrophy. *Cabp4*$^{-/-}$ mice show a progressive retinal phenotype. Therefore, Zeitz et al.[1] hypothesized that mutations in *CABP4* could also lead to cone-rod dystrophy. Sequence analysis of all coding exons of *CABP4* was performed on 85 patients affected with cone or cone-rod dystrophy. No mutations were found in these patients, indicating that mutations in *CABP4* are not a frequent cause of cone or cone-rod dystrophy.

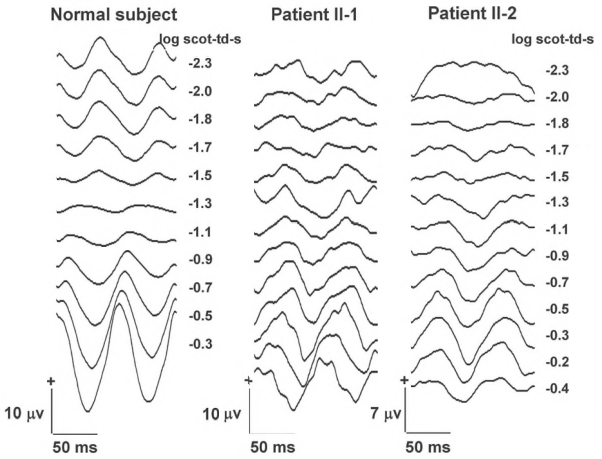

FIGURE 2. Rod ERG responses to 15-Hz flicker stimulation obtained from a normal subject and patients II-1 and II-2. Stimulus intensity was –2.3 log scot-td-s, increasing in steps of approximately 0.25 log scot-td-s up to 0.4 log scot-td-s. In the normal subject, the 15-Hz scotopic flicker ERG showed a minimum response at approximately –1.0 log scot-td-s, caused by destructive interference of the slow, sensitive (between –2.3 and –1.3 log scot-td-s) and fast, insensitive (above –0.9 log scot-td-s) rod pathway signals.[31] In both patients, the amplitudes of the slow, sensitive rod pathway signals were within normal limits. The fast, insensitive rod pathway signals appeared absent or severely subnormal, because no minimum response and phase shift was recorded. Furthermore, from –0.5 log scot-td-s up the amplitudes of the signals were subnormal.

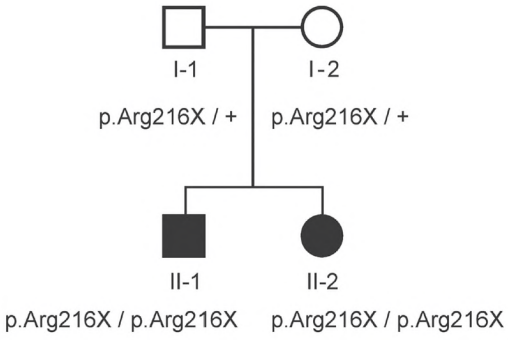

FIGURE 3. Pedigree of a Dutch family with two siblings affected with congenital synaptic cone–rod disorder, caused by a homozygous p.Arg216X mutation.
Black symbols: affected individuals

Expression analysis

Since the premature termination codon is localized more than 55 nucleotides upstream of the last exon-exon boundary (Figure 4), in theory the c.646C>T mutation should result in NMD.[33-35] Considering the absence of NMD as the null hypothesis, comparison of normalized expression levels of *CABP4* of the two patients with four control samples showed a nonsignificant 1.58-fold increase ($P = 0.58$, Student's *t*-test; unequal sample size, equal variance). Repetition of the experiment with RNA from independently grown lymphoblast cell lines confirmed these results and showed that NMD of *CABP4* mRNA of patients carrying a homozygous p.Arg216X mutation does not occur. Comparison of normalized levels of *FTSJ1* in the cDNA of a patient with a p.Q66X mutation in *FTJS1* to four control samples showed a 5.7-fold decrease in *FTSJ1* transcript in the patient ($P = 0.021$), showing that this experiment efficiently demonstrated NMD.

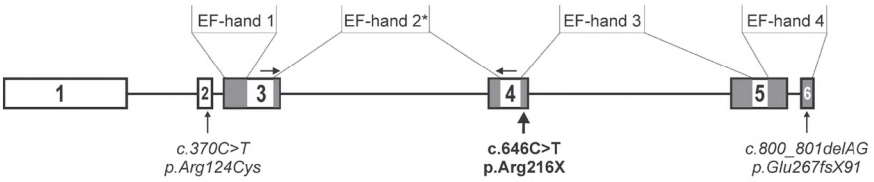

FIGURE 4. The *CABP4* gene. Boxes: exons; lines: introns; gray boxes: parts of the gene that encode the EF hands, the calcium-binding elements in CaBP4; arrows: the location of primers used for quantitative PCR analysis. In bold is the mutation described in this article and in italic are the previously identified mutations in *CABP4*.[1] *EF hand 2 is not functional.

Molecular modeling and structural analysis

Since the premature stop codon does not seem to result in nonsense-mediated degradation of the mutant *CABP4* mRNA, it is likely that a truncated CaBP4 protein of 216 amino acids is present. We predicted the characteristics of this truncated protein by constituting a molecular model, using the crystal structure of calmodulin (Figure 5). The modeled domain of CaBP4 contains important negatively charged residues that can bind Ca^{2+}. The location of these residues results in a typical helix-loop-helix structure, also known as an EF hand. The calmodulin template contains four of such EF hands, but because of the absence of an important negatively charged residue in the second EF hand the wild-type CaBP4 has only three functional calcium-binding EF hands.[15] The nonsense mutation described in this study deletes the functional EF hands 3 and 4 (Figure 5B). For calmodulin, it is known that all four EF hands must be present to fulfill its function.[36] Because of the functional and structural overlap between calmodulin and CaBP4,[15] we conclude that the mutant CaBP4, lacking two functional EF hands, is not able to fulfill its physiological function.

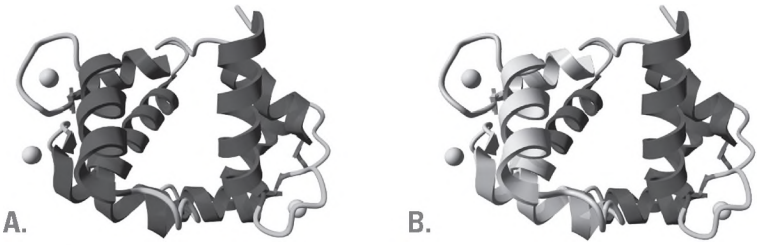

FIGURE 5. **CaBP4 protein model.** ***(See appendix for color figure)***
A. Ribbon model of the calcium binding domains in normal CaBP4.
B. Model showing the deleted calcium binding domains (gray). Yellow balls: calcium atoms.

DISCUSSION

Using a genome-wide homozygosity mapping approach, we detected a novel homozygous nonsense mutation (p.Arg216X) in *CABP4* in two siblings with a remarkable cone-dominated dysfunction. Patients presented with considerably reduced visual acuity at a young age, nystagmus, photophobia, and severely abnormal color vision. Mutations in *CABP4* have been associated with autosomal recessive incomplete congenital stationary night blindness (CSNB2). In two siblings diagnosed CSNB2, but without night blindness, Zeitz et al.[1] discovered a homozygous C-terminal frameshift mutation (p.Glu267fsX91) in the last protein-coding exon, effectively replacing the last 9 amino acids with 91 aberrant amino acids. In a third isolated patients with CSNB2 compound heterozygous (p.Glu267fsX91/p.Arg124Cys) mutations were found. *Cabp4*$^{-/-}$ mice carrying a homozygous null allele show a CSNB2-like phenotype. These mice showed a disturbed transmission of signals from rods and cones to bipolar cells with a more severely disturbed rod than cone function.[15] In contrast to findings in the *Cabp4*$^{-/-}$ mice, our patients with p.Arg216X mutations displayed a prominent cone dysfunction. The presence of this effect was deduced from clinical presentations as well as from ERG responses, which showed an absent cone a-wave in the mixed response and severely reduced amplitude in cone and 30-Hz flicker responses. The rods seemed to function nearly normal: scotopic ERG responses were normal to subnormal, dark-adapted thresholds were only minimally elevated, and patients did not experience night blindness. Another indication that cones were more affected than rods was seen in the 15-Hz flicker stimulation. The fast insensitive rod pathway uses the rod-cone gap junctions and the cone terminal synapse to transmit its signal to the bipolar cells, whereas the slow sensitive rod pathway transmits its signal directly to the rod bipolar cells.[37] Therefore, the combination

of a normal, slow, sensitive rod pathway response to 15-Hz flicker stimulation with an abnormal, fast, insensitive rod pathway response suggests an abnormal function of the cones and/or cone terminal synapses. While Morgans et al.[38] suggest that residual rod function in patients carrying mutations in *CACNA1F* is maintained because rods signal through the rod-cone gap junction, our electrophysiological data suggest that rod function in patients carrying *CABP4* gene mutations is to some extent reduced because of this pathway. In the two patients with the frameshift mutation described by Zeitz et al.,[1] no 15-Hz scotopic measurements, dark adaptometry, and color vision tests were performed, and no differentiation was made between the cone and rod a-wave at the mixed rod-cone ERG response. Therefore, we do not know to what extent the phenotypes of these patients are comparable to ours. The third patient in Zeitz et al.[1] did complain of night blindness and had a mildly elevated threshold on dark adaptometry (1 log unit). Comparison of all five patients described so far suggests that homozygous protein-truncating mutations (nonsense or frameshift) leads to a more severe phenotype, with a reduced visual acuity at a young age (20/100 around the age of 10 years), whereas the patient with a compound heterozygous frameshift/missense mutation showed a relatively preserved visual acuity (20/30 at age 15).[1] The phenotypical similarities in patients carrying protein-truncating mutations do not correspond with the different findings in mRNA expression levels found in Zeitz et al.[1] and in our study. Quantitative PCR analysis of the previously described mutations revealed a 30% to 40% residual amount of *CABP4* transcript in both a homozygous and a compound heterozygous patient,[1] despite the fact that the protein-truncating mutation resides in the last exon and therefore is theoretically not susceptible to nonsense mediated mRNA decay.[33-35] In view of the significant amounts of *CABP4* mRNA in both patients, these mutations could not be conclusively classified as null mutations. The mutation described in our study results in the truncation of the 59 (22%) most C-terminal amino acids. Based on the location of the p.Arg216X mutation in exon 4, the transcribed mRNA should theoretically be degraded through NMD.[33-35] Surprisingly, no difference in expression levels of *CABP4* was found in cDNA of our patients compared with cDNA of control individuals, indicating that NMD does not occur and suggesting the presence of *CABP4* transcripts. To explain why different amounts of *CABP4* mRNA can result in comparable retinal phenotypes, we hypothesize that the differentially truncated CaBP4 proteins both are degraded, or present in a nonfunctional form. Genotype-phenotype correlations based on EBV-LCL mRNA quantification, however, should be interpreted with caution, because *CABP4* mRNA stability may be different in peripheral blood cells versus retinal cells, and because *CABP4* mRNA levels in EBV-LCLs are quite low.

CaBP4 is expressed in the photoreceptor synaptic terminals, both in rods and cones, where it colocalizes and interacts with the α1-subunit of the L-type voltage-dependent calcium channels $Ca_v1.3$[39-41] and $Ca_v1.4$.[15] Although $Ca_v1.4$ channels are localized in the synaptic terminal of both cone and rod photoreceptors, $Ca_v1.3$ channels are only localized in the synaptic terminal of the cones.[38] On binding with these L-type voltage-dependent calcium channels, CaBP4 increases Ca^{2+} influx into the synapse, which increases the amount of neurotransmitter release.[15] The effect of CaBP4 on $Ca_v1.3$ and $Ca_v1.4$ channels, resulting in the maintenance of calcium influx through the channel, is achieved in different ways. In $Ca_v1.3$ channels CaBP4 inhibits a mechanism called calcium-dependent inactivation, a negative feedback mechanism activated by calmodulin that rapidly inactivates calcium channels when intracellular calcium concentrations are elevated.[40,42] $Ca_v1.4$ channels are not subject to this mechanism, but it has been suggested that CaBP4 increases calcium influx through $Ca_v1.4$ channels by shifting the channels to a hyperpolarized voltage.[15] Although CaBP4 interacts differently with the $Ca_v1.3$ and $Ca_v1.4$ channels and distribution of $Ca_v1.3$ and $Ca_v1.4$ channels differs among the synaptic terminals of rods and cones, it remains speculative why dysfunctional human CaBP4 has a stronger effect on cone function than on rod function.

In our young patients with short follow-up no definite conclusions about progression can be drawn. However, a progressive course of the disease was suggested by the fact that all three patients described by Zeitz et al.[1] had slowly progressive visual loss. Furthermore, more pronounced changes in the outer plexiform layer were seen in 6- to 8-months-old $Cabp4^{-/-}$ mice than in 2-month-old mice. The presence of both stationary and *progressive* phenotypes caused by mutations in one gene has been described for mutations in *CACNA1F*, causing both X-linked CSNB2 and progressive cone-rod dystrophy.[32] The absence of *CABP4* mutations in 85 patients from the Netherlands affected with cone or cone-rod dystrophy suggests that *CABP4* mutations are not a major cause for these progressive retinal dystrophies. Of interest, a slowly progressive form of autosomal recessive cone dystrophy has been described, with a rather similar, but milder phenotype than patients carrying mutations in *CABP4*. This disorder is caused by nonsense mutations in the *CACNA2D4* gene, which encodes the $\alpha_2\delta$-subunit of L-type voltage-dependent calcium channels. These patients presented with increasing photophobia and mildly decreasing visual acuity starting around age 30, and no night blindness. Their ERG showed mildly reduced isolated rod responses, electronegative mixed rod-cone responses, markedly diminished cone responses and the wave separation phenomenon at 30-Hz flicker stimulation.[43] Thus, genes

involved in the process of calcium influx in the synaptic terminal seem to lead to a spectrum of phenotypes affecting predominantly cones (*CACNA2D4* and *CABP4*)[1,43] or both rods and cones (*CACNA1F*)[6,11] in either a stationary or slowly progressive course.

In summary, we describe a novel homozygous nonsense mutation in *CABP4* in two siblings with a phenotype in which cones are predominantly affected. Based on the electronegative mixed rod-cone responses on ERG, the disorder has previously been classified as a form of CSNB2. However, four of five patients described with mutations in *CABP4* do not experience night blindness, and a stationary course of the disease is not completely evident. Furthermore, the clinical characteristics are more in agreement with a form of cone dystrophy, like the phenotype associated with mutations in *CACNA2D4*.[43] Moreover, the dysfunctional protein is localized within the photoreceptor synaptic terminal. Therefore, we propose to rename this phenotype congenital cone-rod synaptic disorder.

ACKNOWLEDGEMENTS

The authors thank the patients for their willingness to participate, Christel Beumer and Saskia van der Velde-Visser for technical assistance, and Erik Toonen for help on qPCR experiments.

REFERENCES

1. Zeitz C, Kloeckener-Gruissem B, Forster U, et al. Mutations in CABP4, the gene encoding the Ca2+-binding protein 4, cause autosomal recessive night blindness. Am J Hum Genet. 2006;79:657-667.

2. Carr RE. Congenital stationary nightblindness. Trans Am Ophthalmol Soc. 1974;72:448-487.

3. Dryja TP, Berson EL, Rao VR, Oprian DD. Heterozygous missense mutation in the rhodopsin gene as a cause of congenital stationary night blindness. Nat Genet. 1993;4:280-283.

4. Gal A, Orth U, Baehr W, Schwinger E, Rosenberg T. Heterozygous missense mutation in the rod cGMP phosphodiesterase beta-subunit gene in autosomal dominant stationary night blindness. Nat Genet. 1994;7:551.

5. Dryja TP, Hahn LB, Reboul T, Arnaud B. Missense mutation in the gene encoding the alpha subunit of rod transducin in the Nougaret form of congenital stationary night blindness. Nat Genet. 1996;13:358-360.

6. Bech-Hansen NT, Naylor MJ, Maybaum TA, et al. Loss-of-function mutations in a calcium-channel alpha1-subunit gene in Xp11.23 cause incomplete X-linked congenital stationary night blindness. Nat Genet. 1998;19:264-267.

7. Bech-Hansen NT, Naylor MJ, Maybaum TA, et al. Mutations in NYX, encoding the leucine-rich proteoglycan nyctalopin, cause X-linked complete congenital stationary night blindness. Nat Genet. 2000;26:319-323.

8. Yamamoto S, Sippel KC, Berson EL, Dryja TP. Defects in the rhodopsin kinase gene in the Oguchi form of stationary night blindness. Nat Genet. 1997;15:175-178.

9. Dryja TP, McGee TL, Berson EL, et al. Night blindness and abnormal cone electroretinogram ON responses in patients with mutations in the GRM6 gene encoding mGluR6. Proc Natl Acad Sci U S A. 2005;102:4884-4889.

10. Fuchs S, Nakazawa M, Maw M, Tamai M, Oguchi Y, Gal A. A homozygous 1-base pair deletion in the arrestin gene is a frequent cause of Oguchi disease in Japanese. Nat Genet. 1995;10:360-362.

11. Strom TM, Nyakatura G, Apfelstedt-Sylla E, et al. An L-type calcium-channel gene mutated in incomplete X-linked congenital stationary night blindness. Nat Genet. 1998;19:260-263.

12. Miyake Y, Yagasaki K, Horiguchi M, Kawase Y, Kanda T. Congenital stationary night blindness with negative electroretinogram. A new classification. Arch Ophthalmol. 1986;104:1013-1020.

13. Miyake Y, Horiguchi M, Ota I, Shiroyama N. Characteristic ERG-flicker anomaly in incomplete congenital stationary night blindness. Invest Ophthalmol Vis Sci. 1987;28:1816-1823.

14. Zeitz C, van Genderen MM, Neidhardt J, et al. Mutations in GRM6 cause autosomal recessive congenital stationary night blindness with a distinctive scotopic 15-Hz flicker electroretinogram. Invest Ophthalmol Vis Sci. 2005;46:4328-4335.

15. Haeseleer F, Imanishi Y, Maeda T, et al. Essential role of Ca2+-binding protein 4, a Cav1.4 channel regulator, in photoreceptor synaptic function. Nat Neurosci. 2004;7:1079-1087.

16. Marmor MF, Holder GE, Seeliger MW, Yamamoto S. Standard for clinical electroretinography (2004 update). Doc Ophthalmol. 2004;108:107-114.

17. Miller SA, Dykes DD, Polesky HF. A simple salting out procedure for extracting DNA from human nucleated cells. Nucleic Acids Res. 1988;16:1215.

18. Nannya Y, Sanada M, Nakazaki K, et al. A robust algorithm for copy number detection using high-density oligonucleotide single nucleotide polymorphism genotyping arrays. Cancer Res. 2005;65:6071-6079.

19. Little S. Amplification-refractory mutation system (ARMS) analysis of point mutations. Curr Protoc Hum Genet. 2001;Chapter 9:Unit 9.8.

20. Jaakson K, Zernant J, Kulm M, et al. Genotyping microarray (gene chip) for the ABCR (ABCA4) gene. Hum Mutat. 2003;22:395-403.

21. Rozen S, Skaletsky H. Primer3 on the WWW for general users and for biologist programmers. Methods Mol Biol. 2000;132:365-386.

22. Wall FE, Henkel RD, Stern MP, Jenson HB, Moyer MP. An efficient method for routine Epstein-Barr virus immortalization of human B lymphocytes. In Vitro Cell Dev Biol Anim. 1995;31:156-159.

23. Livak KJ, Schmittgen TD. Analysis of relative gene expression data using real-time quantitative PCR and the 2(-Delta Delta C(T)) Method. Methods. 2001;25:402-408.

24. Pfaffl MW. A new mathematical model for relative quantification in real-time RT-PCR. Nucleic Acids Res. 2001;29:e45.

25. de Brouwer APM, van Bokhoven H., Kremer H. Comparison of 12 reference genes for normalization of gene expression levels in Epstein-Barr virus-transformed lymphoblastoid cell lines and fibroblasts. Mol Diagn Ther. 2006;10:197-204.

26. Freude K, Hoffmann K, Jensen LR, et al. Mutations in the FTSJ1 gene coding for a novel S-adenosylmethionine-binding protein cause nonsyndromic X-linked mental retardation. Am J Hum Genet. 2004;75:305-309.

27. Haeseleer F, Sokal I, Verlinde CL, et al. Five members of a novel Ca(2+)-binding protein (CABP) subfamily with similarity to calmodulin. J Biol Chem. 2000;275:1247-1260.

28. Vriend G. WHAT IF: a molecular modeling and drug design program. J Mol Graph. 1990;8:52-6, 29.

29. Krieger E, Koraimann G, Vriend G. Increasing the precision of comparative models with YASARA NOVA- a self-parameterizing force field. Proteins. 2002;47:393-402.

30. van Genderen MM, Riemslag F, Jorritsma F, Hoeben F, Meire F, Stilma J. The key role of electrophysiology in the diagnosis of visually impaired children. Acta Ophthalmol Scand. 2006;84:799-806.

31. Scholl HP, Langrova H, Weber BH, Zrenner E, Apfelstedt-Sylla E. Clinical electrophysiology of two rod pathways: normative values and clinical application. Graefes Arch Clin Exp Ophthalmol. 2001;239:71-80.

32. Jalkanen R, Mantyjarvi M, Tobias R, et al. X linked cone-rod dystrophy, CORDX3, is caused by a mutation in the CACNA1F gene. J Med Genet. 2006;43:699-704.

33. Nagy E, Maquat LE. A rule for termination-codon position within intron-containing genes: when nonsense affects RNA abundance. Trends Biochem Sci. 1998;23:198-199.

34. Cheng J, Belgrader P, Zhou X, Maquat LE. Introns are cis effectors of the nonsense-codon-mediated reduction in nuclear mRNA abundance. Mol Cell Biol. 1994;14:6317-6325.

35. Zhang J, Sun X, Qian Y, Maquat LE. Intron function in the nonsense-mediated decay of beta-globin mRNA: indications that pre-mRNA splicing in the nucleus can influence mRNA translation in the cytoplasm. RNA. 1998;4:801-815.

36. Forsén S, Vogel H J, Drakenberg T Calcium and Cell Function (E. Chueng, ed). In: Academis Press, San Diego, CA; 1986:113-157.

37. Wässle H. Parallel processing in the mammalian retina. Nat Rev Neurosci. 2004;5:747-757.

38. Morgans CW, Bayley PR, Oesch NW, Ren G, Akileswaran L, Taylor WR. Photoreceptor calcium channels: insight from night blindness. Vis Neurosci. 2005;22:561-568.

39. Yang PS, Alseikhan BA, Hiel H, et al. Switching of Ca2+-dependent inactivation of Ca(v)1.3 channels by calcium binding proteins of auditory hair cells. J Neurosci. 2006;26:10677-10689.

40. Cui G, Meyer AC, Calin-Jageman I, et al. Ca2+-binding proteins tune Ca2+-feedback to Cav1.3 channels in mouse auditory hair cells. J Physiol. 2007;585:791-803.

41. Lee A, Jimenez A, Cui G, Haeseleer F. Phosphorylation of the Ca2+-binding protein CaBP4 by protein kinase C zeta in photoreceptors. J Neurosci. 2007;27:12743-12754.

42. Budde T, Meuth S, Pape HC. Calcium-dependent inactivation of neuronal calcium channels. Nat Rev Neurosci. 2002;3:873-883.

43. Wycisk KA, Zeitz C, Feil S, et al. Mutation in the auxiliary calcium-channel subunit CACNA2D4 causes autosomal recessive cone dystrophy. Am J Hum Genet. 2006;79:973-977.

Adapted from: *Investigative Ophthalmology & Visual Science.* 2010 Febr.

Karin W. Littink,[1,2] Jan-Willem R. Pott,[3] Rob W.J. Collin,[2,4,5] Hester Y. Kroes,[6] Joke B.G.M. Verheij,[7] Ellen A.W. Blokland,[2] Marta de Castro Miró,[2] Carel B. Hoyng,[5] Caroline C.W. Klaver,[8,9] Robert K. Koenekoop,[10] Klaus Rohrschneider,[11] Frans P.M. Cremers,[2,4] L. Ingeborgh van den Born[1] and Anneke I. den Hollander[4,5]

[1] The Rotterdam Eye Hospital, Rotterdam, The Netherlands; [2] Department of Human Genetics, Radboud University Nijmegen Medical Centre, Nijmegen, The Netherlands; [3] Department of Ophthalmology, University Medical Centre Groningen, Groningen, The Netherlands; [4] Nijmegen Centre for Molecular Life Sciences, Radboud University Nijmegen Medical Centre, Nijmegen, The Netherlands; [5] Department of Ophthalmology, Radboud University Nijmegen Medical Centre, Nijmegen, The Netherlands; [6] Department of Medical Genetics, University Medical Centre Utrecht, Utrecht, The Netherlands; [7] Department of Clinical Genetics, University Medical Centre Groningen, Groningen, The Netherlands; [8] Department of Ophthalmology and [9] Department of Epidemiology, Erasmus Medical Centre, Rotterdam, The Netherlands; [10] McGill Ocular Genetics Laboratory, Montreal Children's Hospital Research Institute, McGill University Health Centre, Montreal, Quebec, Canada, and [11] Department of Ophthalmology, University of Heidelberg, Heidelberg, Germany.

CHAPTER 4

A NOVEL NONSENSE MUTATION IN *CEP290* INDUCES EXON SKIPPING AND LEADS TO A RELATIVELY MILD RETINAL PHENOTYPE

ABSTRACT

PURPOSE. To identify the genetic defect in a family with variable retinal phenotypes. The proband had a diagnosis of Leber congenital amaurosis (LCA), whereas her two cousins had an early-onset severe retinal dystrophy (EOSRD) with useful vision. A distant family member was affected by retinitis pigmentosa (RP).

METHODS. DNA samples of the affected family members were genotyped with 250K genome-wide SNP microarrays. Genetic defects were localized by linkage analysis and homozygosity mapping, and candidate genes were analyzed by sequencing. Patients underwent a full ophthalmic examination.

RESULTS. Compound heterozygous mutations in *CEP290* were identified in the proband and her two cousins: the frequent c.2991+1655A>G founder mutation and a novel nonsense mutation in exon 7 (c.451C>T, p.Arg151X). The proband had nystagmus, hyperopia, a flat electroretinogram (ERG), and decreased visual acuity (20/250) from birth. The two cousins had minimal scotopic ERG responses at the age of 2. In one of these patients, visual acuity had reached a level of 20/32 at age 5, which is high for patients with *CEP290* mutations. Analysis of the *CEP290* mRNA in affected individuals revealed altered splice forms in which either exon 7 or exons 7 and 8 were skipped. In both mutant cDNA products, the open reading frame was not disrupted. Furthermore, homozygosity mapping and mutation analysis in the distant family member affected by RP revealed a homozygous mutation in *MERTK*, but no *CEP290* mutations. This *MERTK* mutation was heterozygously present in the most severely affected (LCA) patient, but was absent in the two more mildly affected cousins.

CONCLUSIONS. A novel nonsense mutation in *CEP290* results in nonsense-associated altered splicing. That the remaining open reading frame is intact may explain the less severe phenotype observed in the two affected cousins. The additional heterozygous mutation in *MERTK* may clarify the more severe phenotype in the proband. This study extends the phenotypic spectrum of *CEP290*-associated diseases at the mild end.

INTRODUCTION

Mutations in *CEP290* cause a broad spectrum of diseases, ranging from Meckel-Gruber syndrome (MKS), a lethal multisystemic disorder, and Joubert syndrome (JBTS) at the more severe end, to Leber congenital amaurosis (LCA), at the milder end of the clinical spectrum.[1-5] In addition, several families with Senior Løken syndrome (SLSN) and one case of Bardet-Biedl syndrome (BBS) have been associated with mutations in *CEP290*.[6,7] The *CEP290* gene encodes a ciliary and centrosomal protein that is present in cells of different tissues, explaining the variable set of symptoms, including renal abnormalities (MKS, JBTS, SLSN, and BBS), neurologic abnormalities (MKS, JBTS, and BBS), retinal degeneration (JBTS, SLSN, BBS, and LCA), and polydactyly (MKS and BBS).

CEP290-associated LCA is a single-organ disease affecting the retina.[4,5] Mutations in *CEP290* are the most common cause of LCA, responsible for up to 6% to 22% of cases.[4,5,8,9] A founder mutation in intron 26 (c.2991+1655A>G), leading to the insertion of a cryptic exon with a premature stop codon, is the most prevalent *CEP290* mutation in LCA patients.[4,10] Since a fraction of wild-type *CEP290* mRNA remains in patients carrying the intronic mutation, it is hypothesized that this hypomorphic character of the mutation explains why the mutation leads to LCA, instead of a multiorgan disease.[4] The *CEP290*-associated retinal phenotype is classified by Perrault et al.[5] as a cone–rod type of LCA (type I as classified by Hanein et al.[11]), with a visual acuity of 20/400 or lower, high hyperopia (+6 or more), slight photo-aversion, and a salt-and-pepper appearance of the retina, with macular degeneration in the first decade, changing to the typical appearance of retinitis pigmentosa (RP) at later stages.[5] In this study, we examined three patients with a LCA-like phenotype. However, two of them retained useful vision, and we therefore classified their disease as early-onset severe retinal dystrophy (EOSRD), which is considered to be milder than LCA. The less severe phenotype is caused by a novel nonsense mutation that induces exon skipping without disrupting the open reading frame. In addition, we report on the finding that one individual with the same set of *CEP290* variants showed an LCA phenotype, which may be caused by the cumulative effect of a heterozygous *MERTK* frameshift mutation.

METHODS

This study was approved by the ethics review board of The Rotterdam Eye Hospital and adhered to the tenets of the Declaration of Helsinki. Informed consents were signed by all participants and, in the case of minors, by their parents.

Clinical evaluation

The affected individuals (VI-3, VI-4, and VI-6; Figure 1) visited the University Medical Centre Groningen for the first time at the age of 6 months and were seen for follow-up examinations regularly thereafter for up to 11 years. The examinations included electroretinograms (ERGs), recorded according to the protocol of the International Society for Clinical Electrophysiology of Vision (ISCEV).[12] The three patients were clinically re-evaluated at The Rotterdam Eye Hospital recently. Parents were extensively interviewed about the medical history of their children. Clinical evaluation included best corrected visual acuity using ETDRS charts and was expressed as Snellen equivalents, objective refractive error after cycloplegia, biomicroscopy, and fundoscopy. Visual fields were assessed with Goldmann kinetic perimetry (targets V-4e to I-4e for patients VI-3 and VI-4, and V-4e to II-4e for patient VI-6). Color vision was tested with the American Optical Hardy-Rand-Rittler Test (AO-HRR) and the Farnsworth Panel D-15 Test (saturated and desaturated) in all patients and by the Ishihara Test for Color Blindness in patient VI-4. Additional tests included fundus photography and spectral domain optical coherence tomography (OCT; Spectralis; Heidelberg Engineering, Heidelberg, Germany) for evaluating the in vivo retinal structure. Autofluorescence images (30°) were obtained with a confocal scanning laser ophthalmoscope with 488-nm excitation (Retinogram Angiograph 2; Heidelberg Engineering, Heidelberg, Germany) to detect alterations of the retinal pigment epithelium and lipofuscin accumulation. Kidney function was assessed by serum analyses of sodium, potassium, and creatinine levels. A magnetic resonance imaging (MRI) scan of the brain was performed in patient VI-3 to exclude brain abnormalities, including the molar tooth sign typical of JBTS. Electroretinography was repeated in patient VI-3. Ophthalmic examination and ERG were also performed in the parents to search for clinical abnormalities in mutation carriers.

Molecular genetic analysis

Blood samples for molecular genetic analysis were obtained from all family members (Figure 1). Total genomic DNA was extracted from leukocytes by a standard salting-out procedure.[13] DNA samples of the affected subjects, including a distant family member affected by RP (VI-3, VI-4, VI-6, and V-1; Figure 1), were genotyped for 262,000 single nucleotide polymorphisms (SNPs; GeneChip Mapping 250K *Nsp*I array; Affymetrix, Santa Clara, CA). Array experiments were performed according to protocols provided by the manufacturer. Multipoint linkage analysis was performed with GeneHunter ver. 2.1r5[14] in the easyLINKAGE-Plus software package,[15] with use of the Caucasian allele frequencies. Homozygosity mapping was performed with the software package CNAG.[16] Mutation analysis of the *CEP290* gene was performed

using previously described PCR primers and conditions.[1] Primers for the *MERTK* gene were designed by primer3 software[17] and are listed together with the PCR conditions in Supplementary Table S1. Direct sequencing was performed in sense and antisense direction on an automated sequencer (BigDye Terminator, ver. 3, model 3730 DNA analyzer; Applied Biosystems, Inc. [ABI], Foster City, CA). Segregation analysis of the *CEP290* and *MERTK* mutations in all family members was performed by sequencing. Eighty-five LCA patients and 123 patients affected by cone–rod dystrophy (CRD) were screened for the *CEP290* c.2991+1655A>G mutation by allele-specific PCR[18] and for the p.Arg151X mutation by restriction fragment length polymorphism analysis using *Taq*I (ABI; Supplementary Table S1). To determine the effect of p.Arg151X on the *CEP290* mRNA level, we collected blood samples (PAX vials; Qiagen, Venlo, The Netherlands) of the three affected children (VI-3, VI-4, and VI-6, Figure 1) and six control individuals and isolated the RNA (PAXgene Blood RNA kit 50 ver. 2; Qiagen) according to the protocol provided by the manufacturer. Total RNA (1.5 μg) was reverse transcribed

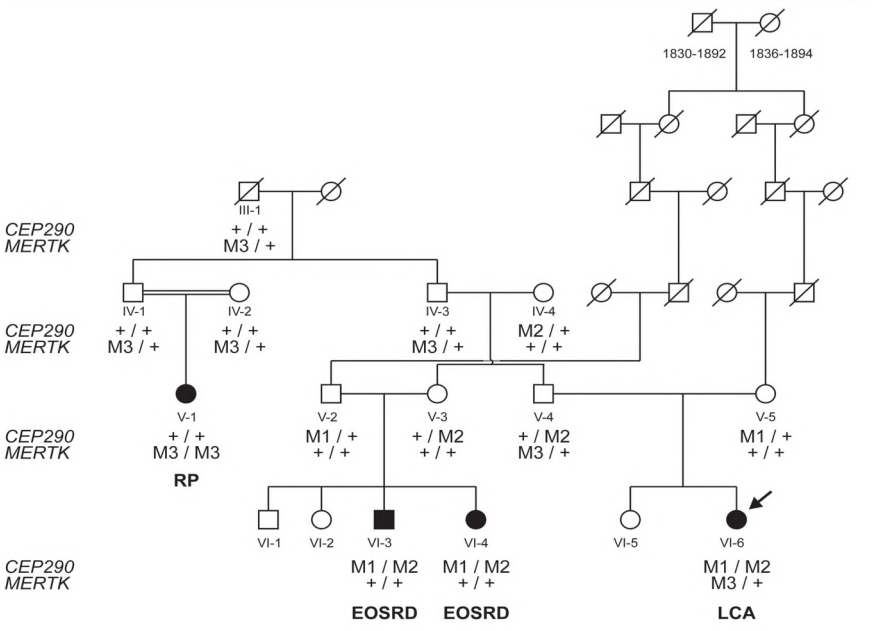

FIGURE 1. Pedigree with inherited retinal diseases and pathologic *CEP290* and *MERTK* variants. The proband (VI-6; arrow) is affected by LCA, two cousins (VI-3 and VI-4) are affected by EOSRD, and one distant family member (V-1) is affected by RP. Mutations in *CEP290* and *MERTK* are indicated. For reasons of privacy, mutations in the unaffected siblings are not presented. M1, *CEP290* c.451C>T, (p.Arg151X; Δexon7; Δexons7-8); M2, *CEP290* c.2991+1655A>G (p.Cys998X;wildtype); and M3, *MERTK* c.1179dup, p.Leu394SerfsX3; +, wild-type.

to cDNA with M-MLV reverse transcriptase (Invitrogen, Breda, The Netherlands). RT-PCR experiments were performed on 2.5 µL of synthesized cDNA or human retina Marathon-Ready cDNA (Clontech, Temecula, CA), with primers in exon 5 and 10 (35 cycles), followed by nested PCR on 0.5 µL, with the same forward primer in exon 5 and a reverse primer in exon 9 (15 cycles; Supplementary Table S1).

RESULTS

Clinical features

Individuals VI-3, VI-4, and VI-6 visited the ophthalmologist within 6 months after birth because of nystagmus and lack of fixation. Ophthalmic assessment revealed a vertical nystagmus, normal pupil responses, a high hyperopia, and essentially normal-appearing fundi. In all three individuals, ERG was performed at the age of 2 years. In patient VI-6, both scotopic and photopic responses were nonrecordable. In patients VI-3 and VI-4, photopic responses were nonrecordable, whereas the scotopic responses were severely reduced, but measurable (15% of normal values). Patient VI-3 was evaluated by a pediatric neurologist because of the vertical nystagmus, but intracranial abnormalities were excluded by neurologic assessment and by an MRI scan of the brain. The patients' histories did not reveal any abnormalities about pregnancy and delivery. Beside the ophthalmic symptoms, no other abnormalities in motor or cognitive development were reported, and their intelligence was normal. An overview of the most recent clinical data is presented in Table 1. In summary, all three patients experienced night blindness and no photophobia. Patients VI-4 and VI-6 displayed mild exotropia. Visual acuity varied from 20/40 in the best eye of patient VI-3 to 20/125 in patient VI-4 and 20/250 in patient VI-6 at ages 11, 8, and 9, respectively (Figure 2).

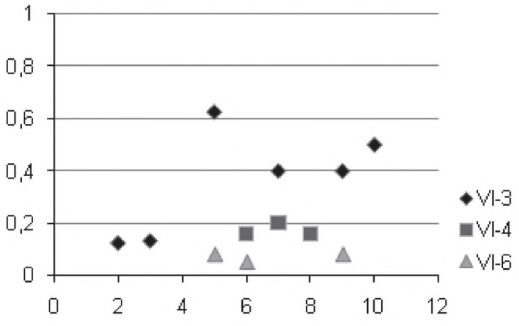

FIGURE 2. Visual acuity of patients with EOSRD and LCA. The course of visual acuity is shown in decimals (y-axis) with age (x-axis) in patients VI-3 and VI-4 (EOSRD) and patient VI-6 (LCA). The improvement in visual acuity at age 5 in patient VI-3 is most likely the effect of better performance at visual acuity assessment.

TABLE 1. Clinical characteristics of three patients with mutations in the *CEP290* gene

Patient	Age (yrs)	Nystagmus	Visual acuity		Refractive error*		Color vision†	Ophthalmoscopy	Goldmann perimetry	ERG	
			RE	LE	RE	LE				Rod‡	Cone§
IV-3	11	Mild horizontal with slightly rotating component	20/80	20/40	+8.75	+8.75	Sat.: normal Desat: mild aspecific errors	Pink optic disc with scleral rim, mild attenuation of vessels, absent macula and fovea with subtle RPE changes. Faint white patchy reflex in midperiphery, dot-like RPE atrophy in far periphery, no intraretinal pigment	Horizontally constricted field up to 50-60 degrees (15 degrees nasally, 50 degrees temporally)	NR	NR
IV-4	8	Horizontal with rotating component	20/100	20/100	+7.75	+7.75	Normal	Pink optic discs with scleral rim, mild attenuation of the vessels, present foveal reflex, mild wrink-ling ILM. In midperiphery normal aspect of RPE, far periphery dot-like RPE atrophy with small nummular subretinal pigmentations, no intraretinal pigment	Constriction up to 80 degrees (10 degrees nasally, 70 degrees temporally	NP1	NP1
IV-6	9	High frequency horizontally and vertically	20/320	20/250	+4.5	+4.5	NP2	Pink optic discs with scleral rim, mild/moderate attenuation of the vessels, absent foveal and macular reflexes, RPE changes in macula, hypopigmented periphery with dot-like RPE atrophy and intraretinal pigmentations	Severely constricted visual field up to 10 degrees	NP1	NP1

*, spherical equivalent in diopters; †, saturated (sat.) and desaturated (desat.) AO-HRR, Panel D-15 Test; ERG, electroretinogram; ‡, isolated rod response; §, single flash cone response; ILM, inner limiting membrane; LE, left eye; NP[1], not performed at this age, because non-responsive at earlier age; NP[2], not able to perform due to low visual acuity; RE, right eye; RPE, retinal pigment epithelium.

On fundoscopy the posterior retina was relatively well preserved in all three patients, with pink optic discs with a scleral rim, attenuated retinal vasculature, and subtle retinal pigment epithelium (RPE) changes in the macular region. In patient VI-3, we found the remnants of a tapetal reflex that had a marbled appearance. This reflex was more pronounced at the age of 5 years and was documented on fundus photographs (Figures 3A, 3B). In the far periphery, subretinal pigmentations were noted in patients VI-3 and VI-4. The periphery in patient VI-6 had a very hypopigmented appearance with intraretinal bone spicule pigmentations (Figure 3E). Visual fields were constricted in all patients, but most severely in VI-6, who was also not able to perform a color vision test. On OCT a preserved photoreceptor layer was noted in the posterior pole in the two patients tested (VI-3 and VI-4; Figure 3D).

Autofluorescence images, which were difficult to obtain because of the nystagmus, showed a mildly reduced intensity of the signal in the posterior pole and midperiphery, with a normal decrease of intensity at the macular region in all three individuals (Figure 3C). Altogether, the phenotype of the proband (VI-6) was most similar to LCA. The phenotype of the two more mildly affected cousins (VI-3 and VI-4) was classified as EOSRD, to emphasize the fact that they were less severely affected.

Ophthalmic examination did not reveal abnormalities in three of four heterozygous carrier parents. In one parent, we detected a choroidal melanoma (V-2; Figure 1). The ERG responses were in the high range of normal in three of the parents (V-3, V-4, and V-5) and completely normal in parent V-2.

Molecular genetics

Genome-wide linkage analysis was performed on DNA of the proband (VI-6) and her two cousins (VI-3 and VI-4). The family, originating from a northern province in The Netherlands, was reported to be non-consanguineous. However, the patients were related through both parental lineages: they were first cousins through one parent and fourth cousins through the other (Figure 1). Linkage analysis revealed only one significant chromosomal region, which localized between SNPs rs10879550 and rs1579244 on 12q21.1-q23.1, with a LOD score of 2.4. The region harbored 68 genes, among which we found *CEP290*, making this the most obvious candidate gene in this family. Mutation analysis of the *CEP290* gene revealed a compound heterozygous combination of the most common *CEP290* founder mutation in intron 26 (c.2991+1655A>G)[4] and a novel nonsense mutation in exon 7 (c.451C>T; p.Arg151X). The mutations segregated with the disease in the family (Figure 1). The deep intronic c.2991+1655A>G variant creates a functional 5′ splice site and the insertion of

a cryptic exon into approximately 50% of the *CEP290* mRNA.[4] The cryptic exon contains a nonsense codon (p.Cys998X), resulting in a predicted truncation of the *CEP290* protein. As ~50% of the *CEP290* mRNA remains wild-type, the c.2991+1655A>G variant can be considered a hypomorphic change.[4] Because patients VI-3 and VI-4 had residual rod function and non-detectable cone ERGs at the age of 2 years, we screened 123 patients affected by CRD for both these *CEP290* mutations.

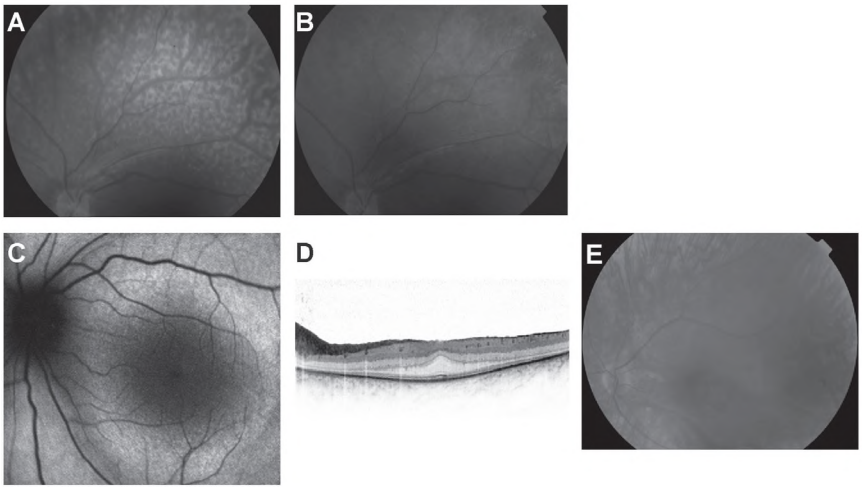

FIGURE 3. Retinal imaging of patients VI-3 and VI-6. ***(See appendix for color figure)***
A. Photograph of the midperipheral fundus of patient VI-3 at the age of 5, showing a marbled appearance. **B.** Fundus photograph of the same patient VI-3 at the age of 11, which shows that the marbled appearance had disappeared, and mild atrophy of the RPE was noted. **C.** Mean autofluorescence image (30°) of the left eye of patient VI-3, calculated from 12 single images (488 nm), showing a well preserved signal in the posterior pole with decreased intensity in the macular region. **D.** Spectral domain OCT of the left eye of patient VI-3 at the age of 11 shows a recognizable photoreceptor layer, intact retinal layers, and disappearance of the foveal dimple. **E.** Fundus photograph of left eye of patient VI-6, showing preserved RPE in the macular region with an extremely hypopigmented area along the vascular arcade, which extends to the periphery.

In addition, 85 LCA patients in whom the c.2991+1655A>G mutation was previously excluded[4] were screened for the p.Arg151X mutation. The c.2991+1655A>G and p.Arg151X mutations were not detected in additional CRD or LCA probands. The novel p.Arg151X mutation was also excluded in 182 alleles of ethnically matched control subjects. Usually, the combination of a hypomorphic change and a truncating change would lead to a LCA phenotype. Since the phenotypes in VI-3 and VI-4 were much

less severe than typical LCA, we hypothesized that the p.Arg151X mutation should have a hypomorphic character. Therefore, using RT-PCR we analyzed *CEP290* mRNA in peripheral blood lymphocytes of the affected children (VI-3, VI-4, and VI-6) and six control individuals. Although splice site and exonic splice enhancer site prediction software[19,20] did not predict an effect on the splicing process, we identified three different RT-PCR products in heterozygous carriers of p.Arg151X when using a forward primer in exon 5 and a reverse primer in exon 10 (Figure 4). One product represented normally spliced mRNA, in which only a minimal fraction of the mutated T-allele was present (Figure 4C). The second PCR product (282 bp) lacked exon 7, and the third product (261 bp) lacked exons 7 and 8 (Figure 4). The removal of exon 7 or exons 7 and 8 does not disrupt the open reading frame. These alternatively spliced products were not detected in six control individuals. It was also not present in human retina cDNA (data not shown). In patients as well as control individuals, we found a weak-intensity PCR product lacking exon 6.

Homozygosity mapping in the distantly related RP patient (V-1; Figure 1) revealed several homozygous segments (Collin et al., manuscript in preparation). Sequence analysis of *MERTK*, a known RP gene located within the patient's largest homozygous region, revealed a homozygous frameshift mutation (c.1179dup, p.Leu394SerfsX3). This mutation was identified heterozygously in the most severely affected (LCA) patient (VI-6) and was not identified in the more mildly affected (EOSRD) patients (VI-3 and VI-4; Figure 1).

DISCUSSION

Using linkage analysis in a family with one proband affected by LCA and her two cousins affected by EOSRD, we localized the genetic defect on 12q21 and detected compound heterozygous mutations in *CEP290* (c.2991+1655A>G and c.451C>T, p.Arg151X). The intronic mutation is known as the most prevalent LCA-causing mutation in *CEP290*.[4,5] The nonsense mutation p.Arg151X has not been described before. The phenotype of the LCA patient was comparable to the *CEP290*-LCA patients previously described[4,5] and consisted of nystagmus, high hyperopia (+4.5 D), night blindness, reduced visual acuity from birth (20/250), fundus abnormalities, and nonrecordable electrophysiological responses. The phenotypes of the two affected cousins were comparable, but less severe, with minimal measurable scotopic responses on ERG and a more functional visual acuity. Lorenz et al.[21] coined the name early-onset severe rod–cone dystrophy to distinguish between true LCA and relatively

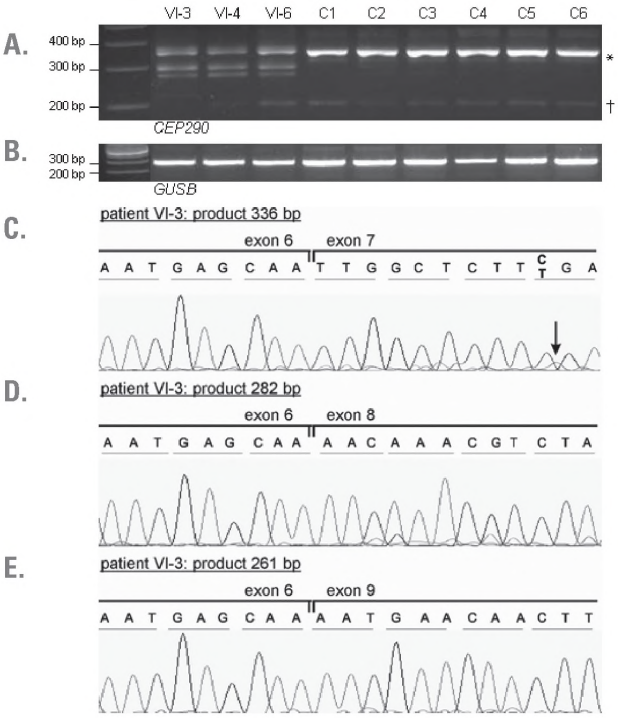

FIGURE 4. ***CEP290*** **cDNA analysis of the effect of the c.451C>T variant on splicing.**
(See appendix for color figure)

A. Agarose (3%) gel electrophoresis showing three major PCR products in carriers of p.Arg151X and one major product in the six control individuals. **B.** Agarose gel electrophoresis showing *GUSB* as the reference gene product. C–E. PCR sequences of cDNA of patient VI-3 (*CEP290* c.451C>T/c.2991+1655A>G), showing **(C)** mRNA containing all exons, but showing a low peak for the mutant heterozygous T at position 451 (arrow). **(D)** mRNA missing exon 7, and **(E)** mRNA missing exons 7 and 8. *Low-intensity product could not be amplified for sequence analysis. Based on the size, it could contain the *CEP290* mRNA lacking exon 8 only, which should be 315 bp; †low-intensity product ~200 bp was analyzed by sequence analysis and appeared to be the *CEP290* mRNA lacking exon 6 only (192 bp). Since *CEP290* lacking exon 6 is present in patients as well as control individuals, it appears to be a normal splice variant.

less severe phenotypes as, for example, observed in patients carrying mutations in *RPE65*. Comparably, we decided that the classification EOSRD would be a more appropriate description of the phenotype of the two affected cousins. That we found a remnant of rod function at the age of 2 years in these two patients suggests that *CEP290*-associated LCA is of the cone–rod type as observed by Perrault et al.[5] On the other hand, visual acuity and color vision were relatively well preserved, suggesting

the opposite. An interesting finding was the marbled appearance of the fundi, which seemed to disappear with age, in patient VI-3. A similar appearance of the fundus was seen in two other patients carrying mutations in *CEP290* (L. Ingeborgh van den Born, personal observation). Perrault et al.[5] showed a similar fundus as well and called it "white dots." The etiology of this fundus abnormality remains unclear, but tapetal reflexes can be pathognomonic for certain diseases, as has been observed in carriers of *RPGR* mutations.[22] The marbled appearance of the fundus may be pathognomonic for the *CEP290*-associated phenotype.

In contrast to the previously described *CEP290*-associated phenotype, we determined a visual acuity that is remarkably high compared with most patients carrying mutations in *CEP290*, especially in patient VI-3 (20/40 at age 11). A well-preserved visual acuity has been reported previously in 4 patients of the 77 *CEP290*-LCA patients who have been described clinically (18 patients from Yzer et al., manuscript in preparation).[4,5,10] Three patients carried the c.2991+1655A>G variant homozygously and had visual acuities of 20/80 and 20/150 at age>40[4] and 20/50 at age 20.[10] One patient carried the c.2991+1655A>G mutation together with a c.5668G>T (p.Gly1890X) nonsense mutation and had a visual acuity of 20/50 at age 19.[10] In most patients, however, the visual acuity ranged from no vision at birth to a maximum of 20/400, as shown in 47 patients by Perrault et al.[5] and in the 18 patients evaluated by Yzer et al. (manuscript in preparation). We hypothesize that the mild phenotype in the two cousins described in this study can be explained by the fact that they carry two mutations with a relatively mild effect on the protein. First, the c.2991+1655A>G mutation affects only part of the mRNA; part of the wild-type mRNA remains present as shown by den Hollander et al.[4] Second, the allele carrying the p.Arg151X mutation is differentially spliced, lacking exon 7 or exons 7 and 8, but remain in frame.
The low peak of the mutated T nucleotide in the mRNA (Figure 4) shows that most of the differentially spliced *CEP290* results from the mutated allele. Usually, the presence of a premature termination codon (PTC) leads to nonsense-mediated mRNA decay, a process that results in the degradation of nonsense-containing mRNAs.[23-25]
We suggest that the different splice products are the result of nonsense-associated altered splicing (NAS), a putative correction mechanism that recognizes an exon with a PTC, and excludes that exon from the mature mRNA.[26-29] One form of NAS is due to the disruption of an exonic splice enhancer (ESE) by a mutation. Since the ESE finder program[20] does not predict a disruption of an ESE, NAS is likely to occur specifically due to the nonsense character of the p.Arg151X mutation. The precise mechanism is not well understood yet.[30] Exons 3 to 17 of the *CEP290* protein are predicted to encode a coiled-coil domain of 506 amino acids. The protein sequences lacking the 18 or 25

amino acids encoded by exon 7 or by exons 7 and 8 are still predicted to encode a coiled-coil domain that is only slightly shorter than the wild-type coiled-coil domain. Therefore, we hypothesize that the altered spliced products encode a stable protein with residual function, resulting in a relatively mild phenotype. Because of technical limitations, it is difficult to quantify the amount of mutant mRNA that is subjected to NAS. Since the mutant splice products are smaller than the wild-type product, they will be amplified more efficiently. In addition, we cannot be certain that the analysis of lymphoblast mRNA is representative of the in vivo situation in the retinas of these patients.

The three patients in this study showed an intrafamilial phenotypic variability that led to different clinical diagnoses. Intrafamilial variability has been reported before in a family with four patients carrying homozygous c.2991+1655A>G mutations.[4] Since the amount of wild-type *CEP290* product, quantified in lymphoblast RNA, was comparable in all patients of that family (data not shown), another variant in other gene(s) may influence the phenotype and the intrafamilial variability. In the family described in this study, the intrafamilial variability between the proband and her two cousins may be explained by the heterozygous p.Leu394SerfsX3 mutation in the *MERTK* gene, which was present in the LCA patient (VI-6) and absent in the two EOSRD patients (VI-3 and VI-4). *MERTK* is associated with autosomal recessive RP[31-33] and is strongly expressed in the RPE and macrophages, where it plays a role in the RPE phagocytosis process.[34] *CEP290* is localized in the connecting cilia of photoreceptors and is suggested to play a role in microtubule-associated protein transport in the cilia.[2, 3, 35] In view of the difference in function and localization, a physical interaction between these proteins seems unlikely. Moreover, one *MERTK* p.Leu394SerfsX3 mutation and one *CEP290* c.2991+1655A>G mutation together do not lead to symptoms of retinal dystrophy (in individual V-4). In addition, human and murine carriers of heterozygous pathogenic *MERTK* mutations do not show signs of retinal dystrophy as well. However, cultured RPE cells from the RCS rats that carry a homozygous truncating deletion in *MERTK* in vitro phagocytose only a few photoreceptor outer segments, in contrast to wild-type cells, in which many phagosomes appear.[36] Therefore, RPE cells with only 50% of the amount of functional MER tyrosine kinase receptor may have a lower turnover of photoreceptor outer segment phagocytosis, which does not have a measurable pathogenic effect in otherwise healthy individuals, but could have a cumulative (or modifying) effect in patients in whom the production of photoreceptor outer segments is disturbed, in this case by two pathogenic mutations in *CEP290*. The phenomenon of modifier alleles has been described more often – for example, tri-allelic mutations resulting

in a more severe phenotype in Bardet-Biedl patients and a modifier *RPGRIP1L* allele that is suggested to result in a more severe retinal phenotype in ciliopathies.[37,38] Nevertheless, it remains speculative whether the *MERTK* mutation functions as a modifier allele. The a priori chance for an individual to carry a pathogenic mutation in a retinal dystrophy gene is ~10%, assuming that there are 67 autosomal recessive retinal dystrophy genes that all account for a similar proportion of cases, as calculated by Rivolta et al.[39] in 2002. Currently, 44 nonsyndromic autosomal recessive retinal dystrophy genes have been identified (http://www.sph.uth.tmc.edu/retnet) that account for ~50% of cases, indicating that the calculation of Rivolta et al.[39] could be realistic. Therefore, we estimate that 10% of retinal dystrophy patients are expected to carry a heterozygous mutation in a second gene. Eventually, the identification of combinations of mutations in more than one retinal dystrophy gene by next-generation sequencing, together with a precise description of phenotypes, may uncover the unknown influences of additional heterozygous mutations.

In conclusion, we found a novel nonsense mutation in exon 7 of *CEP290* that causes a milder phenotype than expected for an early nonsense mutation, most likely due to nonsense-associated altered splicing. Furthermore, we detected a heterozygous *MERTK* mutation in the most severely affected patient that may have a deteriorating effect on the phenotype. In this study, we extended the phenotypic spectrum of *CEP290*-associated diseases at the mildest end.

ACKNOWLEDGMENTS

The authors thank the patients for their willingness to participate; Christel Beumer, Saskia van der Velde-Visser, and Marijke Zonneveld-Vrieling for technical assistance; Peter van Etten and Josine van der Schoot for help on the clinical assessments; and Linda Meiners for evaluating the brain MRI scan in detail. This study was supported by the Stichting Wetenschappelijk Onderzoek Oogziekenhuis Prof. Dr. H.J. Flieringa Foundation, The Rotterdam Eye Hospital (Grant 2005-13); the Netherlands Organization for Scientific Research (Grant 916.56.160); Foundation Fighting Blindness, Owings Mills MD (Grant BR-GE-0507-0381-RAD); the Landelijke Stichting voor Blinden en Slechtzienden; and the Algemene Nederlandse Vereniging ter Voorkoming van Blindheid.

SUPPLEMENTAL DATA

SUPPLEMENTAL TABLE 1. Primers used for sequence analysis of *MERTK*, mutation-specific PCR of the *CEP290* c.2991+1655A>G mutation, PCR for c.451C>T restriction fragment length polymorphism analysis and cDNA PCRs of the *CEP290* mRNA.

Primer *MERTK*	Sequence 5′ - 3′	Size (bp)	PCR mix	Annealing temperature
exon 1 forward	GCCACTCGGCACTCACTG	258	GC rich PCR System	58° C
exon 1 reverse	AGAGGCCCCTGCTTCCTC			
exon 2 forward	CCTAAGAAGTTGGGAACCTAC	586	3 mM MgCl2	58° C
exon 2 reverse	CTGGGCTACAGAATGATACTC			
exon 3 forward	AGTTGAAGAAGTTTCCATCC	241	3 mM MgCl2	58° C
exon 3 reverse	ATTTAACACAGGCCCTAAAAC			
exon 4 forward	GGCTCTGTCTCTGTTTTCAG	294	3 mM MgCl2	58° C
exon 4 reverse	GCCAAACTTTTGATCCTGTC			
exon 5 forward	AGAATTGTAGTGAACAGCAGC	217	3 mM MgCl2	58° C
exon 5 reverse	GCAAGCTCATGCTGTACC			
exon 6 forward	GGTAGCTGTAGCCTGTCATC	247	3 mM MgCl2	58° C
exon 6 reverse	AATCCTTAAACCCACAGAGAG			
exon 7 forward	CCTGACATTCCCACCAC	302	3 mM MgCl2	58° C
exon 7 reverse	GGAAGGGTTTGTTGAATCAC			
exon 8 forward	AAAACCAAACACTTGAAAACC	292	3 mM MgCl2	58° C
exon 8 reverse	ACCAGCAAGTTGAAAGGAG			
exon 9 forward	CAGTTTGCCCAGACCTC	282	3 mM MgCl2	58° C
exon 9 reverse	CAGGTTACTTTCTGGCAATC			
exon 10 forward	TGTTACAAGCCAGTGTTTCTC	294	3 mM MgCl2	58° C
exon 10 reverse	AACAGGAAAGGCATAATCAC			
exon 11 forward	GAAGCTCTGTAGCATCCTTG	235	3 mM MgCl2	58° C
exon 11 reverse	TGATCCTTCTTTGTTCTCAAC			
exon 12 forward	TTATCAAGTGAAAGAAAACACG	371	3 mM MgCl2	58° C
exon 12 reverse	TGTATGTGCTAGGCATTGAAG			
exon 13 forward	CACTGTAGCATTTCTGTGGTC	209	3 mM MgCl2	58° C
exon 13 reverse	ACCCAATACTGAAGCAACTG			
exon 14 forward	ACCCACTCCCCTTAATTG	211	3 mM MgCl2	58° C
exon 14 reverse	CACAGAGCAGATCAGCAG			
exon 15 forward	CGAGGGCTTTTCTGGTC	259	3 mM MgCl2	58° C
exon 15 reverse	TTAGATGATTTGGTTGTCCTG			
exon 16 forward	AACTGCTTGCAAGTTTTCC	247	3 mM MgCl2	58° C
exon 16 reverse	AGGTCCTCTCACTAACCCTG			
exon 17 forward	GACCAGTAATTTAAGGCATTG	285	3 mM MgCl2	58° C
exon 17 reverse	GTCATTTCTTTCAATATGCCC			
exon 18 forward	AAAGTCCATTCAGGCTTTG	279	3 mM MgCl2	58° C
exon 18 reverse	CTGTGTTTCCGAGGTCAG			
exon 19 forward	AATGAATGCTGATTAAAATGTG	688	3 mM MgCl2	58° C
exon 19 reverse	ACAATTGGATTCTCCTACAGC			

*, Roche, Woerden, Netherlands

Primer	Sequence 5' - 3'	Size (bp)	PCR mix	Annealing temperature
***CEP290*, ARMS PCR†** (c.2991+1655A>G)				
c.2991+1655A>G wildtype forward	ACCGCACCTGGCCCCAGTTGTAATTGTGGA			
c.2991+1655A>G mutant forward	ACCGCACCTGGCCCCAGTTGTAATTGTGGg	137	1.5 mM MgCl2	60° C
c.2991+1655A>G reverse	AGTAAGGAGGATGTAAGACTGGAGATAGAG			
†, Amplification-refractory mutation system (ARMS) PCR;				
***CEP290*, RFLP exon 7‡** (c.451C>T, p.Arg151X)				
exon 7 forward	CATTTTCTACTTTGTTAGAGAGGATTT	578	1.5 mM MgCl2	
exon 7 reverse	GAAGACTCCAGTCCTGGTTAAAA			
‡, restriction fragment length polymorphism analysis				
***CEP290*, cDNA primers**				
exon 5 forward	TAATGAAACTGGAAAATGAACTGG			
exon 9 reverse	CACTGTCTTCCCCTCTTCTTG	336	3 mM MgCl2	56° C
exon 10 reverse	TGAACTTCAATTTTCTCATTAGCTTC	433		

REFERENCES

1. Frank V, den Hollander AI, Bruchle NO, et al. Mutations of the CEP290 gene encoding a centrosomal protein cause Meckel-Gruber syndrome. Hum Mutat. 2008;29:45-52.

2. Sayer JA, Otto EA, O'Toole JF, et al. The centrosomal protein nephrocystin-6 is mutated in Joubert syndrome and activates transcription factor ATF4. Nat Genet. 2006;38:674-681.

3. Valente EM, Silhavy JL, Brancati F, et al. Mutations in CEP290, which encodes a centrosomal protein, cause pleiotropic forms of Joubert syndrome. Nat Genet. 2006;38:623-625.

4. den Hollander AI, Koenekoop RK, Yzer S, et al. Mutations in the CEP290 (NPHP6) gene are a frequent cause of Leber congenital amaurosis. Am J Hum Genet. 2006;79:556-561.

5. Perrault I, Delphin N, Hanein S, et al. Spectrum of NPHP6/CEP290 mutations in Leber congenital amaurosis and delineation of the associated phenotype. Hum Mutat. 2007;28:416.

6. Helou J, Otto EA, Attanasio M, et al. Mutation analysis of NPHP6/CEP290 in patients with Joubert syndrome and Senior-Loken syndrome. J Med Genet. 2007;44:657-663.

7. Leitch CC, Zaghloul NA, Davis EE, et al. Hypomorphic mutations in syndromic encephalocele genes are associated with Bardet-Biedl syndrome. Nat Genet. 2008;40:443-448.

8. Vallespin E, Lopez-Martinez MA, Cantalapiedra D, et al. Frequency of CEP290 c.2991+1655A>G mutation in 175 Spanish families affected with Leber congenital amaurosis and early-onset retinitis pigmentosa. Mol Vis. 2007;13:2160-2162.

9. den Hollander AI, Roepman R, Koenekoop RK, Cremers FPM. Leber congenital amaurosis: genes, proteins and disease mechanisms. Prog Retin Eye Res. 2008;27:391-419.

10. Cideciyan AV, Aleman TS, Jacobson SG, et al. Centrosomal-ciliary gene CEP290/NPHP6 mutations result in blindness with unexpected sparing of photoreceptors and visual brain: implications for therapy of Leber congenital amaurosis. Hum Mutat. 2007;28:1074-1083.

11. Hanein S, Perrault I, Gerber S, et al. Leber congenital amaurosis: comprehensive survey of the genetic heterogeneity, refinement of the clinical definition, and genotype-phenotype correlations as a strategy for molecular diagnosis. Hum Mutat. 2004;23:306-317.

12. Marmor MF, Fulton AB, Holder GE, Miyake Y, Brigell M, Bach M. ISCEV Standard for full-field clinical electroretinography (2008 update). Doc Ophthalmol. 2009;118:69-77.

13. Miller SA, Dykes DD, Polesky HF. A simple salting out procedure for extracting DNA from human nucleated cells. Nucleic Acids Res. 1988;16:1215.

14. Kruglyak L, Daly MJ, Reeve-Daly MP, Lander ES. Parametric and nonparametric linkage analysis: a unified multipoint approach. Am J Hum Genet. 1996;58:1347-1363.

15. Hoffmann K, Lindner TH. EasyLINKAGE-Plus-automated linkage analyses using large-scale SNP data. Bioinformatics. 2005;21:3565-3567.

16. Nannya Y, Sanada M, Nakazaki K, et al. A robust algorithm for copy number detection using high-density oligonucleotide single nucleotide polymorphism genotyping arrays. Cancer Res. 2005;65:6071-6079.

17. Rozen S, Skaletsky H. Primer3 on the WWW for general users and for biologist programmers. Methods Mol Biol. 2000;132:365-386.

18. Little S. Amplification-refractory mutation system (ARMS) analysis of point mutations. Curr Protoc Hum Genet. 2001;Chapter 9:Unit 9.8.

19. Reese MG, Eeckman FH, Kulp D, Haussler D. Improved splice site detection in Genie. J Comput Biol. 1997;4:311-323.

20. Cartegni L, Wang J, Zhu Z, Zhang MQ, Krainer AR. ESEfinder: A web resource to identify exonic splicing enhancers. Nucleic Acids Res. 2003;31:3568-3571.

21. Lorenz B, Gyurus P, Preising M, et al. Early-onset severe rod-cone dystrophy in young children with RPE65 mutations. Invest Ophthalmol Vis Sci. 2000;41:2735-2742.

22. van Osch L, van Schooneveld M, Bleeker-Wagemakers EM. Golden tapetal reflex in male patients with X-linked retinitis pigmentosa. Case report and practical implications. Ophthalmic Paediatr Genet. 1990;11:287-291.

23. Nagy E, Maquat LE. A rule for termination-codon position within intron-containing genes: when nonsense affects RNA abundance. Trends Biochem Sci. 1998;23:198-199.

24. Cheng J, Belgrader P, Zhou X, Maquat LE. Introns are cis effectors of the nonsense-codon-mediated reduction in nuclear mRNA abundance. Mol Cell Biol. 1994;14:6317-6325.

25. Zhang J, Sun X, Qian Y, Maquat LE. Intron function in the nonsense-mediated decay of beta-globin mRNA: indications that pre-mRNA splicing in the nucleus can influence mRNA translation in the cytoplasm. RNA. 1998;4:801-815.

26. Dietz HC, Valle D, Francomano CA, Kendzior Jr. RJ, Pyeritz RE, Cutting GR. The skipping of constitutive exons in vivo induced by nonsense mutations. Science. 1993;259:680-683.

27. Valentine CR. The association of nonsense codons with exon skipping. Mutat Res. 1998;411:87-117.

28. Cartegni L, Chew SL, Krainer AR. Listening to silence and understanding nonsense: exonic mutations that affect splicing. Nat Rev Genet. 2002;3:285-298.

29. Wang J, Chang YF, Hamilton JI, Wilkinson MF. Nonsense-associated altered splicing: a frame-dependent response distinct from nonsense-mediated decay. Mol Cell. 2002;10:951-957.

30. Maquat LE. NASty effects on fibrillin pre-mRNA splicing: another case of ESE does it, but proposals for translation-dependent splice site choice live on. Genes Dev. 2002;16:1743-1753.

31. Gal A, Li Y, Thompson DA, et al. Mutations in MERTK, the human orthologue of the RCS rat retinal dystrophy gene, cause retinitis pigmentosa. Nat Genet. 2000;26:270-271.

32. Tada A, Wada Y, Sato H, et al. Screening of the MERTK gene for mutations in Japanese patients with autosomal recessive retinitis pigmentosa. Mol Vis. 2006;12:441-444.

33. Tschernutter M, Jenkins SA, Waseem NH, et al. Clinical characterisation of a family with retinal dystrophy caused by mutation in the Mertk gene. Br J Ophthalmol. 2006;90:718-723.

34. D'Cruz PM, Yasumura D, Weir J, et al. Mutation of the receptor tyrosine kinase gene Mertk in the retinal dystrophic RCS rat. Hum Mol Genet. 2000;9:645-651.

35. Chang B, Khanna H, Hawes N, et al. In-frame deletion in a novel centrosomal/ciliary protein CEP290/NPHP6 perturbs its interaction with RPGR and results in early-onset retinal degeneration in the rd16 mouse. Hum Mol Genet. 2006;15:1847-1857.

36. Edwards RB, Szamier RB. Defective phagocytosis of isolated rod outer segments by RCS rat retinal pigment epithelium in culture. Science. 1977;197:1001-1003.

37. Badano JL, Kim JC, Hoskins BE, et al. Heterozygous mutations in BBS1, BBS2 and BBS6 have a potential epistatic effect on Bardet-Biedl patients with two mutations at a second BBS locus. Hum Mol Genet. 2003;12:1651-1659.

38. Khanna H, Davis EE, Murga-Zamalloa CA, et al. A common allele in RPGRIP1L is a modifier of retinal degeneration in ciliopathies. Nat Genet. 2009;41:739-745.

39. Rivolta C, Sharon D, DeAngelis MM, Dryja TP. Retinitis pigmentosa and allied diseases: numerous diseases, genes, and inheritance patterns. Hum Mol Genet. 2002;11:1219-1227.

Adapted from: *American Journal of Human Genetics*. 2008 Nov;83(5):594-603.

Rob W.J. Collin,[1,2,7] Karin W. Littink,[1,3,7] B. Jeroen Klevering,[4]
L. Ingeborgh van den Born,[3] Robert K. Koenekoop,[5] Marijke N. Zonneveld,[1,3]
Ellen A.W. Blokland,[1] Tim M. Strom,[6] Carel B. Hoyng,[4] Anneke I. den Hollander[1,2,4]
and Frans P.M. Cremers[1,2]

[1] Department of Human Genetics, Radboud University Nijmegen Medical Centre, Nijmegen, The Netherlands; [2] Nijmegen Centre for Molecular Life Sciences, Radboud University Nijmegen Medical Centre, Nijmegen, The Netherlands; [3] The Rotterdam Eye Hospital, Rotterdam, The Netherlands; [4] Department of Ophthalmology, Radboud University Nijmegen Medical Centre, Nijmegen, The Netherlands; [5] McGill Ocular Genetics Laboratory, Montreal Children's Hospital Research Institute, McGill University Health Centre, Montreal, Canada; [6] Institute of Human Genetics, Helmholtz Zentrum München, German Research Center for Environmental Health, Neuherberg, Germany.
[7] These two authors contributed equally to this work.

CHAPTER 5A

IDENTIFICATION OF A 2 MB HUMAN ORTHOLOG OF *DROSOPHILA EYES SHUT/SPACEMAKER* THAT IS MUTATED IN PATIENTS WITH RETINITIS PIGMENTOSA

ABSTRACT

In patients with autosomal-recessive retinitis pigmentosa (arRP), homozygosity mapping was performed for detection of regions harboring genes that might be causative for RP. In one affected sib pair, a shared homozygous region of 5.0 Mb was identified on chromosome 6, within the RP25 locus. One of the genes residing in this interval was the retina-expressed gene *EGFL11*. Several genes resembling *EGFL11* were predicted just centromeric of *EGFL11*. Extensive long-range RT-PCR, combined with 5′- and 3′- RACE analysis, resulted in the identification of a 10-kb transcript, starting with the annotated exons of *EGFL11* and spanning 44 exons and 2 Mb of genomic DNA. The transcript is predicted to encode a 3165-amino acids extracellular protein containing 28 EGF-like and five Laminin A G-like domains. Interestingly, the second part of the protein was found to be the human ortholog of *Drosophila* eyes shut (eys), also known as spacemaker, a protein essential for photoreceptor morphology. Mutation analysis in the sib pair homozygous at RP25 revealed a nonsense mutation (p.Tyr3156X) segregating with RP. The same mutation was identified homozygously in three arRP siblings of an unrelated family. A frameshift mutation (pPro2238ProfsX16) was found in an isolated RP patient. In conclusion, we identified a gene, coined *eyes shut homolog* (*EYS*), consisting of *EGFL11* and the human ortholog of *Drosophila eys*, which is mutated in patients with arRP. With a size of 2 Mb, it is one of the largest human genes, and it is by far the largest retinal dystrophy gene. The discovery of *EYS* might shed light on a critical component of photoreceptor morphogenesis.

INTRODUCTION

Retinitis pigmentosa (RP [MIM 268000]) is made up of a clinically and genetically heterogeneous group of diseases characterized by night blindness and constriction of the visual field, leading to severe visual impairment due to progressive degeneration of photoreceptors and, often, blindness. To date, 21 genes have been described as causing autosomal-recessive RP (arRP) and five loci have been identified for which the causative gene is still unidentified (RetNet web resource). Genes that cause arRP encode proteins that exert their function in different pathways within the retina, such as the phototransduction cascade (*CNGA1*, *CNGB1*, *PDE6A*, *PDE6B*, *RGR*, *RHO*, *SAG* [MIM *123825, *600724, *180071, +180072, *600342, +180380, and *181031, respectively]) or vitamin A metabolism (*ABCA4*, *LRAT*, *RLBP1*, *RPE65* [MIM *601691, +604863, *180090, and +180069, respectively]). Others encode proteins that have a structural or signaling function (*CRB1*, *RP1*, *TULP1*, *USH2A* [MIM +604210, *603937, *602280, and +608400, respectively]), play a role in transcriptional regulation (*NR2E3*, *NRL* [MIM *604485 and +162080, respectively]), or play a role in phagocytosis of the RPE (*MERTK* [MIM +604705]), or their exact role still awaits discovery (*CERKL*, *PRCD*, *PROM1* [MIM *608381, *610598, and *604365, respectively]).[1] *USH2A* is the most frequently mutated gene, causing ~7% of arRP, whereas most other genes account for only 1-2% of arRP cases.[1] Altogether, these 21 known genes are estimated to account for 50% of arRP cases, indicating that more genes await discovery. Mutations at the RP25 locus [MIM #602772] might also represent a significant cause of arRP, given that 10%–25% of Spanish arRP families were previously shown to map to this locus.[2,3] Previous studies have excluded mutations in 60 genes at the RP25 locus.[4-14] Recently, the RP25 locus was significantly reduced by linkage studies in additional Spanish families and the identification of a 100–200 kb deletion in one of the linked families, but the causative gene has not yet been identified.[2,7] Homozygosity mapping has proven to be an effective approach in the search for genes[15-17] and in the discovery of mutations in known arRP genes.[18]

The purpose of this study was to identify retinal dystrophy genes, utilizing homozygosity mapping with SNP microarray technology. Genome-wide homozygosity mapping in a large series of outbred arRP patients revealed a region on chromosome 6q12-q11.1 that was homozygous in two affected siblings and was fully situated within the previously defined RP25 locus.[3] We characterized an exceptionally large gene variant in this region, and we found it to be specifically expressed in the retina. Sequence analysis revealed a homozygous nonsense mutation in these siblings, segregating with RP in the family. Subsequently, the same mutation was detected in an unrelated family with arRP, whereas another mutation was identified in an isolated RP patient.

SUBJECTS AND METHODS

Subjects and clinical evaluation

Five patients from three families (II-1 and II-3 from family A, II-3 and II-6 from family B, and II-1 from family C) received the RP diagnosis several years ago through ophthalmologic examination. The examination included evaluation of best-corrected visual acuity and slit-lamp biomicroscopy, followed by indirect ophthalmoscopy and fundus photography after pupillary dilatation. The size and the extent of the visual-field defects were assessed with Goldmann kinetic perimetry (targets V-4e, II-4e, and I-4e to I-1e; for all patients) and Humphrey static perimetry (30-2; only for patient II-3 in family A). Finally, an electroretinogram (ERG) was recorded in all five patients, in accordance with the protocol of the International Society for Clinical Electrophysiology of Vision (ISCEV).[19] After the nature of this phenotype-genotype study was explained, an informed consent adhering to the tenets of the Declaration of Helsinki was obtained from all patients and from the unaffected siblings of family A and B. Blood samples from these individuals were then collected for future molecular-genetics testing. The initial results of the molecular-genetics analysis warranted further ophthalmologic investigation in the supposedly unaffected individual II-4 from family B. This investigation included all of the elements of the earlier ophthalmologic examination of the affected individuals, with the exception of the visual-field assessment. Furthermore, 142 probands with RP and indications of a recessive mode of inheritance participated in this study. Control DNA samples from 276 unrelated Dutch individuals were used.

Homozygosity mapping and mutation analysis

Genomic DNA was isolated from lymphocytes by standard salting-out procedures.[20] DNA samples of 145 RP patients, mainly of Dutch origin, were genotyped on either the GeneChip Mapping 250K *Nsp*I array, containing 262,000 SNPs, or the GeneChip Genome-Wide Human SNP Array 5.0, which contains 500,568 polymorphic SNPs in addition to 420,000 nonpolymorphic probes for the detection of germline copy-number variations (Affymetrix). Array experiments were performed according to protocols provided by the manufacturer. The 250K SNP genotypes were analyzed with the software package CNAG.[21] Data from the 5.0 array were genotyped with Genotype Console software (Affymetrix), whereas regions of homozygosity were calculated with Partek Genomics Solution (Partek). All 41 coding exons and three noncoding exons of *EYS* were PCR amplified and analyzed in sense and antisense directions with a dye-termination chemistry (BigDye Terminator, version 3 on a 3730 DNA analyzer; Applied Biosystems). Primers for PCR and sequencing of the

44 exons are given in Table S1; PCR conditions are available upon request. A subset of 131 RP patients, mainly from The Netherlands, and a control panel of 276 ethnically matched unrelated and unaffected individuals were screened for the p.Tyr3156X mutation with the amplification-refractory mutation system (ARMS; primers listed in Table S2).

Characterization of the genetic composition of *EYS*

For characterization of the expression of predicted genes encoding EGF-like and/or Laminin A G-like domains (NT_007299.33, NT_007299.34, NT_007299.35, NT_007299.37 and ENST00000237253) in retina, several primers were designed, corresponding to the exons of these gene predictions. Long-range PCRs were performed on human retina Marathon-Ready cDNA (Clontech) with the Advantage cDNA PCR Kit (Clontech), in accordance with the manufacturer's protocol. Nested PCR reactions with the use of a number of these primer combinations resulted in the amplification of PCR products representing parts of a transcript expressed in retina. PCR products were purified on Nucleospin Plasmid Quick Pure columns (Macherey-Nagel) and either directly sequenced or cloned in the pCR4-TOPO vector with the use of the TOPO TA Cloning Kit (Invitrogen) for sequencing with T7 and T3 sequencing primers as described above. Primer sequences are listed in Table S3. To characterize the 5'- and 3'- untranslated regions (UTR) of the detected transcripts, rapid amplification of cDNA ends (5'- and 3'- RACE, Clontech) was performed, in accordance with the manufacturer's protocol, using the Advantage cDNA PCR kit and human retina Marathon-Ready cDNA (Clontech) as a template.

RT-PCR analysis for determining tissue distribution of *EYS*

Total RNA from human placenta, adult brain, testis, kidney, and retina and from fetal heart, skeletal muscle, liver, and lung was obtained from Clontech. For cDNA synthesis, 2 µg of total RNA was incubated with 5 ng/µl of random hexamers ($pd(N)_6$, Pharmacia) and 0.3 mM dNTPs (Invitrogen Life Sciences). Subsequently, cDNA was synthesized with the M-MLV Reverse Transcriptase kit (Invitrogen Life Sciences), with a final concentration of 10 mM DTT, 11 U Reverse Transcriptase, and 0.33 U RNAguard (American Biosciences) per reaction. For detecting the distribution patterns of human *EYS* in various human tissues, RT-PCR was carried out with Advantage Polymerase (Clontech), with the use of various primer pairs equally distributed along the transcript. As a control, b-actin (*ACTB*) was amplified. To verify that the amplified products indeed corresponded to the *EYS* transcript, PCR products were purified and sequenced as described above. Primer sequences are listed in Table S4.

Bioinformatic analysis

Genes and gene-prediction tracks were derived from the UCSC Genome Working Draft, March 2006 assembly (hg18). For identification of homologous proteins of human and *Drosophila eys*, protein blast and tblastn were run under default settings (BLAST web resource). Conserved functional domains within proteins were searched with either the web-based tool SMART[22,23] or Pfam.[24] Prediction of amino acid residues that might be subject to O-linked glycosylation was carried out with the NetOGlyc 3.1 Server.[25]

RESULTS

Homozygosity mapping

In our search for retinal dystrophy genes, homozygosity mapping was conducted in a large series of patients with RP. Genome-wide SNP genotyping revealed two shared homozygous regions ≥ 5 Mb in two affected siblings diagnosed with RP. The largest homozygous region (19.3 Mb) was located on chromosome 2 between SNP_A-1816491 and SNP_A-2053763, whereas the second region, of 5.0 Mb, was located at chromosome 6q12-q11.1 between SNP_A-2144407 and SNP_A-1833968. The region on chromosome 6 overlapped with a well-known and published locus for arRP, namely RP25,[3] for which the causative gene has not yet been identified (Figure 1A). Therefore, a search for candidate genes residing within this homozygous interval was conducted. Within the homozygous region shared with the RP25 locus, five genes are known to reside (Figure 1A), of which *EGFL11* was found to be expressed in the eye, according to the Unigene database. RT-PCR analysis confirmed abundant expression of this gene in human retina (data not shown).

Identification of *EYS* exons

The *EGFL11* gene is made up of 12 exons and encodes a protein with several EGF-like domains. Sequence analysis of the annotated *EGFL11* gene in one of the two affected siblings did not reveal any causative sequence variants. Centromeric to *EGFL11*, several other genes encoding EGF-like domains were predicted, including NT_007299.37, ENST00000237253, NT_007299.35, NT_007299.34, and NT_007299.33. To test the hypothesis that exons of these gene-prediction tracks were part of a longer isoform of the *EGFL11* gene, extensive long-range RT-PCR experiments were performed, combined with 5'- and 3'- RACE experiments using human retina cDNA as a template. Interestingly, these analyses showed that in addition to a transcript corresponding to the annotated *EGFL11* gene, a second transcript

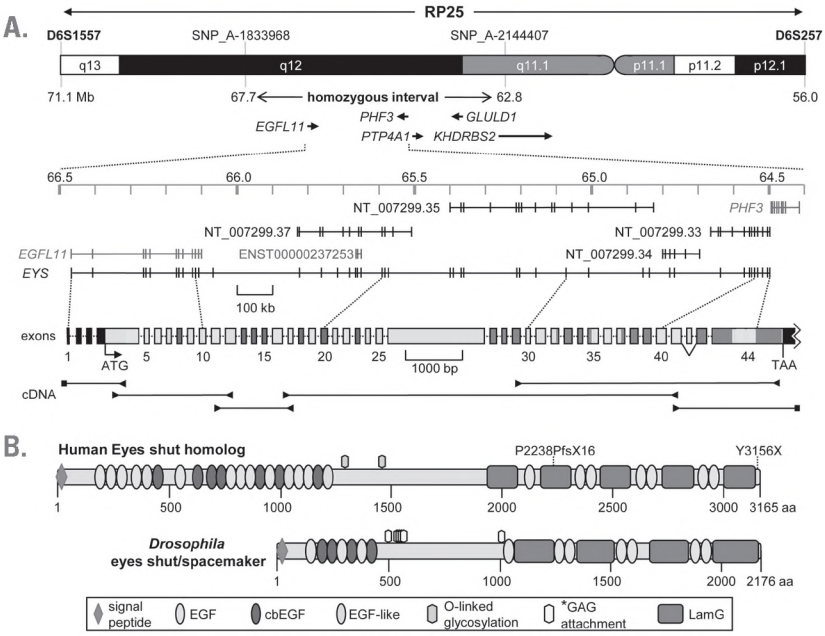

FIGURE 1. Genomic structure, cDNA fragments, and protein domains of *EYS*.
(See appendix for color figure)

A. Upper panel: the RP25 chromosomal region at 6p12.1-q133, the 5.0 Mb homozygous region identified in family A, and the five known genes within the homozygous region. Exons 1 and 2 of *KHDRBS2* reside in the critical region. In the middle, the exon predictions are depicted on the basis of RefSeq (in blue), Genescan (in black), and Ensembl (in red), with the use of the March 2006 UCSC genome build (hg18). Below the genomic-exon annotation is the exon structure of human *EYS* (exons drawn to scale; intron sizes can be found in the top panel). The complete nucleotide sequence of human *EYS* cDNA is presented in Figure S2. For details of the exon-intron structure, see Table S5. The 5'- and 3'- UTRs are indicated in black boxes; the colors of the protein-coding exons correspond with those of the protein domains in **(B)**. Lower panel: reverse-transcription PCR fragments of human *EYS* with retina RNA and *EYS*-specific primers (arrowheads) or 5'- and 3'- RACE adaptor primers (squares). The 5'-UTR, the open reading frame, and the 3'-UTR altogether measure 10,475 nucleotides (see Table S5). Exon 42 (63 bp) is alternatively spliced in retina RNA (see Figure 2). For details of RT-PCR studies, see Figure S1. **B.** Protein-domain structure of *EYS* and its *Drosophila* ortholog (GenBank ID ABH07112.1). Note the conspicuous conservation of the order of EGF-like and Laminin A G-like domains between human and *Drosophila*. The p.Pro2238ProfsX16 frameshift mutation truncates several EGF-like and Laminin A G-like domains, whereas the carboxy-terminal p.Tyr3156X mutation truncates the last ten amino acids of human *EYS*. Abbreviations are as follows: EGF, epidermal growth factor domain; cbEGF, calcium-binding EGF-like domain; EGF-like, EGF-like domain; LamG, Laminin A G-like domain. The asterisk denotes glycosaminoglycan (GAG) attachment sites predicted by Husain and coworkers.[26] Two putative O-glycosylation sites are predicted in the human protein (Thr1268 and Thr1424). Detailed characteristics of the human EYS protein domains are presented in Figure S2

was present, containing several exons of these gene predictions. This larger transcript started at the previously annotated *EGFL11* gene and extended up to the final exon of NT_007299.33 (Figure 1A). In total, this extended variant of *EGFL11* spans almost 2 Mb of genomic DNA and contains 44 exons, of which several had not previously been predicted by gene-prediction programs. The transcript contains 10,475 nucleotides, including the 3′ untranslated region and poly-A tail. A detailed overview of the identification and characterization of the transcript is presented in Figure S1. The protein encoded by this transcript is made up of 3165 amino acids and is predicted to contain a signal peptide for secretion into the extracellular environment. In addition, the protein harbors 28 EGF-like and 5 Laminin A G-like domains (Figure 1B). Subsequently, BLAST analyses were performed for the identification of potential orthologs of this human protein in lower species. These analyses led us to discover that the second part of this protein is homologous to *Drosophila eyes shut (eys)*, also known as *spacemaker*, a protein essential for photoreceptor development and morphology in the insect eye.[26, 27]

The domain organization of *eys* is comparable to that of the human *eys* homolog protein, with 14 EGF-like and four Laminin A G-like domains positioned in a similar order (Figure 1B). Initially, the *Drosophila eys* protein was described as a proteoglycan related to agrin and perlecan.[26] However, with the sequence of the *Drosophila* protein used as input in a BLAST search for human orthologs, *eys* homolog protein, rather than *agrin* and *perlecan*, was found to be the closest relative. In addition, the signaling molecules Notch-1 and -2 and the Crumbs-1 and -2 homolog proteins were identified as relatives of *Drosophila eys* (data not shown). These analyses show that the gene identified in this study is the true ortholog of *Drosophila eys*. Therefore, we propose to name the human gene *eyes shut homolog (EYS)*.

Tissue distribution of *EYS* mRNA

For study of the tissue distribution of human *EYS*, RT-PCR analysis was performed on cDNA from various tissues, including retina. In total, five primer pairs were used, distributed along the transcript. All five primer pairs that were used showed either specific or enriched expression of *EYS* in retina, although for one primer pair (exons 41–44), weak PCR products were also observed in the other tissues (Figure 2). This primer pair also amplified two fragments, and sequence analysis showed that the fragments represent alternatively spliced mRNA products of the *EYS* gene, either lacking or containing exon 42 (63 bp). Together, these results show that this gene is abundantly expressed in retina and support the hypothesis that the encoded protein plays an important role in vision.

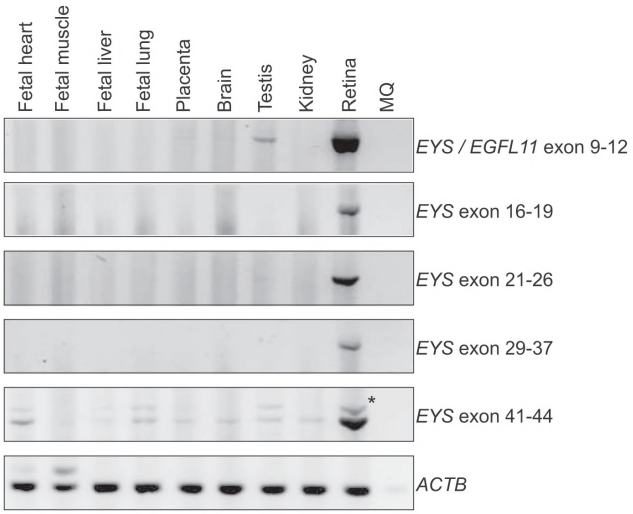

FIGURE 2. Tissue distribution of *EYS*.

RT-PCR analysis was performed on total RNA from various tissues. The expression of *EYS* was determined with the use of several primer pairs distributed along the transcript (see Table S4). The weak PCR product detected with primers from exon 41 to exon 44 is indicated by an asterisk and represents a transcript resulting from alternative splicing. *ACTB* (lower panel) was used as a control.

Mutation analysis

After this transcript was identified, the SNP data were reanalyzed in an attempt to identify RP patients who carry homozygous regions (threshold was set at >200 consecutive homozygous SNP calls) encompassing this new gene. On the basis of these data, ten arRP patients, including one of the affected individuals of the family described above (Figure 3A, family A), were selected for further mutation analysis of this gene. Sequence analysis of all 44 exons and flanking intronic sequences of the human *EYS* gene revealed a homozygous mutation, c.9468T>A, in the last exon (Figure 3B), present in the proband of family A. At the protein level, this mutation results in premature termination of the encoded protein at position 3156 (p.Tyr3156X). The mutation was confirmed to be homozygously present in his affected sibling and either absent or heterozygously present in four unaffected siblings (Figure 3A, family A). For detecting whether this mutation occurs more frequently in arRP patients, allele-specific PCR was conducted on another group of 131 unrelated probands affected with RP, resulting in the identification of a second proband carrying this mutation. The mutation was also homozygously present in her affected siblings,

but not in her four unaffected family members (Figure 3A, family B). Microsatellite and SNP analysis in the region within and surrounding the *EYS* gene revealed that p.Tyr3156X was present at the same haplotype in both families, suggesting a founder effect. The p.Tyr3156X mutation was excluded from 552 alleles of ethnically matched control individuals. The nonsense mutation described here results in the absence of the ten C-terminal amino acids of the human EYS protein. Sequence comparison of the C-terminal amino acids of the human EYS protein and various vertebrate and invertebrate orthologs revealed that some of the amino acids that are absent in the human mutant EYS protein are well conserved, even up to zebrafish, and thus may be crucial for proper function of the EYS protein in vertebrates (Figure 3C). Sequence analysis in the other nine patients whose DNA was homozygous at the region harboring the *EYS* gene revealed a second mutation, namely a homozygous 1-bp deletion in exon 33 (c.6714delT; Figure 3B). At the protein level, this mutation is predicted to result in a frameshift and premature termination (p.Pro2238ProfsX16) of *EYS*. Given that premature truncation is predicted to occur within the second Laminin A G-like domain, the mutant protein will lack six EGF-like and three Laminin A G-like domains (Figure 1B).

FIGURE 3. **Mutation analysis of *EYS* in RP patients.** ***(See appendix for color figure)***

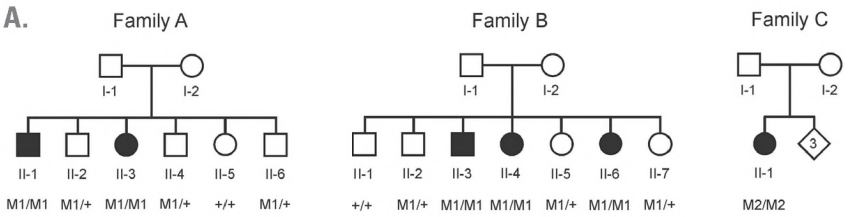

A. Pedigrees of three families with individuals affected with RP. Below the individuals, genotypes are presented for either the p.Tyr3156X change (M1, families A and B) or the p.Pro2238ProfsX16 change (M2, family C) detected to segregate with the disease. M1/M1 and M2/M2 represent homozygous mutants; M1/+ indicates heterozygous carriers, whereas +/+ indicates individuals carrying two wild-type alleles.

B. Upper panel: partial sequence of the *EYS* gene showing the nonsense c.9486T>A change, in an affected individual (family A, II-1) and an unaffected sibling (family A, II-5). The mutation replaces a tyrosine residue by a termination codon (p.Tyr3156X). Preceding amino acids are indicated above the sequence trace. Lower panel: partial sequence of the *EYS* gene showing the c.6714delT change, in an affected individual (family C, II-1) and a control individual. The mutation results in a frame shift and, eventually, in premature termination of the protein (p.Pro2238ProfsX16). Amino acids are indicated above the sequence trace.

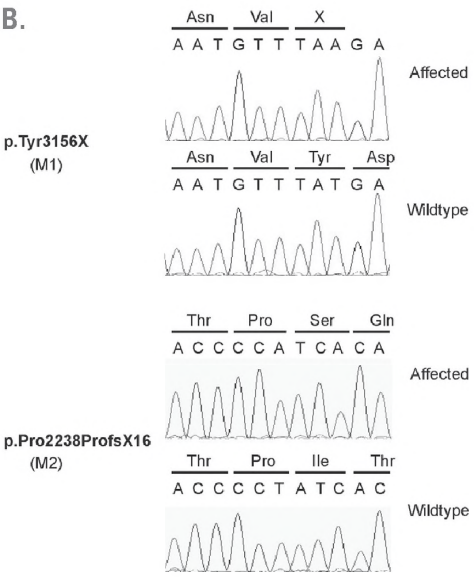

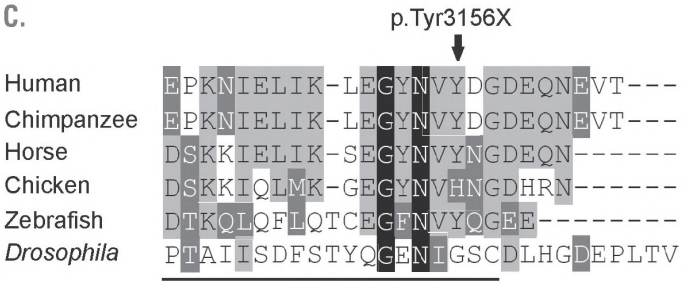

C. Sequence comparison of the 25 most C-terminal amino acids of the human EYS protein and several vertebrate and invertebrate orthologs. Residues identical in all sequences are white on a black background, whereas similar amino acids are white on a gray background. Residues that are present in at least three of the six proteins are indicated in black on a light gray background. Residues constituting the most C-terminal Laminin A G-like domain in the *Drosophila* protein are underlined. Accession numbers of the protein sequences used for sequence comparison are as follows: chimpanzee, XM_527426.2 (RefSeq); horse, XM_001918159.1 (RefSeq); chicken, XM_426198.2 (RefSeq); zebrafish, BX005106.5 (EMBL); *Drosophila*, ABH07112.1 (GenBank).

TABLE 1. Clinical characteristics of patients with mutations in *EYS*

ID	Age* (yrs)	Sex	Age of onset (yrs)	Initial symptom	Visual acuity OD	Visual acuity OS	Ophthalmoscopy	Goldmann Kinetic Perimetry	ERG Rod	ERG Cone	Phenotype
Family A											
II-1	61	M	12	Night blindness and photophobia	20/100	20/40	Pallor of the optic disc, attenuated retinal vasculature, bone spicules in midperiphery and atrophic lesion in the posterior pole.	Constricted visual fields (50-80 degrees). Marked decrease of the central visual field (I-4e not observed)	NR	NR	RP
II-3	57	F	28	Night blindness and photophobia	20/50	20/80	Mild attenuation of the retinal vessels and RPE alterations in the central macula.	Large central scotomas without constriction of the peripheral visual field.	↓	↓↓	CRD
Family B											
II-3	53	F	45	Night blindness	20/20	20/20	Normal aspect of the optic disc, attenuated retinal vasculature and bone spicules in midperiphery.	Constricted visual fields (50-60 degrees)	NR	NR	RP
II-4	52	F	46	Night blindness	20/25	20/20	Normal aspect of the optic disc, attenuated retinal vessels and bone spicules in the nasal fundus.	NP	↓↓	↓	RP
II-6	49	F	42	Night blindness	20/20	20/20	Mild pallor of the optic disc, severely attenuated vasculature and bone spicules throughout entire retina.	Severely constricted visual fields, with some residual visual field temporally.	NR	NR	RP
Family C											
II-2	48	F	13	Night blindness	20/50	20/40	Pallor of the optic disc, attenuated vasculature, RPE alterations in the central macula, extensive bone spicule pigmentation throughout entire retina.	Severely constricted (<5 degrees) visual fields	NR	NR	RP

*Current age; M, male; F, female; RP, retinitis pigmentosa; CRD, cone-rod dystrophy; RPE, retinal pigment epithelium; NP, not performed; ERG, electroretinogram; ↓, decreased; ↓↓, severely decreased; NR, non-recordable

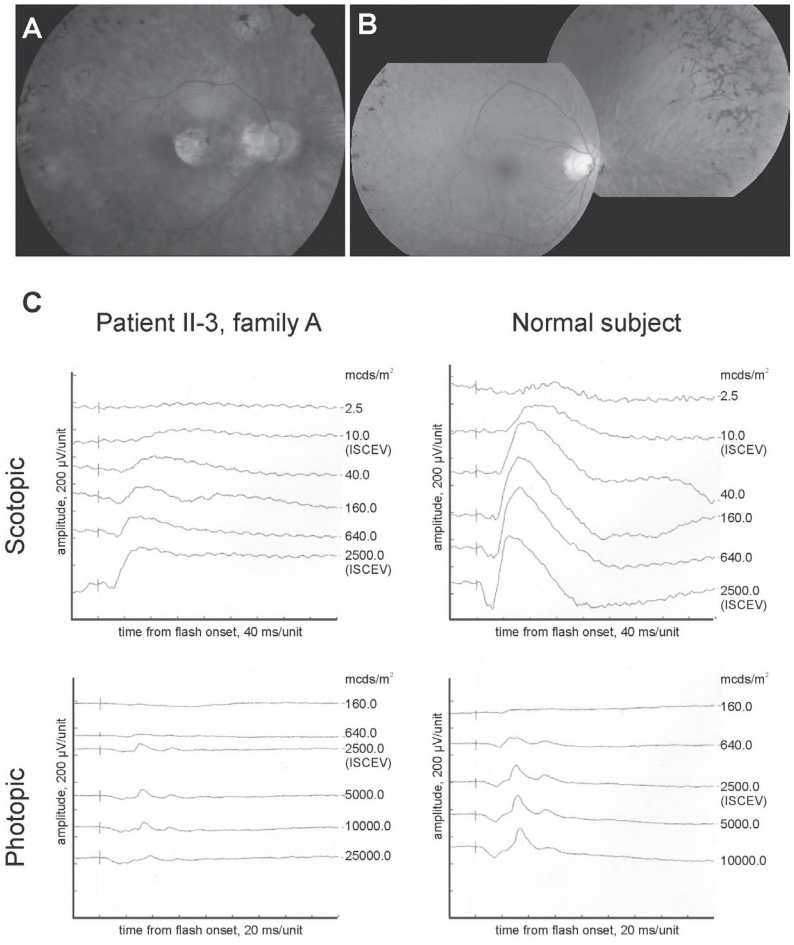

FIGURE 4. Clinical characteristics of RP patients with a homozygous p.Tyr3156X mutation in *EYS*. ***(See appendix for color figure)***

A. Fundus photograph of the right eye of patient II-1 of family A, showing mild pallor of the optic disc, a peripapillary crescent, attenuated retinal vessels, and bone-spicule pigmentations. An area of sharply demarcated chorioretinal atrophy is located nasal to the fovea, with similar atrophic lesions along the vascular arcades, conflating to diffuse atrophy in the midperiphery.

B. Fundus photograph of the posterior pole and nasal peripheral retina of the right eye of patient II-6 of family B, showing mild pallor of the optic disc, severely attenuated vessels, pronounced atrophic changes in the (mid) periphery that spare the posterior pole, and extensive bone spicules in the peripheral retina.

C. Scotopic and photopic ERG of the right eye of patient II-3 of family A and a normal subject. Scotopic mixed response (ISCEV measurement; 2500 mcds/m2) had a b-wave amplitude of 274 µV (normal > 195 µV, mean 424 µV). The b-wave amplitude of the photopic response (ISCEV measurement; 2500 mcds/m2) was 58.8 µV (normal > 69 µV, mean 79 µV).

Clinical characteristics

Clinical examination of the affected individuals of families A, B, and C showed that all patients, with the exception of patient II-3 of family A, displayed characteristic RP abnormalities, including night blindness as the initial symptom, retinal bone-spicule pigmentations and attenuated retinal vessels (Figures 4A and 4B), constriction of the visual fields, and a non-recordable ERG or ERG responses in a rod-cone pattern. A posterior subcapsular cataract could be observed in patient II-1 of family A (age 53) and in patient II-1 of family C (age 39). Patient II-3 of family A also demonstrated a photoreceptor dystrophy, but in this patient, the cones were more severely affected than were the rods (cone-rod pattern; Figure 4C). This is also reflected by the central scotomas on the kinetic visual field. Fundus abnormalities included central abnormalities at the level of the RPE and moderate attenuation of the retinal vessels. The clinical characteristics of the patients in families A, B, and C are summarized in Table 1.

DISCUSSION

In the present study, we describe an extended transcript of the *EGFL11* gene, containing 33 as-yet-uncharacterized exons downstream of the previously annotated gene. The resulting transcript is more than 10 kb in size and is abundantly expressed in human retina. The protein encoded by this gene is predicted to contain 28 EGF-like and five Laminin A G-like domains. Interestingly, the second part of the protein was found to be homologous to the *Drosophila* eys protein. Therefore, we name the corresponding human gene *eyes shut homolog* (*EYS*). In two unrelated families, the same homozygous nonsense mutation (p.Tyr3156X) was identified as segregating with arRP, whereas in an isolated patient, a homozygous frameshift mutation was identified (p.Pro2238ProfsX16). The patients of all three families display typical signs of RP, with night blindness, fundus abnormalities (including bone-spicule pigmentations and narrowing of the retinal vessels), constriction of the visual fields, and evidence of cone- and rod-photoreceptor abnormalities on the ERG. Although all affected individuals share a similar molecular defect, there are, nevertheless, differences in the ensuing photoreceptor dystrophy. Although the affected individual of family C is the youngest of all patients described in this study, she is the only one who is legally blind, a result of her severely constricted visual fields. The phenotype of family A, on the other hand, shows a more prominent involvement of cone degeneration compared to the other families. This is reflected by the moderate to severe impairment of the visual acuity (see Table 1), the cone and mixed rod-cone responses of the ERG, and the photophobia as an early symptom. In patient II-3, especially, the ERG shows

relatively more impairment of the cone-photoreceptor system compared to the rod-photoreceptor system. The visual fields in this patient are not constricted, as in the other patients, but show bilateral central scotomas, also indicative of cone-rod dystrophy (CRD). Her elder brother (II-1) also shows central fundus lesions, but his ERG (at age 60) no longer shows either cone nor rod activity. We do not know whether a cone-rod pattern of deterioration was present in the earlier stages of his disease. Family B, finally, has a relatively late onset of a classic form of RP, with preservation of central vision. In this regard, the phenotype in this family is relatively mild compared to many forms of arRP. In two patients, cataracts were observed at a relatively young age. The development of cataracts, however, is often seen in patients affected by RP at an early age and is not exclusively present in patients with RP due to *EYS* mutations. It appears that in this type of photoreceptor dystrophy, like in many forms of inherited retinal diseases, other modifying factors besides the genetic defect in *EYS* exert their influence on the phenotypic outcome and explain the intra- and interfamilial variability.

The frameshift mutation identified in the isolated RP patient (family C) results in the absence of 927 amino acids that altogether form six EGF-like and three Laminin A G-like domains. As a result of the absence of these functionally important domains, the truncated protein will probably have little or no residual function. Alternatively, the mRNA is degraded via a mechanism called nonsense mediated decay.[28] Premature termination of the EYS protein due to the nonsense mutation in families A and B results only in the absence of the ten C-terminal amino acids that apparently fulfill a crucial function. Although the C-terminal amino acids of *Drosophila eys* are not highly conserved compared to the human protein, several residues of this segment are conserved in vertebrate species, including zebrafish. These results may indicate that during evolution of the vertebrate eye, the C-terminal part of EYS became essential for proper functioning of the entire protein.

The *EYS* gene is located on chromosome 6q12 and resides within the 15 Mb RP25 locus.[2,3] Recently, a ~100 kb clone from a tiling-path array located within the RP25 interval was found to be deleted in all affected members of a Spanish family linked to RP25,[7] suggesting that genes residing within this deletion might be underlying RP in families linked to RP25. On the basis of the array-CGH data, the total length of the deletion was predicted to be 100–200 kb in size, spanning *EYS* exons 14–19. Altogether, these data support our conclusion that *EYS* is the gene responsible for RP in families that link to the RP25 locus. The prevalence of *EYS* mutations remains to be established, because we have thus far only fully analyzed the presence

of mutations in the 44 exons and flanking intronic sequences of *EYS* in ten patients with arRP. The human EYS protein is composed of 3165 amino acids and has a number of remarkable features. The first part of the protein corresponds to the previously annotated EGFL11 protein, which seems not to be present in *Drosophila*. The second part of human EYS is the ortholog of the *Drosophila* eys protein. Whereas the domain organization is similar between human and *Drosophila eys*, other features are not conserved. In both proteins, a less conserved region of the protein, located between the first series of EGF-like domains and the C-terminal end (with both EGF-like and Laminin A G-like domains), is present. In *Drosophila eys*, multiple sites for the attachment of glycosaminoglycan side chains are predicted in this region, and indeed, the protein is heavily glycosylated in the insect eye.[26] The consensus for such an attachment is composed of a serine residue directly followed by a glycine residue, with either a second serine-glycine tandem or a series of acidic amino acids in close proximity.[29] Several of these serine-glycine clusters are found in *Drosophila eys*, but, remarkably, they are not conserved in the human ortholog. Apparently, extensive glycosylation is not required for proper functioning of the human eys homolog protein in the retina.

Drosophila eys is an extracellular matrix protein that occupies the interrhabdomeral space.[26, 27] The generation of the interrhabdomeral space has been a critical event in the transition of compound eyes from a closed to an open system. In insects with a "fused rhabdomer" configuration, such as bees, photoreceptors 1–6 within one ommatidium behave as one photosensitive system and collect light from the same area. In contrast, in insects with an open system, such as flies, photoreceptors 1–6 detect light from different areas in the visual field, because they are isolated from each other. Consequently, flies have an improved angular sensitivity, allowing the detection of smaller moving objects. Both mutant *Drosophila* lines *eys* and *prominin* (*prom*) showed a failure of interrhabdomeral space separation.[27] *Drosophila* prom, a pentaspan transmembrane protein, is present throughout rhabdomer biogenesis and, at the time of eclosion, is selectively localized to the stalk membrane and the tips of the rhabdomer microvilli. There is evidence that *eys* binds to *prom* in orchestrating the open-rhabdomer configuration. Interestingly, *Drosophila* crumbs, a single-span transmembrane protein consisting of 30 extracellular EGF-like and four Laminin A G-like domains, is also expressed at the stalk membrane.

What function can be attributed to Eys, Prom, and Crumbs in mammalian photoreceptors? In the mouse embryonic eye, Prom1 is located between the progenitors of the photoreceptor and retinal pigment epithelium (RPE) cells, whereas

in adult murine retina, Prom1 was found at the microvilli of the RPE cells and in the rod outer segment (ROS) layer, with a high concentration in the plasmamembrane evaginations.[30] Mutations in human *PROM1* are associated with arRP[30,31] or macular degeneration.[32] Crumbs homolog 1 (*Crb1*) is expressed in mouse Müller cells, at the outer limiting membrane opposing photoreceptor cell inner segments, the functional equivalent of the Drosophila photoreceptor stalk.[33] Loss-of-function mutations in human *CRB1* result in Leber congenital amaurosis or arRP.[34-36]

We hypothesize three different functions for human EYS. First, through an interaction with PROM1, EYS could be involved in ROS disc morphogenesis. Second, EYS might interact directly or indirectly with the extracellular domain of CRB1 or its homolog CRB2 and in this way form a critical component of Müller cell-photoreceptor cell and photoreceptor cell-photoreceptor cell interactions. Third, reminiscent of the function of its *Drosophila* ortholog, EYS might be sequestered in the extracellular matrix, also known as the subretinal space, between the (developing) photoreceptors and RPE.

In conclusion, we have identified the human ortholog of *Drosophila eyes shut*, a 3165-amino acids extracellular protein that is encoded by one of the largest human genes described thus far. The 2 Mb size of this gene, which we have coined *eyes shut homolog* (*EYS*), is a little shorter of that of the dystrophin gene mutated in X-linked Duchenne and Becker muscular dystrophies, which spans 2.2 Mb.[37,38] *EYS* is mutated in six patients of three families with arRP and, on the basis of previous linkage studies, is probably an important cause of inherited retinal blindness. On the basis of the function of its *Drosophila* counterpart (*eys*) and interactor (*prom*), it probably serves an important function in photoreceptor morphogenesis.

WEB RESOURCES

The URLs for data presented herein are as follows:
NCBI BLAST, http://blast.ncbi.nlm.nih.gov/Blast.cgi/
NetOGlyc 3.1 Server, http://www.cbs.dtu.dk/services/NetOGlyc/
OMIM, http://www.ncbi.nlm.nih.gov/Omim/
Pfam, http://pfam.sanger.ac.uk/
RetNet, http://www.sph.uth.tmc.edu/Retnet/
SMART, http://smart.embl-heidelberg.de/
UCSC Genome Browser build hg18, March 2006, http://www.genome.ucsc.edu
Unigene, http://www.ncbi.nlm.nih.gov/unigene

ACCESSION NUMBERS

For our human cDNA encoding the human ortholog of *Drosophila eys*, an accession number was requested at the EMBL Nucleotide Sequence Database and was provided; namely, FM209056. After a request to the Human Gene Nomenclature Committee was submitted, the human gene is now officially named *eyes shut homolog*, abbreviated *EYS*.

ACKNOWLEDGMENTS

The authors thank Christel Beumer, Sylvia van Beersum, Diana Cremers, Irma Lopez, Saskia van der Velde-Visser, and Erwin van Wijk for excellent technical assistance and Jayne Hehir-Kwa for data analysis. We also thank all of the participating RP patients and their families. This study was financially supported by: the Dutch Organisation for Scientific Research (grant 916.56.160 to A.I.d.H.), the Foundation Fighting Blindness USA (grant BR-GE-0606-0349-RAD to A.I.d.H.), Stichting Wetenschappelijk Onderzoek Oogziekenhuis Rotterdam (grant 2005-13 to L.I.v.d.B., A.I.d.H., and F.P.M.C.), Fonds de la recherche 'en sante' Quebec (to R.K.K), the Foundation Fighting Blindness-Canada (to R.K.K and F.P.M.C), Toronto Dominion financial group (to R.K.K), Algemene Nederlandse Vereniging ter Voorkoming van Blindheid (to F.P.M.C.), Landelijke Stichting voor Blinden en Slechtzienden (to F.P.M.C.), Rotterdamse Vereniging Blindenbelangen (to F.P.M.C.), Stichting Blindenhulp (to F.P.M.C.), and Stichting Ondersteuning Oogheelkunde 's-Gravenhage (to F.P.M.C.).

SUPPLEMENTAL DATA

SUPPLEMENTAL TABLE S1. Primers used for genomic sequence analysis of human *EYS*

Exon	Forward (5' > 3')	Reverse (5' > 3')	Amplicon length (basepairs)
1	TTATGTCAGCCTGCACATGG	GTAGTTGTGTTCAGCTAGGC	286
2	AGCTAAAGGCAGGATACTGG	ATGGAAAGCAGGGAATGAGG	315
3	GAAGACTCATTCTAGGTTAGTC	CACTGCAAAGATAGTGTCACC	472
4A	CTTAAAACACCATTTTGCAGC	ATGTGTCCCAACACTCAGCC	498
4B	ACTTCTACAGAGATTGCTGG	AGATTCCTGGCAGAACTGC	376
4C	GTGGTCCATCACCTTGTCC	TAGAGACGGGGTTTCACCG	486
5	AGAATTGAGGGAAAACTGATGG	CATAAAAGAGTTCAGTATATATACC	322
6	TCTATGCTCATTTCTTCTTTCCTTC	AAAATAAGTAGACCGTTCTTGTTCG	403
7	TTCTCCAGGTAAGAACCCATTC	TTAAGTAAAAGTTAGGGTTAAAACCAG	311
8	TTGGAATAATGTTAATAGGCTTTTC	TGGCTAAGATTAATAAGAGCATTTG	285

Exon	Forward (5′ > 3′)	Reverse (5′ > 3′)	Amplicon length (basepairs)
9	GGCTTTTGAACATGGATATGAC	AGATTTCCTAGGATGTAGTTGGTG	559
10	GGAACTTATTTTGTGGCAGATG	GACTGTTGAGAATTTGTTTACGAAG	427
11	GGTTTCATCTTAGTAGACAGAGAGGC	CATTGTTACCATGAAACAGTTCG	368
12	TGCACCCCACAACTATCTTC	AATTGCCCAAAGAAGCAATC	570
13	TTCAGATGTCATCCTAAGTGG	CAGACAAGAGACAGAAGTGC	293
14	GGATATTTTCATTGTTGCTTTGC	TGAATCCAATAAGTGAACAGTTTG	655
15	GAGATATCAAAATGGCCAGGAG	ATCCCAAGGACACTGAGCAC	273
16	CACCACATACTATTAGTTCAAG	ATTTTAGGAGGCCATCATCC	447
17-18	ATTCTTTAGACTACCACTGATTC	ACATAATGAGCACATGTGTGC	551
19	AGCAGAACAAAATTTTGCAAGG	CATCTGGCAGATTATTTCAGG	425
20	AGAGAGGTCTTCATTTCTTGG	AGCTCTTGTTTTATGAAAGAGC	395
21	AAACCCAGGAATAAACTCTGC	GGAAGAAATGACTCTGAAACC	322
22	GTCAAACAAGTTTGCACATCAG	GAAAGCAAAACATGGGAGTG	531
23	AACTCATTGTCACCCCAAGG	TCCTGATGAAAGCCTAAGTGC	486
24	AATGGCACCACGGATAAGAG	GAGGAATGCCGAGAAAAGTG	572
25	GAGCTATCCAATATGTCTATGG	GCAGAAAATATGCTTTTACCAC	378
26A	TTATCCCAGTGCCAAAGTGG	AGTAATGACTGCCTGTTTAGC	525
26B	ACTGTTGCTTTATCTGCTACC	GAACATGTTGCACATGTTTGG	434
26C	TACTGAGGCTTCAAGCAACC	GTGGGTCCCATAGTTATGCC	555
26D	ATCCATTGTCCCTTCACAAAC	TACAGACATGGAGGAAGACG	439
26E	GATTTTTCAGAAGTCACCACC	CTGATTACAATGAGGCTGTTC	410
27	AAAGAGGCAGGAAAGAGACG	AGGAAGAGACATCCTGGTGG	443
28	ACTTCATGTCTCTCCAAAGTG	ATTGTTAGGGATAGCCTTTGC	273
29	TGCTTCTGGCTTTGTTTTATTG	TGGAAAAACAGACTGACATTGG	521
30	TGCATACCCTGACCAGTTTG	CGTAGGAATGTGAAGCAAAAAC	335
31	GTTAAACCTTGATCAGTATTGG	ACAGCTGTTTCTTGTTTGTGC	475
32	TGCTTCATGCACTGGTCTGG	GTGTTACCTTTTCAAATGAATGC	552
33	CTAATAGCACTCCTACCAACC	TCTGTAGTCCCAACTACTTGG	465
34	CTTGAAAATGTCCACACTTGG	TTTCTGGTGCTTTGTTGAGAG	405
35	AACTAGCCAACAATAGCAACC	CTCTCAGAGGACAATACTGC	447
36	AGTGGAAAGCACACAGCTAC	TTGATCAGTCAAGTGCTATCC	458
37	TTAGTTGCTCAATGCTGAAGG	CAATTAGAGTGTCCCTGAGG	410
38	CAGCCAGTTGCACATATACC	GTGAACTTCGTGGATGTAGG	438
39	AGCAGAGAATTGAGTGGTATC	GAAAGCAATCCATATAGCTGG	410
40	TCTCTGCGCATTTCTGTATTC	ATGTGCATCTGTTTGTGTTCC	438
41	AAATTGACAAGTTAGCATCAGG	AAGTACTAGTCTATCTGTGAAG	432
42	GAACTGCAGGACAGATGTAC	CCTAATTCTAAGCTCCAATCC	323
43	TTGATGTACTCACCTACAAGC	ACGCATACACTTGCAGTGAC	444
44A	CACAATTGTGCTCAAGATCTG	TACATTTGAGCCACCTTTTGC	511
44B	TGAACCTGTAGGTTTTCAAGG	TGAACTGGAGGTTTCTCATTC	422
44C	TTCTTACAGTTGCCTGTGTAC	TTTATGTGGATCAATATCCTCG	424
44D	TTCTGTTGTAATAAATGGCACC	ACAATCAGAACCTTCAGTGAC	394

SUPPLEMENTAL TABLE S2. ARMS-primers used for screening c.9468T>A, p.Tyr3156X

ARMS primer	Forward (5′ > 3′)	Reverse (5′ > 3′)	Amplicon length (basepairs)
wildtype combination	CAGTCTAATTCTTTCCGAGGATATTGATCC	TATGTAACCTCATTTTGTTCATCTCCATAA	249
mutant combination	TGAACTAATTAAATTAGAAGGATACAATGTTTAA	GGTAATATAGTAAACAGTTGATTCCCCGTA	169

SUPPLEMENTAL TABLE S3. Primers used for cDNA sequence analysis of human *EYS*

Number*	Exon	Forward (5′ > 3′)	Reverse (5′ > 3′)	Comment
AP		CCATCCTAATACGACTCACTATAGGGC		RACE adaptor primer (Clontech)
NAP		ACTCACTATAGGGCTCGAGCGGC		RACE nested adaptor primer (Clontech)
1	4	GTGGTCCATCACCTTGTCC		
2	4		TGAGGGTTGTGGATGCCATTCTTCCAC	5′ RACE nested PCR
3	11	GAGTGAAGAAGACAGTCAGGAATATCGG		
4	11	GTTTTCTCAGATGGGCTGGCAACATG		Nested PCR
5	12		GCTACAGTTACAATTGTGCG	
6	13		TGCAGGGATGTGAAGCACACTCATC	5′ RACE PCR
7	17	CCTTTCCTGCCAGGATTATGGTGACTG		Nested PCR
8	17		GCAGGAAAGGAAGAGGCAGTCTTTCAC	Nested PCR
9	29	AGGATCTGTCTTCATTGGTG		
10	41	CACCACTGTAGCAGAGGAGCAACCTG		3′ RACE PCR
11	41	GGAACCACTGGAATCTACTGTGAAC		3′ RACE nested PCR
12	41		GAAATGCAGGTTGCTCCTCTGCTACAG	
13	41		ACAGTGGTGTGGAGGGTCATGTTCAG	Nested PCR
14	44		TACATTTGAGCCACCTTTTGC	

*, numbers corresponding to primers in Supplemental Figure S1. AP, adaptor primer; NAP, nested adaptor primer; RACE, Rapid Amplification of cDNA Ends.

SUPPLEMENTAL TABLE S4. Primers used for RT-PCR of human *EYS*

Exon	Forward (5′ > 3′)	Reverse (5′ > 3′)
9-12	CTAATTCATCAACACCTCTGC	GCTACAGTTACAATTGTGCG
16-19	TGTACATCTGGATGGACTGG	GCAGTTGTATCCATCAGTCC
21-26	GTTCATGTGATGCAGATGGG	AGTAATGACTGCCTGTTTAGC
29-37	AGGATCTGTCTTCATTGGTG	CAGTGCTGAGTGGTTGTTTG
41-44	ACCCTCCACACCACTGTAGC	GCCTTCTGCACCAACTCTTC
ACTB	GGGACGACATGGAGAAAATC	CAGAGGCGTACAGGGATAGC

SUPPLEMENTAL TABLE S5. Primers used for cDNA sequence analysis of human *EYS*

Exon/intron	Exon size in nucleotides	Intron size in nucleotides
1	43	67.243
2	115	143.785
3	135	252
4	945	3.956
5	114	85.227
6	194	2.569
7	128	17.978
8	115	30.769
9	160	9.281
10	140	8.892
11	167	38.861
12	257	238.136
13	114	59.911
14	122	51.668
15	122	33.050
16	260	9.984
17	97	184
18	108	15.271
19	146	63.875
20	172	934
21	79	8.068
22	200	187.133
23	125	8.588
24	116	24.109
25	193	1.128
26	1.767	150.871
27	191	2.897
28	92	47.334
29	151	80.403
30	113	76.146
31	233	148.590
32	147	15.365
33	154	67.155
34	109	14.472
35	221	120.025
36	173	57.814
37	183	16.966
38	167	809
39	145	9.925
40	175	15.373
41	173	20.486
42	63	15.233
43	162	4.719
44	1.689	
Subtotals:	10.475	1.975.435
Total size human *EYS*:		1.985.910

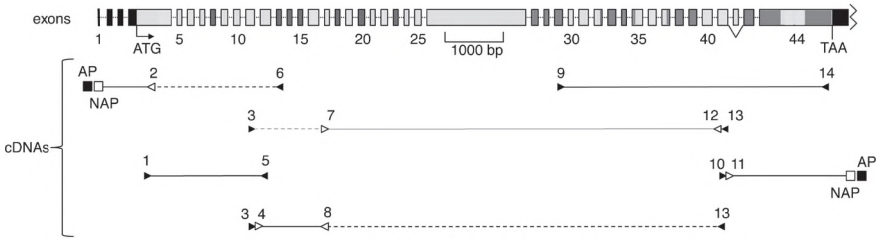

SUPPLEMENTAL FIGURE S1. Details of RT-PCR study of *EYS*.

(See appendix for color figure)

Primer sequences are listed in Supplemental Table S1. AP (filled square) and NAP (open square) denote RACE adaptor and nested adaptor primers, respectively. Filled and open arrowheads represent regular and nested RT-PCR primers. Dashed line denote primary RT-PCR products.

SUPPLEMENTAL FIGURE S2. Detailed characteristics of the human EYS protein domains. *(See appendix for color figure)*

REFERENCES

1. Hartong DT, Berson EL, Dryja TP. Retinitis pigmentosa. Lancet. 2006;368:1795-1809.

2. Barragan I, Abd El-Aziz MM, Borrego S, et al. Linkage validation of RP25 Using the 10K genechip array and further refinement of the locus by new linked families. Ann Hum Genet. 2008;72:454-462.

3. Ruiz A, Borrego S, Marcos I, Antinolo G. A major locus for autosomal recessive retinitis pigmentosa on 6q, determined by homozygosity mapping of chromosomal regions that contain gamma-aminobutyric acid-receptor clusters. Am J Hum Genet. 1998;62:1452-1459.

4. Abd El-Aziz MM, El-Ashry MF, Barragan I, et al. Molecular genetic analysis of two functional candidate genes in the autosomal recessive retinitis pigmentosa, RP25, locus. Curr Eye Res. 2005;30:1081-1087.

5. Abd El-Aziz MM, Patel RJ, El-Ashry MF, et al. Exclusion of four candidate genes, KHDRBS2, PTP4A1, KIAA1411 and OGFRL1, as causative of autosomal recessive retinitis pigmentosa. Ophthalmic Res. 2006;38:19-23.

6. Abd El-Aziz MM, El-Ashry MF, Chan WM, et al. A novel genetic study of Chinese families with autosomal recessive retinitis pigmentosa. Ann Hum Genet. 2007;71:281-294.

7. Abd El-Aziz MM, Barragan I, O'Driscoll C, et al. Large-scale molecular analysis of a 34 Mb interval on chromosome 6q: major refinement of the RP25 interval. Ann Hum Genet. 2008;72:463-477.

8. Barragan I, Marcos I, Borrego S, Antinolo G. Mutation screening of three candidate genes, ELOVL5, SMAP1 and GLULD1 in autosomal recessive retinitis pigmentosa. Int J Mol Med. 2005;16:1163-1167.

9. Barragan I, Marcos I, Borrego S, Antinolo G. Molecular analysis of RIM1 in autosomal recessive Retinitis pigmentosa. Ophthalmic Res. 2005;37:89-93.

10. Barragan I, Borrego S, Abd El-Aziz MM, et al. Genetic analysis of FAM46A in Spanish families with autosomal recessive retinitis pigmentosa: characterisation of novel VNTRs. Ann Hum Genet. 2008;72:26-34.

11. Li Y, Marcos I, Borrego S, Yu Z, Zhang K, Antinolo G. Evaluation of the ELOVL4 gene in families with retinitis pigmentosa linked to the RP25 locus. J Med Genet. 2001;38:478-480.

12. Marcos I, Ruiz A, Blaschak CJ, Borrego S, Cutting GR, Antinolo G. Mutation analysis of GABRR1 and GABRR2 in autosomal recessive retinitis pigmentosa. J Med Genet. 2000;37:E5.

13. Marcos I, Galan JJ, Borrego S, Antinolo G. Cloning, characterization, and chromosome mapping of the human GlcAT-S gene. J Hum Genet. 2002;47:677-680.

14. Marcos I, Borrego S, Antinolo G. Molecular cloning and characterization of human RAB23, a member of the group of Rab GTPases. Int J Mol Med. 2003;12:983-987.

15. den Hollander AI, Koenekoop RK, Mohamed MD, et al. Mutations in LCA5, encoding the ciliary protein lebercilin, cause Leber congenital amaurosis. Nat Genet. 2007;39:889-895.

16. Helbling-Leclerc A, Zhang X, Topaloglu H, et al. Mutations in the laminin alpha 2-chain gene (LAMA2) cause merosin-deficient congenital muscular dystrophy. Nat Genet. 1995;11:216-218.

17. Perrault I, Rozet JM, Calvas P, et al. Retinal-specific guanylate cyclase gene mutations in Leber's congenital amaurosis. Nat Genet. 1996;14:461-464.

18. den Hollander AI, Lopez I, Yzer S, et al. Identification of novel mutations in patients with Leber congenital amaurosis and juvenile RP by genome-wide homozygosity mapping with SNP microarrays. Invest Ophthalmol Vis Sci. 2007;48:5690-5698.

19. Marmor MF, Holder GE, Seeliger MW, Yamamoto S. Standard for clinical electroretinography (2004 update). Doc Ophthalmol. 2004;108:107-114.

20. Miller SA, Dykes DD, Polesky HF. A simple salting out procedure for extracting DNA from human nucleated cells. Nucleic Acids Res. 1988;16:1215.

21. Nannya Y, Sanada M, Nakazaki K, et al. A robust algorithm for copy number detection using high-density oligonucleotide single nucleotide polymorphism genotyping arrays. Cancer Res. 2005;65:6071-6079.

22. Letunic I, Copley RR, Pils B, Pinkert S, Schultz J, Bork P. SMART 5: domains in the context of genomes and networks. Nucleic Acids Res. 2006;34:D257-D260.

23. Schultz J, Milpetz F, Bork P, Ponting CP. SMART, a simple modular architecture research tool: identification of signaling domains. Proc Natl Acad Sci U S A. 1998;95:5857-5864.

24. Finn RD, Tate J, Mistry J, et al. The Pfam protein families database. Nucleic Acids Res. 2008;36: D281-D288.

25. Julenius K, Molgaard A, Gupta R, Brunak S. Prediction, conservation analysis, and structural characterization of mammalian mucin-type O-glycosylation sites. Glycobiology. 2005;15:153-164.

26. Husain N, Pellikka M, Hong H, et al. The agrin/perlecan-related protein eyes shut is essential for epithelial lumen formation in the Drosophila retina. Dev Cell. 2006;11:483-493.

27. Zelhof AC, Hardy RW, Becker A, Zuker CS. Transforming the architecture of compound eyes. Nature. 2006;443:696-699.

28. Holbrook JA, Neu-Yilik G, Hentze MW, Kulozik AE. Nonsense-mediated decay approaches the clinic. Nat Genet. 2004;36:801-808.

29. Winzen U, Cole GJ, Halfter W. Agrin is a chimeric proteoglycan with the attachment sites for heparan sulfate/chondroitin sulfate located in two multiple serine-glycine clusters. J Biol Chem. 2003;278:30106-30114.

30. Maw MA, Corbeil D, Koch J, et al. A frameshift mutation in prominin (mouse)-like 1 causes human retinal degeneration. Hum Mol Genet. 2000;9:27-34.

31. Zhang Q, Zulfiqar F, Xiao X, et al. Severe retinitis pigmentosa mapped to 4p15 and associated with a novel mutation in the PROM1 gene. Hum Genet. 2007;122:293-299.

32. Yang Z, Chen Y, Lillo C, et al. Mutant prominin 1 found in patients with macular degeneration disrupts photoreceptor disk morphogenesis in mice. J Clin Invest. 2008;118:2908-2916.

33. van Rossum AG, Aartsen WM, Meuleman J, et al. Pals1/Mpp5 is required for correct localization of Crb1 at the subapical region in polarized Muller glia cells. Hum Mol Genet. 2006;15:2659-2672.

34. den Hollander AI, ten Brink JB, de Kok YJ, et al. Mutations in a human homologue of Drosophila crumbs cause retinitis pigmentosa (RP12). Nat Genet. 1999;23:217-221.

35. den Hollander AI, Heckenlively JR, van den Born LI, et al. Leber congenital amaurosis and retinitis pigmentosa with Coats-like exudative vasculopathy are associated with mutations in the crumbs homologue 1 (CRB1) gene. Am J Hum Genet. 2001;69:198-203.

36. Lotery AJ, Jacobson SG, Fishman GA, et al. Mutations in the CRB1 gene cause Leber congenital amaurosis. Arch Ophthalmol. 2001;119:415-420.

37. den Dunnen JT, Grootscholten PM, Bakker E, et al. Topography of the Duchenne muscular dystrophy (DMD) gene: FIGE and cDNA analysis of 194 cases reveals 115 deletions and 13 duplications. Am J Hum Genet. 1989;45:835-847.

38. Koenig M, Hoffman EP, Bertelson CJ, Monaco AP, Feener C, Kunkel LM. Complete cloning of the Duchenne muscular dystrophy (DMD) cDNA and preliminary genomic organization of the DMD gene in normal and affected individuals. Cell. 1987;50:509-517

Adapted from: *Ophthalmology,* 2010 May

Karin W. Littink,[1,2] L. Ingeborgh van den Born,[1] Robert K. Koenekoop,[3] Rob W.J. Collin,[2,4,5] Marijke N. Zonneveld,[1,2] Ellen A.W. Blokland,[2] Hayat Khan,[3] Thomas Theelen,[5] Carel B. Hoyng,[5] Frans P.M. Cremers,[2,4] Anneke I. den Hollander,[4,5] and B. Jeroen Klevering[5]

[1] The Rotterdam Eye Hospital, Rotterdam, The Netherlands; [2] Department of Human Genetics, Radboud University Nijmegen Medical Centre, Nijmegen, The Netherlands; [3] McGill Ocular Genetics Laboratory, Montreal Children's Hospital Research Institute, McGill University Health Centre, Montreal, Canada; [4] Nijmegen Centre for Molecular Life Sciences, Radboud University Nijmegen Medical Centre, Nijmegen, The Netherlands and [5] Department of Ophthalmology, Radboud University Nijmegen Medical Centre, Nijmegen, The Netherlands.

CHAPTER 5B

MUTATIONS IN THE *EYS* GENE ACCOUNT FOR APPROXIMATELY 5% OF AUTOSOMAL RECESSIVE RETINITIS PIGMENTOSA AND CAUSE A FAIRLY HOMOGENEOUS PHENOTYPE

ABSTRACT

AIM. To determine the prevalence of mutations in the *EYS* gene in a cohort of patients affected by autosomal recessive retinitis pigmentosa (RP) and to describe the associated phenotype.

METHODS. DNA of 245 RP patients was selected for mutation analysis. All coding exons of *EYS* were screened for mutations by polymerase chain reaction amplification and sequence analysis. All 12 patients carrying mutations in *EYS* were re-examined, which included Goldmann kinetic perimetry, electroretinography, and high-resolution spectral-domain optical coherence tomography (OCT).

RESULTS. Nine novel truncating mutations and one previously described mutation in *EYS* were identified in 11 families. In addition, 18 missense changes of uncertain pathogenicity were found. Patients carrying mutations in *EYS* demonstrated classic RP with night blindness as the initial symptom, followed by gradual constriction of the visual field and a decline of visual acuity later in life. The onset of symptoms typically occurred between the second and fourth decade of life. The fundus displayed bone spicules increasing in density with age and generalized atrophy of the retinal pigment epithelium and choriocapillaris with relative sparing of the posterior pole until later in the disease process, when atrophic macular changes occurred.

CONCLUSIONS. Mutations in *EYS* account for approximately 5% of autosomal recessive RP patients in a cohort of patients consisting predominantly of patients of western European ancestry. The *EYS*-associated RP phenotype is typical and fairly homogeneous in most patients.

INTRODUCTION

Retinitis pigmentosa (RP; MIM 268000) is a clinically and genetically heterogeneous group of inherited retinal disorders characterized by photoreceptor degeneration. The rod and cone system may be equally affected in RP, but in most patients, rod dysfunction precedes cone dysfunction, resulting in the typical symptoms of night blindness, followed by loss of the (mid)peripheral visual field. In many patients, the cones in the central retina also become affected, resulting in loss of visual acuity in the later stages of the disease. Ophthalmoscopic abnormalities include a waxy pallor of the optic disc, attenuation of retinal vessels, and peripheral bone spicule pigmentations as well as atrophy of the retinal pigment epithelium (RPE). All modes of Mendelian inheritance, including digenic inheritance, have been observed in RP.[1,2] Clinical findings may vary between patients carrying causative mutations in different genes, and a degree of clinical heterogeneity even may be observed in patients carrying different or even identical causative mutations within one specific RP gene.[1] Until recently, mutations in 25 genes have been associated with autosomal recessive RP (arRP; http://www.sph.uth.tmc.edu/Retnet/). Together, these genes account for approximately 50% of arRP cases. The most frequently mutated gene is the *USH2A* gene (MIM +608400), accounting for approximately 7% of arRP cases, whereas most other genes contribute to only 1% to 2% of arRP cases.[1,3,4] Recently, a new gene, *eyes shut homolog* (*EYS*), was identified at the RP25 locus.[5,6] The *EYS* gene is one of the largest genes ever identified and, based on current knowledge, the largest gene that is expressed in the human eye. The human EYS protein is localized at the outer segments of the photoreceptor layer, but its function in human retina remains largely unknown.[6] In *Drosophila*, the *eys* protein plays a critical role in creating the space between the rhabdomeres, a structure comparable with the human photoreceptor.[7] Therefore, the human EYS protein may be essential for the integrity of the outer segment. To date, a total of eight truncating mutations have been detected in *EYS* in eight different arRP families.[5,6] The presence of mutations in families from different ancestral origins, the identification of several independent mutations, and the enormous size of the gene have led to the hypothesis that mutations in *EYS* may be a major cause of RP. Moreover, by linkage analysis, 14% to 25% of Spanish arRP families were shown to map to the RP25 interval.[8,9]

This study attempted to determine the percentage of arRP that can be ascribed to mutations in the *EYS* gene in a cohort of patients mainly of western European ancestry. In addition, a detailed clinical description of the RP patients carrying mutations in *EYS* is provided.

PATIENTS AND METHODS

Subjects

Blood samples were collected of 245 patients who were diagnosed with RP based on ophthalmic examination at The Rotterdam Eye Hospital (by LIvdB), the Radboud University Nijmegen Medical Centre (by BJK and CBH), or The McGill University Health Centre in Montreal (by RKK). Some pedigrees showed a pattern compatible with a recessive mode of inheritance (43%); the other patients were considered isolated cases (57%). In 18% of cases, known mutations in arRP genes were excluded with the arrayed-primer extension microarray for arRP genes (Asper Ophthalmics, Tartu, Estonia). In addition, 36 probands affected by an autosomal recessive form of cone–rod dystrophy and negative for known *ABCA4* mutations were enrolled in this study. After explaining the nature of this genotype-phenotype study, informed consent adhering to the tenets of the Declaration of Helsinki was obtained from all patients and unaffected family members who participated in the molecular study. Blood samples of the affected and unaffected family members were collected for segregation analysis of the genetic defect.

Mutation analysis

Genomic DNA was isolated from lymphocytes by a standard salting-out procedure.[10] All 41 coding and three non-coding exons of *EYS* (FM209056) were amplified by polymerase chain reaction (PCR) using the conditions described by Collin et al.[5] Purified PCR products of the coding exons were analyzed in either sense or antisense direction using dye termination chemistry (BigDye Terminator, version 1.1, on a 3730 DNA analyzer; Applied Biosystems, Inc., Foster City, CA). All sequence variants that were identified were confirmed with independent PCR reactions and were analyzed in sense and antisense direction. To determine whether some variants are common polymorphisms, the missense changes that were found in combination with another missense or truncating changes were screened in DNA samples of 180 unrelated and unaffected ethnically matched subjects using restriction fragment length analysis or allele-specific PCR.[11] Furthermore, all patients who carried only one truncating mutation in *EYS* were screened for the presence of heterozygous deletions of exon 12 or exons 15 through 19, which previously were published by Abd El-Aziz et al.[6] by using primers downstream and upstream of the reported breakpoints. The pathogenicity of the missense changes was evaluated for evolutionary conservation using the BLOSUM62 score,[12] by splice site prediction,[13] by the search for exonic splice enhancers,[14] and by analysis of the

biophysical properties of the side chains of the amino acid substitutions (Project Hope; http://www.cmbi.ru.nl/hope/). Furthermore, because prom1 is known to interact with eys in Drosophila,[7] the *PROM1* gene (NM_006017) was screened in DNA of patients who carried a heterozygous truncating mutation without a second allele to test the hypothesis of digenic inheritance. Primers were designed by ExonPrimer (software designed by T.M. Strom, Helmholtz Center Munich, Munich, Germany).

Clinical evaluation

After approval of the institutional review board was obtained, 12 patients who carried homozygous or compound heterozygous mutations in *EYS* were clinically re-evaluated at The Rotterdam Eye Hospital (by LIvdB), the Department of Ophthalmology at the Radboud University Nijmegen Medical Centre (by BJK), or the Department of Ophthalmology at McGill University Health Centre in Montreal, Canada (by RKK). Clinical evaluation included best-corrected visual acuity and slit-lamp biomicroscopy, followed by ophthalmoscopy after pupillary dilatation. Additional examinations included fundus photography, Goldmann kinetic perimetry (targets V-4e, II-4e, and I-4e to I-1e) to assess the size and extent of the visual field and spectral-domain optical coherence tomography (OCT; Spectralis, Heidelberg Engineering, Heidelberg, Germany) to visualize the in vivo retinal architecture. Electroretinograms were recorded according to the protocol of the International Society for Clinical Electrophysiology of Vision.[15] When available, the medical history was reviewed for a longitudinal evaluation of the *EYS*-associated RP phenotype.

RESULTS

Mutation analysis

Sequence analysis of all 41 coding exons of the *EYS* gene led to the identification of 10 pathogenic variants in 11 different families (Table 1). In 5 families (families B, C, D, J, and K), the truncating mutations conclusively were causative for RP, because they were present on both alleles either homozygously or compound heterozygously and segregated in the RP family (Figure 1). In 1 family (Figure 1, family A), the mutation in *EYS* was causative for only two siblings who carry the frameshift mutation homozygously, whereas one affected sibling carries the mutation heterozygously and two affected siblings do not carry the *EYS* mutation. In three families (families G, H, and L), the truncating mutation was found in combination with a missense change (Table 1).

TABLE 1. Retinitis pigmentosa patients carrying truncating mutation(s) in *EYS*

			Allele 1		Allele 2		Confirmed by segregation analysis
Patient	Inheritance	Country	Mutation	Effect	Mutation	Effect	
A II-1	AR	Canada	c.1644delG	p.Q548QfsX60	c.1644delG	p.Q548QfsX60	Partially
B II-2	Isolated	Netherlands	c.1673G>A	p.W558X	c.2811C>A	p.C937X	Yes
C II-6	AR	Netherlands	c.4350_4356del7	p.K1450KfsX3	c.8710_8717del8	p.T2904KfsX4	Yes
D II-1	Isolated	Netherlands	c.4350_4356del7	p.K1450KfsX3	c.4350_4356del7	p.K1450KfsX3	Yes
E	Isolated	Netherlands	c.4350_4356del7	p.K1450KfsX3	NI		NA
F II-9*	AR	Netherlands	c.4350_4356del7	p.K1450KfsX3	NI		No
G	Isolated	South-Korea /USA	c.4712C>G	p.S1571X	c.6557G>A	p.G2186E	NA
H	Isolated	Curaçao	c.6794delC	p.P2265QfsX46	c.2500G>A	p.V834I	NA
J II-1	Isolated	Netherlands	c.6714delT	p.P2238PfsX16	c.6714delT	p.P2238PfsX16	Yes
K II-2	AR	Netherlands	c.6799_6800delCA	p.Q2267EfsX15	c.6799_6800delCA	p.Q2267EfsX15	Yes
L II-2	Isolated	Netherlands	c.7095T>G	p.Y2365X	c.9047T>A	p.I3016N	Yes

AR, autosomal recessive; fsX#, frameshift that leads to stopcodon # amino acids downstream; NA, no family members available; NI, not identified; X, stopcodon. Nucleotide and amino acid numbering refer to EYS cDNA sequence FM209056. *, mutation in *EYS* is not causative in this patient.

Two of the missense changes (family G, p.G2186E; and family L, p.I3016N) affect amino acids that are conserved in most of the Laminin A G-like domains in *EYS* (Figure 2), and therefore are likely to play a crucial role in this domain. Furthermore, these two changes lead to the substitution of amino acids that evolutionarily are not related, and therefore have a negative BLOSUM62 score.[12, 14] The third missense change (family H, p.V834I) affects an amino acid that is not conserved between the epidermal growth factor (EGF)-like domains of EYS (Figure 2) and has a BLOSUM62 score of 3, indicating that a valine commonly is replaced by a isoleucine during evolution. For family L, segregation of the mutations with the disease was confirmed. For the other two patients carrying missense variants, no family members were available for segregation analysis. In two families (families E and F), only one heterozygous truncating mutation was detected (Table 1).

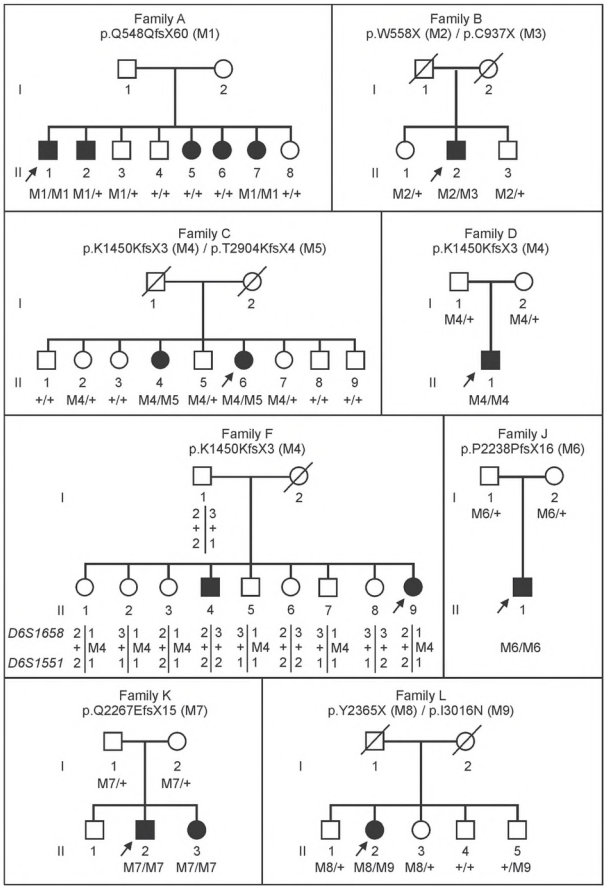

FIGURE 1. Pedigrees of the families that were available for mutation analysis. Pedigrees of 6 families (families B, C, D, J, K, and L) showing segregation of the mutation with the disease. In family A, the mutations are causative in only 2 of 5 patients, and in family F, the mutation is not causative, as shown by the common haplotypes on both alleles in patient II-9 and her unaffected siblings II-1 and II-3. Plus signs indicate a wild-type allele, square boxes indicate men, circles denote women, and affected individuals are pointed out by a black symbol. The probands are indicated with an arrow.

For patient E, no second allele could be identified and no family members were available for segregation analysis. Surprisingly, in family F, the other affected sibling (II-4) did not carry the mutation (Figure 1). Moreover, haplotype analysis around the *EYS* locus revealed the presence of the same second allele in patient II-9 and two of her unaffected siblings (II-1 and II-3) who also carry the p.K1450KfsX3 mutation (Figure 1), suggesting that this mutation in *EYS* is not causative for RP in this family.

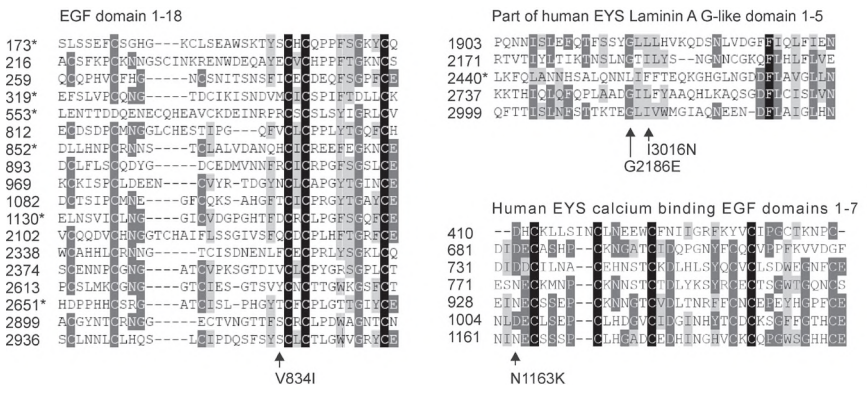

FIGURE 2. Alignment of analogous protein domains within human EYS.
Alignment of analogous domains within the human EYS protein showing amino acids that are conserved throughout the domains that may be essential for a normal function of the domain. Black boxes with white letters denote identical amino acids, conserved amino acids are presented as grey with white letters, and a block of similar amino acids is presented as a grey box with black letters. Sequences were adapted from Collin et al[5] and aligned by Vector NTI version 10 (Invitrogen, Carlsbad, CA). Amino acid position of the first shown amino acid is indicated per domain. *, part of domain not shown; EGF, epidermal growth factor.

In two patients in whom no truncating mutations could be identified and who were therefore not included in the overview of *EYS* RP patients (14613, 28692), more than one heterozygous missense change was found (Table 2). In patient 14613, the p.T1424A change is predicted to affect one of the two predicted glycosylation sites.[16] The other two changes (p.T1993A and p.T2831I) both concern a residue in a Laminin A G-like domain that is not conserved between the EYS Laminin A G-like domains and have a BLOSUM62 score of 0 and –1, respectively. In the other patient (28692), the p.T1993A allele again was found in combination with another heterozygous missense variant (p.I1232F), but this change also is not conserved between the EYS EGF-like domains and has a BLOSUM62 score of 0. Because no family members were available, it could not be determined whether these variants are present on separate alleles and whether they segregate with the disease. All seven missense changes mentioned above were not present in 180 ethnically matched control individuals.

TABLE 2. Heterozygous missense changes in *EYS* identified in retinitis pigmentosa patients

Change	Effect	Prevalence in RP-patients	BLOSUM 62 score	Proof of pathogenicity/non-pathogenicity
Probably pathogenic				
c.2500G>A	p.V834I	1/245	3	Excluded in 180 control subjects, but not conserved throughout EYS EGF domains (Figure 2). However, found in combination with truncating mutation (p.P2265QfsX46)
c.6557G>A	p.G2186E	1/245	-2	Excluded in 180 control subjects, conserved throughout EYS LamG domains (Figure 2), found in combination with nonsense mutation (p.S1571X)
c.9047T>A	p.I3016N	1/245	-3	Excluded in 180 control subjects, conserved throughout EYS LamG domains (Figure 2), found in combination with nonsense mutation (p.Y2365X); segregation with disease confirmed
Unknown pathogenicity				
c.977G>A	p.S326N	1/245	1	Found in patient from consanguineous marriage, so heterozygous change perhaps non-significant
c.1145A>T	p.N382I	1/245	-3	Residue not conserved throughout EYS EGF-like domains
c.1382G>A	p.C461Y	1/245	-2	Not in functional domain, but removal of cysteine in extracellular domain might disrupt secondary structure or protein interaction
c.3489T>A	p.N1163K	1/245	0	Conserved residue (D or N) in cbEGF domains (figure 2)
c.3694A>T	p.I1232F§	1/245	0	Excluded in 180 control subjects, but not conserved residue in EGF-like domain. However, found in combination with other missense variant
c.4531T>C	p.S1511P	1/245	-1	Not in functional domain
c.4270A>G	p.T1424A*	1/245	0	Excluded in 180 control subjects, predicted to disrupt glycosylation site, found in combination with other missense variants
c.4985A>T	p.D1662V	1/245	-3	Not in functional domain
c.5110A>T	p.I1704L	1/245	2	Not in functional domain
c.5401G>A	p.A1801T	1/245	0	Not in functional domain
c.5510G>C	p.W1837S	1/245	-3	Not in functional domain
c.5977A>G	p.T1993A* §	3/245	0	Excluded in 180 control subjects, but non-conserved residue in LamG domain. However, found in combination with other missense variants
c.6188G>T	p.C2063F	1/245	-2	Not in functional domain, but is predicted to form disulphide bond with cysteine at position 2037 (Project Hope), and thus may disrupt secondary structure or protein interaction
c.6452A>G	p.N2151S	1/245	1	Not in functional domain
c.6964A>G	p.I2321V	1/245	3	Not in functional domain
c.7597A>G	p.K2533E	1/245	1	Residue not conserved in LamG domain
c.7751C>G	p.T2584S	2/245	1	Residue not conserved in LamG domain
c.8492C>T	p.T2831I*	2/245	-1	Excluded in 180 control subjects, but not conserved residue in LamG domain. However, found in one patient in combination with two other missense variants
Non-pathogenic				
c.5244A>C	p.L1748F	0/245	0	Found in unaffected family members, while not present in affected family members
c.7666A>T	p.S2556C	43/245	-1	Frequently present in control individuals, both homozygously as heterozygously
c.7796A>G	p.H2599R	4/245	0	Found in unaffected family members, while not present in affected family members

*, p.T1993A, p.T2831I and p.T1424A were all detected in one patient (14613); §, p.T1993A and p.I1232F were detected in one patient (28692); family members were not available for segregation analysis. LamG, Laminin A G-like domain; cbEGF, calcium-binding EGF domain

Furthermore, 18 heterozygous missense changes were identified that were present without a second allele. Table 2 contains further information about these changes, enabling speculation about their pathogenicity.

Three missense changes should be considered benign, because they were found homozygously in control subjects, or were detected in unaffected family members, whereas they were not present in the respective affected family members. In addition, 11 silent changes (i.e., nucleotide changes that do not affect the amino acid) and many intronic variants were identified that are likely to be non-pathogenic, because none of the variants introduce or abolish a splice site or splice enhancer site (data not shown). Abd El-Aziz et al.[6] describe a deletion in *EYS* of exon 12 and a deletion of exons 15 through 19. In an attempt to find the second allele in the patients who carry one heterozygous stop or frameshift mutation, a breakpoint-spanning PCR analysis was conducted to search for the deletions in a heterozygous state. These deletions, as well as the other mutations described by Abd El-Aziz et al.,[6] were not identified in this study. Furthermore, these patients were screened for mutations in *PROM1*, because this gene is known to interact with *spacemaker/eyes shut* (*eys*) in the eye of *Drosophila*.[7] No mutations, however, were found in the coding exons of *PROM1*. Because mutations in *EYS* have been found previously in a patient affected by cone–rod dystrophy,[5] 36 patients affected by cone–rod dystrophy also were screened for mutations in *EYS*, but no mutations were identified in this patient group.

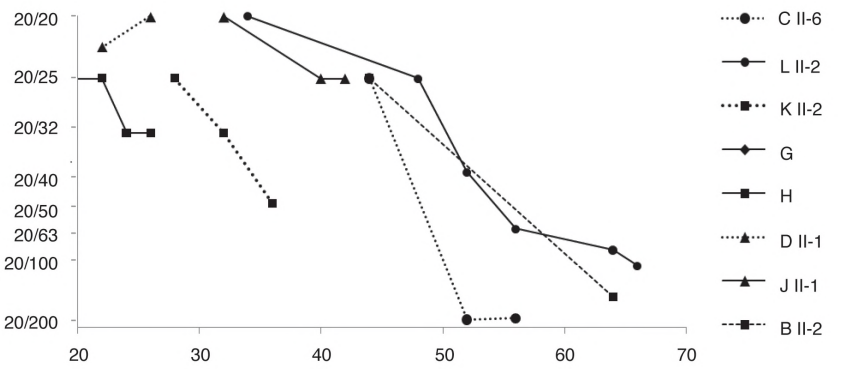

FIGURE 3. **Graph showing changes in visual acuity with age in patients carrying mutations in *EYS*.** The graph shows the change in visual acuity (y-axis) related to the age in years (x-axis). Symbols indicate the moments of assessment of the visual acuity. Improvement of visual acuity in patient DII-1 was the result of successful treatment of cystoid macula edema with Octreotide, and in patient CII-6 visual improvement was the result of cataract extraction

Clinical characteristics

Clinical evaluation of 12 patients carrying pathogenic mutations in *EYS* showed typical RP symptoms of night blindness as the initial symptom and progressive constriction of the visual fields. Table 3 shows an overview of the clinical features of the patients who carry probable causative mutation(s) in *EYS*. The median age of first symptoms was 19 years (range, 14–62 years), including one patient (patient E; Table 3) with an age of onset of 62, which deviates from the others. For those patients with an extended period of clinical follow-up, the decline of visual acuity over the years is depicted in Figure 3. This figure suggests that visual acuity starts to decrease after the age of 30 years and drops to less than 20/200 near the age of 60 years. Posterior subcapsular cataracts were seen in 11 of 12 patients and were encountered at a relatively young age (>26 years).

Ophthalmoscopy showed optic disc pallor in all patients, with multiple nerve head drusen in one patient. Retinal vessels were attenuated, and profound atrophy of the RPE, choriocapillaris, and outer retina at the (mid)peripheral retina was observed in all patients. In the later stages of the disease, the macular region and sometimes the fovea also became affected. In the periphery, variable amounts of intraretinal pigmentations were observed (Figure 4). One patient had fibrous Coats-like lesions on the inferior quadrants. The high-resolution OCT images showed a relative preservation of the retinal layers in the central macula in all patients and marked atrophy of the chorioretinal layers more (mid)peripherally (Figure 5). Reduction of retinal thickness resulting from the loss of neuroretinal tissue is shown in Figure 6. In a patient with end-stage RP, OCT even demonstrated a complete loss of photoreceptors, RPE, and choriocapillaris peripheral to the macula (Figure 7). The profound loss of the normal retinal layers enabled visualization of the entire choriocapillaris and even the sclera in some patients. Interestingly, cellular-sized hyperreflective structures were seen at variable depths, varying from the nerve fiber layer to the RPE (Figure 8). Electroretinography responses at the age of last examination were nonrecordable or showed severe loss of signal in a rod–cone pattern for all patients.

Family ID	ID	Age (yrs)	Sex	Age of onset	Visual acuity (current age) OD	OS	Lens status	Goldmann perimetry
A	II-1	63	M	8	2/400	2/400	NS and PSC cataract	5 degree visual field with V4e target
B	II-2	64	M	36	20/200	LP+	PSC cataract	OD: Central visual field<5 degrees, two peripheral islands. OS: small peripheral island
C	II-4	73	F	21	20/63	20/50	PSC cataract; extraction at age 73 yrs (OU)	Severely constricted visual fields (<10 degrees)
	II-6	69	F	14	HM	HM	PSC cataract; extraction at age 54 yrs (OU)	No longer possible. At age 40: central visual field < 10 degrees
D	II-1	25	M	17	20/20	20/25	Clear	Intact periphery with V-4e, III-4e, mid peripheral sensitivity loss with paracentral scotoma
E	-	64	F	62	20/32	20/25	OD: Posterior cortical cataract	Constricted visual fields up to 30 degrees
G	-	36	F	22	20/25	20/25	Mild PSC cataract	Constricted visual fields up to 15 degrees
H	-	26	M	13	20/32	20/40	Mild PSC cataract	Constriction up to 20 degrees nasally, 70-80 degrees temporally. OS: Relative central scotoma
J	II-1	42	M	22	20/25	20/25	PSC cataract	Mildly constricted visual fields at V-4e, marked constriction of visual fields (<20 degrees) at all other intensities
K	II-2	39	M	15	20/50	20/40	PSC cataract	Marked decrease in visual fields (<30 degrees) with a small temporal islands
	II-3	36	F	17	20/32	20/32	OD: ant/post polar and capsular opacification OS: PSC cataract	Marked decrease of visual field (<20-30 degrees) with residual temporal peninsulas
L	II-2	66	F	35	20/100	CF	PSC cataract	Constricted visual fields (<30-40 degrees), small paracentral scotomas. Loss of sensitivity OS>OD

TABLE 3. Clinical characteristics of retinitis pigmentosa patients carrying mutations in *EYS*.

§, current age; *, recorded elsewhere; ¶, isolated rod response; ǂ, single flash cone response; ↓, 50-100 microvolt; ↓↓, 10-50 microvolt (normal values rod response: ~114 uV, cone response: ~194uV, according to ISCEV with Dawson Trick Litzkow (DTL) electrodes; ant, anterior; CF, counting

Fundoscopy	OCT	ERG Rod¶ (μV)	ERG Cone‡ (μV)
Optic disc pallor, narrow vessels and peripapillary atrophy. Extensive and diffuse choroidal show and choroidal sclerosis, with RPE loss and bone spicule pigmentation.	Extensive remodeling and severe loss of retinal layers.	NR	NR
Optic nerve head drusen, severely attenuated vessels, atrophic macular region with foveal island, relatively preserved RPE midperipheral, atrophic RPE far periphery with bone-spicules and pavingstone-like degenerations.	Severe epiretinal fibrosis. Mild abnormalities in fovea, marked atrophy of the more peripherally located chorioretinal layers.	NR	↓↓
Attenuated retinal vasculature, generalized atrophy with macular sparing, extensive bone spicules throughout periphery.	Complete loss of photoreceptors, RPE and choriocapillaris peripheral to the macula.	NR	NR
Very pale, waxy optic disc. Severely attenuated retinal vasculature, extensive chorioretinal atrophy with minimal residual RPE at macular region. Profound (mid)peripheral pigmentations.	Irregular loss of photoreceptors in the central macula. Severely atrophic retina especially peripheral to the macula. All retinal layers appear to be affected. Focal increased reflectivity in deep layers of neuroretina, possibly RPE cells.	NR	NR
Pink optic disc, moderately attenuated vessels, cystoid maculopathy, in (mid)periphery RPE atrophy with some bone-spicules and some drusen-like deposits.	Virtually normal anatomic aspect of the foveal photoreceptors, with exception of cystoid macular edema. Mild epiretinal fibrosis.	↓↓	↓↓
Pallor of the optic disc, attenuated retinal vasculature, preserved RPE posterior pole, (mid)periphery RPE atrophy with bone-spicules, inferior quadrants (OU) fibrotic lesions resembling old Coats'-like vasculopathy.	NP	↓↓	↓↓
Pink optic disc, severely attenuated vessels with sheathing, preserved RPE macular region, (mid)periphery pronounced RPE atrophy with bone-spicules and some drusen-like deposits.	Normal aspect of foveal anatomy. Chorioretinal atrophy in periphery. Clearly visible choroidal vessels. Hyperreflective structures in variable depths in the nerve fiber layer.	↓↓	↓
Mild pallor optic disc, vessels near normal caliber, preserved RPE posterior pole with mild epiretinal membrane, RPE changes in macula with three intraretinal crystals. OD (mid)periphery atrophic with bone-spicules.	Deepened foveal dimple, almost no outer and inner segments in macular region. In right fovea irregular hyperreflective structure. Outside the macular region generalized atrophy of the retinal layers and RPE.	NR*	NR*
Waxy pallor of the optic disc, attenuated retinal vasculature, generalized chorioretinal atrophy, mild bone spicule pigmentation clustered in periphery.	Relative normal aspect of the fovea. Atrophy of predominantly the deeper layers of the retina in the periphery. Loss of choriocapillaris.	NR	NR
Pink, waxy optic disc. Moderately attenuated retinal vasculature, generalized chorioretinal atrophy with macular sparing, and classic bone spicules in periphery.	Relative sparing of foveal photoreceptors, generalized atrophy of deep retinal layers and choriocapillaris. Deep choroidal vessels clearly visible. Highly irregular hyperreflective structures in retina, possible proliferating and migrating RPE cells.	NR	NR
Waxy optic disc with temporal pallor, attenuated retinal vasculature, extensive chorioretinal atrophy few bone spicules in periphery.	Relative good aspect of central macula and sparing of foveal cones. Severe atrophy of (mid)peripheral retina, with clearly visible larger choroidal vessels. Bone spicules in nerve fiber layer with obscuration of deeper layers.	NR	NR
Pink optic disc. Mild to moderate attenuation of retinal vasculature, marked chorioretinal atrophy extending into the posterior pole. Clustered bone spicule pigmentation in periphery.	Foveal contour present, nevertheless loss of cone outer segments in fovea. Chorioretinal atrophy throughout retina with exception of central macula. Increased visibility of the large choroidal vessels and even sclera due to atrophy of the overlying layers	NR	NR

fingers; ERG, electroretinogram; F, female; HM, hand movements; ID, identification number; LP+, positive for light perception; M, male; NP, not performed; NR, non-recordable; NS, nuclear sclerosis; OCT, optical coherence tomography; OD, right eye; OS, left eye; OU, both eyes; post, posterior; PSC, posterior subcapsular; RPE, retinal pigment epithelium.

FIGURE 4. Fundus photographs of patients carrying mutations in *EYS*. *(See appendix for color figure)*

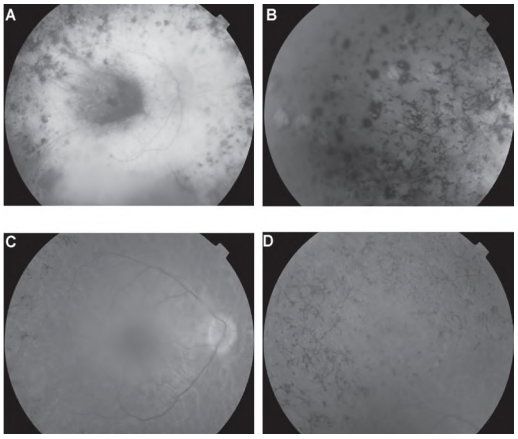

A. Fundus photograph of the central retina of the right eye of patient CII-6 showing the fundus in an end-stage of the disease. The fundus is characterized by a very pale, waxy optic disc, severely attenuated retinal vasculature, and extensive chorioretinal atrophy with minimal residual retinal pigment epithelium at the macular region.

B. Fundus photograph of the temporal peripheral retina of patient C II-6 showing heavy irregular pigmentations in the (mid)peripheral retina.

C. Fundus photograph of the central retina of the right eye of patient KII-2 showing a pink, waxy optic disc, moderately attenuated retinal vessels, and generalized chorioretinal atrophy with macular sparing.

D. Fundus photograph of the upper temporal peripheral retina of patient KII-2 showing classic bone spicules in periphery. The red telangiectatic-like vessels at the temporal retina (Figure 4C, 4D) are not visible with higher resolution and on fluorescein angiography, and therefore seem to be artifacts.

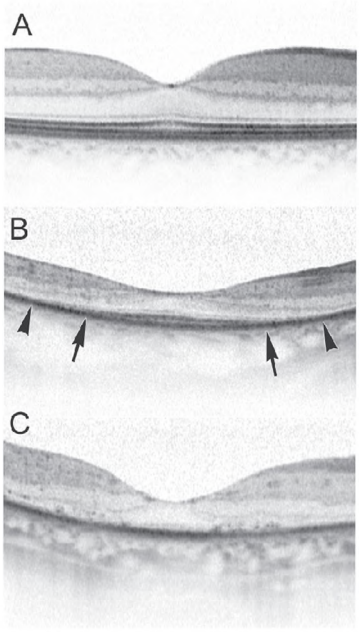

FIGURE 5. Illustration of macular changes by spectral-domain optical coherence tomography.

A. In the healthy, the outer retina constantly shows four highly reflective stripes, representing the photoreceptor outer segment/retinal pigment epithelium complex and the choriocapillary layer.

B. In the earlier stages of retinitis pigmentosa resulting from mutations in *EYS*, the high reflective outer retinal layers are disorganized and lost peripheral to the macula. Frequently, a transition zone may be observed containing a more central margin of photoreceptor outer segment/retinal pigment epithelium loss (arrows) and a more peripheral boundary of total photoreceptor loss (arrowheads), as shown in the right eye of patient KII-3.

C. Optical coherence tomography image of the right eye of patient LII-2 showing a late-stage of *EYS*-related retinitis pigmentosa, total outer retinal loss, and subretinal clump formation at the fovea.

DISCUSSION

This study identified 11 families carrying pathogenic mutations in *EYS*, a gene that recently was found to be mutated in patients with arRP.[5,6] One mutation previously was identified in a Dutch family;[5] the other nine mutations are novel. In one family (family E) with a homozygous frameshift mutation in *EYS*, haplotype analysis revealed that the *EYS* mutation cannot be causative in that family. Previously, mutations in *EYS* were identified in three of 10 patients from the same cohort. Consequently, the molecular cause was identified in 13 arRP families, which brings the prevalence of *EYS* mutations in the total cohort of 255 patients to approximately 5%. Of the 25 genes known to cause arRP, only four are known to be responsible for more than 3% of cases (*USH2A* [7%],[3,4] *ABCA4* [5%–6%],[17] *PDE6B* [4%–5%],[18,19] and *PDE6A* [3%–4%][20]), whereas the other genes account for only 1-2% of patients or less.[1] The prevalence of approximately 5% of *EYS* mutations in the cohort allows for the conclusion that mutations in *EYS* may be one of the major causes of arRP.

Most patients carrying mutations in *EYS* demonstrate the typical RP symptoms of night blindness and progressive constriction of the visual field. The age of first symptoms varied from 14 to 62 years, with a mean age of 19 years. A late onset with mild symptoms has been described previously for patients carrying mutations in *EYS*,

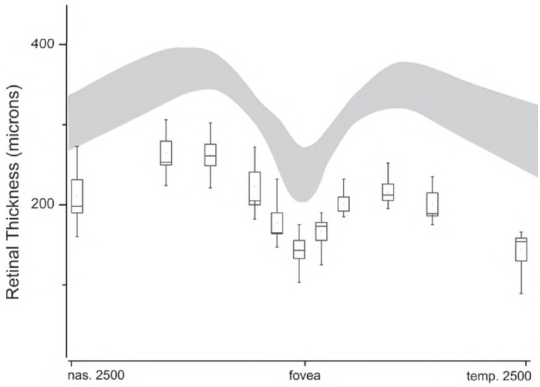

FIGURE 6. Graph showing retinal thickness of *EYS*-associated retinitis pigmentosa patients compared with that of normal individuals.

Retinal thickness across the horizontal meridian with up to 2500 μm of eccentricity from the fovea of 6 patients with autosomal recessive retinitis pigmentosa resulting from mutations in *EYS* (CII-4 and CII-6, JII-1, KII-2 and KII-3, and LII-2; assessed by T.T.) compared with age-matched normal individuals (gray band, ± 2 standard deviations from the mean). Box, mean ± standard deviation; line in box, median; point in box, mean; whisker, range; nas, microns nasal to the fovea.

as well as phenotypic variability in patients carrying identical mutations.[5] Most of the mutations described in this study have a truncating effect on the protein and likely are to result in degradation of the mRNA.

Patients carrying a missense change, which would be expected to result in the mildest phenotype, are not specifically affected more mildly. Therefore, a correlation between the genotype and the severity of the phenotype cannot be determined. Because the age varied in the patients, different stages of the disease could be studied. For most patients, visual acuity was preserved until the fourth decade. Overall, the fundi of all patients were remarkably similar, with generalized and profound chorioretinal atrophy, sparing of the macular region, and bone spicule pigmentations. The high-resolution OCT images showed areas of hyperreflectivity, presumably RPE cells, that appear to be located at different levels in the neuroretina (Figure 8). These OCT data may very well represent migration of RPE cells to the inner retinal layers. Such a process already was suggested in earlier histopathologic studies on bone spicule pigmentation that showed a migration of RPE into the neural retina.[21] Moreover, the severe atrophy of the neuroretinal layers enhanced the penetrating depth of the OCT, enabling visualization of the larger choroidal vessels and sometimes even the sclera (Figure 7).

Posterior subcapsular cataracts were present at an early age, varying from second to fourth decade, in most of the patients (92%), ranging from mild to severe and varying with age. In one patient, visual acuity improved noticeably from hand movements to counting fingers after cataract extraction at age 54 years.

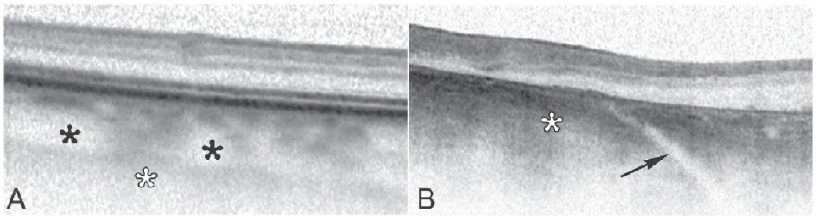

FIGURE 7. Appearance of the peripheral choroid on spectral-domain optical coherence tomography images.

A. In a healthy eye, the choroidal visibility is limited by melanin of the retinal pigment epithelium. Beneath the choriocapillary layer, large choroidal vessels (black asterisks) may be observed.

B. In autosomal recessive retinitis pigmentosa caused by mutations in *EYS*, loss of retinal pigment epithelium results in a dramatically increased visibility of the sclera (white asterisks), as shown in the left eye of patient CII-6. Choroidal vessels cannot be detected any more because of complete atrophy of the choroid. Note the scleral emissary channel (arrow).

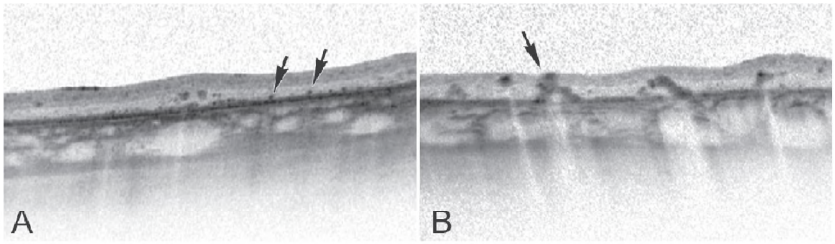

FIGURE 8. Spectral-domain optical coherence tomography image of the equatorial retina in *EYS*-associated autosomal recessive retinitis pigmentosa.
Considerable retinal thinning and disorganization with loss of the typical structure can be observed. At variable retinal levels, highly reflective structures could be observed (arrows) that could occur as single dots in **(A)** the left eye of patient KII-3 or as clusters in **(B)** the right eye of patient KII-2. These changes were colocated with funduscopically visible pigment changes, suggesting transretinal retinal pigment epithelium migration.

The high prevalence of cataracts in *EYS*-associated RP again demonstrates the importance of regular follow-up of patients with inherited retinal disease, because the benefits of cataract surgery in RP patients have been demonstrated even in the presence of relative minor lens opacifications.[22]

Previously described mutations or deletions in *EYS* resulted in premature truncation of the protein.[5,6] Interestingly, 18 missense variants were found as well. Of particular interest are the three missense changes (p.V834I, p.G2186E, p.I3016N) that probably are causative in view of their presence in combination with a truncating mutation. Four of the missense changes were found in combination with one or two other missense variants. One variant (p.T1424A) is predicted to affect a putative glycosylation site, and therefore may be pathogenic. The residues of the other three variants (p.I1232F, p.T1993A, and p.T2831I) are not conserved throughout the EYS EGF-like and Laminin A G-like domains, respectively, and their pathogenicity remains unclear. Of special interest as well is the p.N1163K change, because this particular residue in the calcium-binding EGF domain is a conserved residue involved in calcium binding (Figure 2).[23] Also of interest are two missense changes (p.C461Y and p.C2063F) that are not part of a specific domain, but concern the change of a cysteine residue. Extracellular cysteine residues are known to form disulfide bonds, which are important for the secondary structure of the protein and for protein–protein interaction.[24] Specifically, the cysteine residue at position 2063 is predicted to form a disulfide bond with the cysteine residue at position 2037. Therefore, these missense changes

may have a pathogenic character. Patients in whom a change was identified on only one allele may carry an additional intronic mutation or a heterozygous deletion on the other allele, which cannot be detected by PCR-based mutation screening of the exons. Alternatively, in case of a missense change, the variant could be a nonpathogenic rare variant. In patients with only one clear protein-truncating mutation, *PROM1* was screened for mutations because it has been shown to interact with eys in *Drosophila*,[7] but no mutations were found.

Interestingly, the p.K1450KfsX3 mutation was detected in five patients, all originating from the western part of The Netherlands. Marker analysis showed a common haplotype for markers at 1 Mb of the frameshift mutation for two families and partially the same haplotype for the other two families (data not shown), indicating that this may be a founder mutation in the west of The Netherlands.

In conclusion, this study described nine novel mutations in the *EYS* gene together with a number of possible pathogenic missense changes. The *EYS*-associated RP phenotype is fairly typical with severe atrophy of the neuroretina in the (mid)periphery. Because mutations in *EYS* contribute to a significant proportion of RP patients (approximately 5%), routine diagnostic screening on a genotyping chip is important. By adding the mutations identified in *EYS* by this study and others to the arRP genotyping microarray (Asper Ophthalmics, Tartu, Estonia), the efficiency of this diagnostic tool can be improved significantly. The identification of the genetic cause allows a more precise genetic counseling and, in the future, will be of importance when gene-specific or mutation-specific therapies become available.[25,26]

REFERENCES

1. Hartong DT, Berson EL, Dryja TP. Retinitis pigmentosa. Lancet. 2006;368:1795-1809.

2. Kajiwara K, Berson EL, Dryja TP. Digenic retinitis pigmentosa due to mutations at the unlinked peripherin/RDS and ROM1 loci. Science. 1994;264:1604-1608.

3. Rivolta C, Sweklo EA, Berson EL, Dryja TP. Missense mutation in the USH2A gene: association with recessive retinitis pigmentosa without hearing loss. Am J Hum Genet. 2000;66:1975-1978.

4. Seyedahmadi BJ, Rivolta C, Keene JA, Berson EL, Dryja TP. Comprehensive screening of the USH2A gene in Usher syndrome type II and non-syndromic recessive retinitis pigmentosa. Exp Eye Res. 2004;79:167-173.

5. Collin RWJ, Littink KW, Klevering BJ, et al. Identification of a 2 Mb human ortholog of Drosophila eyes shut/spacemaker that is mutated in patients with retinitis pigmentosa. Am J Hum Genet. 2008;83:594-603.

6. Abd El-Aziz MM, Barragan I, O'Driscoll CA, et al. EYS, encoding an ortholog of Drosophila spacemaker, is mutated in autosomal recessive retinitis pigmentosa. Nat Genet. 2008;40:1285-1287.

7. Zelhof AC, Hardy RW, Becker A, Zuker CS. Transforming the architecture of compound eyes. Nature. 2006;443:696-699.

8. Barragan I, Abd El-Aziz MM, Borrego S, et al. Linkage validation of RP25 Using the 10K genechip array and further refinement of the locus by new linked families. Ann Hum Genet. 2008;72:454-462.

9. Ruiz A, Borrego S, Marcos I, Antinolo G. A major locus for autosomal recessive retinitis pigmentosa on 6q, determined by homozygosity mapping of chromosomal regions that contain gamma-aminobutyric acid-receptor clusters. Am J Hum Genet. 1998;62:1452-1459.

10. Miller SA, Dykes DD, Polesky HF. A simple salting out procedure for extracting DNA from human nucleated cells. Nucleic Acids Res. 1988;16:1215.

11. Little S. Amplification-refractory mutation system (ARMS) analysis of point mutations. Curr Protoc Hum Genet. 2001;Chapter 9:Unit 9.8.

12. Henikoff S, Henikoff JG. Amino acid substitution matrices from protein blocks. Proc Natl Acad Sci U S A. 1992;89:10915-10919.

13. Reese MG, Eeckman FH, Kulp D, Haussler D. Improved splice site detection in Genie. J Comput Biol. 1997;4:311-323.

14. Cartegni L, Wang J, Zhu Z, Zhang MQ, Krainer AR. ESEfinder: A web resource to identify exonic splicing enhancers. Nucleic Acids Res. 2003;31:3568-3571.

15. Marmor MF, Fulton AB, Holder GE, Miyake Y, Brigell M, Bach M. ISCEV Standard for full-field clinical electroretinography (2008 update). Doc Ophthalmol. 2009;118:69-77.

16. Julenius K, Molgaard A, Gupta R, Brunak S. Prediction, conservation analysis, and structural characterization of mammalian mucin-type O-glycosylation sites. Glycobiology. 2005;15:153-164.

17. Klevering BJ, Yzer S, Rohrschneider K, et al. Microarray-based mutation analysis of the ABCA4 (ABCR) gene in autosomal recessive cone-rod dystrophy and retinitis pigmentosa. Eur J Hum Genet. 2004;12:1024-1032.

18. Bayes M, Giordano M, Balcells S, et al. Homozygous tandem duplication within the gene encoding the beta-subunit of rod phosphodiesterase as a cause for autosomal recessive retinitis pigmentosa. Hum Mutat. 1995;5:228-234.

19. McLaughlin ME, Ehrhart TL, Berson EL, Dryja TP. Mutation spectrum of the gene encoding the beta subunit of rod phosphodiesterase among patients with autosomal recessive retinitis pigmentosa. Proc Natl Acad Sci U S A. 1995;92:3249-3253.

20. Dryja TP, Rucinski DE, Chen SH, Berson EL. Frequency of mutations in the gene encoding the alpha subunit of rod cGMP-phosphodiesterase in autosomal recessive retinitis pigmentosa. Invest Ophthalmol Vis Sci. 1999;40:1859-1865.

21. Li ZY, Possin DE, Milam AH. Histopathology of bone spicule pigmentation in retinitis pigmentosa. Ophthalmology. 1995;102:805-816.

22. Jackson H, Garway-Heath D, Rosen P, Bird AC, Tuft SJ. Outcome of cataract surgery in patients with retinitis pigmentosa. Br J Ophthalmol. 2001;85:936-938.

23. Handford PA, Mayhew M, Baron M, Winship PR, Campbell ID, Brownlee GG. Key residues involved in calcium-binding motifs in EGF-like domains. Nature. 1991;351:164-167.

24. Goldberg AF, Loewen CJ, Molday RS. Cysteine residues of photoreceptor peripherin/rds: role in subunit assembly and autosomal dominant retinitis pigmentosa. Biochemistry. 1998;37:680-685.

25. Bainbridge JW, Ali RR. Success in sight: The eyes have it! Ocular gene therapy trials for LCA look promising. Gene Ther. 2008;15:1191-1192.

26. Linde L, Kerem B. Introducing sense into nonsense in treatments of human genetic diseases. Trends Genet. 2008;24:552-563.

Adapted from: *Investigative Ophthalmology & Visual Science.* 2010 Apr;

Dikla Bandah-Rozenfeld,[1] Karin W. Littink,[2,3] Tamar Ben-Yosef,[4] Tim M. Strom,[5] Itay Chowers,[1] Rob W.J. Collin,[3,6,7] Anneke I. den Hollander,[3,6,7] L. Ingeborgh van den Born,[2] Marijke N. Zonneveld,[3] Saul Merin,[1] Eyal Banin,[1] Frans P.M. Cremers[3,6] and Dror Sharon[1]

[1] Department of Ophthalmology, Hadassah-Hebrew University Medical Center, Jerusalem,Israel; [2] The Rotterdam Eye Hospital, Rotterdam, The Netherlands; [3] Department of Human Genetics, Radboud University Nijmegen Medical Centre, Nijmegen, The Netherlands; [4] Department of Genetics, The Rappaport Family Institute for Research in the Medical Sciences, Faculty of Medicine, Technion-Israel Institute of Technology, Haifa, Israel; [5] Institute of Human Genetics, Helmholtz Zentrum Munchen, Neuherberg, Germany; [6] Nijmegen Centre for Molecular Life Sciences, Radboud University Nijmegen Medical Centre, Nijmegen, The Netherlands and [7] Department of Ophthalmology, Radboud University Nijmegen Medical Centre, Nijmegen, The Netherlands.

CHAPTER 5C

NOVEL NULL MUTATIONS IN THE *EYS* GENE ARE A FREQUENT CAUSE OF AUTOSOMAL RECESSIVE RETINITIS PIGMENTOSA IN THE ISRAELI POPULATION

ABSTRACT

PURPOSE. To characterize the role of *EYS*, a recently identified retinal disease gene, in families with inherited retinal degenerations in the Israeli and Palestinian populations.

METHODS. Clinical and molecular analyses included family history, ocular examination, full-field electroretinography (ERG), perimetry, autozygosity mapping, mutation detection, and estimation of the mutation age.

RESULTS. We performed autozygosity mapping in 171 consanguineous Israeli and Palestinian families with inherited retinal degenerations. Large homozygous regions harboring the *EYS* gene were identified in 15 of the families. *EYS* mutation analysis in the 15 index cases, followed by genotyping of specific mutations in additional 121 cases with inherited retinal degenerations, revealed five novel null mutations, two of which are founder mutations, in 10 Israeli and Palestinian families with autosomal recessive retinitis pigmentosa (arRP). The most common mutation we identified was a founder mutation in the Moroccan Jewish sub-population. Using the ESTIAGE program, we estimate that the age of the most recent common ancestor is 26 generations. The retinal phenotype in most patients was a typical yet relatively severe RP, with an early age of onset and non-recordable ERGs upon presentation.

CONCLUSIONS. Our results demonstrate that *EYS* is currently the most commonly mutated arRP gene in the Israeli population, mainly due to founder mutations. *EYS* mutations were associated with an RP phenotype in all patients, and we predict that the gene plays only a minor role in causing other retinal phenotypes.

INTRODUCTION

Retinitis pigmentosa (RP), with a worldwide prevalence of about 1:3,500,[1-3] is a group of hereditary degenerative diseases of the retina and is considered one of the most heterogeneous genetic diseases in humans. The disease appears with different modes of inheritance, including autosomal recessive (50-60%), autosomal dominant (30-40%), or X-linked (5-15%).[4] A total of 25 genes have so far been described to cause non-syndromic autosomal recessive RP (arRP) and four additional loci have been identified by linkage studies (RetNet database; http://www.sph.uth.tmc.edu/RetNet/). In 1998, homozygosity mapping led to the identification of the RP25 locus in Spanish families.[5] Subsequent linkage analyses showed that additional families with arRP from various origins, including Pakistani[6] and Chinese,[7] were linked to the RP25 locus. Extensive fine mapping and sequencing efforts in the RP25 region led to a refinement of the linked region,[8] and eventually to the identification of the causative gene simultaneously by two groups that used different gene hunting strategies.[9, 10] Abd El-Aziz and co-workers used a multi-step analysis in which they excluded 60 of the 110 genes in the RP25 region, refining the locus to a 2.67 cM region, and identified a large genomic deletion in one of the linked families.[10] Collin and co-workers, on the other hand, applied homozygosity mapping in non-consanguineous families, using genome-wide single nucleotide polymorphism (SNP) genotyping.[9] The RP25 gene identified by both studies, termed *EYS* (*eyes shut homolog*), spans almost 2 Mb of genomic sequence and includes 44 exons coding for a 10,475 nucleotide transcript. The gene is abundantly expressed in the human retina[9, 10] and the protein is localized to the outer segments of the photoreceptor cells.[10] The retinal function of the EYS protein is still unknown. It is a large protein, composed of 3165 amino acids, containing a signal peptide, 28 EGF-like and 5 Laminin A G-like domains. The human EYS protein is a homolog of the *Drosophila* eyes shut (spacemaker) protein, which is an extracellular matrix protein essential for photoreceptor development and morphology of the insect eye.[11, 12] Eight *EYS* mutations, all of which are null, have been reported to date, in eight arRP families.[9, 10] Most patients with *EYS* mutations had the clinical diagnosis of RP with an autosomal recessive inheritance pattern,[9, 10] but interestingly, one patient had a cone-rod pattern of photoreceptor loss.[9]

In a study aimed to estimate the prevalence of RP in the Israeli Jewish population, 341,175 individuals aged 17-20 years were screened for visual acuity problems, and those who had a visual acuity lower than 20/25 were further examined by an ophthalmologist. The prevalence in this study was estimated as 1:4,610.[13] Since many RP patients in this age group have relatively preserved visual acuities, this

number is probably an underestimation. The Israeli and Palestinian populations serve as important genetic sources for identifying autosomal recessive disease genes since the Jewish population was divided into isolated ethnic groups during history, leading to relatively high inbreeding levels, and because the Muslim population is enriched with consanguineous marriages. A study conducted in schools for the blind in the West Bank and Gaza in 1992 concluded that 44-85% of the affected children (depending on location) were the offspring of a consanguineous marriage.[14]

Only limited information is currently available on the genetic causes of non-syndromic RP in the Israeli and Palestinian populations, with only a few mutations reported thus far in the *CERKL*, *CRB1*, *NR2E3*, *RDH12*, *TULP1*, and *USH2A* genes.[15-19] As part of our genetic analysis of Israeli and Palestinian families with autosomal recessive retinal degenerations, we used autozygosity mapping as the major mapping tool and identified families with arRP linked to the *EYS* region. Sequence analysis revealed five novel null mutations, two of which were founder mutations, in 10 families with arRP. The phenotype of most affected individuals was typical for arRP although some clinical variation was evident.

METHODS

Patient recruitment

The tenets of the Declaration of Helsinki were followed and informed consent was obtained from all patients who participated in this study prior to donation of a blood sample. Blood samples for DNA analysis were obtained from the index patient as well as other affected and unaffected family members.

Genetic analysis

Genomic DNA was extracted from peripheral blood samples of index cases and their family members using the FlexiGene DNA kit (QIAGEN). Whole genome SNP analysis was performed using the GeneChip Human Mapping 10K Xba 142 2.0 microarray (Affymetrix). Primers for the screening of *EYS* by PCR amplification have been reported previously.[9] PCR was performed in a volume of 25 µl reaction with 35 cycles. Mutation analysis was performed by direct sequencing of purified PCR products.

Genotyping of specific mutations

Two mutations, c.403delA,406G>T,410_424del15 (exon 4) and c.4361_4362CC>AG (exon 26) were genotyped using the restriction enzymes *Dde*I and *Mnl*I, respectively. For the genotyping assay of the c.3715G>T (exon 25) mutation, we designed allele-specific

primers to distinguish between the mutant and normal alleles (primer sequences available on request) and used the *Nla*III enzyme for restriction analysis. The c.1211_1212insA (exon 8) and c.8218_8219delCA (exon 43) mutations were screened by sequencing analysis. The possible effect of sequence changes on the splicing of the corresponding exon was estimated using Splice Site Prediction by Neural Network at http://www.fruitfly.org/.

Estimation of mutation age

We used the ESTIAGE program[20] to calculate the age (in generations) of the most recent common ancestor of patients carrying the c.403delA,406G>T,410_424del15 mutation. ESTIAGE is a likelihood-based method which uses multi locus marker data from patients carrying the same mutation, assuming they descended from a common ancestor who introduced the mutation. An estimate of the number of generations since the most recent common ancestor is obtained from the size of the haplotype shared by the individuals on each side of the disease locus. The method uses the haplotype information in patients carrying the mutation and in controls to identify the most likely positions of recombination events on the ancestral haplotype. This method was reported to be efficient for a very small number of affected individuals in rare diseases. We used SNP genotyping data from 36 markers on eight chromosomes carrying the mutation and 46 population-matched control chromosomes. Allele frequencies were calculated based on the control population.

Clinical evaluation

Complete ophthalmic examinations were performed including refraction, visual acuity, biomicroscopic slit lamp examination, and fundoscopy. Best corrected visual acuity was measured in each eye separately using an ETDRS chart, and presented as a decimal ratio. In patients with visual acuity lower than 20/400, the distance at which fingers could be reliably counted was recorded. Retinal imaging included color fundus photographs, optical coherence tomography (OCT) and fundus autofluorescence (FAF). Retinal function was evaluated according to the level of patient cooperation by full-field electroretinography (ERG), Goldmann kinetic and/or Humphrey static perimetry as previously described.[21] Briefly, full-field ERGs were recorded using corneal electrodes and a computerized system (UTAS 3000, LKC, MD). In the dark-adapted state, rod responses to a dim blue flash (Wratten 47b) and mixed cone-rod responses to a white flash (2.35 cd·sec/m^2) were acquired. Cone responses to 30 Hz flashes of white light (9.4 cd·sec/m^2) were acquired under a background light of 21 cd/m^2. All ERG responses were filtered at 0.3-500 Hz and signal averaging was used.

RESULTS

Autozygosity mapping and *EYS* mutation analysis

We recruited 712 Israeli and Palestinian families with hereditary non-syndromic retinal disease, 307 (including 121 with RP and 43 with Leber congenital amaurosis [LCA]) of which were consanguineous. Aiming to identify the causative gene in the consanguineous families, we used the 10K Affymetrix SNP microarray system for autozygosity mapping in patients from 171 of the families (82 with RP, 28 with LCA, and 61 with cone-dominated diseases). Autozygosity analysis revealed 18 patients from 15 different families (Table 1) who had a large homozygous region harboring the recently identified *EYS* gene and fulfilled two criteria: the genetic size of the homozygous region was at least 10 cM and it was among the 10 largest homozygous regions in the affected individual (Table 1). Interestingly, patients from three of the families (MOL0318, MOL0501, and MOL0662; Figure 1) were of Moroccan Jewish ancestry and shared a large region covered by 44 consecutive homozygous SNP markers. Sequence analysis of the 44 *EYS* exons and exon-intron boundaries in the 15 above-mentioned index cases revealed two novel homozygous null mutations in four families (Table 1 and Figure 2). Patients from the three above-mentioned Moroccan Jewish families were homozygous for a novel complex frameshift mutation c.403delA,406G>T,410_424del15 (hereafter referred to as p.Thr135LeufsX25) in exon 4, which causes a premature stopcodon at position 160 due to a single base pair deletion followed by a 15-bp deletion (Figure 2A). In addition, an isolated case from a consanguineous Palestinian Muslim family (MOL0410; Figure 1 and Table 1) was homozygous for a novel nonsense mutation, c.4361_4362CC>AG (p.Ser1454X), in exon 26 of the *EYS* gene (Figure 2D).

Aiming to assess the frequency of these mutations among patients from the corresponding sub-populations, we screened a set of 56 Jewish families with RP from North-African ancestry (from Morocco, Libya, Tunisia, and Algeria) for the p.Thr135LeufsX25 mutation and 47 Muslim families with RP for the p.Ser1454X mutation. The analysis revealed four additional index patients who were either homozygous (MOL0792 II:2 and MOL0806 III:7) or heterozygous (TB59 III:1 and MOL0626 III:1; Figure 1 and Table 1) or for the p.Thr135LeufsX25 mutation. Screening of the complete *EYS* gene revealed novel heterozygous null mutations in the two latter patients. Patient MOL0626 III:1 (from Moroccan Jewish ancestry) was heterozygous for a frameshift mutation (c.1211_1212insA, p.Asn404LysfsX2; Table 1 and Figure 2B), in exon 8. No additional family members were available to confirm the compound heterozygous state.

Aiming to evaluate the frequency of the c.1211_1212insA mutation in North African Jewish RP patients, we sequenced exon 8 in 47 additional index RP patients, but none of them carried the c.1211_1212insA mutation or any other mutation in this exon. Patient TB59 III:1 was heterozygous for a novel frameshift mutation (c.8218_8219delCA, p.His2740TyrfsX27; Figure 2E), in exon 43. Segregation analysis in family TB59 (Figure 1) revealed that the p.Thr135LeufsX25 mutation was on the maternal allele (of Moroccan Jewish ancestry) and the c.8218_8219delCA mutation was on the paternal allele (of Iraqi Jewish ancestry). We therefore evaluated the

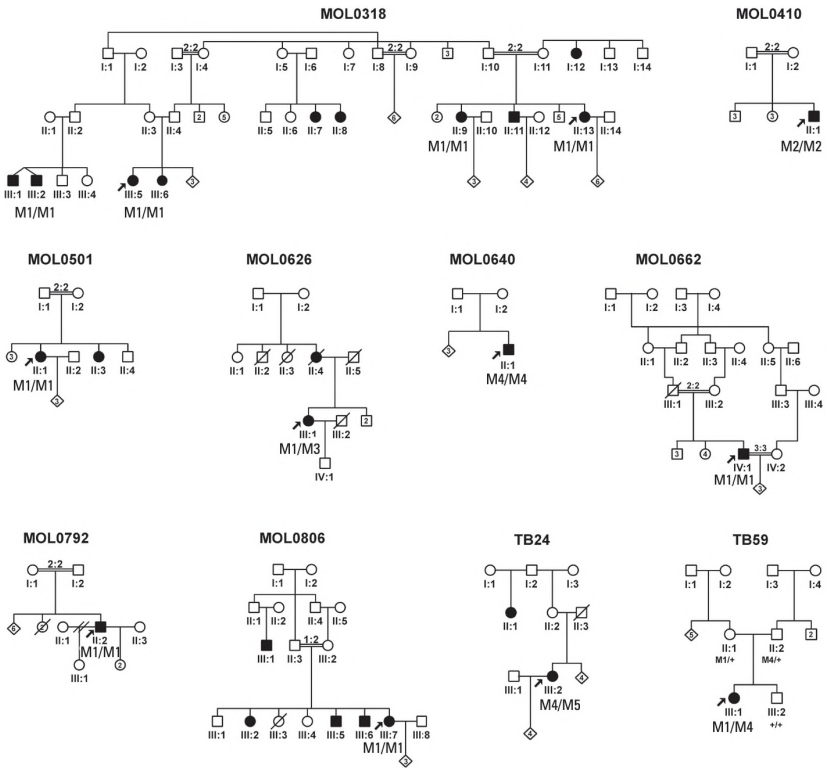

FIGURE 1. **Israeli and Palestinian families with *EYS* mutations.**
Numbers above the pedigrees indicate the family serial number, numbers within symbols represent the number of siblings, numbers below symbols indicate the generation and individual numbers, arrows represent index cases, and a double horizontal line designates consanguinity with an indication of the consanguinity level (e.g. 2:2 designates first cousin marriages). For each recruited individual, the *EYS* genotype is depicted below the individual symbol. M1, p.Thr135LeufsX25; M2, p.Ser1454X; M3, p.Asn404LysfsX2; M4, p.His2740TyrfsX27; M5, p.Glu1239X.

frequency of the c.8218_8219delCA mutation in 31 Oriental Jewish RP patients (mainly from Iran, Iraq, and Afghanistan) and identified two non-consanguineous patients from Iraqi Jewish origin who were either homozygous (MOL0640 II:1) or heterozygous (TB24 III:2) for the mutation. All the alleles carrying the c.8218_8219delCA mutation were from an Iraqi Jewish origin and shared an identical haplotype within *EYS*, indicating a founder mutation.

Sequencing analysis of the remaining exons in TB24 III:2 revealed yet another novel nonsense mutation (c.3715G>T, p.Glu1239X), in exon 25 (Table 1 and Figure 2C). The mutation could not be identified in any of 31 additional RP patients from Oriental Jewish origin. In addition, we identified 29 sequence changes in our genetic screen, of which 14 were non-synonymous changes which are known polymorphisms in the SNP database. None of these sequence changes is likely to be pathogenic.

Haplotype analysis and estimation of mutation age

The most common *EYS* mutation identified in this study was the p.Thr135LeufsX25 mutation identified in 7 RP families, all of Moroccan Jewish ancestry, indicating a founder effect. Screening of normal individuals of Moroccan origin revealed that one out of 94 control individuals was heterozygous. Haplotype analysis of four patients who were homozygous for this mutation revealed a shared homozygous region composed of nine SNP markers covering 3.2 Mb or 2.1 cM (Supplementary Figure 1). The shared homozygous region in three of these patients from consanguineous families is much larger, harboring 44 markers along a region of 17 Mb (6.3 cM). Two pieces of evidence suggest that the mutation is relatively young: the relatively large size of the shared homozygous region and the fact that the mutation was found only in Moroccan Jews and not in Jews originating from neighboring countries (Algeria, Libya, and Tunisia). Aiming to estimate the mutation age, we used genotyping data from 36 SNP markers (8 within the *EYS* gene and 28 flanking it) on eight chromosomes carrying the mutation (MOL0318 II:13, MOL0318 III:2, MOL0501 II:1, and MOL0662 IV:1) and 46 population-matched control chromosomes. The data set was analyzed using the ESTIAGE software and the number of generations since the most recent common ancestor was estimated as 26 (95%, confidence interval of 12-56 generations) or 650 years (based on a mean generation time of 25 years).

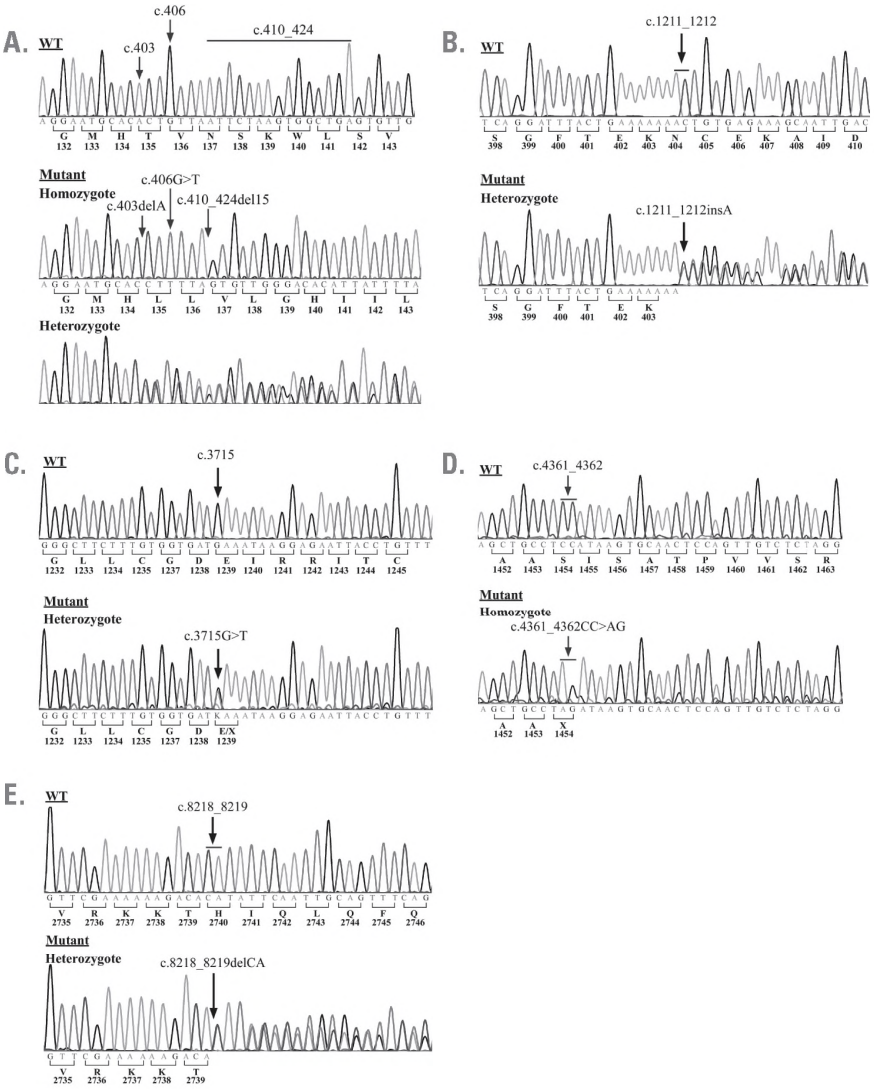

FIGURE 2. **The chromatograms of the five novel *EYS* mutations.** ***(See appendix for color figure)***
For each mutation, the wild-type (wt) sequence is depicted with the homozygous or heterozygous sequences when available. The mutation location is indicated by either an arrow (for a nucleotide change) or a horizontal line (for a sequence change affecting more than a single nucleotide).
A. c. 403delA,406G>T,410_424del15; p.Thr135LeufsX25 (exon 4).
B. c.1211_1212insA; p.Asn404LysfsX2 (exon 8). **C.** c.3715G>T; p.Glu1239X (exon 25).
D. c.4361_4362CC>AG; p.Ser1454X (exon 26). **E.** c.8218_8219delCA; p.His2740TyrfsX27 (exon 43).

TABLE 1. Data regarding patients screened for mutations in the *EYS* gene

Patient ID*	Inheritance pattern and clinical diagnosis†	Level of consanguinity‡	Origin
MOL0139-1 MOL0139-2	arRP	2:1 2:1	Moroccan Jew
MOL0144-1	arRP	3:2	Oriental Jew
MOL0161-1	sSTGD	2:2	Israeli Muslim
MOL0260-1	sRP	2:2	Israeli Muslim
MOL0264-1	sRP	2:2	Israeli Muslim
MOL0318 II:13 **MOL0318 II:9** **MOL0318 III:2** **MOL0318 III:5**	arRP	2:2 2:2 none none	Moroccan Jew
MOL0399-1	sLCA	2:2	Oriental Jew
MOL0400-1	sRP	2:2	Ashkenazi Jew
MOL0410 II:1	sRP	2:2	Palestinian Muslim
MOL0501 II:1	arRP	2:2	Moroccan Jew
MOL0615-1	sLCA	2:2	Israeli Muslim
MOL0626 III:1	arRP	none	Moroccan Jew
MOL0631-1	arRP	2:2	Moroccan Jew
MOL0640 II:1	sRP- sector	none	Iraqi Jew
MOL0652-1	arRP	2:2	Israeli Muslim
MOL0662 IV:1	sRP	2:2	Moroccan Jew
MOL0788-1	sRP	2:2	Ashkenazi Jew
MOL0792 II:2	sRP	2:2	Moroccan Jew
MOL0806 III:7	arRP	2:1	Moroccan Jew
TB24 III:2	sRP	none	Moroccan/ Iraqi Jew
TB59 III:1	sRP	none	Iraqi Jew

*, In bold are patients in whom EYS mutations were identified. The corresponding family trees are shown in Figure 1. †, arRP, autosomal recessive retinitis pigmentosa; sRP, simplex retinitis pigmentosa; sSTGD, simplex Stargardt disease; sLCA, simplex Leber congenital amaurosis. ‡, Level of consanguinity is measured by the number of generations separating the spouse from the

Number of consecutive homozygous SNPs	Size of homozygous region (in Mb and cM)§	Rank among homozygous regions (based on genetic size)	Mutation 1 Mutation 2‖
169 332	50 Mb; 39 cM 90 Mb; 70 cM	2nd 1st	none
113	33 Mb; 27 cM	2nd	none
236	60 Mb; 43 cM	1st	none
277	72 Mb; 53 cM	1st	none
118	34 Mb; 16 cM	4th	none
243 200 9 NP	65 Mb; 72 cM 55 Mb; 49 cM 3.2Mb; 1.5 cM NP	 1st 1st	 p.Thr135LeufsX25 p.Thr135LeufsX25
396	103 Mb; 80 cM	1st	none
107	30 Mb; 13 cM	3rd	none
122	37 Mb; 20 cM	5th	p.Ser1454X p.Ser1454X
175	44 Mb; 24 cM	1st	p.Thr135LeufsX25 p.Thr135LeufsX25
157	42 Mb; 20 cM	1st	none
NP	NP	NP	p.Thr135LeufsX25 p.Asn404LysfsX2
254	70 Mb; 71 cM	1st	none
NP	NP	NP	p.His2740TyrfsX27 p.His2740TyrfsX27
102	28 Mb; 18 cM	4th	none
60	20 Mb; 10 cM	7th	p.Thr135LeufsX25 p.Thr135LeufsX25
69	24 Mb; 12 cM	9th	none
NP	NP	NP	p.Thr135LeufsX25 p.Thr135LeufsX25
NP	NP	NP	p.Thr135LeufsX25 p.Thr135LeufsX25
NP	NP	NP	p.Glu1239X p.His2740TyrfsX27
NP	NP	NP	p.Thr135LeufsX25 p.His2740TyrfsX27

common ancestor (e.g. 2:2 designates first cousins, 2:1 designates marriage between an uncle and his niece). § Data are based on 10K SNP analysis (see Materials and Methods). ‖, The predicted effect of the mutation on the protein sequence is presented. See Supplementary Table for additional information. NP, not performed

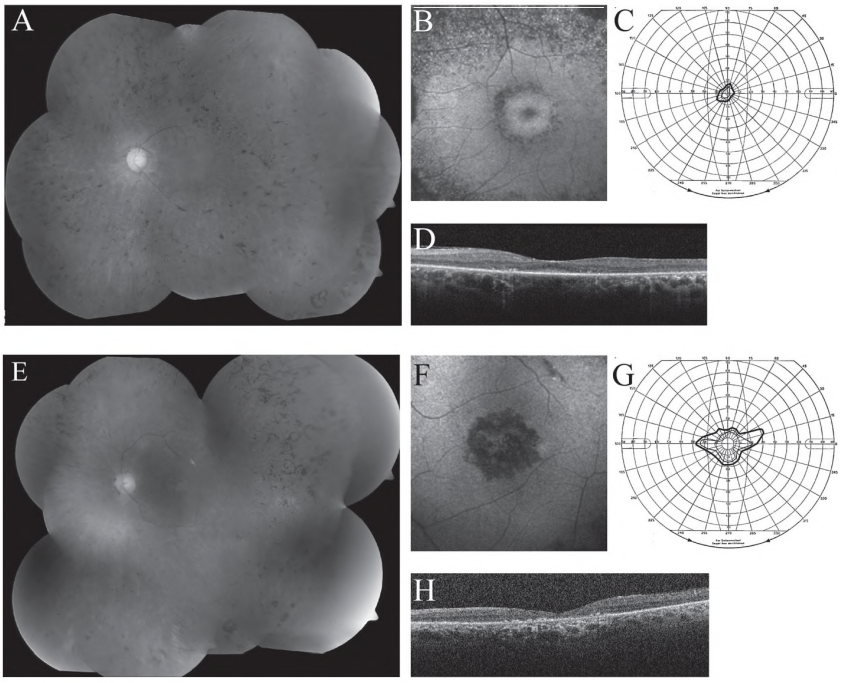

FIGURE 3. **Fundus imaging and visual fields.** ***(See appendix for color figure)***
Representative fundus images and Goldman visual fields of the left eyes of patient TB24 III:2 (panels A-D) at age 63 and patient MOL0501 II:3 (panels E-H) at age 52 are shown. The typical funduscopic findings of RP are present, including bone spicule-like pigmentation, pallor of the optic discs, and narrowing of blood vessels (A,E). Macular involvement is evident also on autofluorescence imaging (B,F) and OCT, with retinal thinning and atrophy (D,H). Note more severe foveal atrophy in patient MOL0501 II:3 which correlates with the lower visual acuity of this patient (Table 2). Visual fields are markedly constricted in both patients (C,G).

Ocular phenotype associated with *EYS* mutations

We clinically examined 15 patients with *EYS* mutations and performed ERG testing in 11 of them (Table 2). All patients with *EYS* mutations showed characteristic manifestations of RP, with a relatively severe course of disease. Night vision, visual fields, and ERG responses were markedly impaired already at early ages. Both myopic and hyperopic refractive errors were present. Fundus appearance was typical for RP including bone spicule-like pigmentation, pallor of the optic discs, and narrowing of blood vessels. Representative fundus mosaics of the left eyes of patient TB24 III:2 at age 63 and patient MOL0501 II:3 at age 52 are shown in Figures 3A and 3E, respectively.

TABLE 2. Clinical data of patients carrying *EYS* mutations

Patient ID	Sex, age	Age of onset	Age of diagnosis	Refraction	Visual Acuity	FFERG
MOL0318 III:1	M 19		19	NA	NA	Extinguished Extinguished
MOL0318 II:9	F 51	12	36	Myopia	CF 2m CF 2m	Extinguished Extinguished
MOL0318 II:9	F 38			-3.50/-1.00×35° -5.00/-0.50×160°	0.3 0.15	NP
MOL0318 II:11	M 32	8	32	-4.50/-1.00×35° -6.00/-0.50×170°	0.15 0.15	NP
MOL0318 II:13	F 36	22	36	NA	NA	Extinguished Extinguished
MOL0318 III:2	M 21		19	NA	NA	Extinguished NP
MOL0318 III:5	F 19	18	18	NA	0.7 0.7	NP Extinguished
MOL0410 II:1	M 21		21	-2.0/-0.25×35° -2.0/-1.0×140°	0.5 0.8	Extinguished Extinguished
MOL0501 II-1	F 33		33	NA	0.1 0.25	Extinguished Extinguished
MOL0626 III:1	F 50	50	50	NA	0.4 0.4	Extinguished Extinguished
MOL0640 II:1	M 47		20	NA	0.5 0.6	27; 53/97; 8, 36 29; 31/81; 7, 36
MOL0662 IV:1	M 41		41	NA	0.15 0.15	NP
MOL0792 II:2	M 57		57	-0.75/-3.00×40° -2.50/-1.50×50°	CF 2.5m CF 1m	NP
TB24 III:2	F 55	37	40	-0.75/-0.25×18° +0.25/-1.5×132°	0.5 0.4	Extinguished Extinguished
TB59 III:1	F 19	15	19	+3.50/-0.75×160° +4.25/-0.50×44°	0.8 0.8	Extinguished Extinguished

*, Full Field Electroretinogram including the following responses: rod response b-wave amplitude (in μV, normal > 200μV); mixed cone-rod a/b wave (in μV, normal a-wave > 90μV, normal b-wave > 400μV); cone response (in μV, normal > 60μV), implicit time (in msec, normal ≤ 33 msec). CF, counting fingers; F, female; FFERG, full-field electroretinogram; M, male; m, meter; NA, Not available; NP, not performed. First line (2nd -6th column) indicates the right eye, second line indicates the left eye.

Macular involvement is evident also on FAF imaging (Figures 3 B and 3F) and OCT, with retinal thinning and atrophy (Figures 3D and 3H). Visual fields in these two patients are markedly constricted (Figures 3C and 3G). In almost all patients for whom ERG data were available (ages between 19-51 years), both scotopic and photopic full-field ERG responses were extinguished, indicating severe retinal involvement (Table 2). Only in one patient (MOL0640 III:1) scotopic as well as photopic ERG responses were measurable, although also severely reduced. This patient initially presented with sector RP – based on funduscopic and visual field findings – at the age of 25 which later progressed to widespread, generalized retinal involvement. The mean 30 Hz cone flicker ERG amplitude measured at our centre on the first ERG test performed in each patient was significantly lower in the *EYS* group as compared to pooled, first test-ERG amplitudes in RP patients in our population (Figure 4). The *EYS* group included 11 patients with a mean age of 34 years and mean ± SD amplitude of 0.65 μV ± 2.17. The control RP group included 240 patients with a mean age of 29.8 years and mean ± SD amplitude of 17.7 μV ± 22.2 (p-value for cone flicker ERG amplitude difference < 0.01).

DISCUSSION

EYS represents a major arRP gene, as can be appreciated from the widespread ethnic origins of families with arRP due to *EYS* mutations thus far reported.[9,10] In the present study, we show that mutations in *EYS* are currently the most frequent cause of non-syndromic arRP in the Israeli population, mainly due to founder mutations in two ethnic groups (Moroccan and Oriental Jews). The five novel *EYS* mutations reported here account for at least 7% of the arRP families (10 out of 141 families) that we have thus far recruited from the Israeli and Palestinian populations. The most common mutation we identified in this study (p.Thr135LeufsX25) is a founder mutation in the Moroccan Jewish population accounting for about 19% (12 out of 64 chromosomes) of non-syndromic arRP alleles in this population, and is therefore currently the most common cause of RP in Jews of Moroccan ancestry.

Similar to previous studies, most of our patients with *EYS* mutations manifested typical and rather severe arRP. One exception is an isolated case who initially presented with a milder phenotype (sector RP) and was homozygous for a null mutation in exon 43. Although one might expect that the nonsense-mediated mRNA decay (NMD) mechanism would prevent protein production of this mutant allele, it is tempting to speculate that some transcripts will escape degradation, as reported in many

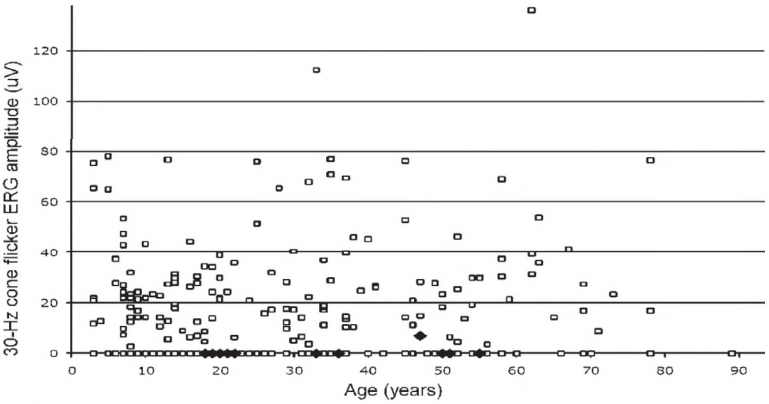

FIGURE 4. A graph representing cone 30-Hz ERG amplitude (Y-axis) versus the age (X-axis) at which ERG data was first obtained from 11 patients with EYS mutations (filled diamonds) versus 240 patients diagnosed with RP (open squares). Each data point represents the average cone flicker amplitude of the two eyes of each patient.

other cases (see Holbrook et al.[22] for review), manifesting a milder, more localized, phenotype. Mutations that are likely to result in a similar effect, however, were reported to cause the typical widespread and severe RP phenotype.[9] Only one patient to date was reported to manifest a different retinal phenotype, cone-rod dystrophy (CRD), due to a null mutation located at the very end of the carboxy-terminus of *EYS*, thereby resulting in the absence of only the last 10 amino acids. Her older sibling, though, displayed RP,[9] probably due to other factors influencing clinical expression. We included 61 families with autosomal recessive cone dominated diseases (mainly CRD) in our autozygosity analysis, but only one (in which no *EYS* mutations were identified) was homozygous at the *EYS* locus, indicating that mutations in *EYS* are a rare cause of CRD in our population. It is interesting to note that all *EYS* mutations thus far reported,[9, 10] as well as the five novel mutations reported here, are null mutations (either frameshift or nonsense). A large number of *EYS* missense changes are known – some of which appear as entries at dbSNP – but none of them is currently considered as a cause of disease. Such missense changes, in combination with a null mutation on the counter allele, might result in a milder retinal phenotype. Another possible explanation for the lack of pathogenic missense mutations in *EYS* is the ability of the protein to tolerate single amino-acid alterations, affecting only a specific protein domain, due to the multiple functional domains (e.g. EGF-like and Laminin A G-like domains) in the EYS protein. This phenomenon resembles the mutation spectrum of well-studied retinal genes, including *CHM23* and the *RPGR-ORF15* terminal exon,[24-26] in which only null mutations have been reported so far. Such genes will therefore cause a retinal phenotype only if no protein is generated. One can also

assume that some of the polymorphic missense changes might result in an expressed protein with reduced activity. This makes *EYS* an attractive candidate for modulating retinal disease severity in cases caused by mutations in other retinal genes, mainly those encoding proteins that interact with *EYS*, such as *PROM1*.[9] Since *EYS* was only recently identified, further *EYS* mutation analyses are likely to result in a more accurate and comprehensive *EYS* mutation spectrum.

The most common mutation we identified here (p.Thr135LeufsX25) is a founder mutation in the Moroccan Jewish sub-population. The history of the Jewish population in North Africa (including Morocco, Algeria, Libya, and Tunisia) is ancient and complicated. The population was founded about 2,000-2,600 years ago and since then underwent a number of historic events that had a dramatic effect on the population size, including a few waves of immigrations (during the first temple period about 600 years BCE and in 1492 due to the expulsion from Spain), the conversion of Berber tribes to Judaism (during the sixth and seventh centuries), and the persecution of a major part of the community in 1033 and 1232. By 1948, the Jewish Moroccan population (the major North African Jewish population) was estimated to contain 270,000 individuals, most of whom immigrated to Israel once the state was established in 1948. Using the ESTIAGE program, which was designed for rare diseases, we estimated the age of the most recent common ancestor to be relatively young, 26 generations (or 650 years) ago. This young age is supported by the fact that the mutation was found in Jews originated from Morocco (and not other North African countries), and by the relatively large size of the shared homozygous region in most of the studied patients. To date, the estimated ages of only two founder mutations in the Moroccan Jewish population have been reported and found to be relatively ancient (2,600-2,700 years ago).[27, 28]

In summary, in this study we report the mutation spectrum of *EYS* in a cohort of Israeli and Palestinian RP patients which includes five novel mutations and show that *EYS* is the most frequently mutated arRP gene currently known in the Israeli population.

ACKNOWLEDGEMENTS

We thank the patients and their families for participating in this study. We thank Ms. Lina Bida, Ms. Ruhama Neis, Mrs. Inbar Erdinest and Dr. Alex Obolensky for excellent technical assistance. This work was supported by the Foundation Fighting Blindness (FFB grant number BR-GE-0607-0395-HUJ), the Stichting Wetenschappelijk Onderzoek Oogziekenhuis Prof. Dr. H.J. Flieringa, Rotterdam, and the Yedidut 1 Research Fund.

SUPPLEMENTAL DATA

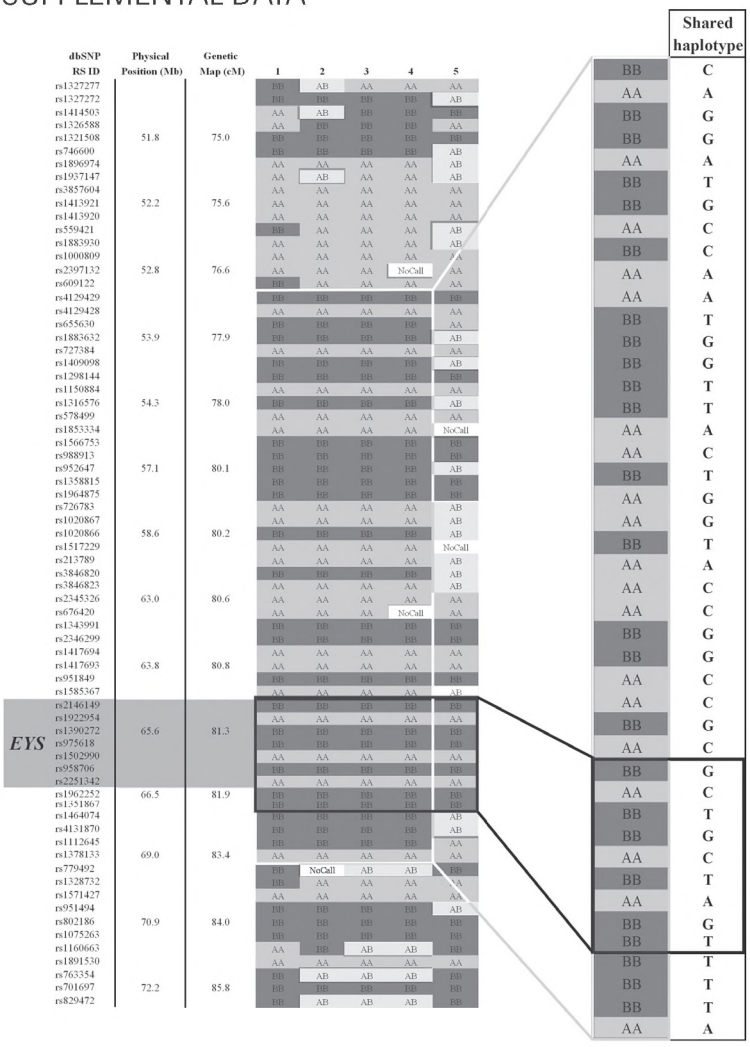

SUPPLEMENTARY FIGURE 1. ***(See appendix for color figure)***

The autozygous region identified in Moroccan Jewish patients who are homozygous for the c.403delA,406G>T,410_424del15 mutation. The appropriate region of the Affymetrix 10K microarray analysis is depicted, covering the *EYS* gene and flanking markers on chromosome 6. The genotype data of the following patients are presented: 1, MOL0501 II:1; 2, MOL0662 IV:3; 3, MOL0318 II:13; 4, MOL0318 II-9; 5, MOL0318 III:5. For each marker, the genotype is presented as homozygous (AA or BB), heterozygous (AB) or unknown (NoCall). The A and B alleles were arbitrarily determined for each allele by Affymetrix and the corresponding nucleotide is presented on the right along the shared homozygous region. Red indicates 'AA' genotype; blue indicaties 'BB' genotype, and green indicates 'AB' genotype.

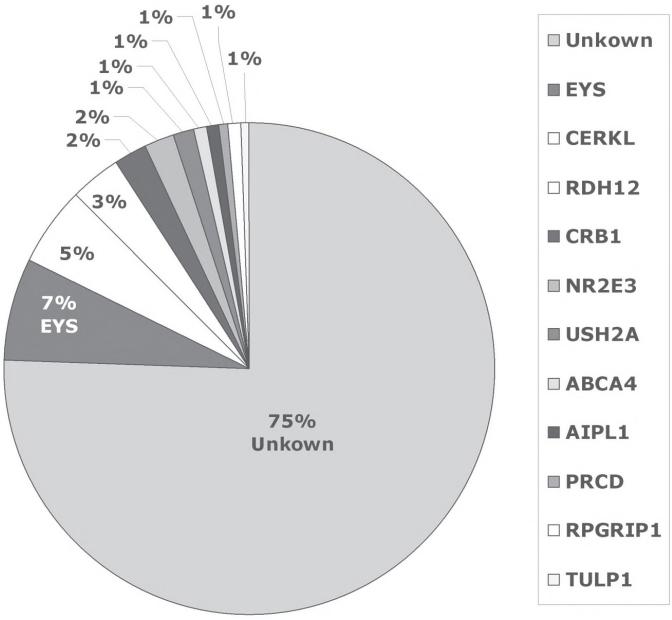

SUPPLEMENTARY FIGURE 2. A pie chart showing the contribution of arRP genes in the Israeli and Palestinian populations. *(See appendix for color figure)*

REFERENCES

1. Bunker CH, Berson EL, Bromley WC, Hayes RP, Roderick TH. Prevalence of retinitis pigmentosa in Maine. Am J Ophthalmol. 1984;97:357-365.

2. Rosenberg T. Epidemiology of hereditary ocular disorders. Dev Ophthalmol. 2003;37:16-33.

3. Bundey S, Crews SJ. A study of retinitis pigmentosa in the City of Birmingham. II Clinical and genetic heterogeneity. J Med Genet. 1984;21:421-428.

4. Hartong DT, Berson EL, Dryja TP. Retinitis pigmentosa. Lancet. 2006;368:1795-1809.

5. Ruiz A, Borrego S, Marcos I, Antinolo G. A major locus for autosomal recessive retinitis pigmentosa on 6q, determined by homozygosity mapping of chromosomal regions that contain gamma-aminobutyric acid-receptor clusters. Am J Hum Genet. 1998;62:1452-1459.

6. Khaliq S, Hameed A, Ismail M, et al. Refinement of the locus for autosomal recessive Retinitis pigmentosa (RP25) linked to chromosome 6q in a family of Pakistani origin. Am J Hum Genet. 1999;65:571-574.

7. Abd El-Aziz MM, El-Ashry MF, Chan WM, et al. A novel genetic study of Chinese families with autosomal recessive retinitis pigmentosa. Ann Hum Genet. 2007;71:281-294.

8. Abd El-Aziz MM, Barragan I, O'Driscoll C, et al. Large-scale molecular analysis of a 34 Mb interval on chromosome 6q: major refinement of the RP25 interval. Ann Hum Genet. 2008;72:463-477.

9. Collin RWJ, Littink KW, Klevering BJ, et al. Identification of a 2 Mb human ortholog of Drosophila eyes shut/spacemaker that is mutated in patients with retinitis pigmentosa. Am J Hum Genet. 2008;83:594-603.

10. Abd El-Aziz MM, Barragan I, O'Driscoll CA, et al. EYS, encoding an ortholog of Drosophila spacemaker, is mutated in autosomal recessive retinitis pigmentosa. Nat Genet. 2008;40:1285-1287.

11. Husain N, Pellikka M, Hong H, et al. The agrin/perlecan-related protein eyes shut is essential for epithelial lumen formation in the Drosophila retina. Dev Cell. 2006;11:483-493.

12. Zelhof AC, Hardy RW, Becker A, Zuker CS. Transforming the architecture of compound eyes. Nature. 2006;443:696-699.

13. Rosner M, Hefetz L, Abraham FA. The prevalence of retinitis pigmentosa and congenital stationary night blindness in Israel. Am J Ophthalmol. 1993;116:373-374.

14. Elder MJ, De Cock R. Childhood blindness in the West Bank and Gaza Strip: prevalence, aetiology and hereditary factors. Eye (Lond). 1993;7 (Pt 4):580-583.

15. Kaiserman N, Obolensky A, Banin E, Sharon D. Novel USH2A mutations in Israeli patients with retinitis pigmentosa and Usher syndrome type 2. Arch Ophthalmol. 2007;125:219-224.

16. Auslender N, Sharon D, Abbasi AH, Garzozi HJ, Banin E, Ben-Yosef T. A common founder mutation of CERKL underlies autosomal recessive retinal degeneration with early macular involvement among Yemenite Jews. Invest Ophthalmol Vis Sci. 2007;48:5431-5438.

17. Bandah D, Merin S, Ashhab M, Banin E, Sharon D. The spectrum of retinal diseases caused by NR2E3 mutations in Israeli and Palestinian patients. Arch Ophthalmol. 2009;127:297-302.

18. Abbasi AH, Garzozi HJ, Ben-Yosef T. A novel splice-site mutation of TULP1 underlies severe early-onset retinitis pigmentosa in a consanguineous Israeli Muslim Arab family. Mol Vis. 2008;14:675-682.

19. Benayoun L, Spiegel R, Auslender N, et al. Genetic heterogeneity in two consanguineous families segregating early onset retinal degeneration: the pitfalls of homozygosity mapping. Am J Med Genet A. 2009;149A:650-656.

20. Genin E, Tullio-Pelet A, Begeot F, Lyonnet S, Abel L. Estimating the age of rare disease mutations: the example of Triple-A syndrome. J Med Genet. 2004;41:445-449.

21. Banin E, Shalev RS, Obolensky A, Neis R, Chowers I, Gross-Tsur V. Retinal function abnormalities in patients treated with vigabatrin. Arch Ophthalmol. 2003;121:811-816.

22. Holbrook JA, Neu-Yilik G, Hentze MW, Kulozik AE. Nonsense-mediated decay approaches the clinic. Nat Genet. 2004;36:801-808.

23. van den Hurk JA, Schwartz M, van Bokhoven H, et al. Molecular basis of choroideremia (CHM): mutations involving the Rab escort protein-1 (REP-1) gene. Hum Mutat. 1997;9:110-117.

24. Vervoort R, Lennon A, Bird AC, et al. Mutational hot spot within a new RPGR exon in X-linked retinitis pigmentosa. Nat Genet. 2000;25:462-466.

25. Vervoort R, Wright AF. Mutations of RPGR in X-linked retinitis pigmentosa (RP3). Hum Mutat. 2002;19:486-500.

26. Sharon D, Sandberg MA, Rabe VW, Stillberger M, Dryja TP, Berson EL. RP2 and RPGR mutations and clinical correlations in patients with X-linked retinitis pigmentosa. Am J Hum Genet. 2003;73:1131-1146.

27. Abidi O, Boulouiz R, Nahili H, et al. The analysis of three markers flanking GJB2 gene suggests a single origin of the most common 35delG mutation in the Moroccan population. Biochem Biophys Res Commun. 2008;377:971-974.

28. Mor-Cohen R, Zivelin A, Fromovich-Amit Y, Kovalski V, Rosenberg N, Seligsohn U. Age estimates of ancestral mutations causing factor VII deficiency and Dubin-Johnson syndrome in Iranian and Moroccan Jews are consistent with ancient Jewish migrations. Blood Coagul Fibrinolysis. 2007;18:139-144.

CHAPTER 6

GENERAL DISCUSSION

In this thesis we identified the genetic defects mainly in patients with cone-rod dystrophy or retinitis pigmentosa, using high density genome-wide SNP arrays, followed by homozygosity mapping or linkage analysis.

STRENGTH AND LIMITATIONS OF HOMOZYGOSITY MAPPING

In this thesis, 108 CRD patients (95 probands) were analyzed by genome-wide SNP genotyping arrays, followed by a search for homozygous regions. This led to the identification of the causative mutation in 8.5% of probands (Chapter 2). Mutations were detected in 2 out of 7 consanguineous probands (28%) and 6 out of 88 non-consanguineous probands (7%). A comparable effectiveness of homozygosity mapping has been described previously in LCA patients, for which the mutation was detected in 30% of consanguineous families and in 3% of non-consanguineous families.[1] In a group of consanguineous patients affected by Bardet-Biedl syndrome (BBS), homozygosity mapping led to the identification of the mutation in all families.[2]

These numbers implicate that homozygosity mapping is mostly effective in consanguineous patients. However, this approach has advantages and disadvantages in both types of families. In a sporadic patient from a consanguineous family, the chance that the mutation occurs homozygously is high, but the homozygous regions are large and numerous. For diagnostic purposes in a genetically heterogeneous disease, several homozygous regions may overlap with known disease-associated genes, which may complicate the search for the causative mutation.[3] When searching for new disease genes, the total size of homozygous regions may be so large, that finding the causative gene defect may be too challenging. In non-consanguineous patients, on the other hand, the chances are lower that an affected individual carries homozygous mutations. However, if an individual carries homozygous mutations, the chances to find them are higher because of a limited number and smaller size of homozygous regions. This is shown by the identification of the *EYS* gene (Chapter 5A). Several other studies have also led to the identification of new mutations or disease loci using homozygosity mapping in non-consanguineous families.[4-6] Homozygosity mapping can thus be effective in both consanguineous and non-consanguineous families, when using the right families for the right purposes (Table 1).

Which non-consanguineous families are most suitable for this type of research, and in which of the regions can the causative mutation be found? First of all, a detailed pedigree of the family, including information about the origin of the maternal and

TABLE 1. **Suitability of type of families in relation to purpose of screening.**

Type of family / Purpose	Consanguineous siblings	Consanguineous sporadic patient	Non-consanguineous siblings		Non-consanguineous sporadic patient	
			Isolated population*	Mixed population	Isolated population*	Mixed population
Diagnostic screening	++++	+++	++++	+/-	+	-
Discovery of novel gene	++	+	++++	+/-	+	-

++++/+++ highly suitable; ++/+, suitable; +/-, possibly suitable; -, unsuitable.
*, isolated is used here in a broad perspective, namely all families in which the parents have a higher than average chance to be related. For example, a family in which the grandparents originate from the same village or the same geographical region, a population that is isolated based on religious or cultural dissimilarities from the surrounding population, an island population, a population with a relatively high rate of inbreeding, etc.

paternal grandparents, is useful to estimate the chances for successful homozygosity mapping. Estimating relative relatedness based on a higher percentage of genome-wide homozygosity than expected, appeared to be unreliable in a population in which genealogy was known and whose DNAs were analyzed for ~10,000 SNPs (10K array).[7] On the other hand, it is stated that the proportion of the genome that is homozygous in an individual (the inbreeding coefficient) is a measure of the degree of relatedness between his/her parents.[8-11] Moreover, the percentage of homozygosity was higher than the average in patients in whom a mutation was detected by homozygosity mapping (1.06% versus 0.47%; Chapter 2). Altogether, the value of this percentage in estimating the probability to find a homozygous mutation remains debatable. The observation that many mutations are located in (one of) the largest regions[1,12] is logical as larger regions on average contain more genes, and thus have a higher chance to harbor the mutation.

There are several explanations why we did not detect the causative mutations in 87 out of 95 probands (91.5%). First, 49 of the patients were not screened for mutations in *ABCA4*. Based on the published 40% prevalence of *ABCA4* mutations in CRD patients, we expect ~20 of the patients studied in this thesis to carry a mutation in this gene. CRD is usually caused by a compound heterozygous combination of a null mutation

and a moderately severe *ABCA4* mutation.[13] For example, in a total of 32 CRD patients 15 compound heterozygous mutation, 14 heterozygous mutations, and only three homozygous mutation were previously detected.[14, 15] Consequently, homozygosity mapping may not be an efficient tool to detect *ABCA4* mutations in CRD patients. Furthermore, patients may carry an intronic or a promoter mutation in one of the arCRD genes, which cannot be detected by sequencing exons and intron-exon boundaries. Alternatively, the causative gene defect could reside in a region that is smaller than our minimum threshold. Also, our cohort contains 52 sporadic male patients, of which 46 remain unsolved. The inheritance in some of these men could be X-linked, with mutations in X-linked CRD genes such as *RPGR*. And finally, several patients are expected to carry mutations in novel CRD genes, which remain to be identified in future studies.

Approximately 35% of patients from an average population, like the cohort studied in this thesis, carry a homozygous defect,[16-20] and thus the maximum percentage of detectable mutations is expected to be ~35% (= 26 patients). The dataset described in Chapter 2 already led to the identification of a mutation in 8 probands, and will thus theoretically lead to the discovery of mutations in new genes in approximately 18 more patients. Especially in combination with next generation sequencing, as will be explained in one of the subsequent paragraphs, this dataset represents a valuable resource to identify new genes associated with CRD.

In conclusion, homozygosity mapping can be a powerful, but not necessarily an efficient method to detect new genes and new mutations in consanguineous as well as non-consanguineous patients, as shown in this thesis by the discovery of a new gene (Chapter 5A), and the identification of 9 novel mutations in ten families (Chapter 2). Altogether, we identified the genetic defect in patients of a total of 32 families (Chapter 2, 3, 4, 5ABC). In the further paragraphs, the value of this molecular knowledge in scientific terms, and the actual benefit for the patient will be discussed.

INSIGHT INTO ETIOLOGY OF RETINAL DYSTROPHIES

Prior to the genetic era, many components of the phototransduction cascade were discovered by physiologists, who clarified small parts of the whole mechanism, for example through electrophysiological experiments on animal photoreceptor cells.[21] Currently, additional components of the visual processes are mostly elucidated by the identification of protein networks,[22] and by genetic studies, like the discovery of *EYS*

(Chapter 5A). The identification of new genes associated with retinal dystrophies may lead to insights into new pathways that can play a role in the etiology of these diseases. The mechanisms of autosomal recessive retinal dystrophy, as far as known now, include mainly disruption of photoreceptor outer segment morphogenesis, interruption of the transport across the photoreceptor connecting cilium, a defective retinoid cycle, dysfunction of the RPE cells, and defective phototransduction through continuous activation or inactivation.[23,24] Still, the function of (newly) identified disease-associated genes (for example, *ADAM9*, *EYS*, *PRCD*, *RD3*, *SPATA7*; Table 1, Chapter 1) remain to be elucidated. Usually, the function emerges from studies on protein localization and interactions, and/or information about retinal abnormalities in spontaneous or transgenic animal models.[23,25 and refs therein] With regard to *EYS*, the hypothesized role of the EYS protein (photoreceptor morphogenesis) was derived from studies in the *Drosophila* eye, in which *eys* has a function in maintaining the interrhabdomeral space, and interacts with other proteins that are associated with human retinal dystrophies (*CRB1*, *PROM1*),[26] as discussed in Chapter 5A. The function of *EYS* in the human retina, however, remains to be determined.

Although some protein functions are already elucidated, clinical information can confirm what was presumed before, and can add new insights. For example, the role of CaBP4 in the synaptic terminal[27] was corroborated by the phenotype of two patients carrying mutations in *CABP4* (Chapter 3), since their electro-negative mixed ERG responses demonstrate that the transmission from photoreceptor cells to the bipolar cells is disturbed. New insight was gained, as we observed that mutations in *CABP4* lead to a disturbed cone function, but relatively preserved rod function. CaBP4 in mice was previously found to be expressed in cones and rods.[28] In humans, either *CABP4* may be expressed predominantly in cones, or disturbance of its function may have a greater effect in cones than in rods.

GENETIC KNOWLEDGE MAY LEAD TO NEW THERAPEUTIC POSSIBILITIES

The very best example of the necessity of identifying the genetic defect is the success of the *RPE65* gene therapy clinical trials.[29-33] Although retinal dystrophies have always been considered untreatable, patients who are visually severely handicapped due to mutations in *RPE65* can now be treated by a subretinal injection of recombinant adeno-associated virus (AAV) carrying *RPE65* complementary DNA (cDNA) to supply functional *RPE65* to the RPE cells. Phase-I clinical trials revealed

no undesirable side-effects, and led to the improvement of visual function in most of the 21 treated patients thus far.[29-33] Patients carrying mutations in *RPE65* are suitable for gene-therapy, as they have a useful visual function in childhood, retinal imaging suggests that photoreceptor cell death occurs late in the disease process,[34] *RPE65* is a relatively small gene that can be carried by an AAV-vector, and *RPE65* has an enzymatic function, a deficiency of which can be more easily compensated than for example a gene that plays a role in photoreceptor development. Not all genes will be suitable for AAV-mediated gene-therapy; for example, the *EYS* cDNA is too large to be carried by an AAV-vector.

The identification of genetic defects is necessary to gain a broader understanding of disease mechanisms in general, which in turn can lead to the development of other therapeutic options. An example is the development of a therapy for Duchenne muscular dystrophy (DMD). In the majority of cases, DMD is caused by deletions or duplications in the Duchenne muscular dystrophy (DMD) gene that lead to the truncation of the dystrophin protein.[35] Deletions or duplications in this gene that do not result in protein truncation lead to a relatively mild phenotype: Becker muscular dystrophy.[35, 36] Based on this genetic mechanism, Aartsma et al. developed a mutation-specific therapy in which the disrupted exon, that causes the frameshift, is blocked by so-called antisense oligonucleotides (AONs).[37] The targeted exon(s), which should have a length of a multiple of three nucleotides, is/are then skipped in the splicing process, and as a result the mRNA remains in frame. In this way, the therapy changes DMD into Becker muscular dystrophy, which potentially gives the patient a higher quality of life and longer life expectancy. Proof-of-concept studies in patients affected with DMD showed a partly recovered synthesis of dystrophin, and although the functional improvement of the patients still needs to be tested, this type of therapy seems promising.[38, 39]

Phenotypic variability dependent on the genetic defect has also been found in patients carrying mutations in *CEP290*. Patients carrying two nonsense mutations in *CEP290* usually suffer from a systemic or even lethal disease (Joubert syndrome and Meckel Gruber syndrome, respectively),[40-43] while a nonsense mutation (p.Arg151X) that leads to exon skipping (nonsense-associated altered splicing; NAS) results in a single-organ disease with relatively mild symptoms (early-onset severe retinal dystrophy; EOSRD) (Chapter 4). Possibly, imitating NAS by using antisense oligonucleotides to block an exon that harbors a syndrome-causing nonsense mutation could lead to a milder phenotype. Obviously there are many obstacles, as patients will need to be treated intrauterine to change the disease course.[44-47] This would only be possible if the parents

of a patient are known to carry *CEP290* mutations and if a prenatal diagnostic test can be performed. Furthermore, few nonsense mutations would be suitable for this type of therapy, since it should be located in an exon that has a multiple of three nucleotides that encodes part of a protein domain that can be missed to some extend. Therefore, this therapy is not likely to be of broad use, but in case of mutations in *CEP290*, this type of therapy could be interesting to investigate further.

Another example of mutation-specific therapy is the PTC124 treatment; a method that aims at mutations resulting in a premature termination codon (PTC). A PTC is a signal for a ribosome to stop translation of the mRNA, which subsequently leads to a truncated protein that cannot fulfill its function, and will be degraded by a mechanism called nonsense mediated mRNA decay.[49-51] Initially, high concentrations of aminoglycosides were found to promote read-through of a PTC.[52,53] However, clinical trials revealed some disadvantages, including a low potency and a high renal and otic toxicity.[54-57] Subsequently, a high-throughput screening of low molecular-weight compounds led to the identification of PTC124 as nonsense-suppressor with a highest affinity for UGA stopcodons, followed by UAG and UAA.[58] PTC124 recognizes a PTC as being premature, and instead of ending the translation, a random amino acid is inserted at that position. The ribosome will then continue to translate the mRNA, which will thus result in a full-length protein. Patients affected by cystic fibrosis due to nonsense mutations in CFTR have been treated in a phase-II clinical trial, which resulted in an increase in chloride transport in most of the 23 treated patients, implicating a restoration of the function of CFTR.[59,60] PTC124 has also been used in DMD patients, which shows that this type of treatment may be of broader use, and thus may be of interest for patients affected by a retinal dystrophy due to a nonsense mutation.[61]

In conclusion, although many experimental treatments are still far from clinical applications, an increase in molecular genetic knowledge may provide new suggestions to develop novel therapies. Molecular genetic testing in a patient will become essential to determine the eligibility for gene- or mutation-specific therapies.

BENEFIT OF MOLECULAR KNOWLEDGE IN THE CLINIC

Although the perspective on therapy for retinal dystrophies looks more promising than it ever did, only few patients can as yet enjoy its benefits. Therefore, the question arises: what does the molecular knowledge currently bring to the patient? The answer to this question will be different for every patient, depending on his/her personal situation and personality; some people for example prefer to know the disease prognosis, while others prefer not to know. Some reasons in favor of molecular screening are mentioned below.

Perhaps the most important aspect of a molecular diagnosis is genetic counseling; patients may have considerable worries about passing on the mutation to their children. Detailed documentation of the family history can often provide the mode of inheritance. However, in isolated cases or in small families, the distinction between autosomal recessive, autosomal dominant and X-linked recessive inheritance can be difficult, while this knowledge has a great influence on the predictions about heritability (Figure 1). Discussing heredity is an issue in which the clinician can provide a clear answer, with which he/she can take away some of the patient´s worries. Furthermore, knowing the genetic defect may improve diagnostic accuracy.[62] Some retinal dystrophies have a very similar presentation in the initial stage, and a study from Weiss and Biersdorf in 1989 showed that a patient with retinal dystrophy or congenital blindness on average visited seven ophthalmologists before the diagnosis was made.[63] Although this number may not be accurate currently, determining the correct diagnosis can still be a challenge, especially in very young patients who are not yet able to participate well in ophthalmic examinations and/or ERG recordings. Therefore, knowing the genetic cause may give a better clue towards the final diagnosis in an early stage of the disease, and can distinguish between a stationary or a progressive disorder.[62] Another argument in favor of finding the genetic cause is that dietary advice may be dependent on the genetic defect. Vitamin A supplementation can be helpful for slowing down progression in patients with retinal dystrophy,[64] but probably has a detrimental effect on the phenotype of patients carrying mutations in *ABCA4*, as was shown in *Abca4*$^{-/-}$ mice.[65] Furthermore, a molecular diagnosis may be of great help to a patient when syndrome-causing mutations would be detected in an early stage. For example, an LCA patient who is affected due to mutations in *IQCB1* (*NPHP5*), is at high risk to develop nephronophthisis later in life (known as Senior-Løken Syndrome).[66, 67] When mutations in *IQCB1* are detected, an early clinical assessment of the kidney function may lead to the diagnosis of nephronophthisis in an early stage, when dietary restrictions and taking preventive medications may postpone the moment that a patient becomes dialysis-dependent (N.C. van de Kar, personal communication, 2010).

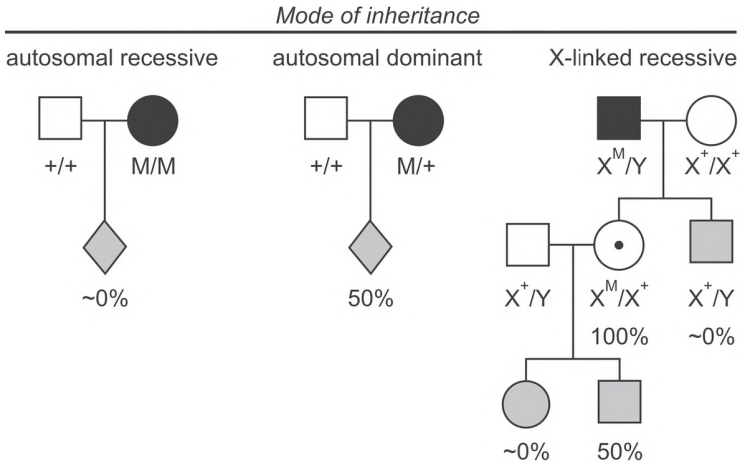

FIGURE 1. Recurrence risk when one of the parents is affected or mutation carrier, presented with different modes of inheritance.
Circle, woman; square, man; diamond shape, either boy or girl; dot within symbol, carrier of mutation; black symbol, affected person; grey symbol, no affected status known, chance to become affected is indicated; +, normal allele; M, mutant allele; X^+, normal X-chromosome; X^M, X-chromosome with mutation.

The last and probably most complex argument for genetic screening is its contribution to predicting the prognosis of the disease. For some genetic defects, a reliable prediction about the disease prognosis can be given. For example, some LCA-associated genes lead to a phenotype with clear characteristics (in refractory error, photophobia or night blindness, progressivity) specific for mutations in that particular gene.[62, 68] Knowledge of the genetic defect in a child carrying a mutation in such a gene provides therefore a reasonably reliable prognosis.

This thesis, on the other hand, shows several examples in which a genetic diagnosis cannot be used for establishing a prognosis (Chapter 3, 4 and 5A). First, mutations in *CABP4* were previously associated with congenital stationary night blindness (CSNB).[69] However, in the patients carrying mutations in *CABP4* (Chapter 3), the cones were primarily affected, and the rods were relatively spared. Also, the course of disease seemed to be progressive during childhood in previously published patients carrying mutations in *CABP4*.[69] Chapter 4 shows that a nonsense mutation in *CEP290*, usually causing LCA, unexpectedly led to a relatively mild phenotype, in which the visual acuity is higher than usually seen in LCA patients. In Chapter 5 two families are presented in whom the patients carried the same p.Tyr3156X mutation in the

EYS gene, but the age of onset in one family is much earlier (adolescence) than in the other family (forties), and their visual field defects differ as well (central defects versus a relatively well-preserved visual field). Two siblings from another family even received two different diagnoses (CRD and RP, respectively). Overall, we found that most of the patients carrying mutations in *EYS* had a more severe phenotype with earlier loss of visual acuity and peripheral visual field (Chapter 5A, 5B, 5C) than the two families with p.Tyr3156X mutations.

In conclusion, knowing the molecular defect may be of benefit for a patient with regard to genetic counseling, diagnostic accuracy, dietary advice, and early detection of systemic abnormalities. However, with regard to prognostic counseling, molecular diagnoses must be provided with great care, and a prognosis should only be made when combining the genetic information carefully with the clinical appearance. Predicting the course of a retinal disease may become more reliable when large genotype-phenotype studies, including detailed documentation of follow-up examinations, will be performed.

PHENOTYPIC VARIABILITY AND MODIFIER ALLELES

Besides the above-mentioned examples of phenotypic variability, many other publications show variability associated with mutations in one gene as well.[48, 70-74] This diversity in phenotypes may be explained by the characteristics of the causative mutation (allelic heterogeneity), by environmental influences and/or by modifier alleles.[75] A clear example of allelic heterogeneity is the *ABCA4* gene, in which mutations can lead to Stargardt disease (STGD1), CRD and RP, and variants can even be 'only' a risk-factor for age-related macular degeneration.[14, 76, 77] In this gene, a genotype-phenotype correlation explains the variability of the phenotypes, since combinations of so-called hypomorphic or mild mutations with severe mutations lead to the mildest phenotype (STGD1), and combinations of null mutations lead to the most severe phenotype (RP).[78, 79]

Intriguing is the large variability among patients carrying the same genetic defect,[48] which cannot be attributed to allelic heterogeneity. The variation in phenotypes is regularly attributed to the presence of a modifier allele.[48, 80-90 and Chapter 4] A modifier allele is a genetic variant that by itself does not cause a disease, but that does exert a modifying effect on a disease, either deteriorating or ameliorating the phenotype.[75, 91, 92] Modifier alleles have been described in Joubert syndrome and

BBS, which both involve retinal dystrophy, and the modifying effect of these alleles was confirmed in zebrafish.[86-88, 93, 94] In case of the heterozygous frameshift mutation in *MERTK* as hypothesized modifier of the *CEP290*-associated phenotype (Chapter 4), only segregation analysis substantiated this hypothesis. Further evidence for the functional relevance of the *MERTK* variant can be obtained by using animal model (mouse, zebrafish) studies.

Is it possible that heterozygous mutations frequently influence disease severity? [48, 80-90 Chapter 5A] Rivolta et al.[95] already calculated a carrier frequency for arRP gene defects of 10%, assuming that a total of 67 arRP genes could be causative, each for an equal percentage of patients. Currently, 26 genes are implicated in arRP, and each gene is mutated in a different percentage of patients. Therefore, a more accurate calculation based on the Hardy Weinberg equilibrium (Supplemental Table 1) shows that with the current knowledge, we can predict a carrier frequency of 1/8 in the general population. It is estimated that mutations in these genes account for ~50% of arRP. Assuming that many more genes will be identified, all contributing to a small percentage of cases, the total carrier frequency could even be as high as 1/4. Therefore, the chance to carry an additional mutation in one of the arRP genes is rather high. The 'mutational load' in the general population may be substantially higher as this estimate does not include mutations associated with other autosomal recessive retinal dystrophies. It is anticipated that new sequencing technologies in combination with detailed clinical analyses will reveal the role of possible modifier alleles in modifying the phenotype.

Another interesting factor influencing phenotypic variability was shown in transgenic mice, in which a mutated gene was introduced in mouse strains with different genetic backgrounds (congenic mice). Although all mice carried the same mutation, clinical appearance varied considerably dependent on the genetic background.[96, 97] This shows that it is the mutation in its genomic context that causes a disease, and that the inheritance of retinal dystrophies is possibly more complex than is currently thought.

CURRENT MOLECULAR (DIAGNOSTIC) SCREENING

Since most retinal dystrophies are genetically extremely heterogeneous (Chapter 1, Table 1), for each disease many genes need to be screened to find the genetic cause. Since a few years, high-throughput screening methods, like the arrayed primer extension (APEX) micro-array (Asper Ophthalmics, Tartu, Estonia), have enhanced diagnostic screening tremendously, leading to a rapid mutation detection

in ~33% of CRD patients,[15] 50-60% of LCA patients (A.I. den Hollander, personal communication 2010),[17] and ~15% of CSNB patients.[98] The APEX micro-array harbors oligonucleotides that can test for the presence of previously identified mutations in all genes associated with one disease (for example, autosomal recessive, autosomal dominant or X-linked RP, LCA, CSNB, BBS, Usher syndrome) or all known mutations in one gene (for example, *ABCA4*) (www.asperophthalmics.com). The limitation of this screening method is that unknown mutations in the known genes are not identified unless they are point mutations that accidentally occur at the same position as the known variants, and mutations in unknown genes can never be found in this way. Furthermore, the distinction between for example RP, LCA, CSNB, and CRD can be difficult, and it may therefore not be straightforward to choose the correct APEX array. Moreover, CRD patients can now only be screened for mutations in *ABCA4*. Also, due to the rapid detection of new mutations it is difficult to keep the APEX microarrays up to date. Ideally, there would be a screening method in which all known genes for all retinal dystrophies, including syndromic variants, could be fully screened in order to be able to detect all mutations in the known genes.
A microarray-based resequencing technology is available and used for diagnostic purposes, for example a microarray that can screen up to ~30,000 nucleotides from 11 arRP genes.[99] This microarray is able to screen all nucleotides of all genes included. However, it is not a flexible and cheap method, as updated versions need to be 'redesigned' and material costs are high. Also, it is not sensitive enough as it is not able to detect small deletions or duplications associated with arRP that constitute a significant fraction (5 – 15%) of mutations.

NEXT GENERATION SEQUENCING AND IDENTIFYING NOVEL RETINAL DYSTROPHY GENES

With the introduction of new sequencing technologies, collectively called 'next generation sequencing' (NGS), comprehensive analysis of all known retinal dystrophy genes may become cost-effective.[100-102] Based on the difference in capacity of the various platforms used, either selected genomic regions, selected genes, or the entire genome are sequenced. Currently, NGS is deployed to sequence all exons of the whole genome ('exome sequencing'), or to sequence a targeted region, that is established by homozygosity mapping or linkage analysis ('targeted sequencing'). In a research setting, NGS already led to the identification of new disease genes,[101, 103, 104] and it is likely to be instrumental to identify many new retinal dystrophy genes in the near future.

FUTURE PERSPECTIVE OF HOMOZYGOSITY MAPPING

Exome sequencing will likely be the most cost-efficient screening method in the near future. Figure 2 depicts a prediction for the future routes of genetic screening. In a diagnostic setting, exome sequencing, followed by bio-informatic focus on the known retinal dystrophy genes, will lead to the identification of the causative mutation in more than 50% of patients. If no mutation is detected in the known retinal dystrophy genes, the search for a genetic cause will probably be performed in a research setting. There are three potential outcomes when evaluating the results of exome sequencing (Figure 2). The quickest road to the identification of a causative mutation and the highest guarantee that a variant indeed is causative for a retinal dystrophy, is when homozygous or compound heterozygous truncating mutations are detected in a gene that is highly expressed in the retina and/or likely to be involved in a retinal

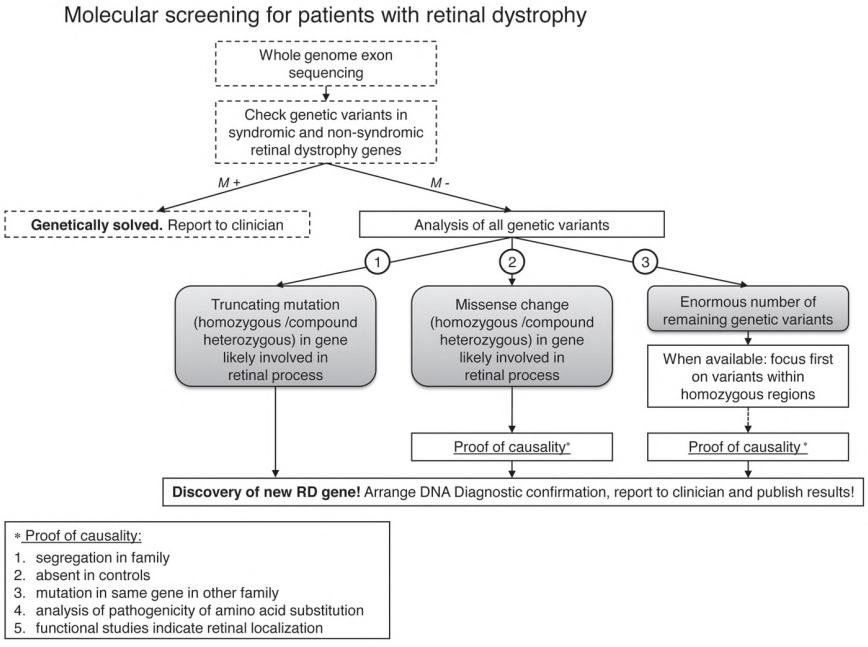

FIGURE 2. Flowchart of proposed molecular screening for diagnostic and research purposes. M +, mutation detected; M -, no mutation detected; dotted boxes, performed in diagnostic setting; full-lined boxes, performed in research setting. Dotted arrow implicates that the process of finding the causative variant from the remaining variants will be very challenging.

process. Second, homozygous or compound heterozygous missense changes can be detected in genes involved in retinal processes. An unambiguous protocol to evaluate pathogenicity needs to be developed in order to prove that a variant is indeed causing the disease, as listed in Figure 2. The third, and by far the most challenging possibility, is to detect the causative variant among the remaining hundreds or thousands of variants, which could be variants that are not clearly truncating, or variants residing in genes of which a role in a retinal process could be difficult to prove. At this stage, homozygosity mapping or linkage analysis resulting in a significant lod-score could be of value, by pointing out homozygous regions that one could first focus on, thereby decreasing the number of variants that need to be verified. Although more insight into pathogenicity of variants will become available, determining which of the variants in all exons of ~25,000 genes may still be challenging.

SUPPLEMENTAL DATA

SUPPLEMENTAL TABLE 1. Carrier frequencies of causative variants in RP genes.

A. Carrier frequencies of mutations in known arRP genes. **B.** Carrier frequencies of mutations in known arRP genes and of 43 hypothesized arRP genes

A	gene	%	q^2 *	2pq*
	EYS	5	1/70000	1/132
	USH2A	5	1/70000	1/132
	PDE6A	4	1/87500	1/148
	PDE6B	4	1/87500	1/148
	CNGA1	2	1/175000	1/210
	CRB1	2	1/175000	1/210
	RPE65	2	1/175000	1/210
	SAG	2	1/175000	1/210
	ABCA4	1,5	1/233333	1/242
	CERKL	1,5	1/233333	1/242
	CNGB1	1,5	1/233333	1/242
	IDH3B	1,5	1/233333	1/242
	LRAT	1,5	1/233333	1/242
	MERTK	1,5	1/233333	1/242
	NR2E3	1,5	1/233333	1/242
	NRL	1,5	1/233333	1/242
	PROM1	1,5	1/233333	1/242
	RGR	1,5	1/233333	1/242
	RHO	1,5	1/233333	1/242
	RLBP1	1,5	1/233333	1/242
	RP1	1,5	1/233333	1/242
	SPATA7	1,5	1/233333	1/242
	TULP1	1,5	1/233333	1/242
	PRCD	0,5	1/700000	1/418
	IRBP	0,5	1/700000	1/418
	Total	50%	~1/7000	1/8

B	gene	%	q^2	2pq*
	EYS	5	1/70000	1/132
	USH2A	5	1/70000	1/132
	PDE6A	4	1/87500	1/148
	PDE6B	4	1/87500	1/148
	CNGA1	2	1/175000	1/210
	CRB1	2	1/175000	1/210
	RPE65	2	1/175000	1/210
	SAG	2	1/175000	1/210
	gene A	2	1/175000	1/210
	gene B	2	1/175000	1/210
	gene C	2	1/175000	1/210
	ABCA4	1,5	1/233333	1/242
	CERKL	1,5	1/233333	1/242
	CNGB1	1,5	1/233333	1/242
	IDH3B	1,5	1/233333	1/242
	LRAT	1,5	1/233333	1/242
	MERTK	1,5	1/233333	1/242
	NR2E3	1,5	1/233333	1/242
	NRL	1,5	1/233333	1/242
	PROM1	1,5	1/233333	1/242
	RGR	1,5	1/233333	1/242
	RHO	1,5	1/233333	1/242
	RLBP1	1,5	1/233333	1/242
	RP1	1,5	1/233333	1/242
	SPATA7	1,5	1/233333	1/242
	TULP1	1,5	1/233333	1/242
	16x new gene	16 x 1,5	16 x 1/233333	16 x 1/242
	17x new gene	17 x 1	17 x 1/350000	17 x 1/296
	7x new gene	7 x 0,5	7 x 1/700000	7 x 1/419
	PRCD	0,5	1/700000	1/419
	IRBP	0,5	1/700000	1/419
	Total	100%	~1/3500	1/4

In a Hardy-Weinberg equilibrium, the frequency of the wild-type allele is denoted p and of the recessive mutant allele q, p+q=1, in which p is assumed to be close to 1. *, q^2 is the prevalence of a homozygous recessive allele, and 2pq is the carrier frequency, and $p^2 + 2pq + q^2=1$.
%, percentage of patients affected by mutations in that gene. Assumption: prevalence arRP 1:3500.

REFERENCES

1. den Hollander AI, Lopez I, Yzer S, et al. Identification of novel mutations in patients with Leber congenital amaurosis and juvenile RP by genome-wide homozygosity mapping with SNP microarrays. Invest Ophthalmol Vis Sci. 2007;48:5690-5698.

2. Abu Safieh L., Aldahmesh M, Shamseldin H, et al. Clinical and molecular characterization of Bardet-Biedl syndrome in consanguineous populations: the power of homozygosity mapping. J Med Genet. 2009.

3. Hildebrandt F, Heeringa SF, Ruschendorf F, et al. A systematic approach to mapping recessive disease genes in individuals from outbred populations. PLoS Genet. 2009;5:e1000353.

4. Megarbane A, Slim R, Nurnberg G, Ebermann I, Nurnberg P, Bolz HJ. A novel VPS13B mutation in two brothers with Cohen syndrome, cutis verticis gyrata and sensorineural deafness. Eur J Hum Genet. 2009;17:1076-1079.

5. Connell F, Kalidas K, Ostergaard P, et al. Linkage and sequence analysis indicate that CCBE1 is mutated in recessively inherited generalised lymphatic dysplasia. Hum Genet. 2010;127:231-241.

6. Hamanoue H, Megarbane A, Tohma T, et al. A locus for ophthalmo-acromelic syndrome mapped to 10p11.23. Am J Med Genet A. 2009;149A:336-342.

7. Carothers AD, Rudan I, Kolcic I, et al. Estimating human inbreeding coefficients: comparison of genealogical and marker heterozygosity approaches. Ann Hum Genet. 2006;70:666-676.

8. Hartl DL, Clark AG. Principles of population genetics. Sunderland, MA: Sinauer Associates; 2010

9. Broman KW, Weber JL. Long homozygous chromosomal segments in reference families from the centre d'Etude du polymorphisme humain. Am J Hum Genet. 1999;65:1493-1500.

10. McQuillan R, Leutenegger AL, Abdel-Rahman R, et al. Runs of homozygosity in European populations. Am J Hum Genet. 2008;83:359-372.

11. Gibson J, Morton NE, Collins A. Extended tracts of homozygosity in outbred human populations. Hum Mol Genet. 2006;15:789-795.

12. Schraders M, Lee K, Oostrik J, et al. Homozygosity mapping reveals mutations of GRXCR1 as a cause of autosomal-recessive nonsyndromic hearing impairment. Am J Hum Genet. 2010;86:138-147.

13. Maugeri A, van Driel MA, van de Pol DJ, et al. The 2588G-->C mutation in the ABCR gene is a mild frequent founder mutation in the Western European population and allows the classification of ABCR mutations in patients with Stargardt disease. Am J Hum Genet. 1999;64:1024-1035.

14. Maugeri A, Klevering BJ, Rohrschneider K, et al. Mutations in the ABCA4 (ABCR) gene are the major cause of autosomal recessive cone-rod dystrophy. Am J Hum Genet. 2000;67:960-966.

15. Klevering BJ, Yzer S, Rohrschneider K, et al. Microarray-based mutation analysis of the ABCA4 (ABCR) gene in autosomal recessive cone-rod dystrophy and retinitis pigmentosa. Eur J Hum Genet. 2004;12:1024-1032.

16. Roux AF, Faugere V, Le Guedard S, et al. Survey of the frequency of USH1 gene mutations in a cohort of Usher patients shows the importance of cadherin 23 and protocadherin 15 genes and establishes a detection rate of above 90%. J Med Genet. 2006;43:763-768.

17. Yzer S, Leroy BP, De Baere E, et al. Microarray-based mutation detection and phenotypic characterization of patients with Leber congenital amaurosis. Invest Ophthalmol Vis Sci. 2006;47:1167-1176.

18. Krone N, Braun A, Roscher AA, Knorr D, Schwarz HP. Predicting phenotype in steroid 21-hydroxylase deficiency? Comprehensive genotyping in 155 unrelated, well defined patients from southern Germany. J Clin Endocrinol Metab. 2000;85:1059-1065.

19. Sandoval N, Platzer M, Rosenthal A, et al. Characterization of ATM gene mutations in 66 ataxia telangiectasia families. Hum Mol Genet. 1999;8:69-79.

20. Wissinger B, Gamer D, Jagle H, et al. CNGA3 mutations in hereditary cone photoreceptor disorders. Am J Hum Genet. 2001;69:722-737.

21. Baylor DA. Photoreceptor signals and vision. Proctor lecture. Invest Ophthalmol Vis Sci. 1987;28:34-49.

22. Liu Q, Tan G, Levenkova N, et al. The proteome of the mouse photoreceptor sensory cilium complex. Mol Cell Proteomics. 2007;6:1299-1317.

23. Pierce EA. Pathways to photoreceptor cell death in inherited retinal degenerations. Bioessays. 2001;23:605-618.

24. den Hollander AI, Roepman R, Koenekoop RK, Cremers FPM. Leber congenital amaurosis: genes, proteins and disease mechanisms. Prog Retin Eye Res. 2008;27:391-419.

25. den Hollander AI, Black A, Bennett J, Cremers FPM. Lighting a candle in the dark: advances in genetics and gene therapy of recessive retinal dystrophies. J Clin Invest. 2010.

26. Zelhof AC, Hardy RW, Becker A, Zuker CS. Transforming the architecture of compound eyes. Nature. 2006;443:696-699.

27. Haeseleer F, Imanishi Y, Maeda T, et al. Essential role of Ca2+-binding protein 4, a Cav1.4 channel regulator, in photoreceptor synaptic function. Nat Neurosci. 2004;7:1079-1087.

28. Maeda T, Lem J, Palczewski K, Haeseleer F. A critical role of CaBP4 in the cone synapse. Invest Ophthalmol Vis Sci. 2005;46:4320-4327.

29. Bainbridge JW, Smith AJ, Barker SS, et al. Effect of gene therapy on visual function in Leber's congenital amaurosis. N Engl J Med. 2008;358:2231-2239.

30. Maguire AM, Simonelli F, Pierce EA, et al. Safety and efficacy of gene transfer for Leber's congenital amaurosis. N Engl J Med. 2008;358:2240-2248.

31. Maguire AM, High KA, Auricchio A, et al. Age-dependent effects of RPE65 gene therapy for Leber's congenital amaurosis: a phase 1 dose-escalation trial. Lancet. 2009;374:1597-1605.

32. Cideciyan AV, Hauswirth WW, Aleman TS, et al. Human RPE65 gene therapy for Leber congenital amaurosis: persistence of early visual improvements and safety at 1 year. Hum Gene Ther. 2009;20:999-1004.

33. Hauswirth WW, Aleman TS, Kaushal S, et al. Treatment of leber congenital amaurosis due to RPE65 mutations by ocular subretinal injection of adeno-associated virus gene vector: short-term results of a phase I trial. Hum Gene Ther. 2008;19:979-990.

34. Paunescu K, Wabbels B, Preising MN, Lorenz B. Longitudinal and cross-sectional study of patients with early-onset severe retinal dystrophy associated with RPE65 mutations. Graefes Arch Clin Exp Ophthalmol. 2005;243:417-426.

35. Hoffman EP, Fischbeck KH, Brown RH, et al. Characterization of dystrophin in muscle-biopsy specimens from patients with Duchenne's or Becker's muscular dystrophy. N Engl J Med. 1988;318:1363-1368.

36. Monaco AP, Bertelson CJ, Liechti-Gallati S, Moser H, Kunkel LM. An explanation for the phenotypic differences between patients bearing partial deletions of the DMD locus. Genomics. 1988;2:90-95.

37. Aartsma-Rus A, De Winter CL, Janson AA, et al. Functional analysis of 114 exon-internal AONs for targeted DMD exon skipping: indication for steric hindrance of SR protein binding sites. Oligonucleotides. 2005;15:284-297.

38. van Deutekom JC, Janson AA, Ginjaar IB, et al. Local dystrophin restoration with antisense oligonucleotide PRO051. N Engl J Med. 2007;357:2677-2686.

39. Kinali M, Arechavala-Gomeza V, Feng L, et al. Local restoration of dystrophin expression with the morpholino oligomer AVI-4658 in Duchenne muscular dystrophy: a single-blind, placebo-controlled, dose-escalation, proof-of-concept study. Lancet Neurol. 2009;8:918-928.

40. Sayer JA, Otto EA, O'Toole JF, et al. The centrosomal protein nephrocystin-6 is mutated in Joubert syndrome and activates transcription factor ATF4. Nat Genet. 2006;38:674-681.

41. Valente EM, Silhavy JL, Brancati F, et al. Mutations in CEP290, which encodes a centrosomal protein, cause pleiotropic forms of Joubert syndrome. Nat Genet. 2006;38:623-625.

42. Helou J, Otto EA, Attanasio M, et al. Mutation analysis of NPHP6/CEP290 in patients with Joubert syndrome and Senior-Loken syndrome. J Med Genet. 2007;44:657-663.

43. Frank V, den Hollander AI, Bruchle NO, et al. Mutations of the CEP290 gene encoding a centrosomal protein cause Meckel-Gruber syndrome. Hum Mutat. 2008;29:45-52.

44. Shen JS, Meng XL, Yokoo T, et al. Widespread and highly persistent gene transfer to the CNS by retrovirus vector in utero: implication for gene therapy to Krabbe disease. J Gene Med. 2005;7:540-551.

45. David AL, Peebles DM, Gregory L, et al. Clinically applicable procedure for gene delivery to fetal gut by ultrasound-guided gastric injection: toward prenatal prevention of early-onset intestinal diseases. Hum Gene Ther. 2006;17:767-779.

46. Coutelle C, Themis M, Waddington SN, et al. Gene therapy progress and prospects: fetal gene therapy--first proofs of concept--some adverse effects. Gene Ther. 2005;12:1601-1607.

47. David AL, Peebles D. Gene therapy for the fetus: is there a future? Best Pract Res Clin Obstet Gynaecol. 2008;22:203-218.

48. den Hollander AI, Koenekoop RK, Yzer S, et al. Mutations in the CEP290 (NPHP6) gene are a frequent cause of Leber congenital amaurosis. Am J Hum Genet. 2006;79:556-561.

49. Nagy E, Maquat LE. A rule for termination-codon position within intron-containing genes: when nonsense affects RNA abundance. Trends Biochem Sci. 1998;23:198-199.

50. Cheng J, Belgrader P, Zhou X, Maquat LE. Introns are cis effectors of the nonsense-codon-mediated reduction in nuclear mRNA abundance. Mol Cell Biol. 1994;14:6317-6325.

51. Zhang J, Sun X, Qian Y, Maquat LE. Intron function in the nonsense-mediated decay of beta-globin mRNA: indications that pre-mRNA splicing in the nucleus can influence mRNA translation in the cytoplasm. RNA. 1998;4:801-815.

52. Manuvakhova M, Keeling K, Bedwell DM. Aminoglycoside antibiotics mediate context-dependent suppression of termination codons in a mammalian translation system. RNA. 2000;6:1044-1055.

53. Barton-Davis ER, Cordier L, Shoturma DI, Leland SE, Sweeney HL. Aminoglycoside antibiotics restore dystrophin function to skeletal muscles of mdx mice. J Clin Invest. 1999;104:375-381.

54. Wagner KR, Hamed S, Hadley DW, et al. Gentamicin treatment of Duchenne and Becker muscular dystrophy due to nonsense mutations. Ann Neurol. 2001;49:706-711.

55. Clancy JP, Bebok Z, Ruiz F, et al. Evidence that systemic gentamicin suppresses premature stop mutations in patients with cystic fibrosis. Am J Respir Crit Care Med. 2001;163:1683-1692.

56. Politano L, Nigro G, Nigro V, et al. Gentamicin administration in Duchenne patients with premature stop codon. Preliminary results. Acta Myol. 2003;22:15-21.

57. Wilschanski M, Yahav Y, Yaacov Y, et al. Gentamicin-induced correction of CFTR function in patients with cystic fibrosis and CFTR stop mutations. N Engl J Med. 2003;349:1433-1441.

58. Welch EM, Barton ER, Zhuo J, et al. PTC124 targets genetic disorders caused by nonsense mutations. Nature. 2007;447:87-91.

59. Du M, Liu X, Welch EM, Hirawat S, Peltz SW, Bedwell DM. PTC124 is an orally bioavailable compound that promotes suppression of the human CFTR-G542X nonsense allele in a CF mouse model. Proc Natl Acad Sci U S A. 2008;105:2064-2069.

60. Hirawat S, Welch EM, Elfring GL, et al. Safety, tolerability, and pharmacokinetics of PTC124, a nonaminoglycoside nonsense mutation suppressor, following single- and multiple-dose administration to healthy male and female adult volunteers. J Clin Pharmacol. 2007;47:430-444.

61. Linde L, Kerem B. Introducing sense into nonsense in treatments of human genetic diseases. Trends Genet. 2008;24:552-563.

62. Koenekoop RK, Lopez I, den Hollander AI, Allikmets R, Cremers FPM. Genetic testing for retinal dystrophies and dysfunctions: benefits, dilemmas and solutions. Clin Experiment Ophthalmol. 2007;35:473-485.

63. Weiss AH, Biersdorf WR. Visual sensory disorders in congenital nystagmus. Ophthalmology. 1989;96:517-523.

64. Berson EL, Rosner B, Sandberg MA, et al. A randomized trial of vitamin A and vitamin E supplementation for retinitis pigmentosa. Arch Ophthalmol. 1993;111:761-772.

65. Radu RA, Yuan Q, Hu J, et al. Accelerated accumulation of lipofuscin pigments in the RPE of a mouse model for ABCA4-mediated retinal dystrophies following Vitamin A supplementation. Invest Ophthalmol Vis Sci. 2008;49:3821-3829.

66. Loken AC, Hanssen O, Halvoren S, Jolster NJ. Hereditary renal dysplasia and blindness. Acta Paediatr. 1961;50:177-184.

67. Estrada-Cuzcano AI, Koenekoop RK, Kohl S, et al. IQCB1 mutations in patients with Leber congenital amaurosis. Invest Ophthalmol Vis Sci. 2010:submitted.

68. Hanein S, Perrault I, Gerber S, et al. Leber congenital amaurosis: comprehensive survey of the genetic heterogeneity, refinement of the clinical definition, and genotype-phenotype correlations as a strategy for molecular diagnosis. Hum Mutat. 2004;23:306-317.

69. Zeitz C, Kloeckener-Gruissem B, Forster U, et al. Mutations in CABP4, the gene encoding the Ca2+-binding protein 4, cause autosomal recessive night blindness. Am J Hum Genet. 2006;79:657-667.

70. Michaelides M, Wilkie SE, Jenkins S, et al. Mutation in the gene GUCA1A, encoding guanylate cyclase-activating protein 1, causes cone, cone-rod, and macular dystrophy. Ophthalmology. 2005;112:1442-1447.

71. Renner AB, Fiebig BS, Weber BH, et al. Phenotypic variability and long-term follow-up of patients with known and novel PRPH2/RDS gene mutations. Am J Ophthalmol. 2009;147:518-530.

72. Abd El-Aziz MM, O'Driscoll CA, Kaye RS, et al. Identification of novel mutations in the ortholog of Drosophila eyes shut gene (EYS) causing autosomal recessive retinitis pigmentosa. Invest Ophthalmol Vis Sci. 2010.

73. Bandah D, Merin S, Ashhab M, Banin E, Sharon D. The spectrum of retinal diseases caused by NR2E3 mutations in Israeli and Palestinian patients. Arch Ophthalmol. 2009;127:297-302.

74. Mataftsi A, Schorderet DF, Chachoua L, et al. Novel TULP1 mutation causing leber congenital amaurosis or early onset retinal degeneration. Invest Ophthalmol Vis Sci. 2007;48:5160-5167.

75. Haider NB, Ikeda A, Naggert JK, Nishina PM. Genetic modifiers of vision and hearing. Hum Mol Genet. 2002;11:1195-1206.

76. Allikmets R, Singh N, Sun H, et al. A photoreceptor cell-specific ATP-binding transporter gene (ABCR) is mutated in recessive Stargardt macular dystrophy. Nat Genet. 1997;15:236-246.

77. Martinez-Mir A, Paloma E, Allikmets R, et al. Retinitis pigmentosa caused by a homozygous mutation in the Stargardt disease gene ABCR. Nat Genet. 1998;18:11-12.

78. van Driel MA, Maugeri A, Klevering BJ, Hoyng CB, Cremers FPM. ABCR unites what ophthalmologists divide(s). Ophthalmic Genet. 1998;19:117-122.

79. Cremers FPM, van de Pol DJ, van Driel M, et al. Autosomal recessive retinitis pigmentosa and cone-rod dystrophy caused by splice site mutations in the Stargardt's disease gene ABCR. Hum Mol Genet. 1998;7:355-362.

80. Jacobson SG, Cideciyan AV, Iannaccone A, et al. Disease expression of RP1 mutations causing autosomal dominant retinitis pigmentosa. Invest Ophthalmol Vis Sci. 2000;41:1898-1908.

81. Silva E, Dharmaraj S, Li YY, et al. A missense mutation in GUCY2D acts as a genetic modifier in RPE65-related Leber Congenital Amaurosis. Ophthalmic Genet. 2004;25:205-217.

82. Thompson DA, Janecke AR, Lange J, et al. Retinal degeneration associated with RDH12 mutations results from decreased 11-cis retinal synthesis due to disruption of the visual cycle. Hum Mol Genet. 2005;14:3865-3875.

83. Yzer S, Fishman GA, Racine J, et al. CRB1 heterozygotes with regional retinal dysfunction: implications for genetic testing of Leber congenital amaurosis. Invest Ophthalmol Vis Sci. 2006;47:3736-3744.

84. Passerini I, Sodi A, Giambene B, Menchini U, Torricelli F. Phenotypic intrafamilial variability associated with S212G mutation in the RDS/peripherin gene. Eur J Ophthalmol. 2007;17:1000-1003.

85. Walia S, Fishman GA, Swaroop A, et al. Discordant phenotypes in fraternal twins having an identical mutation in exon ORF15 of the RPGR gene. Arch Ophthalmol. 2008;126:379-384.

86. Khanna H, Davis EE, Murga-Zamalloa CA, et al. A common allele in RPGRIP1L is a modifier of retinal degeneration in ciliopathies. Nat Genet. 2009;41:739-745.

87. Leitch CC, Zaghloul NA, Davis EE, et al. Hypomorphic mutations in syndromic encephalocele genes are associated with Bardet-Biedl syndrome. Nat Genet. 2008;40:443-448.

88. Badano JL, Leitch CC, Ansley SJ, et al. Dissection of epistasis in oligogenic Bardet-Biedl syndrome. Nature. 2006;439:326-330.

89. Schorderet DF, Escher P. NR2E3 mutations in enhanced S-cone sensitivity syndrome (ESCS), Goldmann-Favre syndrome (GFS), clumped pigmentary retinal degeneration (CPRD), and retinitis pigmentosa (RP). Hum Mutat. 2009;30:1475-1485.

90. Louie CM, Caridi G, Lopes VS, et al. AHI1 is required for photoreceptor outer segment development and is a modifier for retinal degeneration in nephronophthisis. Nat Genet. 2010;42:175-180.

91. Nadeau JH. Modifier genes in mice and humans. Nat Rev Genet. 2001;2:165-174.

92. Samardzija M, Wenzel A, Naash M, Reme CE, Grimm C. Rpe65 as a modifier gene for inherited retinal degeneration. Eur J Neurosci. 2006;23:1028-1034.

93. Stoetzel C, Laurier V, Davis EE, et al. BBS10 encodes a vertebrate-specific chaperonin-like protein and is a major BBS locus. Nat Genet. 2006;38:521-524.

94. Stoetzel C, Muller J, Laurier V, et al. Identification of a novel BBS gene (BBS12) highlights the major role of a vertebrate-specific branch of chaperonin-related proteins in Bardet-Biedl syndrome. Am J Hum Genet. 2007;80:1-11.

95. Rivolta C, Sharon D, DeAngelis MM, Dryja TP. Retinitis pigmentosa and allied diseases: numerous diseases, genes, and inheritance patterns. Hum Mol Genet. 2002;11:1219-1227.

96. Liu Q, Saveliev A, Pierce EA. The severity of retinal degeneration in Rp1h gene-targeted mice is dependent on genetic background. Invest Ophthalmol Vis Sci. 2009;50:1566-1574.

97. Brunner S, Skosyrski S, Kirschner-Schwabe R, et al. Cone versus rod disease in a mutant Rpgr mouse caused by different genetic backgrounds. Invest Ophthalmol Vis Sci. 2010;51:1106-1115.

98. Zeitz C, Labs S, Lorenz B, et al. Genotyping microarray for CSNB-associated genes. Invest Ophthalmol Vis Sci. 2009;50:5919-5926.

99. Mandal MN, Heckenlively JR, Burch T, et al. Sequencing arrays for screening multiple genes associated with early-onset human retinal degenerations on a high-throughput platform. Invest Ophthalmol Vis Sci. 2005;46:3355-3362.

100. Ng SB, Turner EH, Robertson PD, et al. Targeted capture and massively parallel sequencing of 12 human exomes. Nature. 2009;461:272-276.

101. Choi M, Scholl UI, Ji W, et al. Genetic diagnosis by whole exome capture and massively parallel DNA sequencing. Proc Natl Acad Sci U S A. 2009;106:19096-19101.

102. Hodges E, Xuan Z, Balija V, et al. Genome-wide in situ exon capture for selective resequencing. Nat Genet. 2007;39:1522-1527.

103. Ng SB, Buckingham KJ, Lee C, et al. Exome sequencing identifies the cause of a mendelian disorder. Nat Genet. 2010;42:30-35.

104. Nikopoulos K, Gilissen C, Hoischen A, et al. Next-generation sequencing of a 40 Mb linkage interval reveals TSPAN12 mutations in patients with familial exudative vitreoretinopathy. Am J Hum Genet. 2010;86:240-247.

SUMMARY

Over the last two decades, approximately one hundred genes have been identified, that are associated with retinal dystrophies. In many patients, though, the genetic cause is still unknown. In this thesis, we attempted to identify new genes and gene mutations in patients with autosomal recessive retinal dystrophies, using homozygosity mapping and linkage analysis. We mainly focused on patients affected by cone-rod dystrophy (CRD), but also patients with retinitis pigmentosa (RP) and Leber congenital amaurosis (LCA) were included in this study.

Chapter 1 provides a general introduction to the retinal anatomy, the processes that lead to vision, and an introduction to the clinical and genetic aspects of the three retinal dystrophies involved in this thesis. Furthermore, it describes the rational of homozygosity mapping; a method that is often used for identifying the genetic defect in patients from consanguineous families, but that is relatively new in the search for mutations and new genes in non-consanguineous patients.

In **chapter 2** the results of homozygosity mapping in a cohort of 95 CRD-probands are described. Significant homozygous regions (≥ ~3 Mb) were detected in the majority of non-consanguineous patients (76/99; 77%), and in all (9/9) consanguineous patients. Screening of the known retinal dystrophy genes residing in these homozygous regions led to the detection of new causative mutations in five genes (*ABCA4, CABP4, CERKL, KCVN2* and *PROM1*) in seven probands. Moreover, overlap of a homozygous region with the RP25 locus led to the identification of a new gene (*EYS*). Detailed clinical evaluation of patients carrying mutations in CRD-associated genes (*ABCA4, CERKL, PROM1*) revealed a wide variety of retinal appearances on fundus photographs, autofluorescence and in vivo retinal microscopy. The phenotypes of patients carrying mutations in genes not associated with CRD (*CABP4, EYS, KCNV2*) indeed appeared to be different than CRD.

Chapter 3 describes the detection of the *CABP4* p.Arg216X mutation in two siblings and the associated phenotype. Mutations in *CABP4* were previously described in patients with congenital stationary night blindness (CNSB), whereas the two siblings investigated were initially diagnosed with cone-rod dysfunction. Detailed clinical evaluation, including 15 Hz electroretinogram (ERG) measurements, revealed a distinctive phenotype that was characterized by reduced visual acuity, photophobia, and abnormal color vision. ERGs showed electronegative mixed rod-cone responses and severely reduced cone responses, but with relatively preserved isolated rod responses. Since these patients did not experience night blindness, we considered the name CSNB inappropriate. As the phenotype and the genotype indicated a defect

in the photoreceptor synapse, we introduced a new name for this type of disease, namely congenital cone–rod synaptic disorder.

In **chapter 4** A family is described with four affected individuals; one affected by RP, one affected by LCA, and two affected by a phenotype less severe than LCA, that we coined early-onset severe retinal dystrophy (EOSRD). Linkage analysis followed by mutation analysis in the LCA patient and her two cousins (with EOSRD), revealed compound heterozygous mutations in *CEP290*; the most prevalent LCA-causing mutation c.2991+1655A>G, which is a hypomorphic mutation, and a novel p.Arg151X mutation. Since two nonsense mutations usually lead to a *CEP290*-associated syndrome with at least neurological and renal symptoms, we hypothesized that p.Arg151X represents a hypomorphic mutation in order to cause a relatively mild phenotype. Reverse transcriptase (RT) PCR of *CEP290* mRNA revealed three splice forms in individuals carrying the p.Arg151X mutation; one wildtype PCR product, representing the allele without p.Arg151X, one PCR product missing exon 7, and one PCR product missing exons 7 and 8. The aberrant splice forms are probably caused by a mechanism called nonsense-associated altered splicing. As the mutant mRNA maintain the open reading frame, the predicted proteins – lacking 18 or 25 amino acids, respectively – may maintain functional properties, and p.Arg151X indeed is likely to have a hypomorphic character. Homozygosity mapping in a distant family member affected by RP revealed a homozygous frameshift mutation in *MERTK*. This mutation was heterozygously present in the LCA patients, and absent in the two cousins affected by EOSRD, leading to the hypothesis that the heterozygous *MERTK* mutation may have a modifying effect on the phenotype.

Chapter 5A presents the discovery of *EYS*, which was facilitated by the detection of a homozygous region, shared by two non-consanguineous siblings, that reduced the size of the RP25 locus. The RP25 locus was already defined in 1998, but the causative gene remained undiscovered. Based on several gene-predictions we hypothesized that one gene, residing in the reduced RP25-locus, might be larger than previously assumed. RT-PCR of retinal cDNA indeed revealed a transcript of 10,475 nucleotides in size, spanning approximately 2 million nucleotides of the genome, which makes this newly identified gene one of the largest genes known and the largest gene specifically expressed in the eye. The gene appeared to be an ortholog of the *Drosophila eyes shut* (*eys*)-*spacemaker* gene, and therefore the new human gene was coined *'eyes shut homolog'*, abbreviated *EYS*. Based on the function of *eys* in *Drosophila*, the EYS protein is hypothesized to play a role in the photoreceptor outer segment morphogenesis. Mutation analysis in CRD and RP patients with

a homozygous region at the *EYS* locus revealed two different truncating mutations in three Dutch families. One mutation (p.Tyr3156X) caused CRD in one patient and RP in her brother, and led to a very mild RP in three patients from a second family. Another truncating mutation (p.Pro2238ProfsX16) in a third family led to a classic type of RP.

To decipher the prevalence of *EYS* mutations in RP patients, we performed mutation analysis in 245 RP patients, mainly of Dutch origin. This resulted in the identification of the causative mutations in ten RP families, presented in **chapter 5B**, and with that the prevalence of *EYS* mutations in autosomal recessive RP patients from The Netherlands is estimated to be 5%. **Chapter 5C** presents the prevalence of mutations in *EYS* in the Israelian and Palestinian populations. Mutation analysis of *EYS* in patients having a homozygous region at the *EYS* locus led to the identification of the causative mutation in four RP patients. Subsequent screening for the identified mutations in a cohort of 177 RP patients revealed six more patients carrying mutations in *EYS*. The prevalence of *EYS* mutations in autosomal recessive RP patients from the Israelian and Palestinian population is estimated to be 7%.

The age of onset of the *EYS*-associated RP phenotype was between the second and fourth decade of life in Dutch (**5B**) as well as Israelian-Palestinian (**5C**) patients, starting with night blindness, followed by gradual constriction of the visual field, and a decline of visual acuity later in life. The fundus displayed bone spicules, generalized atrophy of the retinal pigment epithelium and choriocapillaris, and atrophic macular changes occurring later in life. Altogether, the *EYS*-associated phenotype in the Dutch and the Israelian-Palestinian cohorts seemed to be rather homogeneous.

In **Chapter 6** the results described in this thesis are discussed in order to point out the implications for scientists, ophthalmologists and patients. The strengths and limitations of homozygosity mapping are discussed, leading to the conclusion that homozygosity mapping can be effective in consanguineous as well as non-consanguineous families. Identifying the genetic defects in patients with retinal dystrophies is of importance for providing clear information about heredity, it gives insight in disease etiology, and it is indispensable for developing new therapies, and to determine which patients will be eligible for gene therapy. Providing information about the prognosis based on the genetic defect remains difficult in patients with retinal dystrophy, because we do not yet know the impact of modifier alleles. As calculated in the discussion, approximately 1/4 people likely carry a mutation in one of the autosomal recessive RP genes, and therefore patients have a high chance to carry a third mutation (a so-called modifier allele) that may have an additional deteriorating effect on the photoreceptor.

In the near future, the current molecular screening technologies will be expanded with next generation sequencing (NGS) methods, which are able to screen millions of nucleotides in one experiment. Upon identifying a novel retinal disease gene by NGS, homozygosity mapping data can be used to select patients for sequence analysis in order to identify other patients with mutations in the same gene. As whole genome exon (exome) NGS reveals an enormous number of sequence variants in each patient, homozygosity mapping in a subset of patients may also facilitate the discrimination of pathologic versus benign variants.

SAMENVATTING

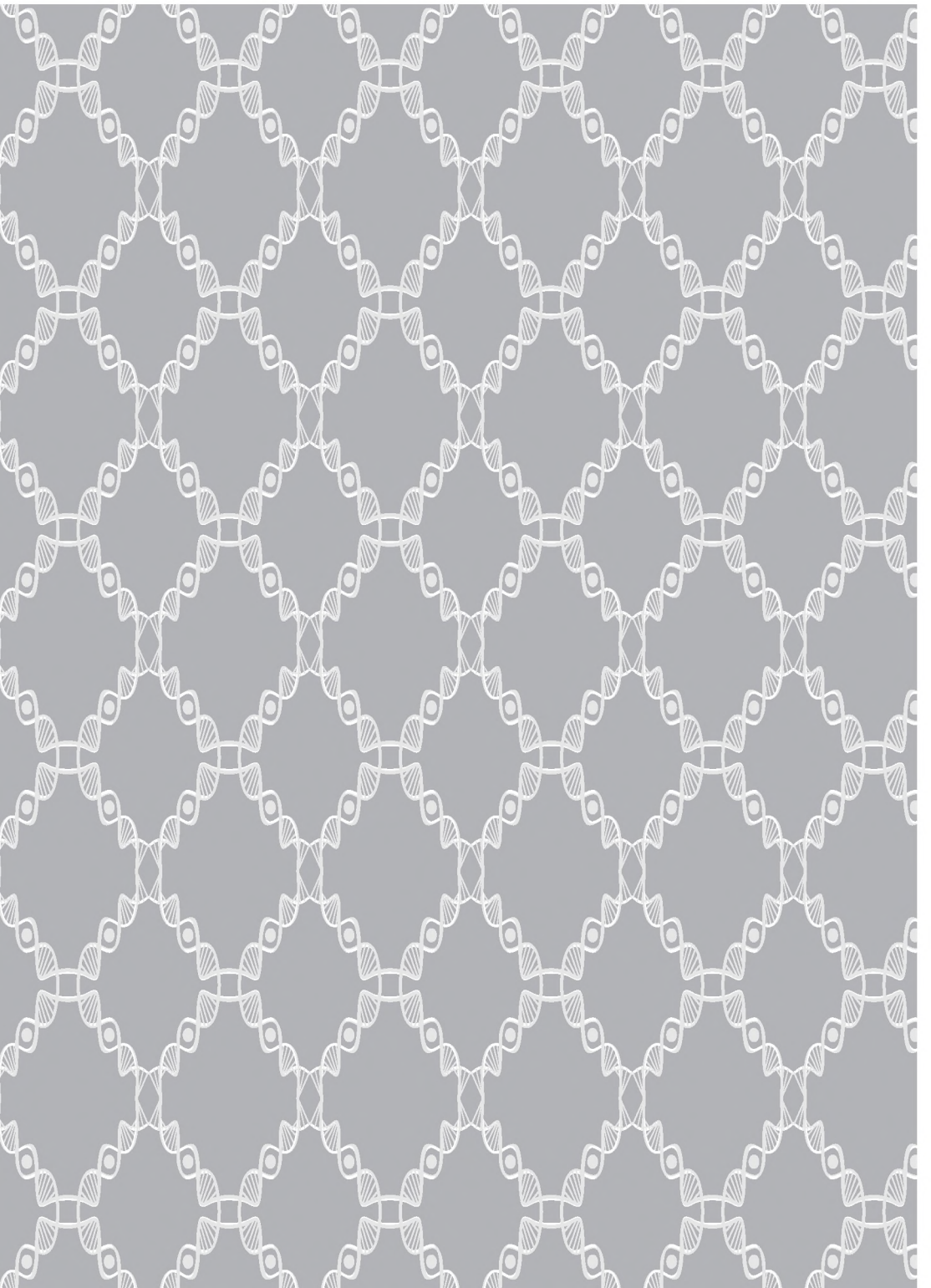

De afgelopen twee decennia zijn er ongeveer honderd genen ontdekt die geassocieerd zijn met retina dystrofie. Echter, bij veel patiënten is het genetisch defect nog onbekend. In dit proefschrift hebben we getracht om met behulp van homozygotie mapping en koppelingsstudies analyse nieuwe genen en genmutaties te identificeren bij patiënten met een autosomaal recessieve kegel-staaf dystrofie (CRD), retinitis pigmentosa (RP) en amaurosis congenita van Leber (LCA).

Hoofdstuk 1 bevat een algemene inleiding in de anatomie van de retina, de processen die leiden tot zicht, en een introductie in de klinische en genetische aspecten van de drie vormen van retina dystrofie die in dit proefschrift aan bod komen. Daarnaast wordt het principe van homozygotie mapping uitgelegd. Homozygotie mapping is een methode die regelmatig gebruikt wordt om het genetisch defect op te sporen in families waarin de ouders van een patiënt aan elkaar gerelateerd zijn (consanguine families). De methode is echter nog relatief ongebruikelijk voor het opsporen van mutaties en nieuwe genen in niet-consanguine families.

In **hoofdstuk 2** worden de resultaten beschreven van homozygotie mapping bij 95 CRD probanden. Significante homozygote gebieden (≥ ~3 Mb) werden gevonden in de meerderheid van de niet-consanguine patiënten (76/99; 77%) en in alle (9/9) consanguine patiënten. Mutatie analyse van de bekende retina dystrofie genen die zich in een homozygotie gebied bevonden heeft geleid tot het vinden van de oorzakelijke mutatie in vijf genen (*ABCA4*, *CABP4*, *CERKL*, *KCVN2* en *PROM1*) bij zeven patiënten. Daarnaast bleek een homozygoot gebied te overlappen met het RP25 locus, wat leidde tot de ontdekking van een nieuw RP gen (*EYS*). Fundus foto s, autofluorescentie en OCT onderzoeken bij patiënten met een mutatie in een CRD gen (*ABCA4*, *CERKL*, *PROM1*) toonden een grote variatie in de gevonden retina afwijkingen. Het fenotype van patiënten met mutaties in een gen dat niet geassocieerd is met CRD bleek inderdaad geen CRD te zijn.

Hoofdstuk 3 beschrijft de ontdekking van de *CABP4* p.Arg216X mutatie en het bijbehorende fenotype. Mutaties in *CABP4* waren voorheen geassocieerd met congenitale stationaire nachtblindheid (CSNB), terwijl beide patiënten met de p.Arg216X mutatie de diagnose 'kegel-staaf dysfunctie' hadden gekregen. Oogheelkundig onderzoek, inclusief een 15 Hz electroretinogram (ERG), toonde een fenotype gekarakteriseerd door een verlaagde visus, fotofobie en abnormaal kleurenzien. Het ERG toonde electronegatieve gemengde staaf-kegel responsies, extreem verlaagde kegel responsies, maar relatief gespaarde staaf responsies. Het feit dat de patiënten niet nachtblind zijn, maakte de naam CSNB ongeschikt. Omdat

het fenotype en genotype wijzen op een defect in de fotoreceptor synaps, hebben we de naam 'congenitale kegel-staaf synaps aandoening' voorgesteld voor dit fenotype.

In **hoofdstuk 4** wordt een familie beschreven met vier aangedane personen: één met RP, één met LCA en twee personen met een fenotype dat milder is dan LCA, dat we juveniele ernstige retina dystrofie (EOSRD) hebben genoemd. Linkage analyse gevolgd door mutatie analyse in de LCA patiënte en haar neefje en nichtje met EOSRD bracht samengestelde heterozygote mutaties in *CEP290* aan het licht: de veelvoorkomende LCA-veroorzakende hypomorfe c.2991+1655A>G mutatie en de nieuwe p.Arg151X mutatie. Twee stopmutaties leiden meestal tot een syndroom met neurologische en renale symptomen. Daarom zou de p.Arg151X mutatie een hypomorfe mutatie moeten zijn om een relatief mild fenotype te kunnen veroorzaken. Bij reverse transcriptase (RT) PCR van het *CEP290* mRNA vonden we drie verschillende splice-varianten: een wildtype PCR product dat afkomstig is van het allel zonder p.Arg151X, een product waarbij exon 7 ontbreekt, en een product waarbij exon 7 en 8 ontbreken. The afwijkende splice-vormen worden waarschijnlijk veroorzaakt door een mechanisme dat 'nonsense-associated altered splicing' wordt genoemd. Aangezien het mutante mRNA het open reading frame behoudt, zal het afgelezen eiwit – dat 18 of 25 aminozuren mist – mogelijk nog functioneel zijn. De p.Arg151X mutatie lijkt daarmee dus inderdaad een hypomorfe mutatie te zijn. Homozygotie mapping in een familielid met RP leidde daarnaast tot het vinden van een mutatie in *MERTK*. Deze mutatie was ook heterozygoot aanwezig bij de LCA patiënte, en afwezig bij de twee patiënten met EOSRD. Onze hypothese is dat deze heterozygote *MERTK* mutatie een modificerend effect heeft op het fenotype.

Hoofdstuk 5A presenteert de ontdekking van het *EYS* gen. Een Nederlandse broer en zus bleken een homozygoot gebied te delen binnen het 15 Mb RP25 locus. Het RP25 locus was al beschreven in 1998, maar het oorzakelijke gen was nog onbekend. Binnen het 5 Mb homozygote gebied dat de patiënten deelden bleek een gen te liggen waarvan we voorspelden dat het een groter gen zou zijn dan voorheen werd aangenomen. Met behulp van RT-PCR van retina cDNA vonden we inderdaad een transcript van 10.475 nucleotiden lang, dat zich over 2 miljoen basen in het genoom uitspreid en daarmee één van de langste genen is in het genoom, en het langste gen dat specifiek tot expressie komt in het oog. Het gen bleek een ortholoog te zijn van het *eyes shut* (*eys*)-*spacemaker* gen in *Drosophila*, en is daarom *'eyes shut homoloog'* genoemd, afgekort als *EYS*. Gebaseerd op de functie van *eys* in *Drosophila*, lijkt het EYS eiwit een rol te spelen in de ontwikkeling van het fotoreceptor buitensegment. Bij CRD en RP patiënten met een homozygoot gebied rond *EYS* werden twee

verschillende mutaties in patiënten uit drie Nederlandse families ontdekt. De homozygote p.Tyr3156X mutatie veroorzaakt CRD in een patiënte en RP bij haar broer, en leidt tot een mild en laat-optredende vorm van RP in een andere familie. De tweede geïdentificeerde mutatie (p.Pro2238ProfsX16) leidde tot een klassiek RP fenotype in een derde familie.

Om de prevalentie te bepalen van mutaties in *EYS* bij RP patiënten, hebben we mutatie analyse uitgevoerd bij 245 RP patiënten, waarvan de meeste Nederlands. Dit resulteerde in de identificatie van de oorzakelijke mutaties bij 10 RP families, beschreven in **hoofdstuk 5B**, en daarmee lijkt de prevalentie van *EYS* in autosomaal recessieve RP patiënten in Nederland ongeveer 5% te zijn. **Hoofdstuk 5C** presenteert de prevalentie van *EYS* mutaties in de Israelische-Palestijnse populatie. Mutatie analyse van *EYS* bij patiënten met een homozygoot gebied rond *EYS* heeft geleid tot de identificatie van de mutatie bij vier RP patiënten. Een cohort van 121 RP patiënten is vervolgens gescreend voor de aanwezigheid van deze mutaties, en werden in zes patiënten gevonden. Daarmee lijkt de prevalentie van mutaties in *EYS* in autosomaal recessieve RP patiënten in de Israelische-Palestijnse populatie ongeveer 7% te zijn.

De diagnose RP in het *EYS*-gerelateerde fenotype werd gesteld tussen de 20 en 40 jaar bij zowel de Nederlandse (5B) als de Israelisch- Palestijnse (5C) patiënten, en begint met nachtblindheid gevolgd door verlies van het perifere gezichtsveld en een achteruitgang van de visus later in het beloop. De fundus vertoont beenbalkjes pigmentatie, gegeneraliseerde atrofie van het retina pigment epitheel en de choriocapillaris en atrofische macula veranderingen later in het beloop. Het *EYS*-gerelateerde fenotype lijkt in de Nederlandse en Israelische-Palestijnse patiënten vrij homogeen te zijn.

In **hoofdstuk 6** worden de implicaties van de resultaten uit het hele proefschrift bediscussieerd. Reflectie op de mogelijkheden en onmogelijkheden van homozygotie mapping leidden tot de conclusie dat homozygotie mapping effectief kan zijn in zowel consanguine als niet-consanguine families. Het identificeren van het genetisch defect is van belang om duidelijkheid te krijgen over de overerving, om inzicht te krijgen in de etiologie van de aandoening, voor het ontwikkelen van nieuwe vormen van therapie, en om inzichtelijk te maken welke patiënten in aanmerking kunnen komen voor gentherapie. Een voorspelling van de prognose op basis van het genetisch defect blijft moeilijk, omdat de impact van modificerende allelen op het fenotype nog onduidelijk is. Zoals berekend in de discussie, is waarschijnlijk 1 op de 4 mensen

drager van een mutatie in een autosomaal recessief RP gen, waardoor de kans groot is dat een patiënt een derde mutatie (modifier allel) draagt dat voor een verergering van het fenotype zorgt.

In de nabije toekomst zullen de mogelijkheden voor mutatie analyse uitgebreid worden met zogenaamde 'next generation sequencing' (NGS) technieken, waarbij miljoenen nucleotiden in één experiment gescreend kunnen worden. Wanneer NGS analyses leiden tot de ontdekking van nieuwe genen geassocieerd met retina dystrofie, dan zal homozygotie mapping een rol kunnen spelen in de selectie van patiënten om te screenen voor mutaties in zo'n nieuw gen. Daarnaast zal er een enorme hoeveelheid varianten gevonden worden bij NGS van alle exonen in het genoom (het exoom), en kan homozygotie mapping bij dergelijke analyses bijdragen aan het maken van het onderscheid tussen pathogene en niet-pathogene varianten.

LIST OF PUBLICATIONS

LIST OF PUBLICATIONS

Identification of a 2 Mb human ortholog of *Drosophila eyes shut/spacemaker* that is mutated in patients with retinitis pigmentosa.
Collin RWJ*, Littink KW*, Klevering BJ, van den Born LI, Koenekoop RK, Zonneveld MN, Blokland EA, Strom TM, Hoyng CB, den Hollander AI, Cremers FPM.
Am J Hum Genet. 2008 Nov;83(5):594-603

A novel homozygous nonsense mutation in *CABP4* causes congenital cone-rod synaptic disorder.
Littink KW, van Genderen MM, Collin RWJ, Roosing S, de Brouwer APM, Riemslag FCC, Venselaar H, Thiadens AAHJ, Hoyng CB, Rohrschneider K, den Hollander AI, Cremers FPM, van den Born LI.
Invest Ophthalmol Vis Sci. 2009 May;50(5):2344-50

A novel nonsense mutation in *CEP290* induces exon skipping and leads to a relatively mild retinal phenotype.
Littink KW, Pott JWR, Collin RWJ, Kroes HY, Verheij JBGM, Blokland EAW, de Castro Miró M, Hoyng CB, Klaver CCW, Koenekoop RK, Rohrschneider K, Cremers FPM, van den Born LI, den Hollander AI.
Invest Ophthalmol Vis Sci. 2010 Jul;51(7): 3646-52

Mutations in the *EYS* gene account for approximately 5% of autosomal recessive retinitis pigmentosa and cause a fairly homogeneous phenotype.
Littink KW, van den Born LI, Koenekoop RK, Collin RWJ, Zonneveld MN, Blokland EAW, Khan H, Theelen T, Hoyng CB, Cremers FPM, den Hollander AI, Klevering BJ.
Opthalmology. 2010 May; *Epub ahead of print*

Novel null mutations in the *EYS* gene are a frequent cause of autosomal recessive retinitis pigmentosa in the Israeli population.
Bandah-Rozenfeld D, Littink KW, Ben-Yosef T, Strom TM, Chowers I, Collin RWJ, den Hollander AI, van den Born LI, Zonneveld MN, Merin S, Banin E, Cremers FPM, Sharon D.
Invest Ophthalmol Vis Sci. 2010 Apr; *Epub ahead of print*

Mutations in *C2ORF71* cause autosomal recessive retinitis pigmentosa.
Collin RWJ*, Safieh C*, Littink KW, Shalev SA, Garzozi HJ, Rizel L, Cremers FPM, den Hollander AI, Klevering BJ#, Ben-Yosef T#.
Am J Hum Genet. 2010 May;86(5):783-8.

Homozygosity mapping in patients with cone-rod dystrophy: novel mutations and clinical characterizations.
Littink KW*, Koenekoop RK*, van den Born LI, Collin RWJ, Moruz L, Veltman JA, Roosing S, Zonneveld MN, Omar A, Darvish M, Lopez I, Kroes HY, van Genderen MM, Hoyng CB, Rohrschneider K, van Schooneveld MJ, Cremers FPM, den Hollander AI.
Invest Ophthalmol Vis Sci. 2010 June; *Epub ahead of print*

Mutation spectrum of *EYS* in Spanish patients with autosomal recessive retinitis pigmentosa.
Barragán I, Borrego S, Pieras JI, González-Del Pozo M, Santoyo J, Ayuso C, Baiget M, Millán JM, Mena M, Abd El-Aziz MM, Audo I, Zeitz C, Littink KW, Dopazo J, Bhattacharya SS, Antinolo G
Hum Mut. 2010; in press

* Both first authors contributed equally
# Both last authors contributed equally

CURRICULUM VITAE

CURRICULUM VITAE

Karin Willemijn Littink werd geboren op 25 juni 1981 in Sleeuwijk. Zij volgde haar gymnasium opleiding op het Alexander Hegius Lyceum (tegenwoordig: Etty Hillesum Lyceum) in Deventer, en startte aansluitend in 1999 haar studie Geneeskunde aan de Katholieke Universiteit Nijmegen (tegenwoordig: Radboud Universiteit Nijmegen).
In het studiejaar 2001-2002 onderbrak zij haar studie om een jaar als fulltime commissielid en vicevoorzitter de Batavierenrace ('s werelds grootste estafetteloop) te organiseren.
Van 2002 tot en met 2007 vervolgde zij haar studie Geneeskunde en liep zij stage onder begeleiding van Dr. Robert Koenekoop in het McGill Ocular Genetics Laboratory (Montréal Children's Hospital Research Institute, McGill University Health Centre) in Montréal, Canada. Daar verzamelde ze klinische gegevens van patiënten met autosomaal dominante retinitis pigmentosa uit één grote familie, en deed ze de genetische screening bij andere retina dystrofie patiënten.
Na deze eerste kennismaking met moleculaire genetica begon zij in februari 2007 aan haar promotie-onderzoek, in het blindheid-genetica lab onder begeleiding van Prof. Dr. Frans Cremers, Dr. Ingeborgh van den Born en Dr. Anneke den Hollander, in een samenwerkingsverband tussen Het Oogziekenhuis Rotterdam en de sectie Moleculaire genetica van de afdeling Antropogenetica in het UMC St Radboud.
De resultaten daarvan zijn in dit proefschrift beschreven.
In 2010 ontving zij een Young Investigators Travel Award voor de 'XIVth International Symposium on Retinal Degeneration' in Mont-Tremblant, Canada. Van juni tot november 2010 was zij werkzaam als project manager voor een TOP-subsidie project in blindheid- en doofheidgenetica, onder supervisie van Prof. Dr. Frans Cremers, Dr. Hannie Kremer en Dr. Anneke den Hollander.
Na een korte kennismaking met oogheelkunde in Indonesië, zal zij per 1 februari 2011 starten met de opleiding tot oogarts in Het Oogziekenhuis Rotterdam.

CURRICULUM VITAE

Karin Willemijn Littink was born on June 25th 1981 in Sleeuwijk, the Netherlands. She attended secondary school at Alexander Hegius Lyceum (currently: Etty Hillesum Lyceum) in Deventer, and thereafter started her medical studies in 1999 at the Catholic University Nijmegen (currently: Radboud University Nijmegen).
In the college year 2001-2002 she temporarily delayed her studies to participate as fulltime organizer and vice-president of the Batavierenrace, the world largest running relay.
From 2002 to 2007 she continued her medical studies and did her scientific internship under the supervision of Dr. Robert Koenekoop in the McGill Ocular Genetics Laboratory (Montréal Children's Hospital Research Institute, McGill University Health Centre) in Montréal, Canada. She collected DNA and clinical data from a large family with autosomal dominant retinitis pigmentosa, and screened several other retinal dystrophy patients in order to identify the genetic defect.
After this introduction into molecular genetics, she started her PhD research in February 2007 in the blindness-genetics lab supervised by Prof. Dr. Frans Cremers, Dr. Ingeborgh van den Born and Dr. Anneke den Hollander. The project was a collaboration between The Rotterdam Eye Hospital and the division of Molecular Genetics in the Department of Human Genetics at Radboud University Nijmegen Medical Centre. The results of this study are presented in this thesis.
In 2010 she was awarded a Young Investigators Travel Grant to attend the 'XIVth International Symposium on Retinal Degeneration' in Mont-Tremblant, Canada.
From June to November 2010 she worked as a project manager to start up a TOP subsidy project in the genetics of blindness and of non-syndromic hearing loss, under supervision of Prof. Dr. Frans Cremers, Dr. Hannie Kremer, and Dr. Anneke den Hollander.
After a short introduction to ophthalmology in Indonesia, she will start her formal training as an ophthalmologist in February 2011 at The Rotterdam Eye Hospital.

DANKWOORD

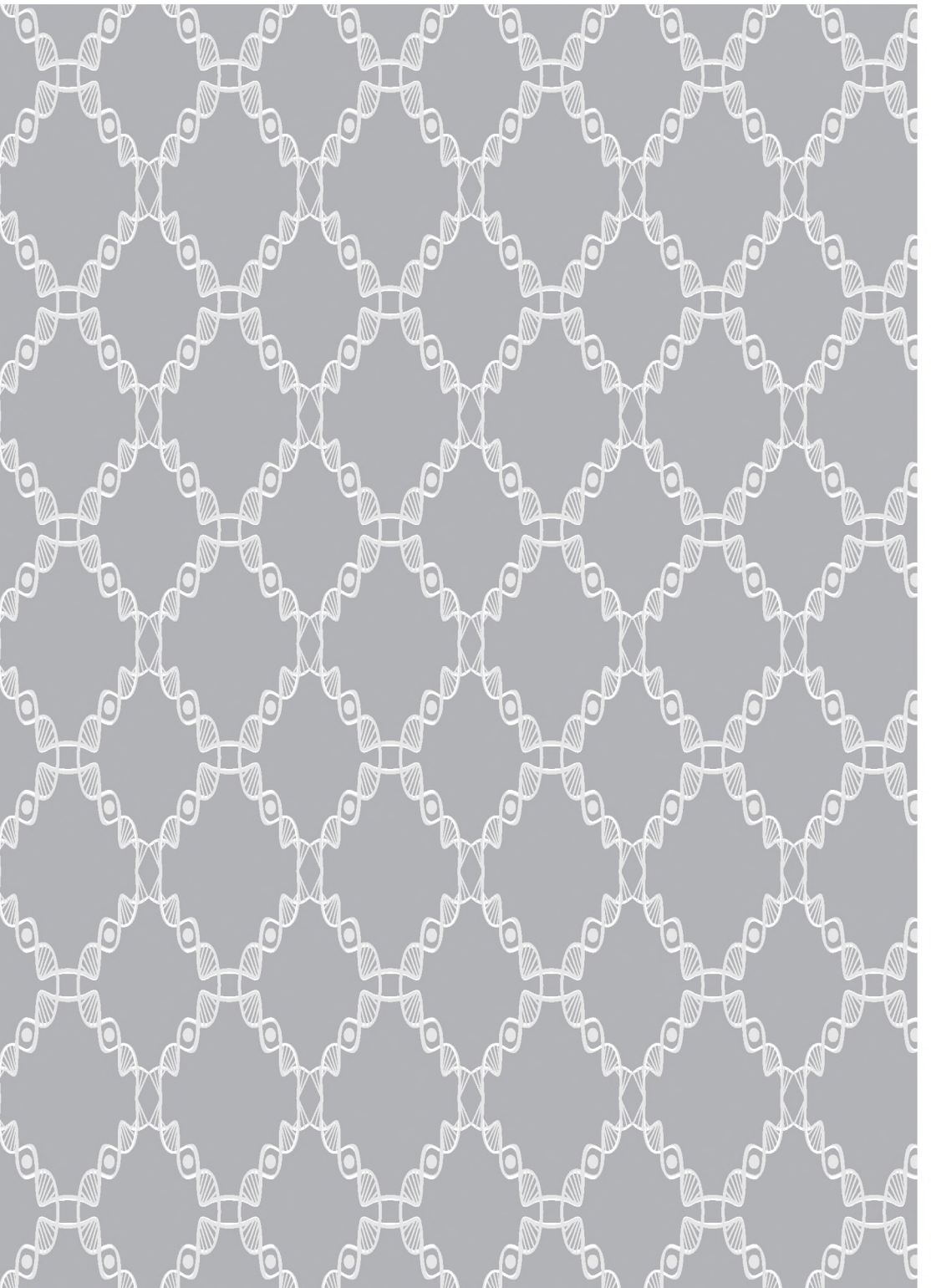

DANKWOORD

Sommige promovendi zijn opgelucht als het boekje dan eindelijk af is, anderen willen er eigenlijk niet meer mee ophouden. Misschien verwachtte ik de eerste maanden tot de eerste groep te behoren; nu weet ik dat ik duidelijk tot de laatste groep behoor. Onderzoek doen is leuk! Zeker ook door alle mensen die aan dit onderzoek hebben bijgedragen, en die mijn tijd als promovenda zo leuk hebben gemaakt.

Allereerst heel veel dank aan mijn promotor Frans Cremers en co-promotores Ingeborgh van den Born en Anneke den Hollander.

Beste Frans, ik ben blij dat jij mijn promotor bent. Ik heb erg veel van je geleerd door jouw oog voor detail en je kritische blik. In het begin ging jouw kennis vaak iets te snel voor mij - terwijl jij dacht dat ik mijn 7-jaar oude minimale genetica-kennis nog wel paraat zou hebben. Maar jouw manier van begeleiden, waarin je mij ook de kans gaf om mijn kennis van buiten het lab in te zetten, gaven mij steeds meer vertrouwen in mezelf binnen dit onderzoek. Niet alleen je begeleiding op onderzoeksterrein, maar ook jouw aandacht voor factoren rondom onderzoek, zoals persoonlijke ontwikkeling, 'verplichte' koffie-pauzes en het stimuleren van alle initiatieven op het gebied van uitjes en gezelligheid, maken jou een superleuke 'baas', ook al mogen we dat woord niet gebruiken...!

Beste Ingeborgh, je hebt mij vanaf het begin altijd weten te motiveren. Zeker toen ik het allemaal nog wat moeilijk vond in het lab, zorgden de telefoongesprekken met jou weer voor positievere gedachten. Maar eigenlijk zijn die telefoongesprekken alle drie de jaren belangrijk gebleven. Jij luisterde naar alles wat ik maar kwijt wilde, en dat heeft me veel geholpen. Daarnaast was jij voor mij de belangrijke link naar de klinische wereld, en heeft jouw kennis en kritische blik op de klinische en genetische data veel toegevoegd aan alle artikelen in dit proefschrift. Jij bent als 'physician-researcher' echt een voorbeeld voor me en ik hoop dat we samen nog veel artikelen kunnen schrijven.

Beste Anneke, jouw begeleiding begon al toen ik nog in Montréal mijn wetenschappelijke stage deed en ik je nog maar een paar keer had gezien. Jouw prettige manier van begeleiden - toen al - is altijd zo gebleven. Ondanks jouw volle agenda kon ik altijd op je rekenen, je reageerde altijd hartstikke snel op al mijn vragen en e-mails, en je wist de tijdsdruk die ik soms voelde fijn te relativeren. Ook bedankt voor jouw talent om een kromme zin helemaal mooi te maken door een paar woorden aan te passen. Een manuscript dat door jou gezien was kwam per definitie mooier terug!

Beste Rob, jij bent co-auteur van alle artikelen in dit boekje en dat laat duidelijk zien wat jouw aandeel aan dit proefschrift is. Het begon met *EYS*, en hopelijk is het nog lang niet voorbij. Jij nam me mee in de wereld van RACE, minipreppen, kloneren (klonen :-)), en dat RNA niet eng is, en daarmee raakte ik pas echt verzeild in de labwereld. En ARVO's en RD2010 samen, supergezellig. Ik heb heel erg veel van je geleerd! Superbedankt voor alles: it was bery bery nEYS, HOEIII!

Heel erg veel dank ook aan Marijke en Ellen; zonder jullie (en de honderden of door *EYS* waarschijnlijk wel duizenden PCRs die jullie gedaan hebben) was dit proefschrift er niet geweest. PCR-en ging nog nooit zo efficiënt als toen we met z'n drieën *EYS* onder handen namen! Marijke, niet alleen jouw inzicht en bijdrage in het project, maar ook het feit dat je een geweldige 'lab-coach' voor me was (Het kleine boek van Knorretje ligt nog steeds binnen handbereik) hebben veel bijgedragen aan dit boekje en aan mijn plezier op het lab. Ellen, ook jij hebt superveel werk verzet voor de artikelen in dit boek. Hartstikke bedankt daarvoor en voor de gezellige lab-buurvrouw die je was! Irma, I also want to thank you here, because you were my first lab mentor, who guided me through my first steps into the lab world. And beside that you made me a big sushi-fan as well! Muchas gracias por todo!

Lieve Suus en Syl, jullie staan naast me de grote dag en daar ben ik erg trots op! Ook ben ik superblij met de tijd die ik met jullie in het lab én buiten het lab heb doorgebracht; jullie zijn echte vriendinnen voor me geworden. Suus, jouw creativiteit in mailtjes, epjes-post en nooit-grappigs als het werk (of de vierdaagse!) wel een beetje afleiding kon gebruiken maakten me altijd aan het lachen. Syl, alles wat jij zegt lijkt gewoon altijd te kloppen, met jouw goede adviezen bent jij echt mijn orakel. Jullie zijn allebei geweldig!! Bedankt dat jullie mijn paranimfen willen zijn.

Bjorn, 'mijn' student; ik vond het heel erg leuk om je te begeleiden en om te zien hoe jij het naar je zin had in onze groep. Ik zal mijn best doen om alle door jou vergaarde RLBP1/RDH5/LRAT data snel te kunnen submitten, beloofd.

Ook veel dank aan Saskia, Christel en Tesy voor het zo nauwkeurig bijhouden van alle DNA's en bijbehorende gegevens. Zolang jullie in de buurt zijn is altijd alles terug te vinden.

Many many thanks to all the lab colleagues. Especially the blindness genetics colleagues, and all foreign guests who stayed with us for a while: Susanne, Marijke, Alejo, Kostas, Rob, Ellen, Frederieke, Alberta, Anneke, Frans, Maleeha, Kentar,

Almudena, Marta, Imran, Ajmal, Simone, Krysta, Anna; I had so much fun with you! Inside the lab, with our stupid language jokes ("How goes it? It goes"), the running through the lab after discovering a mutation, champagne after the first EYS publication, home-made bami and pisang goreng from Kentar, sneaking through the lab to decorate for Frans' anniversary, etc etc. But also outside the lab, with the 'moleculinary dinners', the PROM1-dinner, the afternoons out, SinterKostas and his black Petes, goodbye-dinners and -lunches for our guests (who became more like close colleagues to us...). Special thanks also to Arijit and Arjan; those first months, they seem so far away. But in those months that I spent in the postdoc room with you, you established a really nice scientific basis for me and helped me to understand what science is about.

Ook alle andere Antropogenetica collega's (en niet-collega's) bedankt! Met name Peer, Christian, Eugene, Gleb, Andrew, Jamie, Heleen, Sonja, alias "het vrijdagavond onderzoeksteam", Konny (next year we will do the vierdaagse together! uhm...?), Ramprasath (was also great to meet your parents, cousin!), Alejandro and Sandra (for the nice picnics/dinners the Latin American way), Alfi (hope to see you soon in Indonesia), Erwin, Ferry, Erik, Alex, Marloes, Eveline, Martijn (met jullie erbij is het altijd een leuk feestje; bij de 4Daagse Woensdagavond op het Koningsplein, Vastelaovend, na het Dagje Uit, enz), de Dagje-Uit Commissie 2009 (was eigenlijk wel erg gezellig om te organiseren!). Alle "The Fast and the Curious" en "2 Fast, 2 Curious"-hardlopers bij de Zevenheuvelenloop en de Bruggenloop (ik train wel weer mee dit jaar!), en natuurlijk het 4daagse-team en alle supporters bedankt. Het was echt geweldig om op zo'n gezellige en talentvolle afdeling te werken!

Veel dank ook aan alle oogartsen, klinisch genetici en alle andere co-auteurs die een bijdrage hebben geleverd aan dit onderzoek / Many thanks to all the ophthalmologists, clinical geneticists and other collaborators who contributed generously to this research; especially Jeroen Klevering, Mies van Genderen, Frans Riemslag, Jan Willem Pott, Carel Hoyng, Caroline Klaver, Mary van Schooneveld, Klaus Rohrschneider, Dror Sharon, Dikla Bandah-Rozenfeld, Eric Pierce, Hester Kroes, Joke Verheij, and Robert Koenekoop. Robert, jij ook extra bedankt voor de geweldige tijd die ik in jouw lab had in Montréal, jouw vermogen mij zo te motiveren voor de genetische onderzoeks-wereld en alles wat ik toen en daarna van je geleerd heb. Ook wil ik graag alle patiënten bedanken die – vaak zonder enig eigenbelang en soms van heel ver – een keer naar het ziekenhuis kwamen om nog een extra onderzoek te ondergaan.
Ook alle collega arts-onderzoekers in het ROI bedankt. Ook al werkte ik nogal op grote afstand van het ROI, bij de gelegenheden waarin ik jullie tegenkwam (NOG, ARVO) voelde ik me toch een beetje collega. Suzanne, bedankt voor alle interessante data

waar ik mee verder kon werken, en voor het delen van jouw ervaringen. En Linda, via deze weg nog eens veel succes gewenst met jouw RP onderzoeksproject!

Nicole van de Kar en Lucy Platvoet; jullie beiden zijn voor mij een soort mentor. Misschien wisten jullie het niet eens, maar jullie hebben een groot aandeel gehad in mijn motivatie om me in de onderzoekswereld te (blijven) storten. Bedankt voor alle inspirerende en motiverende woorden.

Het eind van dit onderzoek betekent ook een eind aan een lange tijd in Nijmegen. Daarom wil ik dit dankwoord ook gebruiken om mijn vrienden te bedanken voor de geweldige tijd die ik dankzij jullie en met jullie in Nijmegen en buiten Nijmegen heb gehad. Studievrienden, WW41-ers, bunnies, huisgenoten, Bata-vrienden; hopelijk volgen er nog veel meer biertjes bij de Kluizenaar, bij de Foyer (oh nee, die is gesloten; nieuwe leuke kroeg vinden...), films bij Lux, vakanties, East of Easterns, dagen van het Levenslied, Batavierenraces, Hart-van-Brabantlopen, zomerfeesten, enz. Hopelijk komen er leuke nieuwe Rotterdamse tradities bij zoals De Parade of het zomercarnaval in Rotterdam; mijn deur zal wagenwijd open staan! Met name Heleen en Gabie, al vanaf het allereerste Nijmeegse begin in 1999 zijn jullie in het dagelijks leven mijn 'paranimfen' geweest; superbedankt daarvoor!

Als laatsten, de allerbelangrijksten:
Pap, mam, Sas, Rob en oma; 'gewoon' bedankt, omdat jullie er altijd zijn!
(Mooi verhaal, lekker kort!)

Dear Alejo, being together with you is the best result of this research! :-) Thank you for our wonderful time together!

COLOR FIGURES

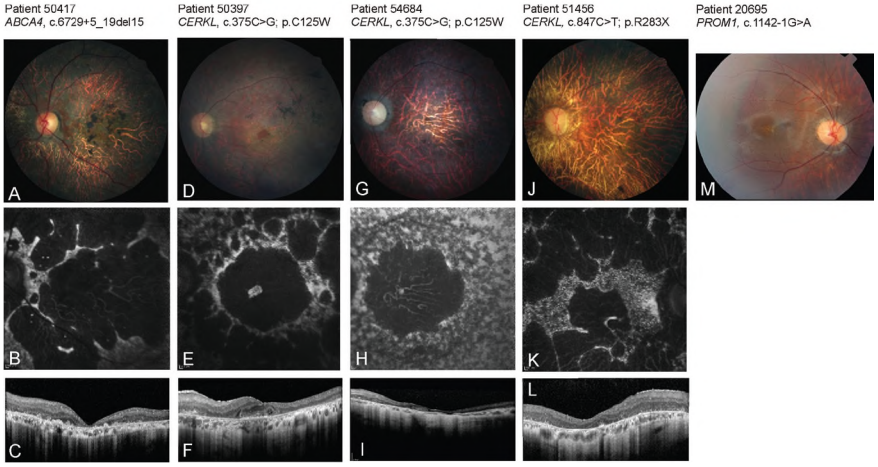

FIGURE 3. Fundus photographs, autofluorescence and spectral domain (Spectralis) OCT images of CRD patients with conclusive genetic defects.

The retina of patient 50417 (*ABCA4*, c.6729+5_19del15; age 44) shows (**A**) extensive retinal pigment epithelium (RPE) cell loss, choroidal sclerosis and pigmentary macular changes on fundoscopy, (**B**) marked loss of central lipofuscin accumulation on fundus autofluoresence (FAF), and (**C**) a disorganized retina in which the six layers are not detectable, the fovea is extremely thin, with loss of the inner/outer segment junction. Extensive debris accumulation is noted. Patient 50397 (*CERKL*, p.C125W; age 48) has (**D**) a pigmentary maculopathy with choroidal sclerosis, (**E**) absence of central FAF, except in a tiny island, indicating nearly complete loss of lipofuscin deposition, and (**F**) very extensive retinal remodeling and an unusual subretinal cystic structure in the fovea. His older brother (54684, age 51), although carrying the same mutation in *CERKL*, has (**G**) extensive retinal, RPE and optic disc atrophy and sclerosis, (**H**) loss of central FAF, with a peculiar salt and pepper pattern of FAF outside the central retina, and (**I**) thinning and disorganization of the retina. A *CERKL* nonsense mutation (p.R238X) in patient 51456 (age 53) resulted in (**J**) extensive choroidal sclerosis, (**K**) loss of FAF, and (**L**) retinal remodeling with loss of inner/outer segment junction. The retina of patient 20695 (*PROM1*, c.1142-1G>A; age 18) showed (**M**) central atrophic lesions in the fovea and severely attenuated retinal vessels. No autofluorescence and spectral domain OCT images were available for this patient.

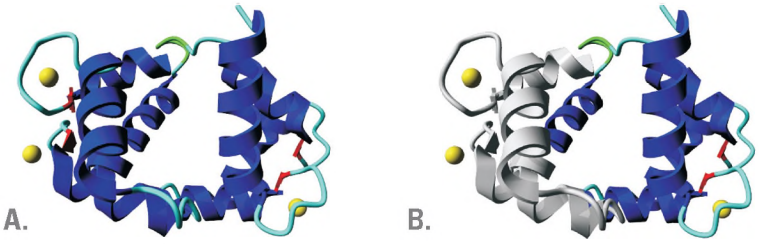

FIGURE 5. **CaBP4 protein model.**

A. Ribbon model of the calcium binding domains in normal CaBP4.
B. Model showing the deleted calcium binding domains (gray). Yellow balls: calcium atoms.

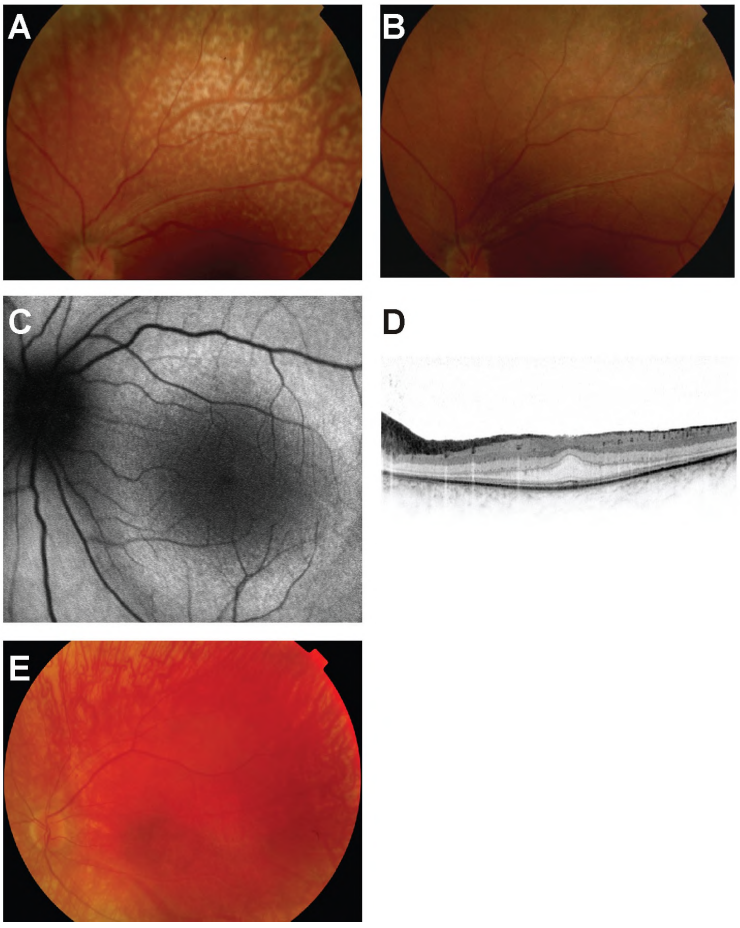

FIGURE 3. **Retinal imaging of patients VI-3 and VI-6.**

A. Photograph of the midperipheral fundus of patient VI-3 at the age of 5, showing a marbled appearance. **B.** Fundus photograph of the same patient VI-3 at the age of 11, which shows that the marbled appearance had disappeared, and mild atrophy of the RPE was noted. **C.** Mean autofluorescence image (30°) of the left eye of patient VI-3, calculated from 12 single images (488 nm), showing a well preserved signal in the posterior pole with decreased intensity in the macular region. **D.** Spectral domain OCT of the left eye of patient VI-3 at the age of 11 shows a recognizable photoreceptor layer, intact retinal layers, and disappearance of the foveal dimple. **E.** Fundus photograph of left eye of patient VI-6, showing preserved RPE in the macular region with an extremely hypopigmented area along the vascular arcade, which extends to the periphery.

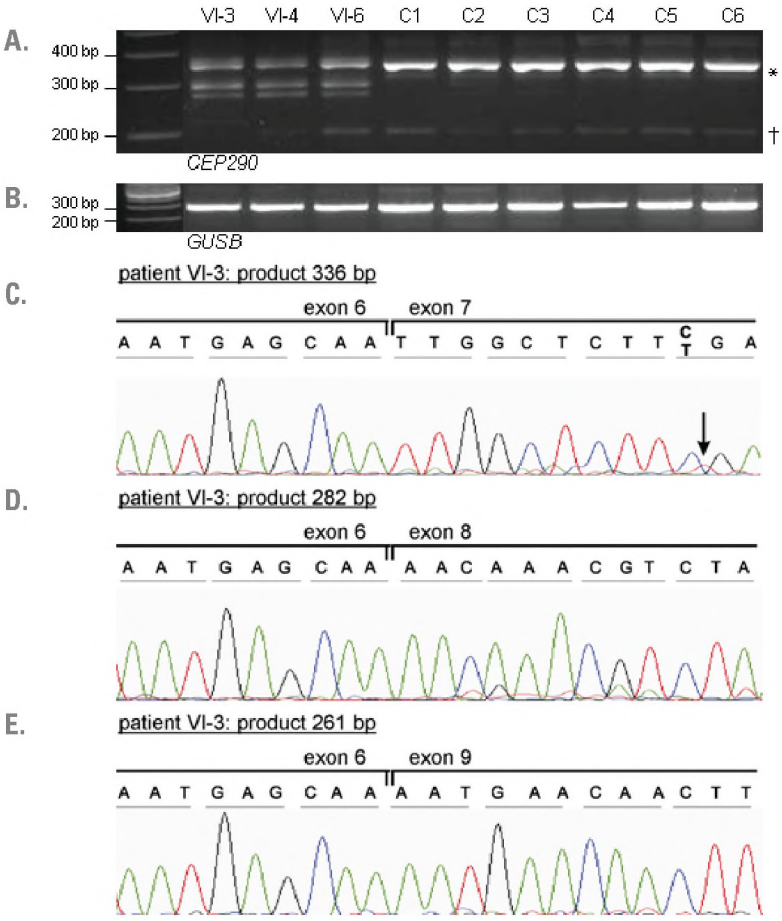

FIGURE 4. ***CEP290*** **cDNA analysis of the effect of the c.451C>T variant on splicing.**

A. Agarose (3%) gel electrophoresis showing three major PCR products in carriers of p.Arg151X and one major product in the six control individuals. **B.** Agarose gel electrophoresis showing GUSB as the reference gene product. C–E. PCR sequences of cDNA of patient VI-3 (CEP290 c.451C>T/c.2991+1655A>G), showing **(C)** mRNA containing all exons, but showing a low peak for the mutant heterozygous T at position 451 (arrow). **(D)** mRNA missing exon 7, and **(E)** mRNA missing exons 7 and 8. *Low-intensity product could not be amplified for sequence analysis. Based on the size, it could contain the CEP290 mRNA lacking exon 8 only, which should be 315 bp; †low-intensity product ~200 bp was analyzed by sequence analysis and appeared to be the CEP290 mRNA lacking exon 6 only (192 bp). Since CEP290 lacking exon 6 is present in patients as well as control individuals, it appears to be a normal splice variant

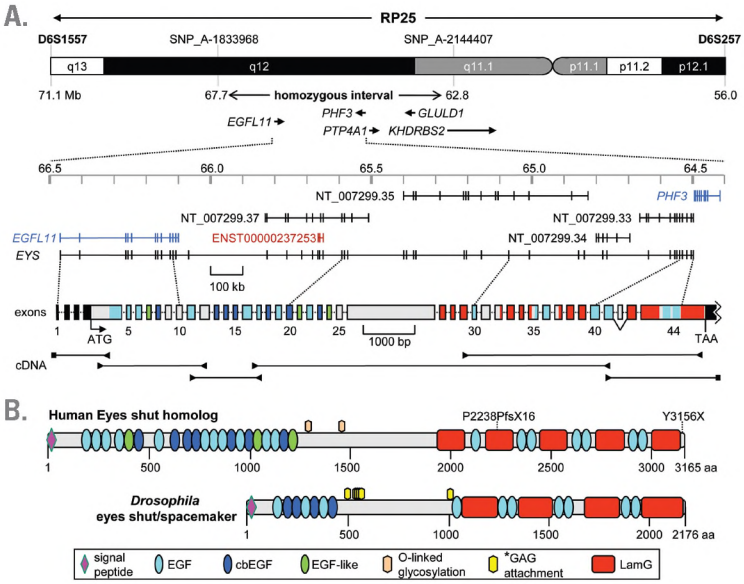

FIGURE 1. Genomic structure, cDNA fragments, and protein domains of *EYS*.

A. Upper panel: the RP25 chromosomal region at 6p12.1-q133, the 5.0 Mb homozygous region identified in family A, and the five known genes within the homozygous region. Exons 1 and 2 of *KHDRBS2* reside in the critical region. In the middle, the exon predictions are depicted on the basis of RefSeq (in blue), Genescan (in black), and Ensembl (in red), with the use of the March 2006 UCSC genome build (hg18). Below the genomic-exon annotation is the exon structure of human *EYS* (exons drawn to scale; intron sizes can be found in the top panel). The complete nucleotide sequence of human *EYS* cDNA is presented in Figure S2. For details of the exon-intron structure, see Table S5. The 5'- and 3'- UTRs are indicated in black boxes; the colors of the protein-coding exons correspond with those of the protein domains in **(B)**. Lower panel: reverse-transcription PCR fragments of human *EYS* with retina RNA and *EYS*-specific primers (arrowheads) or 5'- and 3'- RACE adaptor primers (squares). The 5'-UTR, the open reading frame, and the 3'-UTR altogether measure 10,475 nucleotides (see Table S5). Exon 42 (63 bp) is alternatively spliced in retina RNA (see Figure 2). For details of RT-PCR studies, see Figure S1. **B.** Protein-domain structure of *EYS* and its *Drosophila* ortholog (GenBank ID ABH07112.1). Note the conspicuous conservation of the order of EGF-like and Laminin A G-like domains between human and *Drosophila*. The p.Pro2238ProfsX16 frameshift mutation truncates several EGF-like and Laminin A G-like domains, whereas the carboxy-terminal p.Tyr3156X mutation truncates the last ten amino acids of human *EYS*. Abbreviations are as follows: EGF, epidermal growth factor domain; cbEGF, calcium-binding EGF-like domain; EGF-like, EGF-like domain; LamG, Laminin A G-like domain. The asterisk denotes glycosaminoglycan (GAG) attachment sites predicted by Husain and coworkers.[26] Two putative O-glycosylation sites are predicted in the human protein (Thr1268 and Thr1424). Detailed characteristics of the human EYS protein domains are presented in Figure S2

FIGURE 3. Mutation analysis of *EYS* in RP patients.

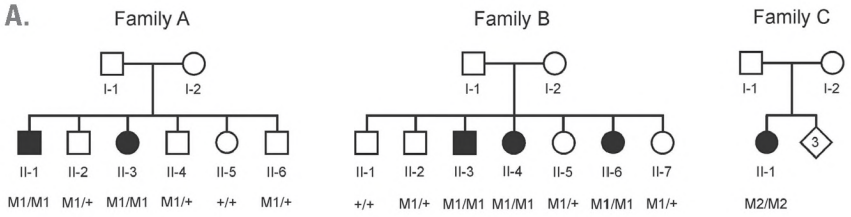

A. Pedigrees of three families with individuals affected with RP. Below the individuals, genotypes are presented for either the p.Tyr3156X change (M1, families A and B) or the p.Pro2238ProfsX16 change (M2, family C) detected to segregate with the disease. M1/M1 and M2/M2 represent homozygous mutants; M1/+ indicates heterozygous carriers, whereas +/+ indicates individuals carrying two wild-type alleles.

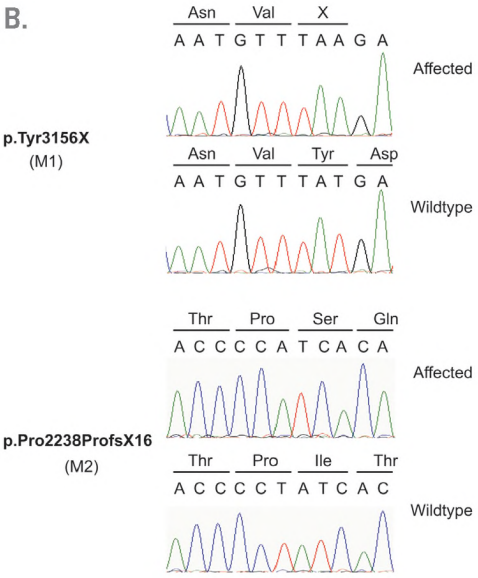

B. Upper panel: partial sequence of the *EYS* gene showing the nonsense c.9486T>A change, in an affected individual (family A, II-1) and an unaffected sibling (family A, II-5). The mutation replaces a tyrosine residue by a termination codon (p.Tyr3156X). Preceding amino acids are indicated above the sequence trace. Lower panel: partial sequence of the *EYS* gene showing the c.6714delT change, in an affected individual (family C, II-1) and a control individual. The mutation results in a frame shift and, eventually, in premature termination of the protein (p.Pro2238ProfsX16). Amino acids are indicated above the sequence trace.

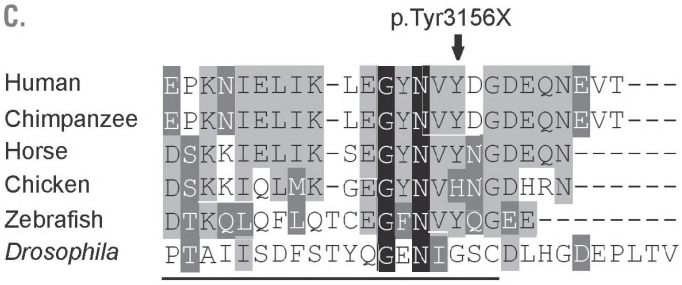

C. Sequence comparison of the 25 most C-terminal amino acids of the human EYS protein and several vertebrate and invertebrate orthologs. Residues identical in all sequences are white on a black background, whereas similar amino acids are white on a gray background. Residues that are present in at least three of the six proteins are indicated in black on a light gray background. Residues constituting the most C-terminal Laminin A G-like domain in the *Drosophila* protein are underlined. Accession numbers of the protein sequences used for sequence comparison are as follows: chimpanzee, XM_527426.2 (RefSeq); horse, XM_001918159.1 (RefSeq); chicken, XM_426198.2 (RefSeq); zebrafish, BX005106.5 (EMBL); *Drosophila*, ABH07112.1 (GenBank).

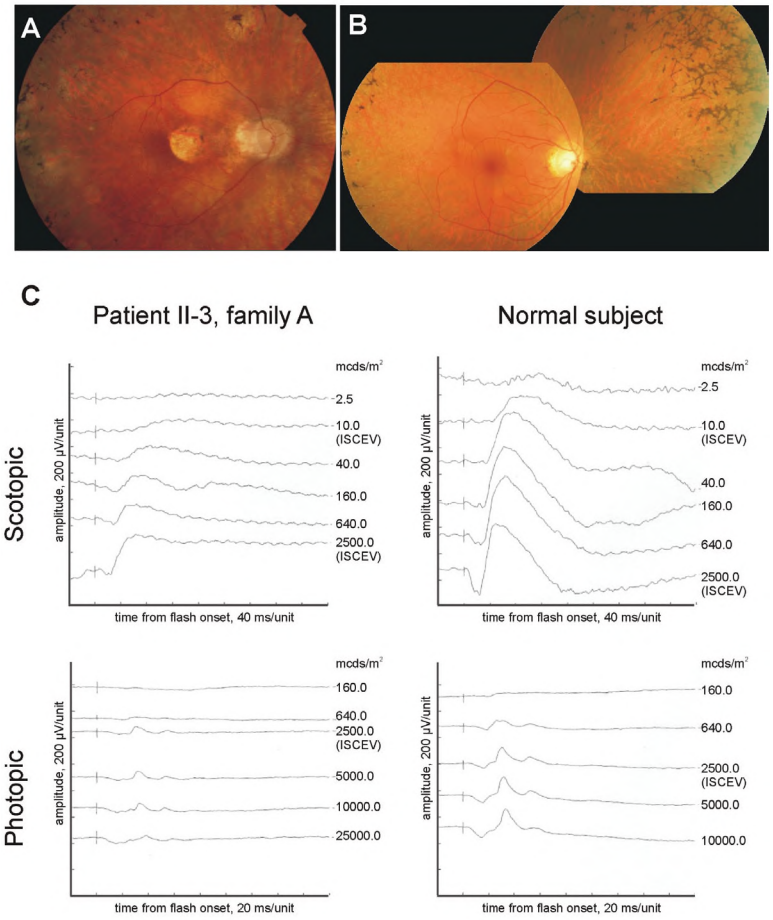

FIGURE 4. **Clinical characteristics of RP patients with a homozygous p.Tyr3156X mutation in *EYS*.**

A. Fundus photograph of the right eye of patient II-1 of family A, showing mild pallor of the optic disc, a peripapillary crescent, attenuated retinal vessels, and bone-spicule pigmentations. An area of sharply demarcated chorioretinal atrophy is located nasal to the fovea, with similar atrophic lesions along the vascular arcades, conflating to diffuse atrophy in the midperiphery.
B. Fundus photograph of the posterior pole and nasal peripheral retina of the right eye of patient II-6 of family B, showing mild pallor of the optic disc, severely attenuated vessels, pronounced atrophic changes in the (mid) periphery that spare the posterior pole, and extensive bone spicules in the peripheral retina.
C. Scotopic and photopic ERG of the right eye of patient II-3 of family A and a normal subject. Scotopic mixed response (ISCEV measurement; 2500 mcds/m2) had a b-wave amplitude of 274 µV (normal > 195 µV, mean 424 µV). The b-wave amplitude of the photopic response (ISCEV measurement; 2500 mcds/m2) was 58.8 µV (normal > 69 µV, mean 79 µV).

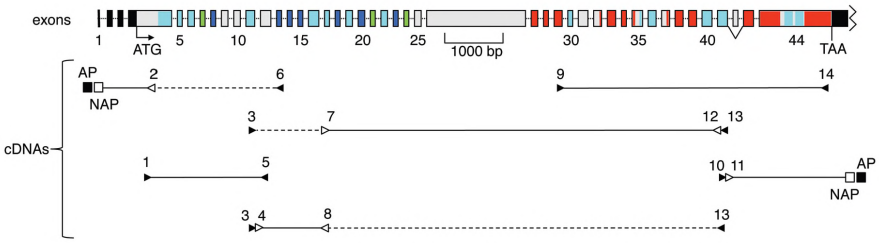

SUPPLEMENTAL FIGURE S1. Details of RT-PCR study of *EYS*.

Primer sequences are listed in Supplemental Table S1. AP (filled square) and NAP (open square) denote RACE adaptor and nested adaptor primers, respectively. Filled and open arrowheads represent regular and nested RT-PCR primers. Dashed line denote primary RT-PCR products.

SUPPLEMENTAL FIGURE S2. Detailed characteristics of the human EYS protein domains.

Protein motifs:

Signal peptide; EGF-domains; Calcium-binding EGF-domains; EGF-like domains; O-linked glycosylation; Laminin A G-like domains

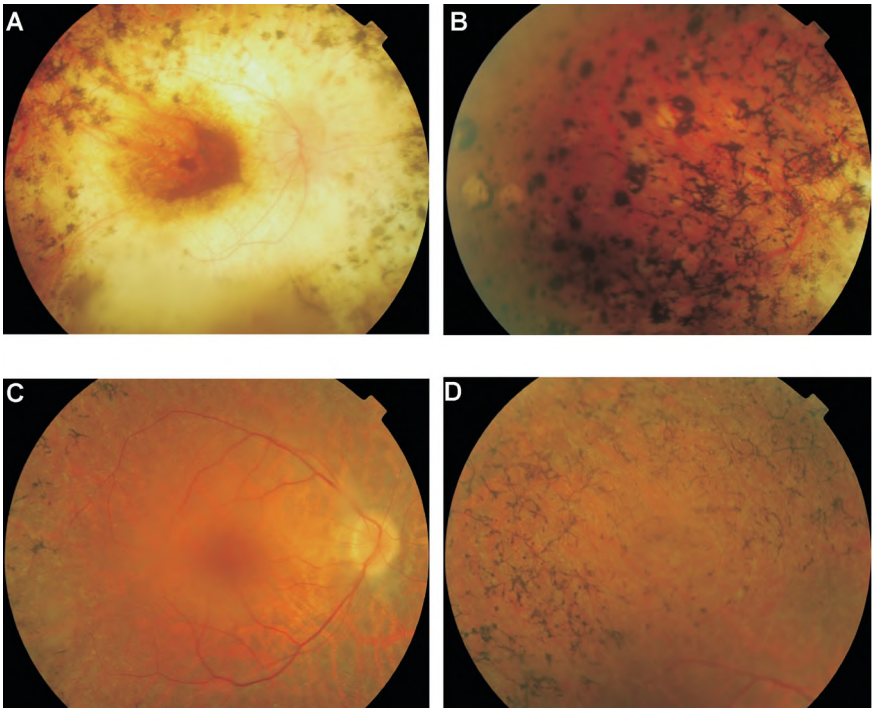

FIGURE 4. **Fundus photographs of patients carrying mutations in *EYS*.**

A. Fundus photograph of the central retina of the right eye of patient CII-6 showing the fundus in an end-stage of the disease. The fundus is characterized by a very pale, waxy optic disc, severely attenuated retinal vasculature, and extensive chorioretinal atrophy with minimal residual retinal pigment epithelium at the macular region.
B. Fundus photograph of the temporal peripheral retina of patient C II-6 showing heavy irregular pigmentations in the (mid)peripheral retina.
C. Fundus photograph of the central retina of the right eye of patient KII-2 showing a pink, waxy optic disc, moderately attenuated retinal vessels, and generalized chorioretinal atrophy with macular sparing.
D. Fundus photograph of the upper temporal peripheral retina of patient KII-2 showing classic bone spicules in periphery. The red telangiectatic-like vessels at the temporal retina (Figure 4C, 4D) are not visible with higher resolution and on fluorescein angiography, and therefore seem to be artifacts.

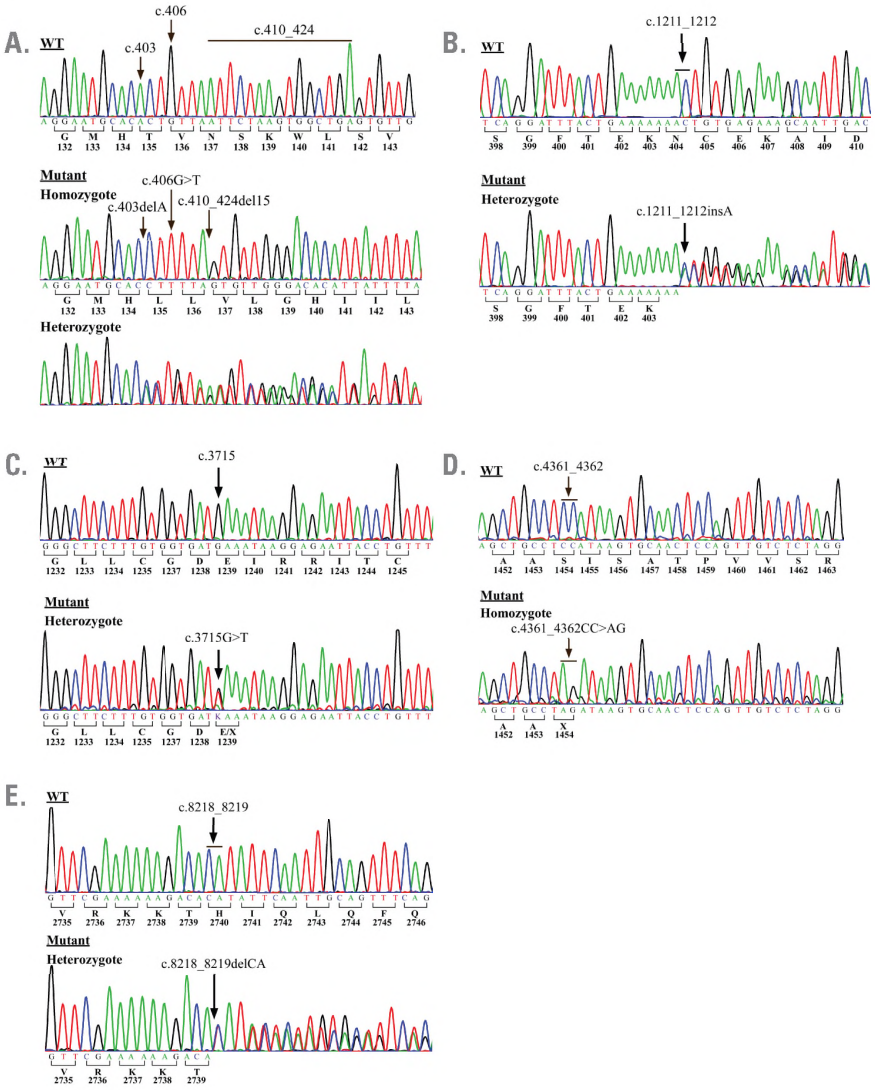

FIGURE 2. **The chromatograms of the five novel *EYS* mutations.**

For each mutation, the wild-type (wt) sequence is depicted with the homozygous or heterozygous sequences when available. The mutation location is indicated by either an arrow (for a nucleotide change) or a horizontal line (for a sequence change affecting more than a single nucleotide).
A. c. 403delA,406G>T,410_424del15; p.Thr135LeufsX25 (exon 4).
B. c.1211_1212insA; p.Asn404LysfsX2 (exon 8). **C.** c.3715G>T; p.Glu1239X (exon 25).
D. c.4361_4362CC>AG; p.Ser1454X (exon 26). **E.** c.8218_8219delCA; p.His2740TyrfsX27 (exon 43).

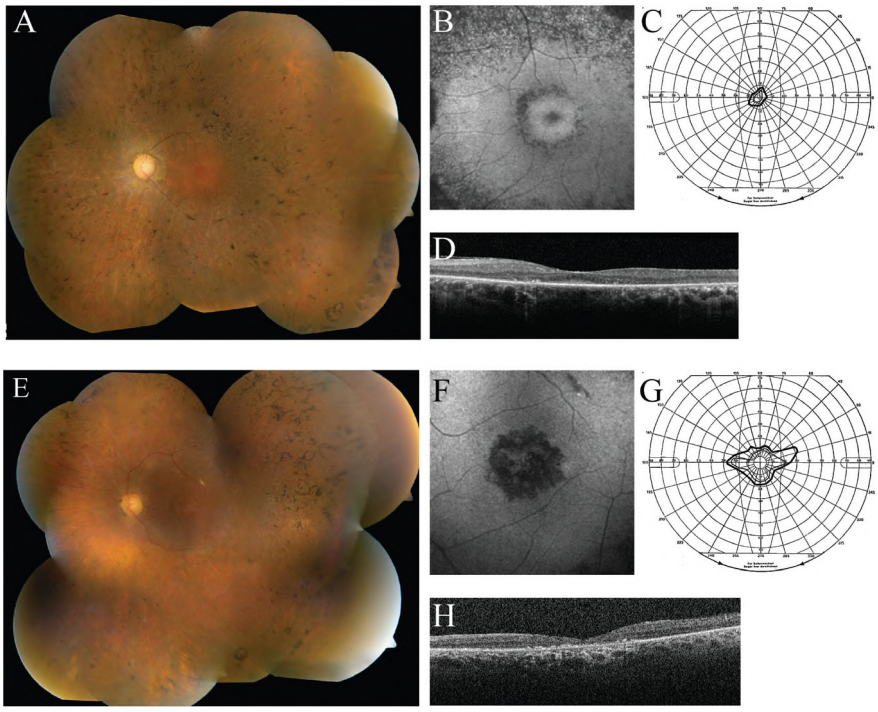

FIGURE 3. **Fundus imaging and visual fields.**

Representative fundus images and Goldman visual fields of the left eyes of patient TB24 III:2 (panels A-D) at age 63 and patient MOL0501 II:3 (panels E-H) at age 52 are shown. The typical funduscopic findings of RP are present, including bone spicule-like pigmentation, pallor of the optic discs, and narrowing of blood vessels (A,E). Macular involvement is evident also on autofluorescence imaging (B,F) and OCT, with retinal thinning and atrophy (D,H). Note more severe foveal atrophy in patient MOL0501 II:3 which correlates with the lower visual acuity of this patient (Table 2). Visual fields are markedly constricted in both patients (C,G).

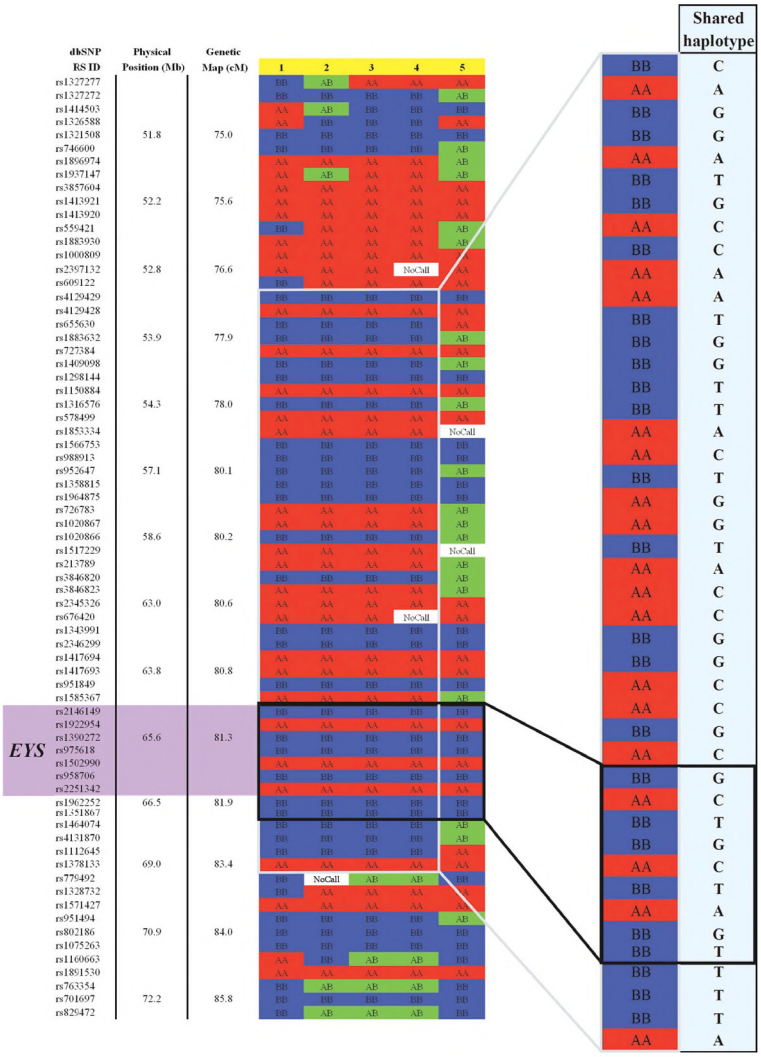

SUPPLEMENTARY FIGURE 1.

The autozygous region identified in Moroccan Jewish patients who are homozygous for the c.403delA,406G>T,410_424del15 mutation. The appropriate region of the Affymetrix 10K microarray analysis is depicted, covering the *EYS* gene and flanking markers on chromosome 6. The genotype data of the following patients are presented: 1, MOL0501 II:1; 2, MOL0662 IV:3; 3, MOL0318 II:13; 4, MOL0318 II-9; 5, MOL0318 III:5. For each marker, the genotype is presented as homozygous (AA or BB), heterozygous (AB) or unknown (NoCall). The A and B alleles were arbitrarily determined for each allele by Affymetrix and the corresponding nucleotide is presented on the right along the shared homozygous region. Red indicates 'AA' genotype; blue indicaties 'BB' genotype, and green indicates 'AB' genotype.

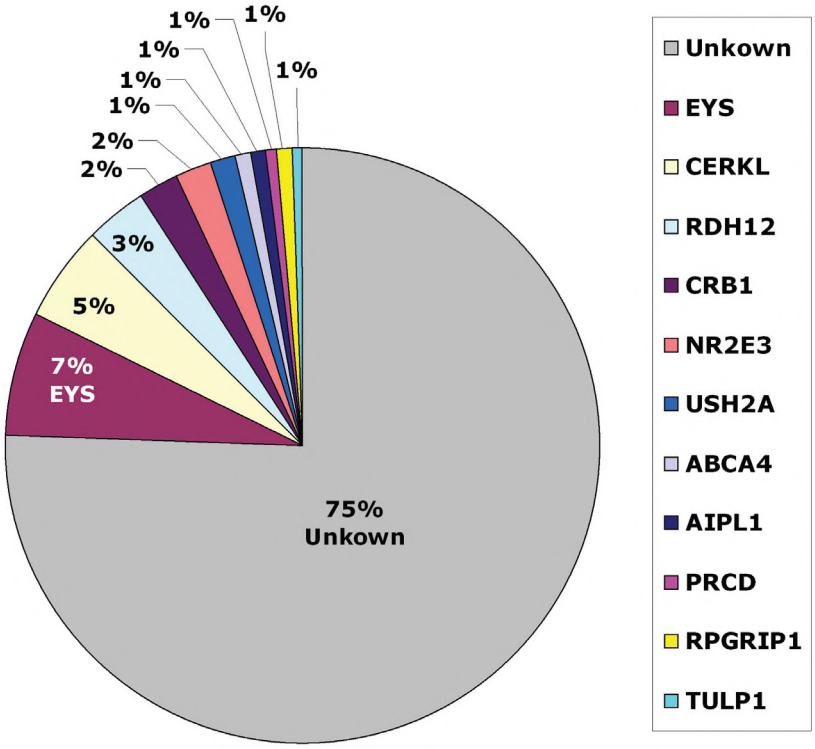

SUPPLEMENTARY FIGURE 2. A pie chart showing the contribution of arRP genes in the Israeli and Palestinian populations.

ABBREVIATIONS

aa	amino acid
AAV	adeno-associated virus
ad	autosomal dominant
APEX	allele-specific primer extension
ar	autosomal recessive
ARMS	amplification-refractory mutation system
BBS	Bardet-Biedl syndrome
bp	base pair
cDNA	complementary deoxyribonucleic acid
CF	counting fingers
CRD	cone-rod dystrophy
CSNB	congenital stationary night blindness
DNA	deoxyribonucleic acid
EBV-LCL	Epstein-Barr virus transformed lymphoblastoid cell lines
EGF	epidermal growth factor
EOSRD	early-onset severe retinal dystrophy
ERG	electroretinogram
ESE	exonic splice enhancer
FAF	fundus autofluorescence
HM	hand movements
ISCEV	international society for clinical electrophysiology of vision
JBTS	Joubert syndrome
LCA	Leber congenital amaurosis
LP	light perception
Mb	megabases
MIM	Mendelian inheritance in man
MKS	Meckel-Gruber syndrome
mM	millimolar
mRNA	messenger ribonucleic acid
µV	microvolt
NAS	nonsense-associated altered splicing
NGS	next generation sequencing
NMD	nonsense-mediated decay
NP	not performed
NR	non recordable
nt	nucleotide
OCT	optical coherence tomography
OD	right eye (oculo dextro)
OMIM	online Mendelian inheritance in man
OS	left eye (oculo sinistro)
PCR	polymerase chain reaction
PTC	premature termination codon
RACE	rapid amplification of cDNA ends
RP	retinitis pigmentosa
RPE	retinal pigment epithelium
SLSN	Senior Løken syndrome
SNP	single nucleotide polymorphism
STGD	Stargardt disease
UTR	untranslated regions
wt	wildtype